ISSN 2413-5577

№ 2 Апрель – Июнь 2026

Экологическая безопасность прибрежной и шельфовой зон моря

Ecological Safety of Coastal and Shelf Zones of Sea

No. 2 April – June 2026

ecological-safety.ru

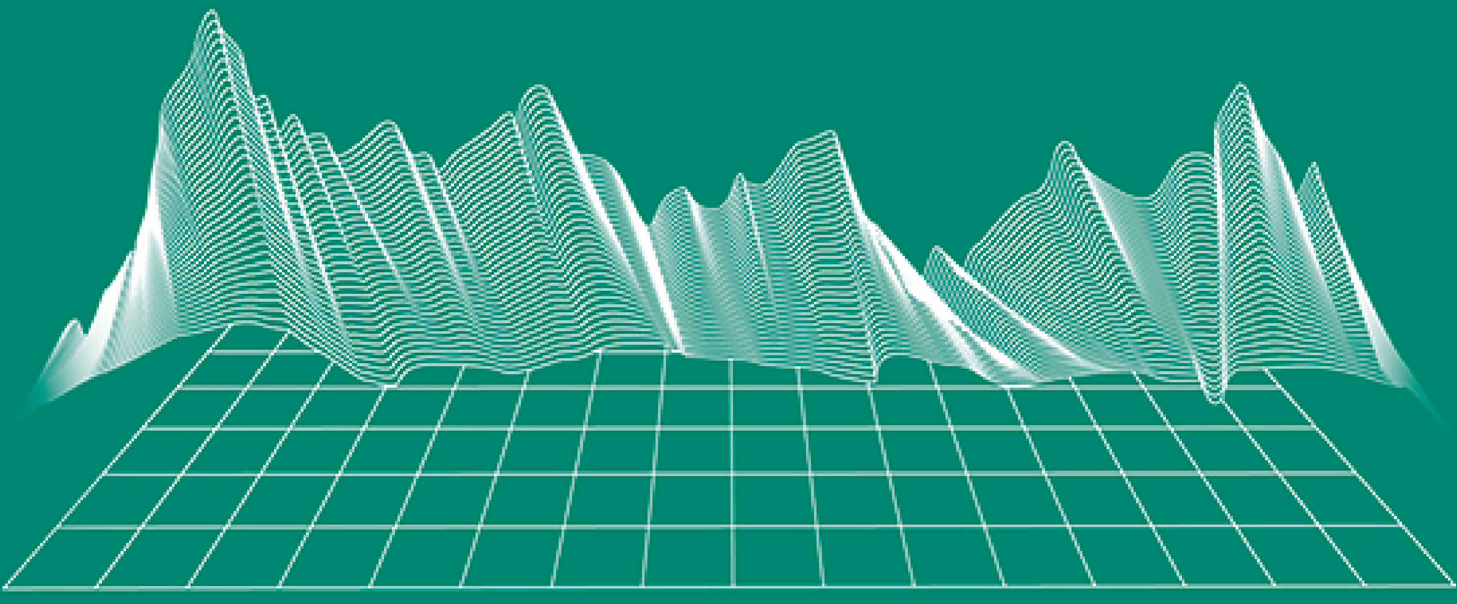

No. 2, 2026
April – June

Publication frequency:
Quarterly

16+

ECOLOGICAL SAFETY OF COASTAL AND SHELF ZONES OF SEA

Scientific and theoretical journal

FOUNDER AND PUBLISHER:
Federal State Budget Scientific Institution
Federal Research Centre
"Marine Hydrophysical Institute of RAS"

Journal is on the list of peer reviewed academic journals of the Higher Attestation Commission of the Russian Federation, where one may publish main research results of a Ph.D. thesis in the following field:

1.6.14 – Geomorphology and paleography (geographical sciences),
1.6.17 – Oceanology (geographical sciences, physical and mathematical sciences, technical sciences),
1.6.18 – Atmosphere and Climate Sciences (geographical, physical and mathematical sciences),
1.6.20 – Geoinformatics and cartography (geographical sciences),
1.6.21 – Geoecology (geographical sciences),
1.5.16 – Hydrobiology (biological sciences).

Journal is under the scientific and methodological guidance of the Earth Sciences Department of the Russian Academy of Sciences.

Journal is registered by the Federal Service for Supervision of Communications, Information Technology, and Mass Media (registration number ПИ № ФС77-73714 of 21 September 2018 and Эл № ФС77-82679 of 21 January 2022).

Journal coverage: The Russian Federation, other countries.

The Journal is indexed in and reposited at Russian Index of Science Citation (RISC), International Interactive Information and Bibliography System EBSCO, indexed in Scopus.

Journal is in the catalog of scientific periodicals of the Russian Science Citation Index (RSCI) on the platform of the scientific electronic library eLibrary.ru, Cyberleninka.

There is no fee for publishing articles.

e-mail: ecology-safety@mhi-ras.ru

website: http://ecological-safety.ru

Founder, Publisher and Editorial Office address:

2, Kapitanskaya St.,
Sevastopol, 299011, Russia

Phone, fax: + 7 (8692) 54-57-16

EDITORIAL BOARD

Yuri N. Goryachkin – **Editor-in-Chief**, Chief Researcher of FSBSI FRC MHI, Dr.Sci. (Geogr.), Scopus ID: 6507545681, ResearcherID: I-3062-2015, ORCID 0000-0002-2807-201X (Sevastopol, Russia)

Vitaly I. Ryabushko – **Deputy Editor-in-Chief**, Chief Researcher, Head of Department of FSBSI FRC A. O. Kovalevsky Institute of Biology of the Southern Seas of RAS, Dr.Sci. (Biol.), ResearcherID: H-4163-2014, ORCID ID: 0000-0001-5052-2024 (Sevastopol, Russia)

Elena E. Sovga – **Deputy Editor-in-Chief**, Leading Researcher of FSBSI FRC MHI, Dr.Sci. (Geogr.), Scopus ID: 7801406819, ResearcherID: A-9774-2018 (Sevastopol, Russia)

Vladimir V. Fomin – **Deputy Editor-in-Chief**, Chief Researcher, Head of Department of FSBSI FRC MHI, Dr.Sci. (Phys.-Math.), ResearcherID: H-8185-2015, ORCID ID: 0000-0002-9070-4460 (Sevastopol, Russia)

Tatyana V. Khmara – **Executive Editor**, Researcher of FSBSI FRC MHI, Scopus ID: 6506060413, ResearcherID: C-2358-2016 (Sevastopol, Russia)

Sergey V. Berdnikov – Chairman of FSBSI FRC Southern Scientific Centre of RAS, Dr.Sci. (Geogr.), ORCID ID: 0000-0002-3095-5532 (Rostov-on-Don, Russia)

Valery G. Bondur – Director of FSBSI Institute for Scientific Research of Aerospace Monitoring “AEROCOSMOS”, vice-president of RAS, academician of RAS, Dr.Sci. (Tech.), ORCID ID: 0000-0002-2049-6176 (Moscow, Russia)

Temir A. Britayev – Chief Researcher of IEE RAS, Dr.Sci. (Biol.), ORCID ID: 0000-0003-4707-3496, ResearcherID: D-6202-2014, Scopus Author ID: 6603206198 (Moscow, Russia)

Elena F. Vasechkina – Deputy Director of FSBSI FRC MHI, Dr.Sci. (Geogr.), ResearcherID: P-2178-2017 (Sevastopol, Russia)

Isaac Gertman – Head of Department of Israel Oceanographic and Limnological Research Institute, Head of Israel Marine Data Center, Ph.D. (Geogr.), ORCID ID: 0000-0002-6953-6722 (Haifa, Israel)

Sergey G. Demyshev – Chief Researcher, Head of Department of FSBSI FRC MHI, Dr.Sci. (Phys.-Math.), ResearcherID C-1729-2016, ORCID ID: 0000-0002-5405-2282 (Sevastopol, Russia)

Nikolay A. Diansky – Chief Researcher of Lomonosov Moscow State University, associate professor, Dr.Sci. (Phys.-Math.), ResearcherID: R-8307-2018, ORCID ID: 0000-0002-6785-1956 (Moscow, Russia)

Vladimir A. Dulov – Chief Researcher of FSBSI FRC MHI, professor, Dr.Sci. (Phys.-Math.), ResearcherID: F-8868-2014, ORCID ID: 0000-0002-0038-7255 (Sevastopol, Russia)

Victor N. Egorov – Scientific Supervisor of FSBSI FRC A. O. Kovalevsky Institute of Biology of the Southern Seas of RAS, academician of RAS, professor, Dr.Sci. (Biol.), ORCID ID: 0000-0002-4233-3212 (Sevastopol, Russia)

Vladimir V. Efimov – Chief Researcher, Head of Department of FSBSI FRC MHI, Dr.Sci. (Phys.-Math.), ResearcherID: P-2063-2017 (Sevastopol, Russia)

Vladimir B. Zalesny – Leading Researcher of FSBSI Institute of Numerical Mathematics of RAS, professor, Dr.Sci. (Phys.-Math.), ORCID ID: 0000-0003-3829-3374 (Moscow, Russia)

Andrey G. Zatsepin – Chief Researcher, Head of Laboratory of P.P. Shirshov Institute of Oceanology of RAS, Dr.Sci. (Phys.-Math.), ORCID ID: 0000-0002-5527-5234 (Moscow, Russia)

Sergey K. Konovalov – Director of FSBSI FRC MHI, corresponding member of RAS, Dr.Sci. (Geogr.), ORCID ID: 0000-0002-5200-8448 (Sevastopol, Russia)

Gennady K. Korotaev – Chief Researcher, Scientific Supervisor of FSBSI FRC MHI, corresponding member of RAS, professor, Dr.Sci. (Phys.-Math.), ResearcherID: K-3408-2017 (Sevastopol, Russia)

Arseniy A. Kubryakov – Leading Researcher, Deputy Director of FSBSI FRC MHI, Ph.D. (Phys.-Math.), ORCID ID: 0000-0003-3561-5913 (Sevastopol, Russia)

Alexander S. Kuznetsov – Leading Researcher, Head of Department of FSBSI FRC MHI, Ph.D. (Tech.), ORCID ID: 0000-0002-5690-5349 (Sevastopol, Russia)

Michael E. Lee – Chief Researcher, Head of Department of FSBSI FRC MHI, Dr.Sci. (Phys.-Math.), professor, ORCID ID: 0000-0002-2292-1877 (Sevastopol, Russia)

Pavel R. Makarevich – Chief Researcher of MMBI KSC RAS, Dr.Sci. (Biol.), ORCID ID: 0000-0002-7581-862X, ResearcherID: F-8521-2016, Scopus Author ID: 6603137602 (Murmansk, Russia)

Ludmila V. Malakhova – Leading Researcher of A. O. Kovalevsky Institute of Biology of the Southern Seas of RAS, Ph.D. (Biol.), ResearcherID: E-9401-2016, ORCID: 0000-0001-8810-7264 (Sevastopol, Russia)

Gennady G. Matishov – Deputy Academician – Secretary of Earth Sciences Department of RAS, Head of Section of Oceanology, Physics of Atmosphere and Geography, Scientific Supervisor of FSBSI FRC Southern Scientific Centre of RAS, Scientific Supervisor of FSBSI Murmansk Marine Biological Institute KSC of RAS, academician of RAS, Dr.Sci. (Geogr.), professor, ORCID ID: 0000-0003-4430-5220 (Rostov-on-Don, Russia)

Ekaterina A. Pozachenyuk – Head of Department in Tavrida Academy of V. I. Vernadsky Crimean Federal University, professor, Dr.Sci. (Geogr.), ORCID ID: 0000-0002-4837-1009 (Simferopol, Russia)

Alexander V. Prazukin – Leading Researcher of FSBSI FRC A. O. Kovalevsky Institute of Biology of the Southern Seas of RAS, Dr.Sci. (Biol.), ResearcherID: H-2051-2016, ORCID ID: 0000-0001-9766-6041 (Sevastopol, Russia)

Dimitar I. Trukhchev – Institute of Metal Science, equipment, and technologies “Academician A. Balevski” with Center for Hydro- and Aerodynamics at the Bulgarian Academy of Sciences, Dr.Sci. (Phys.-Math.), professor (Varna, Bulgaria)

Naum B. Shapiro – Leading Researcher of FSBSI FRC MHI, Dr.Sci. (Phys.-Math.), ResearcherID: A-8585-2017 (Sevastopol, Russia)

РЕДАКЦИОННАЯ КОЛЛЕГИЯ

Горячкин Юрий Николаевич – **главный редактор**, главный научный сотрудник ФГБУН ФИЦ МГИ, д. г. н., Scopus Author ID: 6507545681, ResearcherID: I-3062-2015, ORCID ID: 0000-0002-2807-201X (Севастополь, Россия)

Рябушко Виталий Иванович – **заместитель главного редактора**, главный научный сотрудник, заведующий отделом ФГБУН ФИЦ ИнБЮМ им. А.О. Ковалевского РАН, д. б. н., ResearcherID: H-4163-2014, ORCID ID: 0000-0001-5052-2024 (Севастополь, Россия)

Совга Елена Евгеньевна – **заместитель главного редактора**, ведущий научный сотрудник ФГБУН ФИЦ МГИ, д. г. н., Scopus Author ID: 7801406819, ResearcherID: A-9774-2018 (Севастополь, Россия)

Фомин Владимир Владимирович – **заместитель главного редактора**, главный научный сотрудник, заведующий отделом ФГБУН ФИЦ МГИ, д. ф.-м. н., ResearcherID: H-8185-2015, ORCID ID: 0000-0002-9070-4460 (Севастополь, Россия)

Хмара Татьяна Викторовна – **ответственный секретарь**, научный сотрудник ФГБУН ФИЦ МГИ, Scopus Author ID: 6506060413, ResearcherID: C-2358-2016 (Севастополь, Россия)

Бердников Сергей Владимирович – председатель ФГБУН ФИЦ ЮНЦ РАН, д. г. н., ORCID ID: 0000-0002-3095-5532 (Ростов-на-Дону, Россия)

Бондур Валерий Григорьевич – директор ФГБНУ НИИ «АЭРОКОСМОС», вице-президент РАН, академик РАН, д. т. н., ORCID ID: 0000-0002-2049-6176 (Москва, Россия)

Бритаев Темир Аланович – главный научный сотрудник ФГБУН ИПЭЭ, д. б. н., ORCID ID: 0000-0003-4707-3496, ResearcherID: D-6202-2014, Scopus Author ID: 6603206198 (Москва, Россия)

Васечкина Елена Федоровна – заместитель директора ФГБУН ФИЦ МГИ, д. г. н., ResearcherID: P-2178-2017 (Севастополь, Россия)

Гертман Исаак – глава департамента Израильского океанографического и лимнологического исследовательского центра, руководитель Израильского морского центра данных, к. г. н., ORCID ID: 0000-0002-6953-6722 (Хайфа, Израиль)

Демышев Сергей Германович – главный научный сотрудник, заведующий отделом ФГБУН ФИЦ МГИ, д. ф.-м. н., ResearcherID: C-1729-2016, ORCID ID: 0000-0002-5405-2282 (Севастополь, Россия)

Дианский Николай Ардальянович – главный научный сотрудник МГУ им. М. В. Ломоносова, доцент, д. ф.-м. н., ResearcherID: R-8307-2018, ORCID ID: 0000-0002-6785-1956 (Москва, Россия)

Дулов Владимир Александрович – главный научный сотрудник ФГБУН ФИЦ МГИ, профессор, д. ф.-м. н., ResearcherID: F-8868-2014, ORCID ID: 0000-0002-0038-7255 (Севастополь, Россия)

Егоров Виктор Николаевич – научный руководитель ФГБУН ФИЦ ИнБЮМ им. А.О. Ковалевского РАН, академик РАН, профессор, д. б. н., ORCID ID: 0000-0002-4233-3212 (Севастополь, Россия)

Ефимов Владимир Васильевич – главный научный сотрудник, заведующий отделом ФГБУН ФИЦ МГИ, д. ф.-м. н., ResearcherID: P-2063-2017 (Севастополь, Россия)

Залесный Владимир Борисович – ведущий научный сотрудник ФГБУН ИВМ РАН, профессор, д. ф.-м. н., ORCID ID: 0000-0003-3829-3374 (Москва, Россия)

Зацепин Андрей Георгиевич – главный научный сотрудник, руководитель лаборатории ФГБУН ИО им. П.П. Ширшова РАН, д. ф.-м. н., ORCID ID: 0000-0002-5527-5234 (Москва, Россия)

Коновалов Сергей Карпович – директор ФГБУН ФИЦ МГИ, член-корреспондент РАН, д. г. н., ORCID ID: 0000-0002-5200-8448 (Севастополь, Россия)

Коротаев Геннадий Константинович – главный научный сотрудник, научный руководитель ФГБУН ФИЦ МГИ, член-корреспондент РАН, профессор, д. ф.-м. н., ResearcherID: K-3408-2017 (Севастополь, Россия)

Кубряков Арсений Александрович – ведущий научный сотрудник, заместитель директора ФГБУН ФИЦ МГИ, д. ф.-м. н., ORCID ID: 0000-0003-3561-5913 (Севастополь, Россия)

Кузнецов Александр Сергеевич – ведущий научный сотрудник, заведующий отделом ФГБУН ФИЦ МГИ, к. т. н., ORCID ID: 0000-0002-5690-5349 (Севастополь, Россия)

Ли Михаил Ен Гон – главный научный сотрудник, заведующий отделом ФГБУН ФИЦ МГИ, профессор, д. ф.-м. н., ORCID ID: 0000-0002-2292-1877 (Севастополь, Россия)

Макаревич Павел Робертович – главный научный сотрудник ММБИ КНЦ РАН, д. б. н., ORCID ID: 0000-0002-7581-862X, ResearcherID: F-8521-2016, Scopus Author ID: 6603137602 (Мурманск, Россия)

Малахова Людмила Васильевна – ведущий научный сотрудник ФГБУН ФИЦ ИнБЮМ им. А.О. Ковалевского РАН, к. б. н., ResearcherID: E-9401-2016, ORCID ID: 0000-0001-8810-7264 (Севастополь, Россия)

Матишов Геннадий Григорьевич – заместитель академика-секретаря Отделения наук о Земле РАН – руководитель Секции океанологии, физики атмосферы и географии, научный руководитель ФГБУН ФИЦ ЮНЦ РАН, научный руководитель ФГБУН ММБИ КНЦ РАН, академик РАН, профессор, д. г. н., ORCID ID: 0000-0003-4430-5220 (Ростов-на-Дону, Россия)

Празукин Александр Васильевич – ведущий научный сотрудник ФГБУН ФИЦ ИнБЮМ им. А.О. Ковалевского РАН, д. б. н., Researcher ID: H-2051-2016, ORCID ID: 0000-0001-9766-6041 (Севастополь, Россия)

Позаченюк Екатерина Анатольевна – заведующая кафедрой Института «Таврическая академия» ФГАОУ КФУ им. В.И. Вернадского, профессор, д. г. н., ORCID ID: 0000-0002-4837-1009 (Симферополь, Россия)

Трухчев Димитър Иванов – старший научный сотрудник Института океанологии БАН, профессор, д. ф.-м. н. (Варна, Болгария)

Шапиро Наум Борисович – ведущий научный сотрудник ФГБУН ФИЦ МГИ, д. ф.-м. н., ResearcherID: A-8585-2017 (Севастополь, Россия)

CONTENTS

№ 2. 2026 April – June, 2026

СОДЕРЖАНИЕ

№ 2. 2026 Апрель – Июнь, 2026

ISSN 2413-5577, Ecological Safety of Coastal and Shelf Zones of Sea, No. 2, pp. 6–25 (2026)

Original paper

Creation of a Coastal Cadastre for Crimea: Status and Prospects

Yu. N. Goryachkin *, V. V. Dolotov, O. S. Romanyuk

Marine Hydrophysical Institute of RAS, Sevastopol, Russia

* *e-mail: yngor@mhi-ras.ru*

Abstract

The problem of regulating the use of natural resources in the coastal zone of Russia can largely be solved by creating and adopting a national cadastre of marine coasts. Despite years of discussions and some practical steps, it has not yet been established. The aim of the work is to consider the evolution of views on the purpose and content of a cadastre of Russian marine coasts, to highlight the current state of its creation in general for Russia and for the Crimean Peninsula in particular. We used literary sources, departmental reports, materials of various meetings and monitoring observations. There are two stages in setting up the problem of creating a cadastre. There were virtually single scientific publications on the subject in between. The first stage is characterized by maximum cadastre requirements. Whereas in the second stage, there was a marked shift in focus from filling the cadastre with data on natural processes to environmental and socio-economic aspects. Since the coastal line of Russia is almost equal to the equator length and most of it lies in remote areas with a harsh climate, the creation of a unified cadastre does not seem real in the nearest future. It is therefore reasonable to focus on the compilation of cadastres for specific areas that are of great economic importance, such as the Black and Baltic Seas. In this context, we introduce for the first time the initial experience and results of compiling a cadastral survey of the Crimean coastline (1986–1988) into academic discourse and a GIS developed by us, discussing them in detail. Creation of a coastal cadastre for Crimea is of significant scientific and practical importance, as it will allow systematization and analysis of data on the status, morphology and dynamics of the coastal zone of the peninsula and serve as a tool to prevent natural and technological risks as well as promote sustainable development of Crimea.

Keywords: Russia, Crimean Peninsula, coastal cadastre, lithodynamics, GIS

Acknowledgments: The work was carried out under state assignment no. FNNN-2024-0016 of MHI RAS.

For citation: Goryachkin, Yu.N., Dolotov, V.V. and Romanyuk, O.S., 2026. Creation of a Coastal Cadastre for Crimea: Status and Prospects. *Ecological Safety of Coastal and Shelf Zones of Sea*, (2), pp. 6–25.

© Goryachkin Yu. N., Dolotov V. V., Romanyuk O. S., 2026

This work is licensed under a Creative Commons Attribution-Non Commercial 4.0 International (CC BY-NC 4.0) License

Создание кадастра морских берегов Крыма: состояние вопроса и перспектива

Ю. Н. Горячкин *, В. В. Долотов, О. С. Романюк

Морской гидрофизический институт РАН, Севастополь, Россия

* *e-mail: yngor@mhi-ras.ru*

Аннотация

Задачу регулирования природопользования в береговой зоне России во многом можно решить путем создания и принятия на государственном уровне кадастра морских берегов. Несмотря на многолетние обсуждения и некоторые практические шаги, он до настоящего времени не создан. Цель работы – рассмотреть эволюцию взглядов на предназначение и содержание кадастра морских берегов России, осветить современное состояние вопроса его создания в целом для России и для Крымского полуострова, в частности. Использованы литературные источники, ведомственные отчеты, материалы различных совещаний и мониторинговых наблюдений. Выделено два этапа в постановке проблемы создания кадастра. В промежутках между этими этапами по этому вопросу были единичные научные публикации. Для первого этапа характерно выдвижение максимальных требований к содержанию кадастра. На втором этапе отмечено резкое смещение акцентов с наполнения кадастра данными о природных процессах в сторону экологического и социально-экономического аспектов. Поскольку береговая линия России близка по длине к экватору, а бóльшая ее часть находится в труднодоступной и климатически неблагоприятной местности, создание единого кадастра в обозримом будущем не представляется реальным. Поэтому целесообразно сосредоточиться на составлении кадастров отдельных, наиболее важных в хозяйственном отношении территорий, например, Черного и Балтийского морей. В связи с этим впервые вводится в научный оборот и подробно обсуждается первый опыт и результаты создания кадастрового описания берегов Крыма в 1986–1988 гг. и сделанная на его основе авторами настоящей работы ГИС. Создание кадастра морских берегов Крыма имеет важное научное и практическое значение, поскольку он позволит систематизировать и анализировать данные о состоянии, морфологии и динамике береговой зоны полуострова, а также послужит инструментом для предотвращения природных и техногенных рисков и способствует устойчивому развитию Крыма.

Ключевые слова: Россия, Крымский полуостров, кадастр береговой зоны, литодинамика, ГИС

Благодарности: работа выполнена в рамках выполнения государственного задания FNNN-2024-0016 МГИ РАН.

Для цитирования: *Горячкин Ю. Н., Долотов В. В., Романюк О. С.* Создание кадастра морских берегов Крыма: состояние вопроса и перспектива // Экологическая безопасность прибрежной и шельфовой зон моря. 2026. № 2. С. 6–25. EDN GWPAEQ.

Introduction

Studying the processes occurring in the coastal zone of the Russian Federation, forecasting its dynamics, and countering hazardous natural and man-made processes are pressing challenges recognised by the scientific community and administrative bodies. In recent decades, economic operators and state bodies in the Russian Federation have been confronted with adverse processes in the coastal zone, predominantly of anthropogenic origin. Moreover, the situation is complicated by numerous cross-sectoral conflicts. This hinders economic development and poses a threat to the sustainability of the natural environment and its aesthetic appeal. This applies in full to the coastline of the Crimean Peninsula as well.

Among scientists specialising in coastal issues and practising hydraulic engineers, it is widely held that the challenge of regulating land use in the coastal zone can, to a large extent, be addressed through the creation and adoption, at national level, of a coastal register.

The idea of such a cadastre was first implicitly proposed in 1954 by V. P. Zenkovich, the founder of Soviet coastal science [1], who understood the cadastre to mean a scientific description of each section of the coastline, including an analysis of its dynamics, a forecast of expected changes and an assessment of its practical suitability. At the same time, V. V. Longinov, an authoritative scholar in the field of coastal science, expressed himself more clearly and concisely: "A coastal cadastre should be understood as a description of the coastal zone, revealing its nature as an object of practical activity" [2, p. 44].

As early as 2008, during the existence of the Russian Federation, a glossary on the coastal zone cadastre was published [1)]. The glossary defines the cadastre as a constantly updated, refined (detailed) and systematised collection of data on the coastal zone from geographical, administrative, geological-morphological and socio-economic perspectives. It is emphasised that, similarly to other cadastres, it should be an official document for nationwide use, forming an important part of the relevant legislative act at federal level. In the conceptual study [3], the coastal systems cadastre is seen as a methodologically systematised collection of data that quantitatively and qualitatively characterises the phenomena and resources located within the territory under consideration and the adjacent water area, reflecting the high dynamism and complexity of coastal systems.

For Crimea, the first and, to date, only cadastral survey (1986–1988) was carried out at the Institute of Mineral Resources (IMR) (Simferopol) under the supervision of O. S. Romanyuk. The challenges involved in establishing a cadastre for Crimea were discussed in the works of researchers at V. I. Vernadsky Taurida National University and Marine Hydrophysical Institute of the Russian Academy of Sciences [2)] [4–7].

[1)] Gogoberidze, G.G., Zhamoida, V.A., Nesterova, E.N., Ryabchuk, D.V. and Spiridonov, M.A., 2008. *Glossary on the Coastal Zone Cadastre*. Saint Petersburg: RSHU, 95 p. (in Russian).

[2)] Mikhailov, V.A. and Soloviov, V.I., 2013. [*Data Base for the Marine Coast Cadastre*]. Moscow. State Registration Number 2013620057.

Following the change in the political and economic system within the Russian Federation, the role of state regulation of natural resource use has grown in the definitions of the cadastre: the state is considered to act as a mediator for economic entities, and the cadastre should serve as the basis for its activities.

However, despite many years of discussion and some practical steps, no such cadastre currently exists. Although, in our view, it could serve as an effective mechanism for sustainable natural resource management and integrated coastal zone management. The creation of a coastal cadastre would provide a legal framework for regulating relations both between economic operators and between enterprises and state authorities, and would help to reduce natural and man-made risks to coastal systems. This is demonstrated by examples of natural resource cadastres and registers that actually exist and are in operation in the Russian Federation: the State Forest Register, the State Water Register, the State Cadastre of Mineral Deposits and Occurrences, the State Cadastre of Specially Protected Natural Areas, and the State Cadastre of Wildlife. The Land Cadastre deserves special mention, as it contains information on the natural, economic and legal status of land and plays a huge role in the economic life of the Russian Federation.

The aim of this paper is to examine the evolution of views on the purpose and content of the Russian Federation's coastal cadastre, and to highlight the current state of play regarding its establishment, both for the Russian Federation as a whole and, in particular, for the Crimean Peninsula.

Methods and materials

In preparing this article, we drew on academic sources, departmental reports, previously unpublished materials from various meetings and data from monitoring observations and studies conducted by various organisations, including Marine Hydrophysical Institute of the Russian Academy of Sciences. The cadastral GIS was developed as a 32-bit desktop version, using the object-oriented programming language Delphi and the Windows 7–10 operating system. The base map used comprised nine vector layers, including land and seabed relief, as well as a detailed representation of coastal features. All GIS map features are stored in ESRI shapefile formats.

Results and discussion

Definition of a cadastre. According to the definition in the Great Soviet Encyclopaedia [3)], a cadastre (French: *cadastre*) is a list or register compiled by an official body or institution, such as a water cadastre or a land cadastre. In the Great Russian Encyclopaedia [4)], the term "cadastre" is defined as an organised list or register of certain important objects, officially compiled by the state on the basis of data from observations carried out periodically or continuously.

[3)] [Cadastre]. In: A. M. Prokhorov, ed., 1969–1978. [*Great Soviet Encyclopedia*]. Moscow: Sovetskaya Entsiklopediya. Vol. 11, p. 137 (in Russian).

[4)] [Cadastre]. In: Yu. S. Osipov, ed., 2004–2017. [*Great Russian Encyclopedia*]. Moscow. Vol. 12, p. 374 (in Russian).

The Russian Internet Encyclopaedia (RUWIKI) provides a similar definition. In international practice, this term is generally used in the context of land resource management. In the Russian Federation, it is also associated primarily with land relations. This may be why, in Russian legislation, the term "cadastre" is gradually being replaced by the term "register"; however, in essence, the main functions of the cadastre (recording and systematisation) remain unchanged.

Stages in the development of the cadastre concept in Russia. An analysis of publications on the issue of establishing a coastal cadastre reveals two distinct stages: the first during the existence of the USSR (namely, in the mid-1950s) and the second from the beginning of the 21st century. Between these two stages, there were almost no academic publications on this subject.

In brief, the information that a cadastre was meant to contain was defined as follows [1]:

1. An introductory theoretical section setting out general principles regarding the morphology and dynamics of sea coasts, as applicable to the coast in question and necessary for engineering and technical staff to understand the rest of the text.

2. General physical characteristics of the basin, the adjacent land and the coastline proper: the geographical location and outline of the sea, depths, water masses and benthic fauna, climatic conditions (winds, precipitation, temperature and ice conditions); waves and currents, water level patterns; the topography and hydrography of the adjacent land and the water and solid runoff of rivers; the geological structure and geological history of the coasts, economic and geographical characteristics, transport links, major hydraulic engineering structures, a description of sediments (their origin, volume and depositional patterns), and detailed bathymetric profiles of the underwater coastal slope showing the structure of the seabed and the nature of the seabed material.

3. History of the development and study of the basin; archaeological and historical monuments and documents; a review of the literature, maps and archival materials; and a review of our own studies and obtained data.

4. Principles for the coastline zoning and a list of the designated zones.

5. A detailed zone-by-zone description, including an analysis of the dynamics (and regime) of the coastline, with elements of forecasting and an assessment of the coastline for practical purposes.

6. General conclusions by zone, summarising the detailed descriptions and serving as the basis for new scientific findings.

Compiling such an extensive list of information – which the cadastre is required to contain – for the vast majority of coastal areas in the Russian Federation is virtually impossible even now, 70 years on. In paper [2], this list was expanded even further to include seismic conditions, results of dry land and offshore drilling, and much more. To illustrate the level of detail proposed by the author, we will now provide only a description of the necessary information regarding wave conditions:

- statistical data on wave activity;
- progression of storms by stage (developing, mature, dissipating) and by wind action;
- the number of swells;
- areas where waves of various directions and strengths shoal and break;

– the nature of wave breaking and the resulting surf;
– the nature of the resulting translational wave;
– run-up heights of swash flows on the beach and their velocities;
– data on the parameters of waves entering the coastal zone from the open sea, and their parameters prior to breaking;
– the velocities and directions of currents arising in the bottom layer, as well as throughout the entire water column of the coastal zone under various wave conditions;
– information on cross-shore compensation (return) flows, rip currents, and longshore currents in the coastal zone;
– a description of wave refraction and its patterns, where refraction is significant.

Such an extensive list of data was clearly excessive at that stage in the development of coastal science. To be fair, it should be noted that the author of article [2] (V. V. Longinov) contributed significantly to the development of the theory of coastal zone lithodynamics [5), 6)]. It is only now, with the development of mathematical models and computing technology, that it has become possible to solve problems involving the determination of the quantitative characteristics of lithodynamic processes, albeit approximately and with some margin of error, and only for certain regions (see, for example, works [8, 9]).

Overall, the first stage was characterised by the setting of the most stringent requirements for the cadastre content, reflecting the significant advances in coastal science during that period and a certain degree of optimism regarding the future. Of note, these detailed lists did not include a description of the anthropogenic pressure level, due to its negligible role at that time.

In the second stage (early 21st century), the content of the proposed cadastre shows a marked shift from information on natural processes to socio-economic aspects. Thus, paper [10] asserts that the cadastre must include the following information sections: physical-geographical information; administrative and legal information; geological and geomorphological information; resource information; economic information; environmental protection information; and information on hazardous natural and natural-manmade processes.

Elaborating on this approach, the authors [3] propose the creation of a coastline cadastre in the form of a modular information and analytical system, based on three modules: administrative and economic; landscape and geographical; and eco-socio-economic. The authors believe that the landscape-geographical module should include the location of the coastline in the form of linear features; land cover (sand, forests, tundra, marshes, etc.) in the form of polygonal features; the geological and geomorphological structure of the coastline and the shelf area of the coastal waters; the relief of the land-based part of the coastal territory in the form of polygonal features; hydrography (seas, lakes and reservoirs, watercourses, rivers and channels, canals, etc.) in the form of polygonal/linear features; the bathymetry of the seas adjacent to the coastal regions, in the form of polygonal features.

---

5) Longinov, V.V., 1963. [*Dynamics of the Coastal Area of Tideless Seas*]. Moscow: Izd-vo Akademii Nauk, 379 p. (in Russian).

6) Longinov, V.V., 1973. [*Essays on Oceanic Lithodynamics*]. Moscow: Nauka, 244 p. (in Russian).

In this list (albeit not a detailed one), the description of the natural environment is considerably less detailed than was stated in the cadastral drafts at the first stage.

The works of V. P. Zenkovich. It is interesting to note that, for half a century following the publication of articles [1, 2], not a single significant work appeared in which the term “cadastre” featured, apart from V. P. Zenkovich’s brief abstracts in the proceedings of the 9th Congress of the Geographical Society of the USSR [11]. In these, he once again justifies the need to create a coastal zone cadastre as a systematic collection of data on coast types, their morphology, dynamics, stability and degree of economic development, which should serve as a scientific and practical basis for the rational use of coastal areas. Coastal zone monitoring is regarded as an essential complement to the cadastre and is understood as the long-term and regular observation of changes to coastlines with the aim of identifying trends, forecasting hazardous processes and assessing the consequences of human activity. It is also emphasised that only an integrated system of cadastre and monitoring allows for the scientifically sound planning of coastal protection measures and the minimisation of environmental and economic damage. Notably, the author expresses concern as for the deterioration of the natural condition of the coastal system.

During the half-century period mentioned above, scientists’ main efforts were generally directed towards studying individual components of the coastal zone’s natural environment, which was clearly insufficient for compiling a detailed cadastre of the coastline. However, attempts were made to move closer to this goal for certain regions (for example, the Crimean Peninsula). In article [1], V. P. Zenkovich argued that the work carried out by the Institute of Oceanology of the USSR Academy of Sciences between 1945 and 1951 made it possible to create, as a first approximation, a cadastre of the Soviet Black Sea coastline. It is difficult to agree with this, since the seminal work published on the basis of these studies – which played an enormous role in the development of coastal science [7)] – lacks the formal characteristics inherent in a cadastre as a document. The author was apparently aware of this, as he characterised this work as a cadastral description and called for this experience to be extended to all the seas of the USSR.

The development of the concept of a cadastre in the late 20th and early 21st centuries. In the late 20th century, two works by scholars from Saint Petersburg were published, in which the issue of creating a cadastre of marine coasts was raised once again [12, 13]. From this period onwards, discussion of this issue and practical steps were resumed. For instance, work commenced by the All-Russian Geological Research Institute of A. P. Karpinsky (the Karpinsky Institute) and the non-governmental organisation *Yuzhmorgeologiya* along the coasts of the Baltic and Black Seas. A section on the cadastre of the coastal zone of the Black Sea and Sea of Azov, prepared based on the results of these studies, was incorporated into the Law of the Krasnodar Krai of the Russian Federation “On the Coastal Zone of the Black Sea and Sea of Azov within the Krasnodar Krai” (No. 156-КЗ of 18 November 1998). As part of the Russian Shelf Programme, implemented in the early 2000s, it was proposed to establish a separate programme for the comprehensive study of Russia’s

---

[7)] Zenkovich, V.P., 1960. [*Morphology and Dynamics of the Soviet Coasts of the Black Sea*]. Moscow: Izd-vo AN SSSR. Vol. 2, 216 p. (in Russian).

coastlines, entitled Russian Coastlines. One of the intended outcomes of the programme was to create the State Cadastre of Russian Coastal Areas; however, no funding was allocated for this.

The paper [14] raises the issue of establishing a system of coastal and marine cadastres in the Far Eastern region with a view to the rational and integrated management and use of natural resources in coastal zones. The paper also justifies the need to use information-based coastal cadastral systems as a tool for resolving the main conflicts arising from traditional natural resource use, management decision-making, environmental monitoring and nature conservation measures. Researchers from the Karpinsky Institute and the Russian State Hydrometeorological University (RSHU) have, for the first time, developed and published a reference guide [1)], which sets out the key concepts and terminology of the cadastre. The Karpinsky Institute is developing a project named Reference and Information System on the Geology and Resources of the Russian Sector of the Baltic Sea and its Coastal Zone.

In 2012, an article was published by researchers from the RSHU, the Karpinsky Institute and Peter the Great Saint Petersburg Polytechnic University (SPbPU), entitled Concept for the Development of a State Cadastre of the Coastal Zone of the Seas of the Russian Federation [10]. Relying on this work, paper [3] proposed a structure and purpose for the information and analytical system State Cadastre of the Coastal Zone of the Russian Federation, taking into account the spatial hierarchy of coastal territories and coastal zones. A pilot project to create such a system, using the Kaliningrad Region as a case study, was proposed.

A series of meetings and conferences has led to the launch of a project to establish a State Cadastre of the Russian Arctic's coastal zone. A number of steps are being taken to this end [15–17]. An indicator-based approach is being developed to assess the state of the natural and socio-economic environment of the coastal zone [8)] [18, 19].

In October 2022, as part of the First All-Russian Scientific and Practical Conference Russia in the UN Decade of Ocean Sciences, a round-table discussion entitled The Cadastre of Russia's Sea Coasts: Groundwork, Challenges and Prospects took place, in which one of the authors of this article participated. A resolution was adopted, noting "the existence of a substantial foundation for the systematisation of information on the coastlines of the Russian Federation" [20, p. 375]. The operative part drew "the attention of federal and regional administrative bodies to the need to develop a package of regulations governing the inventory of natural resources and features of coastal territories and adjacent waters… including the compilation of the Cadastre of the Russian Federation's Sea Shores and the establishment of a system of natural and economic accounting". It was recommended that "research and development work be initiated on 'The Development of Principles and Tools for the Cadastre of the Sea Coasts of the Russian Federation'" [20, p. 376]. The resolution proposed the Kaliningrad Region as a pilot region for testing the principles and implementing the tools of the Cadastral Register of the Marine Coasts of the Russian Federation.

[8)] Spiridonov, A.I., ed., 1980. [*Four-Language Encyclopedic Dictionary of Physical Geography Terms: Russian, English, German, French*]. Moscow: Sovetskaya Entsiklopediya, 703 p. (in Russian).

The current situation and challenges in establishing a cadastre. At present, the need to establish a cadastre of the country's coastlines is evident to many in the Russian Federation; however, there are also certain difficulties. It must be borne in mind that, according to the Great Russian Encyclopaedia, the total length of the Russian Federation's coastline is approximately 39,053 km, which is almost equal to the length of the equator. Most of the coastline is situated in hard-to-access areas with a harsh climate. Consequently, the task of creating a unified cadastre does not appear feasible in the foreseeable future. Therefore, in our view, the focus should be on compiling cadastres for individual territories of the greatest economic importance, such as the Black and the Baltic Seas.

Another problem is the lack of qualified scientific and engineering staff in organisations conducting research in the coastal zone, as well as their inadequate material resources. Compared with the late Soviet era, the number of staff employed by these organisations has fallen sharply, and some organisations have been wound up altogether. It is worth noting here that, over the past two years, several enthusiasts who championed the idea of creating a cadastre have passed away: the renowned scientists G. G. Gogoberidze, R. D. Kosyan and M. A. Spiridonov, who were highly respected in scientific and administrative circles.

There are also legal issues. These include, first and foremost, ambiguity in defining the types of maritime activities and the difficulty of taking account of all forms of natural resource use in coastal and marine areas, owing to the division of powers between different levels of government in relation to specific activities. For example, the coastal land itself falls under the jurisdiction of regional authorities, while the maritime space off the coast falls under federal jurisdiction.

In our view, many contemporary perspectives on the cadastre content show a certain bias towards socio-economic aspects, to the detriment of the natural and environmental components. There are also doubts regarding the large number of components within the cadastre content itself, as well as the complexity of calculating certain indicators proposed in [19], which makes compiling the cadastre highly problematic.

As noted above, the first – and, until 1986, the only – detailed description of the Soviet Black Sea coastline within the borders of the USSR was compiled at the Institute of Oceanology supervised by V. P. Zenkovich in 1954. According to the supervisor's own conclusion, this document did not constitute a comprehensive cadastre, but could only be regarded as one of its constituent parts, albeit a very significant one. Part of this work was published in 1960 [7)]. In this classic work, considerable attention was paid to the Crimean coast, but only to its western part, from Sivash to Balaklava. The remaining coastlines (the Southern Coast of Crimea and the Kerch Peninsula) were described in a report classified as secret, which was downgraded only after the collapse of the USSR and which remains unpublished so far.

In 1984, the Commission of the Presidium of the Council of Ministers of the USSR on Environmental Protection and the Rational Use of Natural Resources instructed the Academy of Sciences of the USSR, the State Committee for Construction in the USSR and the Ministry of Geology of the USSR to draw up a forecast of the state of the Black Sea coastal zone up to the year 2000, given the development of health resorts and the economic development of this zone; to establish a cadastre of the Black Sea coastline in the coming years and to ensure that the necessary engineering-geological maps of the Black Sea coast were drawn up in 1985–1986. In pursuance of these decisions, the following regulatory documents were issued:

– Order No. 497 of the Ministry of Geology of the USSR dated 21 November 1984 "On the Implementation of Measures in the RSFSR, the Ukrainian SSR and the Georgian SSR to Protect the Black Sea Coastline from Erosion";

– Order No. 22 of the Ministry of Geology of the Ukrainian SSR dated 17 January 1985, which required the IMR to implement Order No. 497;

– Order No. 21 of the IMR dated 2 August 1985, instructing the project leader, E. P. Tikhonenkov, to adopt both orders for guidance and implementation.

By letter No. 03/3-376 dated 2 December 1985, the Ministry of Geology of the Ukrainian SSR instructed the IMR and the Krymgeologiya State Geological Organisation to produce an engineering-geological map of the coastline from the mouth of the Danube to the Kerch Strait. In the course of this work, Resolutions No. 568 of the Council of Ministers of the USSR dated 17 May 1986 and No. 238 of the Council of Ministers of the Ukrainian SSR dated 26 June 1986 were also issued, requiring the drafting of regulations on the procedure for compiling and updating data on the condition of the coastline. The Ministry of Geology of the Ukrainian SSR, in letters No. 03/3-213 of 24 July 1986 and No. 03/3-245 of 11 August 1986, emphasised the importance of the coastal cadastre work and instructed the IMR to submit proposals to higher-level organisations, which was duly carried out.

Under a commercial contract with the Crimean Hydrological Expedition of the Krymgeologiya State Geological Organisation (Krymgeologiya), the IMR drew up an unclassified diagram entitled Zoning of the Crimean Coast According to Dynamic Conditions, which was implemented by the Crimean Regional Executive Committee, the Evpatoria and Feodosia Territorial Councils of the Ukrainian Council for Resort Management, the Geological Inspectorate for the Southern Coast of Crimea under the Crimean Landslide Prevention Administration, and the Simferopol branch of UkrGIINTIZ.

In the course of work on this subject, Resolution No. 568 of the Council of Ministers of the USSR, dated 17 May 1986, and Resolution No. 238 of the Council of Ministers of the Ukrainian SSR, dated 26 June 1986, "On Improving the Effectiveness of Work to Protect the Coasts of the Black and Azov Seas from Erosion" were issued. These resolutions instructed the Academy of Sciences of the Ukrainian SSR, the USSR State Committee for Hydrometeorology and Environmental Monitoring, the USSR Ministry of Geology and the USSR State Committee for Construction were tasked with developing, in collaboration with the Councils of Ministers of the RSFSR, the Ukrainian SSR, the GSSR, and to approve, in the first half of 1987, regulations on the procedure for compiling and updating data on the condition of the coasts and on landslide processes leading to the erosion of the coastal zone of the Black Sea and the Sea of Azov.

The 1988 Cadastre of the Crimean Coast. Between 1986 and 1988, under a commercial contract with the Crimean Hydrological Expedition of the Krymgeologiya, the IMR carried out work "To compile a cadastre of the above-water portion of the Crimean coast at a scale of 1:200,000". The cost amounted to 35,000 Soviet roubles, which, based on the consumer price index and the cost of basic commodities, would roughly correspond to 10 million Russian roubles in 2026. The field and office studies were carried out in fact by two staff members, with one of the authors of this paper acting as the project leader and principal investigator. Use was also made of archival materials from the Krymgeologiya, P. P. Shirshov Institute of Oceanology of the USSR Academy of Sciences, Rostov State University, the Crimean Research Institute of Design (KrymNIIproekt), the Evpatoria Hydrogeological Station of the Regional Council, Ukrzemproekt and VSEGINGEO. Economic and recreational development of the coast was assessed from periodical publications. The terms of reference covered the entire coastline, excluding the Southern Coast of Crimea.

That study was guided by the definition given in work [9]: a cadastre is a systematic collection of data comprising a qualitative and quantitative inventory of objects and phenomena, accompanied by a socio-economic assessment, which is compiled either periodically or through continuous observation of the relevant objects. The main content of the study included:

– zoning of the Crimean coasts into zones for the purposes of a cadastral description of the coastline at a scale of 1 : 200,000;

– compilation of a comprehensive regional-typological characterisation of subordinate taxonomic units;

– identification of the main tasks for the prospective study of the Crimean coastline.

The work proceeded in four stages: (1) analysis of published and archival material covering up to 100 years; (2) fieldwork and collected data processing; (3) coastline zoning; and (4) typological characterisation of the identified taxa.

In his book [7], V. P. Zenkovich based his classification of the Black Sea coastline on the tectonic or geological structure of the surrounding areas, as this largely determines the relief of the entire coastal zone, including both the land and the seabed. This approach is, in fact, analogous to engineering-geological classification [9].

The zoning performed by the IMR was based on factors controlling the rate of shoreline transformation (erosion or abrasion, and the transport of eroded material leading to the formation of mobile accumulation landforms) or its dynamics. These factors were grouped into three genetic categories: geological and geomorphological (lithological and stratigraphic rock strength complexes, neotectonic movements, seismic conditions, coastal and beach morphometry and exogenous geological processes (EGP)); hydrometeorological (wind, wave and sea-level regimes) and biological (marine biological productivity affecting EGP). Rock lithology was the key factor for zoning. Based on the main characteristics and with due account of these factors, individual thematic maps were compiled and then combined using a matrix-based approach, which enabled zoning of the coastline by its dynamic conditions at a scale of 1:200,000.

During fieldwork, sampling and the selection of sampling points, as well as the processing of material and analysis of the results, the methodology for coastal studies approved by the Ministry of Geology of the Ukrainian SSR was utilised [10].

---

[9] Popov, I.V., 1961. [*Engineering Geology of the USSR. Part 1. Theoretical Foundations of Regional Engineering Geology*]. Moscow: Izd-vo MGU, 178 p. (in Russian).

[10] Romanyuk, O.S., 1980. [*General Methodological Guidelines for the Study of Exogenous Coastal Processes with a View to Forecasting the Development of the Black Sea and Azov Sea Coasts Within the Ukrainian SSR*]. Simferopol: Institut Mineralnykh Resursov, 120 p. (in Russian).

For typological zoning based on subordinate taxa, the characteristics of approximately 500 coastal points were examined. Neighbouring points were determined to be identical in terms of shore type, which made it possible to identify sections of the coastline as the basis for subordinate taxa.

The following classification principles were applied:

– *hierarchy* – the subdivision of the territory from the general (the whole of Crimea) to the specific (base sections);

– *mutual exclusivity* – each coastal unit falls into only one of the proposed types when classified by a specific criterion: by genesis – erosional, accumulative, or erosional-accumulative; by relation to tectonic structure – longitudinal or transverse, etc;

– *nestedness* – the set of common characteristics grows as the subdivision proceeds (for example, at the regional level only the structural-tectonic feature is common, whereas at the section level a whole range of common characteristics applies);

– *consistency* – taxonomic units are identified according to uniform principles.

The coastal zoning was five-tiered, in contrast to the three-tiered approach used in study [7)]. Below is a brief description of the subordinate taxonomic units used in the zoning of the Crimean coast for cadastral purposes.

A *region* is a territory sharing a common tectonic structure that determines the inherited pattern of coastal development under predominantly unidirectional neotectonic movements.

A *province* is a geomorphologically distinct territory within a region, defined by a subordinate tectonic structure. A province is characterised by a predominantly uniform process (erosion or accumulation), albeit on coastlines of different types (erosional and accumulative).

A *district* is an area delineated within a geomorphological province on the basis of the lithology of the rocks exposed along the coast, which determines the rate of coastal processes common to the province.

A *sub-district* is a territory delineated within a district on the basis of specific hydrodynamic parameters resulting from the spatial heterogeneity of the area.

A *section* is the basic unit in a taxonomic description, the boundaries of which are determined by the similarity of the territory (at a scale of 1:200,000) in terms of coastline type, morphometry, the set of EGP and the relative rate of their occurrence, and suitability for recreational development. In total, 2 regions, 3 provinces, 6 districts, 7 sub-districts and 31 sections were identified (Fig. 1).

The 1988 coastal cadastre was compiled on the basis of an analysis of the characteristics of individual points. The textual and graphical components of the description contained all or most of the following features:

– the point number and its geographical coordinates;

– a hypsometric profile of the coastline extending 2 km inland and up to the 20-metre isobath, or 2 km seaward of the shoreline;

– a geological and geomorphological profile of the coastal outcrop;

– morphometric data for the coastline, either in the profile or in the text;

– a diagram of the grain-size distribution of the sandy component of beach deposits;

– the ratio of light to heavy mineral fractions for sandy deposits, or the mineral composition of gravel and pebble deposits;

– certain characteristics of wind and wave conditions based on available observation points;

– the type of coastline and the developed EGP;

– the degree of development of the surrounding area.

The comprehensiveness of the information on each point depended on the extent to which the area had been developed and studied, and on the availability of permanent EGP observation points. Taxonomic units of various ranks were described according to a standardised plan:

– geographical location;

– coastline type (genetic, morphological, secondary changes, development trend);

– geological characteristics (geological and structural features, lithological and strength complexes), neotectonics, seismicity;

– EGP on the coast, their setting and development trends;

– coastal morphometry (bedrock and beach deposits);

– hydrodynamics and meteorological conditions;

– marine biological productivity as a factor in coastal dynamics;

– the region's economic development (land use) and potential for recreational use;

– coastal protection works.

In addition to the typological zoning of the Crimean coastline and the description of individual locations, the 1988 cadastre contains general sections providing a brief overview of the Crimean Peninsula: a prospective economic assessment of

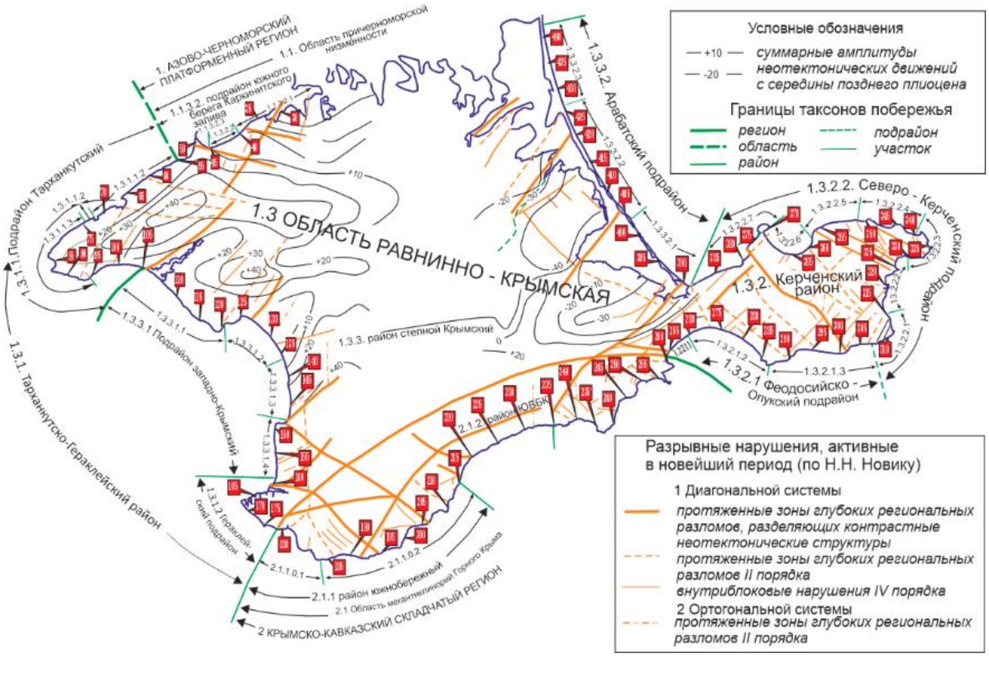

F i g . 1 . Schematic typology zoning of the coast of Crimea (delineation 2025). The full-scale figure is available at: https://ecological-safety.ru/repository/issues/2026/02/01/Fig.1.png (in Russian) the territory; information on the population, the development of the resort and recreational infrastructure, and road construction; an assessment of agricultural land; a description of coastal protection measures; and a natural and climate assessment of the coastline.

General engineering-geological parameters are also provided: the grain-size distribution of sandy beach deposits; the mineral composition of beach deposits; the erosion resistance of rocks; and tectonic processes.

The work on compiling the cadastre was completed during the Soviet Union's collapse; consequently, with a few exceptions, the findings were not incorporated into academic discourse. Of course, it is difficult to describe this work as a fully-featured cadastre, not least because it was not officially recognised by state bodies as a guide to action. Another shortcoming is the lack of in-depth analysis of socio-economic issues.

Following the dissolution of the IMR in 2012, its entire archive – including materials relating to the cadastral survey of Crimea carried out between 1986 and 1988 – was transferred to Kiev. Only a poor-quality photocopy of the report survived, which made it virtually impossible to work with it properly. An analysis of this material revealed that converting it into electronic format would be extremely labour-intensive: it would require retyping the text and redrawing the graphical elements in the appropriate software.

The recent digitisation of the report at Marine Hydrophysical Institute. Between 2024 and 2025, this work was carried out using computer technologies, including the GIS technology. We would like to highlight a few points. The geographical location of the observation points in the original was presented in two formats: cartographic and tabular. However, in the cartographic version, the locations of the points were indicated at intervals of five numbers. The tabular version listed the locations of 269 points, that is, approximately every second one. Furthermore, some of these points were repeated in both versions and were situated quite close together on the map, to the extent that they almost coincided. In addition, it was necessary to take into account that the points on the original diagrams were plotted on a hand-drawn sea boundary, and the accuracy of their positions was questionable.

In contrast, the positions of points in the tables were given relative to reference points, for example, "7 km west of the village of Ishuni" or "2 km east of the town of Atlesh". In such cases, the question arose as to whether the measurement was taken from the boundary of the reference point or from its centre, and what measuring instruments were used. It was subsequently agreed that, where a direction from a feature was specified, the measurement was taken from the boundary of that feature corresponding to that direction; where no direction was specified, the point was located at its centre. In all cases, the points were aligned with the position of the modern coastline, as it is difficult to assess the accuracy of the 1986 coastline delineation; according to our visual assessments, it is extremely low. This is clearly visible on the black-and-white overlays, where the points, converted to GIS format, are shown on the map (Fig. 2).

At the same time, the boundaries of coastal settlements were adjusted and their official names were entered into the system, bringing the total number of digitised settlements in the coastal zone to 353. In addition to this, the linear boundaries

Fig. 2. Location of marked points of the inventory on a modern map of Crimea (black lines with dots represent original fragments of the diagram). The full-scale figure is available at: https://ecological-safety.ru/repository/issues/2026/02/01/Fig.2.png (in Russian)

of cadastral units (regions, provinces, districts, sub-districts and coastal zone sections) and the boundaries of faults were digitised, as well as the total amplitudes of neotectonic movements. The geographical features of all the diagrams and their attribute data were also converted into GIS formats. Moving beyond the work on the text (which mainly involved formatting and organising hyperlinks in HTM format) we would simply note that the total number of pages, comprising 459 figures and 9 tables, amounted to 136. Furthermore, all graphic images (345 in total) were redrawn in colour (unlike the originals), which improved their visual appeal. All 150 photographs were processed to improve image quality using the PhotoVintage software, which employs artificial intelligence algorithms. Most were successfully converted to colour, which not only significantly improved the visual representation of the terrain but also eliminated numerous defects such as scratches and other imperfections.

As the main user interface, we used a representation of the cadastre as a zoomable map with content panels on the left and a display of selected cartographic features on the right (Fig. 3).

The visual representation of the map is based on the display of cadastral data against a background of nine base vector layers (ESRI shapefiles) [11)].

All numerical data associated with geographical features are loaded into the relevant attribute tables and can be accessed by clicking on the feature on the map.

[11)] ESRI, 1998. *ESRI Shapefile Technical Description. An ESRI White Paper*. 34 p.

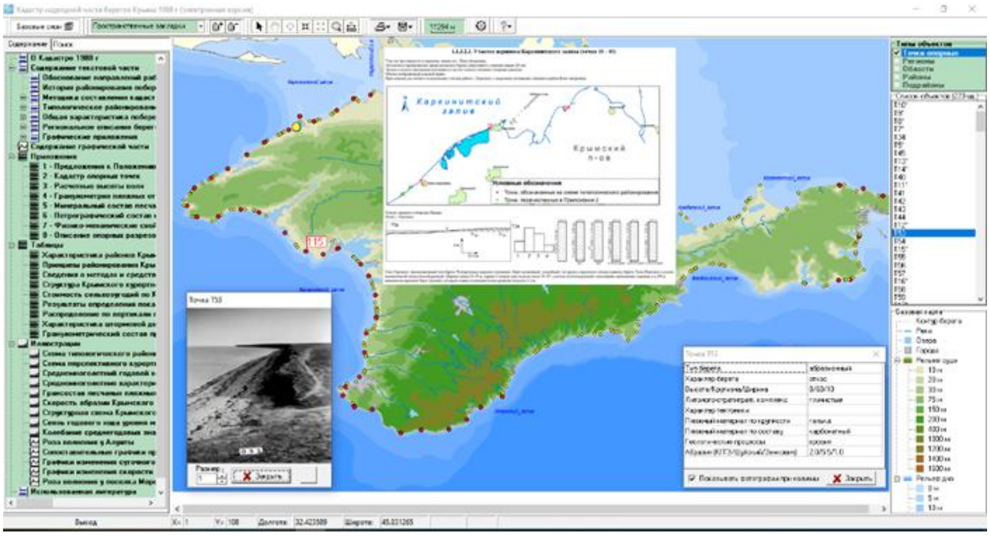

F i g . 3 . The user graphical interface of the GIS Cadastre of the Coast of Crimea, 1988. The full-scale figure is available at: https://ecological-safety.ru/repository/issues/2026/02/01/Fig.3.png (in Russian)

Text blocks containing tabular and graphical data are formatted in HTM and contain a large number of hyperlinks, both within the page (navigation between points on the section) and between pages of general content (see insets in Fig. 3).

We have therefore created the GIS Crimean Coastline Cadastre, 1988, which has enabled us to preserve this vital work for future researchers, make it user-friendly and enhance its accessibility.

Work on the creation of a cadastre of the Crimean coastline in the 21st century. Since the beginning of the 21st century, the issue of creating a cadastre of the Crimean coastline has once again been the subject of discussion in academic and engineering circles. This was prompted by intensive construction in the coastal zone, which was not always legal. Human economic interests came into conflict with the natural evolution of coastal systems. Over considerable stretches, the coastline began to retreat, posing a threat to coastal infrastructure. A significant reduction in beach area and a deterioration in the composition of beach material diminished their recreational appeal.

During this period, papers were published by researchers at Taurida University and Marine Hydrophysical Institute, focusing on the development of the regulatory, informational and methodological framework [2)] for the Crimean coastline cadastre [5–7]. Paper [5] examines models of a coastal zone cadastre and the structure of the geographical information used in such a cadastre; it discusses issues relating to the selection of coastal zone boundaries, the scope of the study, the constituent components of the cadastre (geological-geomorphological, administrative-economic, socio-economic) and the implementation of GIS packages. Going beyond purely theoretical issues, the authors of [4] examine practical aspects of creating the cadastre and the methodology for its compilation. A notable outcome of this work is the certificate of state registration issued for the coastal cadastre database [2)].

Paper [7] proposes a methodology for comprehensive assessment of beaches as recreational objects, encompassing their geomorphological, economic and social components. It is based on algorithms to jointly analyse a large set of parameters and compute certain integral indices. These indices will are expected to enable objective assessment of beach condition, dynamics and development prospects and to support targeted measures to improve recreational comfort and service quality.

As regards the future content of the Crimean coastal cadastre, a large number of publications have appeared over the last 25 years, providing information on individual sections of the coastal zone. It is not possible to provide a complete bibliography here. A significant proportion of these are available at: https://www.coast-crimea.ru/. Of particular note are the comprehensive studies [21–23], which provide information on the entire Crimean coast; these publications contain various cartographic materials and a large number of photographs.

Of note, in the absence of a cadastre of the Crimean coastline and given the real need for one, municipal authorities are themselves creating something akin to a cadastre. These include, for example, lists of beaches with their characteristics in Evpatoria, Sevastopol and Feodosia. There is, in fact, a cadastre (scientific reference guide) of Crimea's marine protected areas [12)], and a cadastre of the Republic of Crimea's coastal lakes [13)]. Details of approximately half of the hydraulic structures along the Crimean coast (particularly on the Southern Coast of Crimea) are recorded in the Russian Register of Hydraulic Structures (available at: http://waterinfo.ru/gts/index.php). This costly work is ongoing.

Over the past 10 years, surveys have been carried out along many stretches of the Crimean coastline for various types of construction work; however, the survey data are generally not accessible to a wide range of researchers. This significantly slows down the process of populating the cadastre with specific information.

At present, it is clear that, despite numerous meetings, conferences and discussions with senior officials of the Republic of Crimea, the creation of a comprehensive cadastre of Crimea's coastline remains in doubt.

It is fair to say that following a meeting between scientists from Marine Hydrophysical Institute of RAS and the Governor of Sevastopol, work in this area was initiated. Commissioned by the Department of Natural Resources and Ecology of the City of Sevastopol (Sevprirodnadzor), engineering-geodetic, morpholythodynamic, engineering-geological, geophysical and environmental surveys were carried out in the coastal zone stretching from Cape Lukul to Cape Karantinny (24 km), engineering-geodetic, morpholithodynamic, engineering-geological, geophysical,

---

[12)] Milchakova, N.A., ed., 2015. [*Marine Protected Areas of Crimea. Scientific Reference Book*]. Sevastopol, Simferopol: N. Orianda, 300 p. (in Russian).

[13)] Vasenko, V.I., Gulov, O.A., Chaban, V.V. et al., 2017. [S*cientific and Practical Report: Cadastral Register of Coastal Lakes in the Republic of Crimea. Types of their Economic Use (as at 1 January 2017)*]. Saki: Fondy GUNPP RK Krymskaya GGRES, 36 p. (in Russian).

environmental and hydrometeorological surveys were carried out. The work was carried out in 2021–2022; the cost of the work amounted to approximately 75 million roubles. As a result, a virtually complete set of data was obtained, necessary for compiling a cadastral register for this part of the coastline.

Marine Hydrophysical Institute of RAS is currently developing a software and information framework for cadastral valuation of recreational and coastal zones along the Crimean coast, and is populating individual subject-specific catalogues with data. To enable comparison of changes over time, the structure of the system will be similar to that of the "1988 Crimean Coast Cadastre" GIS described above. In addition to traditional data, information obtained using modern technologies will be included, i. e. satellite imagery, orthophotos captured by UAVs, results of mathematical modelling of lithodynamics, and so on.

The software and information framework can be used as a basis for creating a comprehensive cadastre of the Crimean coastline. This will require the joint efforts of all relevant organisations.

Conclusion

In our view, the creation of a Crimean coastal cadastre is of significant scientific importance, as it allows the systematisation, analysis and synthesis of data on the state, morphology and dynamics of the peninsula's coastal zone. The cadastre serves as the basis for:

– developing scientifically based methods for monitoring and managing coastal processes;

– studying the patterns of interaction between natural and anthropogenic factors affecting coastal stability;

– modelling erosion, accumulation and transformation of coasts under the influence of hydrometeorological, tectonic and anthropogenic factors;

– creating geoinformation databases necessary for comprehensive geoecological and geomorphological studies.

Thus, the Crimean coastal cadastre should contribute to deepening scientific understanding of the functioning of coastal geosystems and to forming a basis for long-term forecasting of changes in the coastal zone.

From an applied outlook, the Crimean coastal cadastre has high practical significance for economic development and rational nature management. Its use enables:

– assessing the current state of the shoreline;

– justifying engineering protection measures;

– supporting management decisions in planning infrastructure, construction of ports, resort and recreational facilities;

– performing cadastral and environmental monitoring of coastal areas;

– developing the legal and regulatory framework for regulating nature management in the coastal zone.

Furthermore, the cadastre serves as a tool for mitigating natural and man-made risks and contributes to the sustainable development of the coastal regions of Crimea.

REFERENCES

1. Zenkovich, V.P., 1954. [A Coastal Cadastre of Seas of the USSR]. *Trudy Instituta Okeanologii AN SSSR*, 10, pp. 35–43 (in Russian).
2. Longinov, V.V., 1954. [On Compiling a Marine Coastal Cadastre]. *Trudy Instituta Okeanologii AN SSSR*, 10, pp. 44–50 (in Russian).
3. Gogoberidze, G.G., Kosyan, R.D., Ogorodov, S.A., Chubarenko, B.V., Burnashov, E.M. and Rumiantceva, E.A., 2024. Coastal Cadastre of the Russian Federation: Basis, Problems, Prospects. *Journal of Oceanological Research*, 52(2), pp. 183–205. https://doi.org/10.29006/1564-2291.JOR-2024.52(2).10 (in Russian).
4. Mykhailov, V.A., 2011. Applied Aspects of Creation of Coast Cadastre of the Sivash. *Scientific Notes of Tavrida National V.I. Vernadsky University. Geography*, 24(1), pp. 84–88 (in Russian).
5. Skrebets, G.N. and Mykhailov, V.A., 2013. Geographical Principle in the Informative Filling of Cadastre of Sea-Coasts. *Scientific Notes of Tavrida National V.I. Vernadsky University. Geography*, 26(2), pp. 90–96 (in Russian).
6. Orlova, M.S., Dolotov, V.V. and Ivanov, V.A., 2006. [Development of a Cadastral Valuation of Beaches: The Case of the Crimean Coast]. [*Proceedings of the International Conference Latvia–Europe, Europe–Latvia*]. Rēzekne, Latvia, pp. 103–104 (in Russian).
7. Dolotov, V.V., Amosha, A.I., Ivanov, V.A. and Salomatina, L.N., 2006. Main Regulations of Beach's Cadastre Evaluation. *Ecological Safety of Coastal and Shelf Zones and Comprehensive Use of Shelf Resources*, 14, pp. 147–156 (in Russian).
8. Fomin, V.V. and Goryachkin, Yu.N., 2022. Accounting for the Local Wave and Morphodynamic Processes in Coastal Hydraulic Engineering. *Physical Oceanography*, 29(3), pp. 271–290.
9. Kharitonova, L.V., Lazorenko, D.I., Alekseev, D.V. and Fomin, V.V., 2024. Modeling of Artificial Beach Morphodynamics in the Koktebel Village Coastal Zone (Crimea) under the Storm Wave Impact. *Ecological Safety of Coastal and Shelf Zones of Sea*, (3), pp. 93–109.
10. Gogoberidze, G.G., Spiridonov, M.A., Ryabchuk, D.V., Zhamoida, V.A. and Lednova, Yu.A., 2012. Concept of Development of State Cadastre of Marine Coastal Zone of the Russian Federation. *National Interests: Priorities and Security*, 8(27), pp. 2–11 (in Russian).
11. Zenkovich, V.P., 1990. [A Cadastre and Monitoring of the Coastal Area of the Seas of USSR]. In: A. P. Alkhimenko, ed., 1990. [*Geoecology of the World Ocean: Proceedings of the 9th Congress of the Geographic Society of the USSR*]. Leningrad, pp. 120–122 (in Russian).
12. Shurygin, A.G. and Spiridonov, M.A., 1998. [Methodological Recommendations on Compiling a Cadastre of Marine Coasts]. In: VSEGEI, 1998. *Izvestiya VSEGEI*. Saint Petersburg: Izd-vo VSEGEI, pp. 75–76 (in Russian).
13. Viktorov, S.V., Kil'dyushevsky, E.I., Kirsanov, A.A. and Pertsov, A.V., 1999. On the Inventory of Sea Shores. *Otechestvennaya Geologiya*, (6), pp. 77–78 (in Russian).
14. Mayorov, I.S., 2007. [Cadastral Valuations of the Coastal Zone of Russia's Far Eastern Seas]. *Geografiya i Prirodnye Resursy*, (2), pp. 139–143 (in Russian).
15. Rumiantceva, E.A. and Gogoberidze, G.G., 2020. [Automated Information and Analysis System (GIS application) for the Cadastral Register of the Coastal Zone of the Arctic Seas of the Russian Federation]. In: IPMech RAS, 2020. *Waves and Vortices in Complex Media: Proceedings of the 11-th International Conference – Scientific School of Young Scientists (Moscow, December 01–03, 2020)*. Moscow: ISPO-Print, pp. 53–56 (in Russian).

16. Gogoberidze, G.G. and Rumiantceva, E.A., 2020. [A Comprehensive Analysis of the Socio-Economic Situation and Development Trends in the Arctic Coastal Regions of the Russian Federation]. In: G. G. Gogoberidze, ed., 2020. [*Developing Arctics*]. Murmansk: MAGU, pp. 27–54 (in Russian).
17. Gogoberidze, G.G., Levkevich, V.E., Rumiantceva, E.A. and Sergievich, T.V., 2021. Indicator Approach for Analysis of the Socio-Economic State and Development Trends of the Arctic Coastal Regions. *Ekonomicheskaya Nauka Segodnya*, 14, pp. 87–100 (in Russian).
18. Gogoberidze, G.G., Kosyan, R.D. and Rumiantceva, E.A., 2020. Method for Comprehensive Assessment of the Stability of Coastal Eco-Socio-Economic Systems on the Indicator Approach. *Ecological Safety of Coastal and Shelf Zones of Sea*, (3), pp. 122–141. https://doi.org/10.22449/2413-5577-2020-3-122-141 (in Russian).
19. Gogoberidze, G.G., Rumiantceva, E.A. and Kosyan, R.D., 2022. Criterion-Statistical Assessment of the Sustainability of Black Sea Local Coastal Eco-Socio-Economic Systems of the Krasnodar Krai. *Ecological Safety of Coastal and Shelf Zones of Sea*, (1), pp. 113–131. https://doi.org/10.22449/2413-5577-2022-1-113-131
20. MIREA, 2022. [*Russia in the UN Decade of Ocean Science: Proceedings of The First All-Russian Conference with International Participation "Russia in the UN Decade of Ocean Science"*]. Moscow: MIREA, 280 p. (in Russian).
21. Goryachkin, Yu.N., Kosyan, R.D. and Krylenko, V.V., 2018. A Comprehensive Assessment of the Crimea West Coast. *Ecological Safety of Coastal and Shelf Zones of Sea*, (3), pp. 41–55. https://doi.org/10.22449/2413-5577-2018-3-41-55 (in Russian).
22. Goryachkin, Yu.N., ed., 2015. *The Current State of the Coastal Zone of Crimea*. Sevastopol: ECOSI-Gidrofizika, 252 p. (in Russian).
23. Goryachkin, Yu.N. and Dolotov, V.V., 2019. *Sea Coasts of Crimea*. Sevastopol: Colorit, 256 p. (in Russian).

Submitted 03.02.2026; accepted after review 25.02.2026;
revised 19.03.2026; published 30.06.2026

About the authors:

Yuri N. Goryachkin, Chief Researcher, Marine Hydrophysical Institute of RAS (2 Kapitanskaya St., Sevastopol, 299011, Russia), DSc (Geogr.), **ORCID ID: 0000-0002-2807-201X, ResearcherID: I-3062-2015**, *yngor@mhi-ras.ru*

Vyacheslav V. Dolotov, Senior Researcher, Marine Hydrophysical Institute of RAS (2 Kapitanskaya St., Sevastopol, 299011, Russia), PhD (Chem.), **ORCID ID: 0000-0002-1485-2883, ResearcherID: E-5570-2016**, *dolotov_v_v@mhi-ras.ru*

Olga S. Romanyuk, Leading Researcher, Institute of Mineral Resources, Simferopol (1962–2010)

Contribution of the authors:

Yuri N. Goryachkin – problem statement, reviewing and analysing literary and archival sources, preparation of the article

Vyacheslav V. Dolotov – digitisation of the 1988 cadastre, preparation of the article

Olga S. Romanyuk – cadastre development in 1988

All the authors have read and approved the final manuscript.

Original paper

Landscapes of the Coastal Zone of Cape Khako (Abrau Peninsula, Black Sea)

V. V. Solyannikov

Saint Petersburg Branch of the Russian Federal Research Institute of Fisheries and Oceanography ("GosNIORKH" named after L. S. Berg), Saint Petersburg, Russia

e-mail: lacrimas.777@mail.ru

Abstract

The Black Sea coast of the North-Western Caucasus is a key biodiversity hotspot; however, its landscapes are experiencing increasing anthropogenic pressure. Cape Khako, located within the Abrausky State Nature Sanctuary, represents a unique model site for studying the interaction of geomorphological processes and vegetation cover in the coastal zone. The paper aims at a comprehensive analysis of the landscape structure of the coastal zone at Cape Khako, including an examination of its geomorphological structure and the spatial distribution of terrestrial and benthic vegetation, as well as an assessment of the current state of the ecosystems. The study was conducted using landscape-ecological profiling, geobotanical and hydrobiological descriptions, interpretation of satellite imagery and geoinformation mapping. For the first time for this territory, a large-scale geomorphological map has been compiled, and the spatial organization of terrestrial and benthic phytocenoses has been detailed. The study shows that the landscape structure is characterized by the dominance of abrasion-denudation cliffs, complicated by active gravitational processes (landslides, rockfalls), which determines the mosaic pattern of ecotopes. A clear zonation of vegetation was revealed: from shiblyak (deciduous shrubland) and relict krummholz stands of *Pinus pityusa* on upland plains to upland xerophytic communities on steep slopes, which host a number of protected and endemic species. It is shown that in the coastal waters, the distribution of benthic phytocenoses is strictly governed by the geomorphology of the underwater coastal slope. Signs of anthropogenic ecosystem degradation were identified: pyrogenic transformation of vegetation over part of the territory and the emergence of algocenoses dominated by genera *Ulva* and *Ectocarpus* as indicators of the initial stage of eutrophication. The obtained results underscore the high vulnerability of this unique landscape complex and the necessity of applying a systemic approach to its conservation, considering not only the preservation of individual species but also the integrity of the entire system of interconnected geomorphological and biotic processes.

Keywords: cliffs, benthic vegetation, petrophytes, Black Sea, Abrau Peninsula, nature sanctuary

For citation: Solyannikov, V.V., 2026. Landscapes of the Coastal Zone of Cape Khako (Abrau Peninsula, Black Sea). *Ecological Safety of Coastal and Shelf Zones of Sea*, (2), pp. 26–42.

© Solyannikov V. V., 2026

This work is licensed under a Creative Commons Attribution-Non Commercial 4.0 International (CC BY-NC 4.0) License

Ландшафты береговой зоны мыса Хако (полуостров Абрау, Черное море)

В. В. Солянников

Санкт-Петербургский филиал ФГБНУ «Всероссийский научно-исследовательский институт рыбного хозяйства и океанографии» («ГосНИОРХ» им. Л. С. Берга»), Санкт-Петербург, Россия

e-mail: lacrimas.777@mail.ru

Аннотация

Черноморское побережье Северо-Западного Кавказа является ключевым центром биоразнообразия, однако его ландшафты испытывают растущую антропогенную нагрузку. Мыс Хако, расположенный в границах природного заказника «Абраусский», представляет собой уникальный модельный объект для изучения взаимодействия геоморфологических процессов и растительного покрова в условиях прибрежной зоны. Цель работы – комплексный анализ ландшафтной структуры береговой зоны мыса Хако, включающий изучение геоморфологического строения, пространственной организации наземной и донной растительности, а также оценку современного состояния экосистем. Исследование выполнено на основе ландшафтно-экологического профилирования, геоботанических и гидробиологических описаний, дешифрирования космических снимков и геоинформационного картографирования. Впервые для этой территории составлена крупномасштабная геоморфологическая карта и детализирована пространственная организация наземных и донных фитоценозов. Установлено, что ландшафтная структура характеризуется доминированием абразионно-денудационных клифов, осложненных активными гравитационными процессами (оползни, обвалы), что определяет мозаичность экотопов. Выявлена четкая зональность растительности: от шибляков и реликтовых криволесий сосны пицундской на плакорах до нагорно-ксерофитных группировок на крутых склонах, в составе которых отмечено значительное число охраняемых и эндемичных видов. Показано, что в прибрежной зоне распределение донных фитоценозов строго подчинено геоморфологии подводного берегового склона. Выявлены признаки антропогенной деградации экосистем: пирогенная трансформация растительности на части территории и появление альгоценозов с доминированием родов *Ulva* и *Ectocarpus* как индикаторов начальной стадии эвтрофикации. Полученные результаты подчеркивают высокую уязвимость этого уникального ландшафтного комплекса и необходимость применения системного подхода к его охране, учитывающего не только сохранение отдельных видов, но и целостность всей системы взаимосвязанных геоморфологических и биотических процессов.

Ключевые слова: клифы, донная растительность, петрофиты, Черное море, полуостров Абрау, природный заповедник

Для цитирования: *Солянников В. В.* Ландшафты береговой зоны мыса Хако (полуостров Абрау, Черное море) // Экологическая безопасность прибрежной и шельфовой зон моря. № 2. С. 26–42. EDN RHZBCT.

Introduction

The Black Sea coast, particularly within the North-wWestern Caucasus, is recognised as one of the key biodiversity centres at the boundary between Europe and Asia. A complex combination of the Greater Caucasus mountain landscapes and the marine area creates unique conditions for high levels of endemism and the preservation of Tertiary relicts [1, 2]. Coastal terrestrial-aquatic complexes act here as critically important ecotones – transition zones where intense interaction between marine and terrestrial ecosystems occurs, determining their stability and biodiversity.

Despite their ecological value, these landscapes are experiencing increasing anthropogenic pressure associated with recreational activities, urbanisation, and climate change. This leads to habitat fragmentation, degradation of vegetation cover, and disruption of natural geomorphological processes [3, 4]. Under such conditions, specially protected natural areas (SPNAs), such as the Abrausky State Nature Sanctuary, which includes Cape Khako, gain particular significance as refugia for maintaining the populations of rare and endangered species.

Cape Khako is located in the north-western part of the Black Sea coast of the Abrau Peninsula and lies within the boundaries of the Abrausky State Nature Sanctuary. The cape itself represents a morphological structure with a relict abrasion cliff, adjacent to an accumulative terrace. As a continuation of Mount Koldun (the summit of the Navagirsky Ridge), the cape belongs to the Greater Caucasus mountain system. Stratigraphically, the territory is formed by Cretaceous deposits. The coast is represented by the Myskhako suite (K_2m_1ms) and consists predominantly of dark flysch, including clay shales and friable marls that are most susceptible to weathering. The boundary between dark and light flysch passes through this area [5]. The territory is characterised by modern relief-forming processes, primarily of exogenous origin. Along the coastal zone, ancient landforms of abrasion and seismic origin are noted. The combination of active geodynamics, diverse ecotopes, and a Mediterranean-type climate has formed a mosaic of unique plant communities: from relict mixed forests and juniper woodlands to petrophytic mountain-xerophytic communities that include numerous endemic and protected species.

Analysis of published data shows that research on the peninsula is predominantly concentrated within the Utrish Nature Reserve [6, 7], which has a higher conservation status, whereas the Abrausky State Nature Sanctuary, including Cape Khako, remains significantly less studied. Existing works are either of a general nature or focus on individual components of the flora, while comprehensive studies integrating geomorphological and geobotanical approaches in this territory are almost absent. This gap prevents the development of effective measures for the conservation and management of this unique natural complex.

The purpose of this study is to conduct a comprehensive analysis of the landscape structure of the coastal zone of Cape Khako, including detailed geomorphological characterisation, description of the spatial organisation of terrestrial and benthic vegetation, and assessment of the current state of the cape's ecosystems under the influence of natural and anthropogenic factors.

Materials and methods

Comprehensive field studies were carried out in July–August of 2023–2025 and included landscape-ecological profiling, geobotanical and hydrobiological descriptions. The structure of the coastal zone and long-term shoreline dynamics were analysed using interpretation of multi-temporal satellite imagery (Landsat) and route-based field observations. Landscape profiles (transects) were established perpendicular to the shoreline, covering key geomorphological elements of the cape. A set of procedures was performed along the transects: relief parameters (elevation, aspect, slope) and underlying rocks were recorded, and sampling plots for detailed geobotanical descriptions of vegetation cover were established. To create a large-scale (1:5000) geomorphological map with identification of genetic relief types and modern processes, we used the QGIS 3.0.4 software package. The coordinates of observation points were recorded using a GPS receiver (GPS Fields Area Measure). Petrophytic vegetation was described on cliff tops and at their bases. The terrestrial area was divided into plots using a 1 × 1 m frame, and the projective cover of each species was recorded. Marine vegetation was studied according to standard methods [8] using a 0.5 × 0.5 m sampling frame. Benthic phytocenoses were distinguished according to the dominant-based classification by A. A. Kalugina-Gutnik [1)]. Species nomenclature followed current taxonomy: World Register of Marine Species (Available at: https://www.marinespecies.org) – for algae, and Plants of the World Online (Available at: https://powo.science.kew.org) – for vascular plants.

Results and discussion

The geomorphological coast type in the study area is defined as abrasion-accumulative, with a clear predominance of denudation processes on land and active interaction between abrasion and accumulation in the coastal zone (Fig. 1). The diversity of geodynamic processes affecting the contact zone determines the variability of cliff typology. Along the entire cape, three types of cliffs were identified: a cliff with a predominance of abrasion reworking at the base, an abrasion-denudation cliff with widespread development of scree processes, and an abrasion-denudation cliff with widespread development of landslides. At the base of the first type of cliff, forms of wave reworking (a bench and its ridges) are developed.

[1)] Kalugina-Gutnik, A. A., 1975. [*Phytobenthos of the Black Sea*]. Kyiv: Naukova Dumka, 247 p. (in Russian).

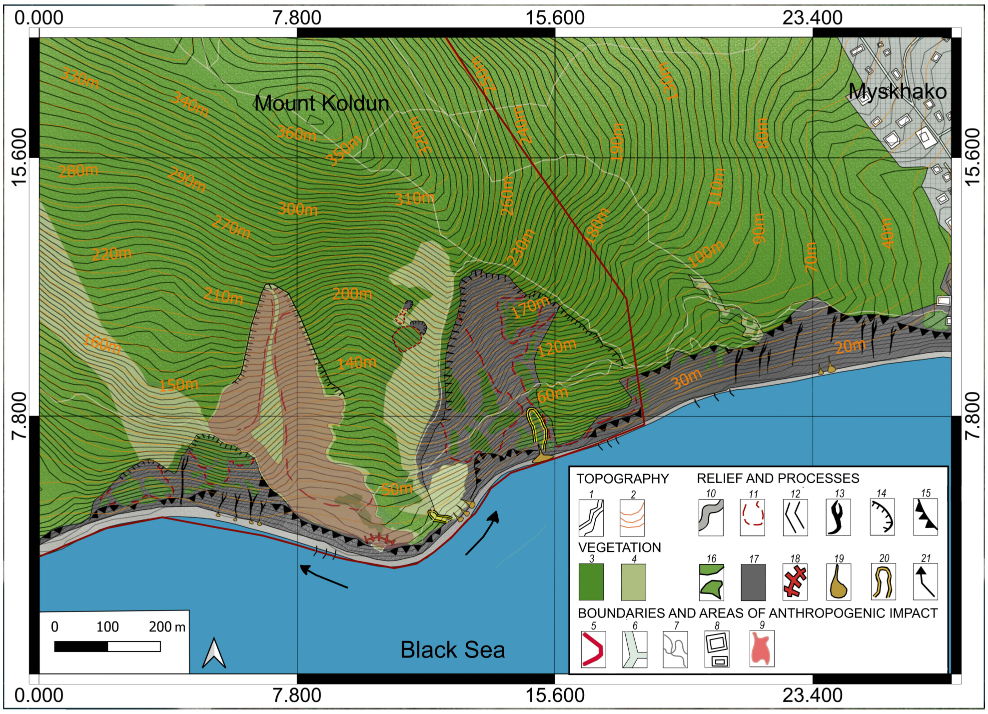

F i g . 1 . Relief features of the coastal zone of Cape Khako. Legend: *1* – contour lines; *2* – spot heights, m; *3* – forest vegetation; *4* – herbaceous vegetation; *5* – protected area boundary; *6* – roads; *7* – informal trails; *8* – cadastral parcels; *9* – post-fire affected areas; *10* – accumulation terrace; *11* – landslide body; *12* – bench ridges; *13* – karren; *14* – landslide head scarp; *15* – abrasional shore; *16* – erosional rock remnant; *17* – cliff face; *18* – lateral detachment crack; *19* – talus (scree); *20* – gully; *21* – direction of alongshore sediment transport

The coastline of the North-Western Caucasus, characterised by alternating capes and bays [9], is of ingressive origin. The formation of such relief is associated with repeated Quaternary transgressions of the Black Sea, which led to the flooding of depressions in the dissected mountain massif and intense abrasion of the most vulnerable areas. Abrasion processes and climatic factors contributing to rock destruction and physical weathering have a significant influence on shoreline straightening [10].

Despite the active straightening typical of flysch shores of the Novorossiysk floristic region, Cape Khako retains its outline and is one of the most stable elements of the bay coast. The relative stability of the cape is explained not only by its structural position but also by active compensatory processes. As part of the mountain massif, the cape receives a constant supply of clastic material as a result of landslide, rockfall and scree, and other slope processes. This constant source of sedimentary material counteracts wave action, compensating for erosion and slowing shoreline straightening.

Abrasion-accumulative processes

The coast in the study area is represented by a relict cliff: its height on the projecting part of the cape is 20–25 m, while on the side walls it reaches 100 m. The absence of active wave-cut niches and the presence of scree and rockfall material at the cliff base indicate the transition of the cliff to a stage of denudation reworking. The overall slope of the drying zone is gentle. According to the E.V. Guryanova scale [11], the wave regime is characterised as almost constant surf (degree II of surf intensity).

Extreme storm events are a key factor in current coastal dynamics. Thus, at the end of December 2023, with wind speeds of 12–17 m/s and wave heights up to 3 m, beach erosion and renewed mechanical abrasion were recorded. Only the lower part of the coastal scarp up to the maximum splash level was abraded. This event activated gravitational processes in the upper part of the slope. However, by June 2024, the beach strip had fully recovered naturally, demonstrating the cyclic nature and reversibility of accumulative processes under this geomorphological regime. The exposed ridges of the underwater bench, forming the ridge-bench landscape, are subject to constant abrasion.

Accumulative landforms are represented by pocket beaches formed in the wave-shadow zone of the cape, where sediment transport is interrupted and local accumulation occurs during alongshore transport. The base of the accumulative terrace consists of large pebbles and boulders. Coastal ridges oriented seawards form from one to three distinct steps. Colluvial deposits, represented by blocks, rubble, and grus, are widely developed at the cliff base as a result of active denudation processes.

Suffosion-karst and slope water-erosion processes

A significant portion of the North-Western Caucasus coastline is occupied by the Upper Cretaceous flysch complex [12]. The flysch layers forming the cape have both parallel and angular orientations. They are dominated by grey platy argillite and friable limestone. These carbonate rocks are subject to karst processes that actively transform the cliff relief. The most common forms are karren – shallow fissures formed by temporary watercourses flowing down the slopes of Mount Koldun. Groundwater outlets are noted at the base of the cliffs, enhancing carbonate dissolution and the removal of fine-grained material.

The central part of Cape Khako is dissected by a shallow gully that developed along a local relief depression (drainage hollow). The formation and further development of the gully are due to the transversely concave profile of the slopes.

During periods of intense precipitation, temporary watercourses (rain runoff) form here, causing linear and sheet erosion. In the lower part of the gully and at the base of the cape, microrelief smoothing and the formation of a gently sloping plateau-like surface are observed. Similar manifestations of slope moistening and surface runoff are also noted in the cliff-edge zone, where they weaken the rock mass and contribute to crack development.

The combination of suffosion-karst processes, groundwater filtration, and water erosion in the cliff-edge zone contributed to the formation and expansion of a lateral detachment crack. By January 2018, a fragment of the bedrock coast had separated from the base of the cape along this crack, forming an erosional remnant (Fig. 2). Further undercutting led to its final separation in 2019.

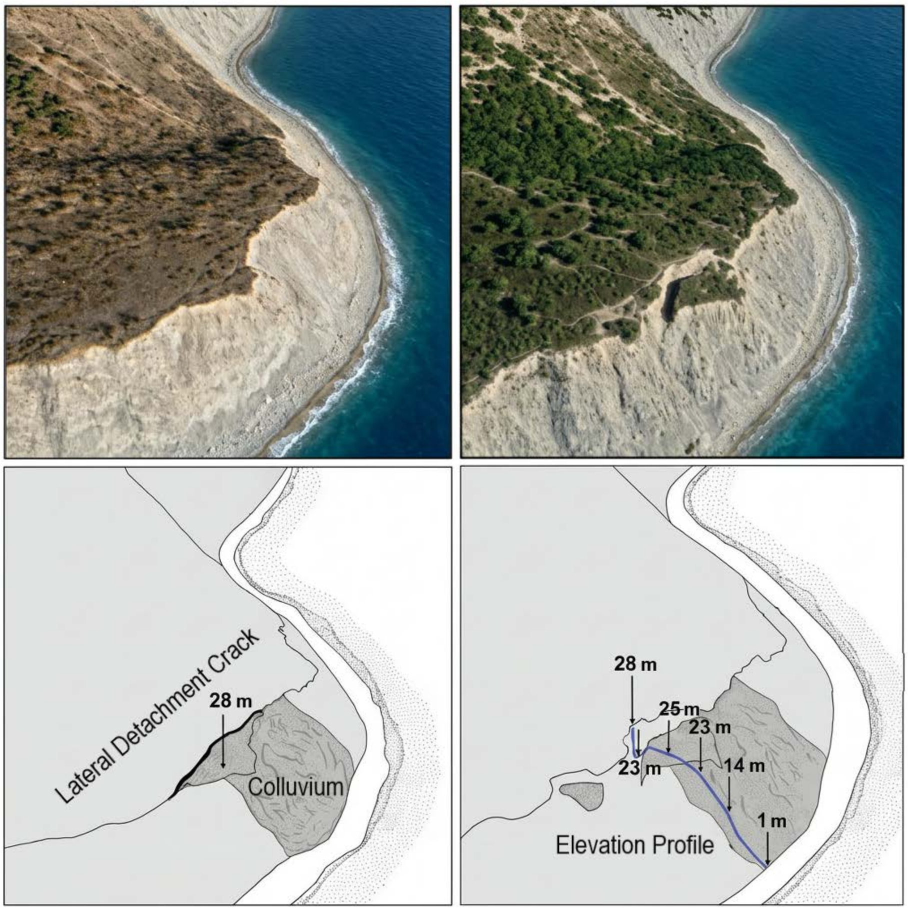

a ***b***

F i g . 2 . Erosional rock remnant at the edge of Cape Khako: *a* – December 2018; *b* – September 2021. Adopted from Google Maps (Available at: https://www.google.ru/maps)

The most important consequence of suffosion-karst processes is the formation of biofilms on cliff surfaces under conditions of constant capillary moistening and shading. The color of these formations varies from brownish-ochre to green. Microscopic analysis revealed the presence of diatoms (Bacillariophyta) – *Navicula* sp., charophytes (Charophyta) – *Mougeotia* sp., and cyanobacteria (Cyanobacteria) – *Chroococcus* sp. Such biofilms play a significant role in primary soil formation and biological weathering, representing an initial stage of successional processes on exposed substrates [13]. Biofilm development clearly demonstrates the close connection between abiotic and biotic processes in the coastal zone, emphasising the ecological significance of these biotopes.

Gravitational processes

Almost the entire cliff zone of the Abrau Peninsula is characterised by ancient landslide blocks [14], the formation of which is due to seismic effects on rocks in the past [15]. Unlike the nearby Cape Bolshoy Utrish, which is a tongue of an ancient landslide, Cape Khako is, in origin, a spur of Mount Koldun. However, sliding of the cape's side walls led to the formation of buttresses – steep projections of an ancient landslide cirque composed of undisturbed rocks. The detachment scarp of landslide masses is recorded at elevations of about 300 m on the southern slope of the Mount Koldun Ridge. Analysis of remote sensing data made it possible to record the activation of gravitational processes in August 2021, when two insequent landslides descended on the south-western slope at elevations of 190–210 m. Their trigger mechanism was likely the abnormally high precipitation (up to 200% of the monthly average) in Krasnodar Krai [2)] during this period [16].

Rockfalls and scree are widely developed at the cliff bases. Rockfalls form mainly under landslide blocks and are represented by blocks of more than 1 m in diameter. Scree occurs mainly on steep scarps in the eastern part and consists of coarse clastic material with an admixture of soil particles. The largest scree cone, with a slope angle of 30–35° and a length of up to 9 m, is noted under the gully in the southern part of the cape.

Vegetation

The vegetation cover of Cape Khako is characterised by pronounced mosaic structure, due to the combination of a complex geomorphological structure, diversity of ecotopes, and significant anthropogenic impact. The formation of plant communities occurs under the influence of specific ecological conditions of the coastal zone, including salinisation, aeolian processes, substrate characteristics, and the dynamics of slope processes. The flora of the cape has a distinctly Mediterranean character and belongs to the Novorossiysk floristic region of the Crimean-Novorossiysk

---

[2)] Ogureeva, G.N., 2013. [*Utrish State Nature Reserve. Atlas*]. Anapa: IP Gushcha E. V. Vol. 2, 88 p. (in Russian).

province. Spatial organisation of vegetation clearly demonstrates a regular succession of communities towards the sea, as reflected in the landscape profile (Fig. 3).

Tree and shrub vegetation

The best-preserved forest communities are distributed on levelled areas and cliff tops with developed rendzina soils. In the eastern part of the cape, juniper-hornbeam-oak shiblyak with *Pistacia mutica* is widespread, representing a variant of Eastern Mediterranean shiblyak typical of the Crimean-Novorossiysk province. The edificatory role in the tree layer is performed by *Quercus pubescens*, with co-dominants *Carpinus orientalis* and junipers (*Juniperus excelsa*, *J. oxycedrus*). *Juniperus foetidissima* and *P. mutica* also play a significant role in stand composition. The well-developed undergrowth is formed by characteristic species with Mediterranean ranges: *Lonicera etrusca*, *Paliurus spina-christi*, *Cotinus coggygria*, and *Jasminum fruticans* with abundant regeneration of *C. orientalis*. The herbaceous layer is distinguished by high floristic richness; the most typical and constant species are *Ruscus aculeatus*, *Agropyron pinifolium*, *Asparagus verticillatus*, *Veronica multifida*, and *Piptatherum holciforme*.

On ancient landslide blocks facing the sea, steep-slope formations of *Pinus pityusa* are formed. These areas are characterised by strong erosional dissection and slope angles of 15–30°. The stand is monodominant, with trunk deformation noted in the pines forming krummholz due to substrate instability and strong wind exposure. The undergrowth is very sparse, represented predominantly by regeneration of *P. pityusa* and *J. fruticans*; the community edges are bordered by *J. excelsa*. On open areas, xerophytic dwarf shrubs occur: *Ephedra distachya*, *Teucrium polium*, *Onosma taurica*, and *Euphorbia petrophila*. In spring (April–May), seasonal synusiae of the ephemeroid *Muscari neglectum* develop in the herbaceous layer.

The central part of the cape, dissected by an erosional gully, is occupied by oak-hornbeam shiblyak with an admixture of *P. pityusa*. Upslope towards the summit of Mount Koldun, the role of pine increases, and it acts here as a codominant. The shrub layer is formed predominantly by *J. fruticans*, *A. verticillatus*, and *Dictamnus albus* L. The herbaceous layer is dominated by *Piptatherum holciforme*, *Origanum vulgare*, *Stachys atherocalyx*, *Aegonychon purpureocaeruleum*, and *Scariola viminea*. The mosaic structure of the phytocenotic structure is manifested in gaps in the stand canopy, where specialised species develop: *Haplophyllum thesioides*, *Fibigia eriocarpa*, *Lomelosia micrantha*, and *Galium xeroticum*. An important phenological feature is the formation of seasonal synusiae of winter–spring ephemeroids *Scilla bifolia* and *Crocus reticulatus* in February.

On open slopes of south-western and south-eastern aspects bordering the gully, sparse shrub phytocenoses dominated by *Rhus coriaria* are concentrated. These communities represent a transition to mountain-xerophytic communities and are characterised by increased insolation and substrate drainage.

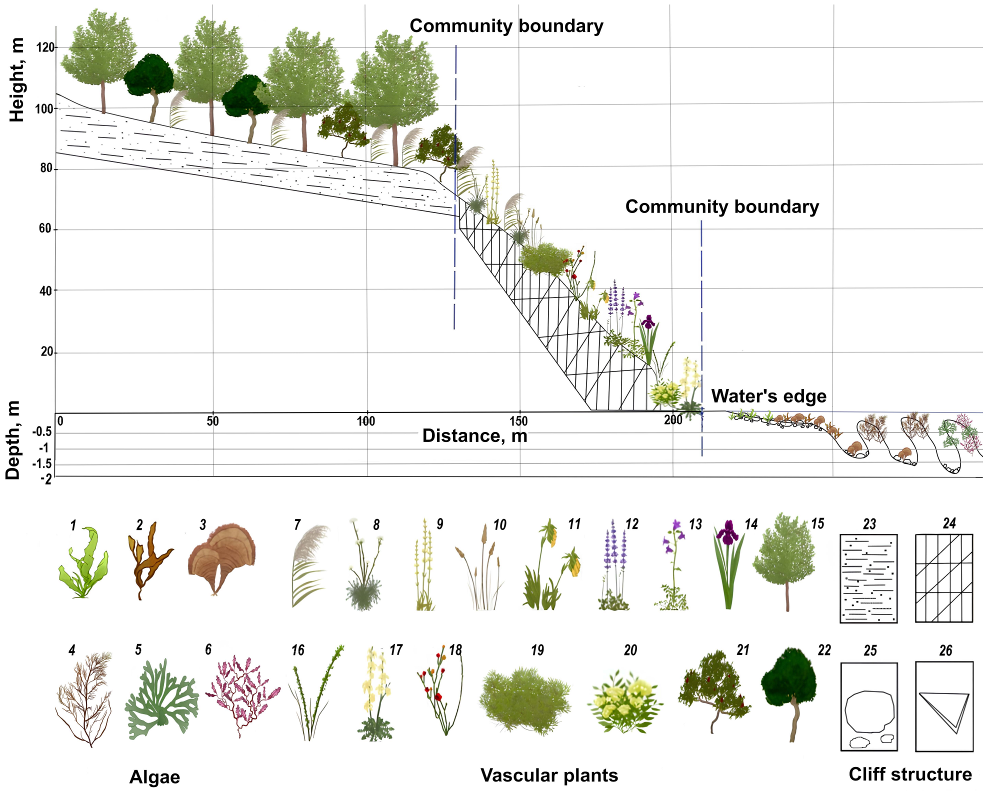

F i g . 3 . Landscape profile across the coastal zone in the area of Cape Khako. Legend: *1* – *Ulva compressa*, *2* – *Dictyota fasciola*, *3* – *Padina pavonica*, *4* – *Cystoseira sensu lato*, *5* – *Codium vermilara*, *6* – *Phyllophora crispa*, *7* – *Phragmites australis*, *8* – *Seseli ponticum*, *9* – *Sideritis taurica*, *10* – *Agropyron pinifolium*, *11* – *Onosma polyphylla*, *12* – *Salvia ringens*, *13* – *Campanula komarovii*, *14* – *Iris pumila*, *15* – *Pinus pityusa*, *16* – *Andrachne telephioides*, *17* – *Matthiola odoratissima*, *18* – *Ephedra distachya*, *19* – *Astracantha arnacantha*, *20* – *Euphorbia petrophila*, *21* – *Rhus coriaria*, *22* – *Juniperus excelsa, 23* – rendzinas, *24* – flysch, *25* – boulders and stones, *26* – bench. Vertically: the heights and depths are shown at different scales

Thus, the forest and shrub vegetation of Cape Khako forms a complex mosaic cover, the spatial organisation of which directly depends on the geomorphological structure of the territory, slope aspect, and associated microclimatic and edaphic conditions. The patterns identified confirm the role of the cape as a refugium for Mediterranean floristic complexes on the Black Sea coast of the Caucasus. Of particular importance is the fact that the core of these communities is formed by species listed in the Red Data Books at both the regional (*J. oxycedrus*, *J. excelsa*) and federal (*Pinus pityusa*) levels, as well as by a significant number of protected and endemic species in the herbaceous layer, emphasising the high conservation significance of these forest areas.

Mountain-xerophytic herbaceous-dwarf shrub communities

Steep slopes of different aspects and landslide body surfaces are occupied by phryganoid formations, representing modifications of classical Mediterranean vegetation types. Their formation is a direct consequence of historical connections between the Black and Mediterranean Seas. The dominance of cushion life forms and species with essential oils (family Lamiaceae) is typical. On open slopes of south-western and south-eastern aspects free of sumac thickets, tomillares dominated by *T. polium* and *Salvia ringens* develop. Total projective cover (TPC) varies from 30 to 50%. The floristic core of the community shows a high concentration of Crimean-Novorossiysk endemics – *Sideritis euxina* Juz., *Onosma taurica* Pall. ex. Willd, and *A. Pinifolium*.

On stabilised cliff edges at various elevations, mountain-xerophytic vegetation represented by phrygana is concentrated. The role of Lamiaceae decreases. The main background is formed by phytocenoses dominated by *E. distachya*, *Galatella villosa* (L.) Rchb. f., *T. polium, A. pinifolium*, *Hedysarum tauricum* Pall. ex Willd., *Jurinea stoechadifolia* (M. Bieb.) DC., *O. taurica* and *Artemisia caucasica* Willd. Their composition and structure are determined by substrate characteristics, slope angle, and slope processes. The most frequent variant is *A. pinifolium* + *J. stoechadifolia* + *E. distachya*. Under the most favourable ecotopic conditions on upland areas, average TPC values of herbaceous cover are close to 60–70%. In addition to the aforementioned codominants, accessory species of mountain-xerophytic communities include *Astragalus arnacantha* M. Bieb., *Astragalus subuliformis* DC., *O. polyphylla*, *Veronica multifida* L., *I. pumila*, *Helianthemum nummularium* (L.) Mill., *Psephellus declinatus* (Bieb.) K. Koch, and *Potentilla taurica* Willd. ex Schltdl.

In the zone of seismic deformations between blocks, landslide deposits (delapsium) are widespread. The substrate is characterised by the absence of clast sorting, with large blocks and fine material found together. The deposits show relative stability due to the presence of clays in the flysch composition. Blocks are cemented by finer fractions. As a result, colluvium gradually becomes overgrown. Phryganoid communities characteristic of successional stages develop here. For example, microgroups with *E. distachya*, *S. euxina, Ptilostemon echinocephalus* (Willd.) Greuter (= *Lamyra echinocephala* (Willd.), *Matthiola odoratissima* (Pall. ex M. Bieb.), *O. polyphylla*, *T. polium*, S. ringens, *A. pinifolium, I. pumila* occur here.

Constant species include: *Teucrium nuchense* K. Koch, *Iberis simplex* DC., *Fumana procumbens* (Dunal) Gren. & Godr., *Euphorbia petrophila* C.A. Mey., *Linaria genistifolia* (L.) Mill., *Linum tauricum* Willd., *Odontarrhena obtusifolia* (Steven ex DC.) C. A. Mey., *Picris pauciflora* Willd., *S. viminea*, *Asperula supina* M. Bieb., *B. squarrosus*. In addition, shrubs and small trees occur – *C. coggygria*, *R. coriaria* and *J. excelsa*. Along erosion furrows, synusiae of *Phragmites australis* (Cav.) Trin. ex Steud are distributed.

At the cliff bases, modern seismogravitational formations – rockfalls and scree – are developed. Scree slopes and detachment slopes are clearly distinguished. The material is represented by colluvial deposits of rubble-block composition with an admixture of clays. Populations of rare and protected species such as *Campanula komarovii* Maleev, *Crambe koktebelica* (Junge) N. Busch, *L. tauricum, H. tauricum*, *E. distachya*, *O. polyphylla*, *S. euxina*, as well as *Glaucium flavum* Crantz characteristic of lithophytic communities on pebble beaches, are noted here. *Sesleria alba* Sm, *E. petrophila, Crepis alpina L.*, *Sonchus oleraceus* L., and sumac regeneration are abundantly represented.

Petrophytic vegetation on mobile substrates is concentrated on scree fans, represented by sparse microgroups of *Seseli ponticum*, *Andrachne telephioides* L, and *P. australis*. TPC in such areas can vary from 5 to 30%. Rocky outcrops on cliff walls of varying slope angles are characterised by chasmophytic communities (*Reseda lutea* L., *Periploca graeca* L., *Centaurea sarandinakiae* N. B. Illar. (= *Centaurea novorossica* Klokov), *S. ponticum, M. odoratissima, L. genistifolia*). They develop in extensive fissures characteristic of the cliff belt of the Black Sea coast [17]. The formation of these communities is associated with flysch rock stratification and denudation processes.

Post-fire vegetation

A significant impact on the western part of Cape Khako resulted from a fire in 2020, which covered an area of about 5.66 ha (56,600 m²), according to analysis of satellite images. As a consequence, the mountain-xerophytic complex was eliminated. The rapid formation of sumac thickets with a high proportion of Christ's thorn was noted, characteristic of the first stages of secondary succession on the Abrau Peninsula [18]. Tomillares are replaced by communities dominated by explerent species – *Malva setigera* K.F. Schimp. & Spenn. (=*Althaea hirsuta*), *Delphinium consolida* L., *Cephalaria transsylvanica* (L.) Schrad. ex Roem. & Schult., *Echinops sphaerocephalus* L., and grasses (*Achnatherum bromoides, Bromus squarrosus* L, *P. holciforme*). Oak-pistachio woodlands occupying a small area of the southwestern tip of the cape also suffered varying degrees of damage.

Vegetation of the western tip of the cape, subjected to pyrogenic transformation, differs sharply from preserved, undisturbed areas. Currently, the structure of the post-fire community is determined by species with active seed regeneration – annuals *B. squarrosus*, *Carthamus glaucus* M.Bieb., *Carthamus lanatus* L., *C. transsylvanica, Rapistrum rugosum* (L.) *All*, and perennials *Salvia tesquicola* Klokov & Pobed., *Centaurea salonitana* Vis., *Galatella linosyris* (L.) Rchb. f., *G. villosa*, *A. pinifolium*, as well as young root-suckering individuals of *Rhus coriaria*. TPC here can reach 90%. A population of *E. distachya* has been preserved on the slopes of small erosion furrows.

Anthropogenic load

In addition to the threat of fire, unregulated recreational activities cause significant damage to the terrestrial ecosystems of the cape. Studies carried out within the Abrausky State Nature Sanctuary [4] record direct signs of high recreational load on coastal landscapes. Such signs include numerous informal trails leading to cliffs, areas with destroyed vegetation cover and trampled rare species, as well as accumulations of domestic waste and campfire sites characteristic of the most visited coastal areas. These disturbances contribute to the intensification of erosion processes and fragmentation of the habitats of protected species.

A particular problem is posed by the network of informal trails penetrating forest areas. As noted above, the forest phytocenoses of Cape Khako are characterised by the development of seasonal synusiae of ephemeroids, which play a key role in ecosystem functioning: after completing their vegetative cycle in early spring, they die off and become a significant source of organic matter for the tree layer. Intensive trampling and soil compaction along trails lead to the suppression and disappearance of these vulnerable species, disrupting the natural cycle of biological turnover and causing degradation of the soil cover [3), 4)].

Anthropogenic impact is also manifested in the aquatic complex. In bays experiencing increased anthropogenic pressure, signs of organic pollution are noted. The most striking example is the area near the pipeline outlet at the boundary between the Myskhako beach and the water area of the sanctuary, through which surface runoff enters the coastal zone. Here, the formation of local microgroups dominated by the filamentous alga *Cladophora laetevirens* (Aresch.) – an indicator species of mesosaprobic conditions – has been recorded, indicating local eutrophication of coastal waters associated with the inflow of polluted runoff. This fact, along with the spread of opportunistic algae (*Ulva*, *Ectocarpus*), confirms that recreational pressure acts as a key factor in the degradation of both terrestrial and marine ecosystems of Cape Khako.

Benthic vegetation

In inland seas such as the Black Sea, daily sea level fluctuations are insignificant and do not exceed 4–9 cm. Due to the absence of tidal phenomena, the littoral is replaced by the pseudolittoral zone, the existence of which is determined by wind-driven level fluctuations [19].

[3)] Rabotnov, T.A., 1983. [*Phytocenology*]. 2nd edition. Moscow: Moscow State University Publishing House, 292 p. (in Russian).

[4)] Zlobin, Yu.A., 1989. [*Principles and Methods of Studying Cenotic Plant Populations: A Study Guide*]. Kazan: Kazan University Publishing House, 148 p. (in Russian).

In the pseudolittoral (depths of 0.1–0.5 m), bench ridges are smoothed by waves, and their height is 10–50 cm. Between them, areas of completely smooth bottom covered with coarse and fine clastic material are located. The pseudolittoral transitions into the sublittoral (depths of 0.5–2.0 m); these bionomic zones represent the upper level of the phytal.

The pseudolittoral is characterised by boulder accumulations, on which annual mesosaprobic communities dominated by *Ulva compressa* + *Ectocarpus siliculosus* (TPC 40–80%) are concentrated. On submerged stones, a seasonal phytocenosis of *Padina pavonica* + *Dictyota fasciola* with a projective cover of 65–100% develops. In the upper sublittoral (depths of 0.7–2.0 m), on bench ridges, a perennial phytocenosis of *Cystoseira bosphorica* (=*Cystoseira crinita*) + *Treptacantha barbata* (=*Cystoseira barbata*) – *Padina pavonica* (TPC 80–100%) develops. The community is polydominant, multi-layered, with the lower layer represented by crustose coralline algae. Constant species include *Cladostephus spongiosum*, *Laurencia obtusa*, *Polysiphonia opaca,* and *Ceramium rubrum*, characteristic of bench ridge slopes. The epiphytic synusia is formed by *Polysiphonia subulifera*, *Cladophoropsis membranacea*, *Corallina elongata* and *Sphacelaria cirrosa*. From a depth of 2.0 m, the phytocenosis of *Codium vermilara* + *Phyllophora crispa* (TPC 30–50%) occurs in fragments, reaching full development at greater depths.

The identified structure of benthic vegetation reflects the gradient of conditions from stressful conditions in the pseudolittoral to more stable conditions in the sublittoral. Communities dominated by *Ulva compressa* and *Ectocarpus siliculosus* are typical pioneer communities colonizing disturbed benthic habitats and indicating significant anthropogenic pressure. At the same time, the presence of stable multispecies phytocenoses with species of the *Cystoseira sensu lato* complex indicates preserved areas with ecological stability. The conservation significance of the aquatic complex is confirmed by records of species included in the Red Data Books at various levels: *P. crispa*, *C. vermilara*, *C. spongiosus*, and *Laurencia coronopus*. The presence of these species underscores the high conservation value of the water area of Cape Khako[5), 6)].

Conclusion

The studies performed made it possible to provide a comprehensive characterisation of the landscape structure of the coastal zone of Cape Khako. It was found that the key role in shaping its structure is played by interrelated abrasion-accumulative and gravitational processes, creating a mosaic of ecotopes with high contrast.

The most important results are as follows:

1. The geomorphological structure of the territory is dominated by a relict cliff complicated by modern landslide and scree processes, and by accumulative terraces with pocket beaches.

---

5) Geltman, D.V., ed., 2024. *Red Data Book of the Russian Federation. Plants and Fungi*. Moscow: VNII “Ekologiya”, 944 p. (in Russian).

6) Livinskaya, S.A., ed., 2017. *Red Book of Krasnodar Territory. Plants and Fungi*. Krasnodar, 2017. 229 p. (in Russian).

2. We identified a clear spatial organisation of vegetation cover, determined by geomorphological conditions: from mixed shiblyaks on upland plains to mountain-xerophytic communities and mobile petrophytic vegetation on steep slopes and in areas of discontinuity.

3. The high conservation significance of the territory was confirmed. The flora of the cape includes a significant number of rare, endemic, and relict species, emphasising its role as an important refugium under conditions of anthropogenic pressure.

4. Signs of ecosystem degradation, caused by both natural factors (landslides) and human activity (fires, recreational pressure, eutrophication of coastal waters) were recorded. Communities dominated by ruderal plant species and opportunistic algae (*Ulva*, *Ectocarpus*) indicate the initial stages of succession and habitat disturbance.

5. Thus, Cape Khako represents a dynamic and vulnerable natural system.

The data obtained provide a scientific basis for developing measures for monitoring and conserving this unique complex. To ensure its sustainability, a systemic approach is required, including not only the protection of individual rare species but also the preservation of the integrity of the entire landscape and natural geomorphological processes. Priority measures should include the restriction of unregulated recreation and the development of a post-fire restoration programme for disturbed phytocenoses.

REFERENCES

1. Demina, O.N., Ogureeva, G.N., Rogal, L.L., Bocharnikov M.V. and Dmitriev, P.A., 2015. Coenotic Diversity and Syntaxonomy of Xerophytic Coniferous Forests and Woodlands in the Utrish Reserve. In: O. N. Bykhalova, ed., 2015. [*Conservation of Biodiversity in the Utrish State Nature Reserve*]. Anapa: OOO Poligraf-Yug, Vol. 3, pp. 80–106 (in Russian).
2. Bocharnikov, M.V., 2021. Spatial Structure of the Vegetation Cover of the Abrau Peninsula (on the Example of the Vodopadnaya Shchel). *Geobotanical Mapping 2021*, pp. 62–83. https://doi.org/10.31111/geobotmap/2021.62 (in Russian).
3. Kalyuzhny, M.A. and Pikalova, N.A., 2024. [A Study of Fire Hazards on the Abrau Peninsula. In: E. I. Zakharchenko, ed., 2024. [*Student Practice: From Introductory to Pre-Graduation: Proceedings of the 3rd All-Russian Scientific and Practical Conference, Krasnodar, 22–23 November 2024*]. Krasnodar: Kuban State University, pp. 159–163 (in Russian).
4. Solyannikov, V.V. and Nyushchenko, E.A., 2025. Vegetation of Coastal Cliffes of the Black Sea on the Border of the Abraussky Natural Reserve. *Povolzhskiy Journal of Ecology*, (2), pp. 240–250. https://doi.org/10.35885/1684-7318-2025-2-240-250 (in Russian).
5. Litvinskaya, S., 2004. *Vegetation of the Russian Blacк Sea Coast (Mediterranean Enclave)*. Krasnodar, 118 p. (in Russian).
6. Popkov, V.I., Krickaya, O.Y., Ostapenko, A.A., Dementjeva, I.E. and Bykhalova, O.N., 2021. Relief and Geological and Geomorphological Conditions for the Formation of Landscapes of the Utrish Reserve. In: O. N. Bykhalova, ed., 2021. [*Terrestrial and Marine Ecosystems of the Abrau Peninsula: History, Current Status, Conservation*]. Anapa: FGBU State Reserve Utrish. Vol. 5, pp. 12–21 (in Russian).

7. Bocharnikov, M.B., 2021. Phytocoenotic Diversity and Spatial Structure of the Vegetation Cover in the Vodopadnaya Valley (Utrish Reserve). In: O. N. Bykhalova, ed., 2021. [*Terrestrial and Marine Ecosystems of the Abrau Peninsula: History, Current Status, Conservation*]. Anapa: FGBU State Reserve Utrish. Vol. 5, pp. 69–78 (in Russian).
8. Blinova, E.I., Pronina, O.A. and Shtrik, V.A., 2005. Methodical Recommendations on Accounting of Stocks of Commercial Seaweeds of the Coastal Zone. In: VNIRO, 2005. [*Methods of Landscape Studies and Stock Assessment of Benthic Invertebrates and Algae of the Marine Coastal Zone*]. Moscow: VNIRO Publ., pp. 80–127 (in Russian).
9. Krylenko, V.V., Kosyan, R.D. and Krylenko, M.V., 2021. The Coasts of the Caucasian North-Western Part of the Black Sea at the Beginning of the XXI Century. *Journal of Oceanological Research*, 49(1), pp. 68–92. https://doi.org/10.29006/1564-2291.JOR-2021.49(1).5 (in Russian).
10. Lipka, O.N., Andreeva, A.P., Bogdanovich, A.Yu., Krylenko, M.V. and Dobrolyubova, K.O., 2021. Weather-Climatic Influences on the Dynamics of Flysch Coastal Cliffs of the Caucasus Black Sea Coast. In: SSC RAS, 2021. *Regularities of Formation and Impact of Marine and Atmospheric Hazardous Phenomena and Disasters on the Coastal Zone of the Russian Federation under the Conditions of Global Climatic and Industrial Challenges ("Dangerous Phenomena – III") in Memory of Corresponding Member RAS D.G. Matishov: Proceedings of the International Scientific Conference (Rostov-on-Don, 15–19 June 2021)*. Rostov-on-Don: SSC RAS Publishers, pp. 188–191 (in Russian).
11. Gurianova, E.F., Zaks, I.G. and Ushakov, P.V., 1930. [Living Conditions on the Littoral of Kola Bay]. *Trudy Leningradskogo Obshchestva Estestvoispytatelei*, 60(2), pp. 2–108 (in Russian).
12. Srybnaja, S.V., 2008. Urgency of Research of a Karst Flishev Adjournment of the Western Caucasus. *Geology, Geography and Global Energy*, (3), pp. 171–173 (in Russian).
13. Viles, H.A., 2012. Microbial Geomorphology: a Neglected Link Between Life and Landscape. *Geomorphology*, 157, pp. 6–16. https://doi.org/10.1016/j.geomorph.2011.03.021
14. Shulyakov, D.Yu., Shulyakova, M.S. and Naumova, A.I., 2015. [Geographical Interpretation of Palaeo-Seismogravitational Displacements on the Abrau Peninsula]. In: A. V. Pogorelov, ed., 2015. [*Geographical Studies of the Krasnodar Krai*]. Krasnodar: KGU. Iss. 9. pp. 25–29 (in Russian).
15. Mironyuk, S.G. and Kropotkin, M.P., 2020. Possible Mechanism and Causes of Landslides of Utrish and the Near Shelf (the Abrau Peninsula). In: SSC RAS, 2020. *Regularities of Formation and Impact of Marine and Atmospheric Hazardous Phenomena and Disasters on the Coastal Zone of the Russian Federation under the Conditions of Global Climatic and Industrial Challenges ("Dangerous Phenomena – II") in Memory of Corresponding Member RAS D.G. Matishov: Proceedings of the International Scientific Conference (Rostov-on-Don, 6–10 July 2020)*. Rostov-on-Don: SSC RAS Publishers, pp. 52–57 (in Russian).
16. Parshina, L.N., 2021. Weather on the Russian Federation Territory in June 2021. *Meteorologiya i Gidrologiya*, (9), pp. 135–138 (in Russian).
17. Agarkova-Lyakh, I.V. and Lyakh, A.M., 2022. Features of the Structure of Marine Coastal Landscapes. *Monitoring Systems of Environment*, (3), pp. 18–26 (in Russian).
18. Andreeva, A.P. and Petrushina, M.N., 2023. Monitoring of Coastal Landscapes in the Utrish Nature Reserve. In: IGCE, 2023. [*Monitoring of the State and Pollution of the Environment: Surface Climate, Pollutants and Climate-Active Substances. Proceedings of the 3rd All-Russian Scientific Conference with International Participation. Moscow, 15–17 November 2023*]. Moscow: IGCE, pp. 323–327 (in Russian).

19. Agarkova-Lyakh, I.V., Frolova, K.V. and Lyakh, A.M., 2022. Adaptation of Coastal Vegetation to the Ecological Conditions of the Land-Sea Contact Zone. *Monitoring Systems of Environment*, (2), pp. 73–83. https://doi.org/10.33075/2220-5861-2022-2-73-83 (in Russian).

Submitted 19.02.2026; accepted after review 04.03.2026;
revised 19.03.2026; published 30.06.2026

About the author:

Vadim V. Solyannikov, Specialist, Laboratory of Hydrobiology, Saint Petersburg Branch of "VNIRO" ("GosNIORKH" named after L. S. Berg) (26, Makarova Emb., 199053, Saint Petersburg, Russia), **ORCID ID: 0009-0005-3889-1237**, *lacrimas.777@mail.ru*

The author has read and approved the final manuscript.

ISSN 2413-5577, Ecological Safety of Coastal and Shelf Zones of Sea, No. 2, pp. 43–56 (2026)

Original paper

Dynamics of the Area and Volume of the Chernorechenskoe Reservoir (Sevastopol)

A. A. Aleskerova [1] *, P. N. Lishaev [1], N. V. Vasilenko [1], A. A. Kubryakov [1], S. V. Stanichny [1], M. G. Grechushnikova [2]

[1] *Marine Hydrophysical Institute of RAS, Sevastopol, Russia*

[2] *Lomonosov Moscow State University, Moscow, Russia*

* *e-mail: annete08@mail.ru*

Abstract

The article aims to quantify the dynamics of the area and volume of the Chernorechenskoe Reservoir (the main water supply of Sevastopol). The study relies on a comprehensive analysis of Sentinel-2 optical satellite data (164 images) with a spatial resolution of 10 m for 2015–2026 to develop and test an automatic algorithm for determining the water surface area, based on a normalized difference water index with adaptive threshold values for different seasons. The obtained water surface areas are integrated with a bathymetric model to calculate the reservoir volume. The obtained results are compared with MERRA-2 precipitation reanalysis data. The minimum values of the reservoir volume were observed in January 2021 (7.4 million m³ with an area of 178.1 hectares) after the low-water year of 2020, and also in September 2025. The maximum volume during the study period did not exceed 45.7 million cubic meters, which is 23% less than the design usable volume. A positive correlation was found between the precipitation amount and reservoir area, taking into account the inertia of the hydrological system. The developed methodology can be used to monitor other reservoirs in the region.

Keywords: Chernorechenskoe Reservoir, satellite monitoring, Sentinel-2, NDWI, bathymetry, reservoir volume, water surface area, Crimea

Acknowledgments: This study was conducted under state assignment of MHI RAS FNNN-2024-0012 “Analysis, diagnosis and real-time forecast of the state of hydrophysical and hydrochemical fields of marine water areas based on mathematical modelling using data from remote and *in situ* methods of measurements”.

For citation: Aleskerova, A.A., Lishaev, P.N., Vasilenko, N.V., Kubryakov, A.A., Stanichny, S.V. and Grechushnikova, M.G., 2026. Dynamics of the Area and Volume of the Chernorechenskoe Reservoir (Sevastopol). *Ecological Safety of Coastal and Shelf Zones of Sea*, (2), pp. 43–56.

© Aleskerova A. A., Lishaev P. N., Vasilenko N. V., Kubryakov A. A., Stanichny S. V., Grechushnikova M. G., 2026

This work is licensed under a Creative Commons Attribution-Non Commercial 4.0 International (CC BY-NC 4.0) License

Динамика площади и объема Чернореченского водохранилища (Севастополь)

А. А. Алескерова [1] *, П. Н. Лишаев [1], Н. В. Василенко [1], А. А. Кубряков [1], С. В. Станичный [1], М. Г. Гречушникова [2]

[1] *Морской гидрофизический институт РАН, Севастополь, Россия*

[2] *Московский государственный университет им. М.В. Ломоносова, Москва, Россия*
* *e-mail: annete08@mail.ru*

Аннотация
Цель исследования – количественная оценка динамики площади и объема Чернореченского водохранилища (основного источника водоснабжения Севастополя). На основе анализа оптических спутниковых данных *Sentinel*-2 (164 снимка) с пространственным разрешением 10 м за 2015–2026 гг. разработан и протестирован автоматический алгоритм определения площади водной поверхности на основе нормализованного разностного водного индекса с адаптивными пороговыми значениями для различных сезонов. Полученные данные о площади водного зеркала интегрированы с батиметрической моделью для расчета объема водохранилища. Результаты сопоставлены с данными реанализа осадков MERRA-2. Установлено, что минимальные значения объема водохранилища наблюдались в январе 2021 г. (7.4 млн м^3 при площади 178.1 га) после маловодного 2020 года, а также в сентябре 2025 г. Максимальный объем за исследуемый период не превышал 45.7 млн м^3, что на 23 % меньше проектного полезного объема. Выявлена положительная корреляция между количеством осадков и площадью водохранилища с учетом инерционности гидрологической системы. Разработанная методика может быть использована для мониторинга других водохранилищ региона.

Ключевые слова: Чернореченское водохранилище, спутниковый мониторинг, *Sentinel*-2, *NDWI*, батиметрия, объем водохранилища, площадь водного зеркала, Крым

Благодарности: исследование выполнено в рамках государственного задания ФГБУН ФИЦ МГИ по теме FNNN-2024-0012 «Анализ, диагноз и оперативный прогноз состояния гидрофизических и гидрохимических полей морских акваторий на основе математического моделирования с использованием данных дистанционных и контактных методов измерений».

Для цитирования: *Алескерова А. А., Лишаев П. Н., Василенко Н. В., Кубряков А. А. и др.* Динамика площади и объема Чернореченского водохранилища (Севастополь) // Экологическая безопасность прибрежной и шельфовой зон моря. 2026. № 2. С. 43–56. EDN JNUHPE.

Introduction

The Chernorechenskoe Reservoir is located in the southwestern part of the Crimean Peninsula on the Chernaya River within the Baydarsky Reserve and is the largest reservoir in Crimea in terms of total and usable volume. It was put into operation in 1956 for water supply to Sevastopol [1, 2]. The Chernorechenskoe Reservoir is replenished by the natural runoff of the Chernaya River [3] and has a mixed feeding regime with a predominance of snow-rain and groundwater feeding [2, 4]. Under conditions of flow regulation by the Chernorechenskoe

Reservoir, floods on the Chernaya River can significantly affect the ecological state of the near-mouth area of Sevastopol Bay, causing freshening of the surface water layer and contributing to pollutants discharge [5].

The Chernorechenskoe Reservoir is a key source of water supply for the population of Sevastopol [6, 7] and meets up to 70% of water demand. The total volume of the reservoir, according to literature data, is 64.2 million m³, and the usable volume is 61.2 million m³ [8]. The annual water consumption[1)] by the city's population alone is 19–20 million m³.

For stable water supply to the city, it is necessary to supply 120 thousand m³ of water per day, and in summer this volume increases to 150–160 thousand m³ [7].

In recent years, the population of Sevastopol has been increasing [9], and at the same time the load on the water supply system is growing. Against this background, there is a threat of water deficit in the region for a number of reasons. This situation is primarily associated with insufficiently efficient use of resource potential, namely losses of channel runoff in the Chernaya River, siltation of the reservoir (about 1.9 cm per year), as well as conveyance losses due to the aging of hydraulic structures [3, 8, 10–12]. In addition, the region's water supply depends on climatic conditions: in low-water years, local shortages of drinking and domestic water occur on the Crimean Peninsula [13].

In past years, critical shallowing of the Chernorechenskoe Reservoir has already been observed. Thus, in 1994, the water surface area of the reservoir decreased to an extreme value of 50.8 hectares (according to Landsat data of 22 August 1994) [14], and in December 2014, to 180 hectares [15]. In 2020, due to record-low annual precipitation, drought conditions were also observed, which led to a noticeable reduction in the water surface area [16].

A systematic assessment of the reservoir morphometric characteristics (volume and water surface area) is required for effective management of resource potential and its forecasting under conditions of climate change and increasing water demand. The regulated flow of the Chernorechenskoe Reservoir allows controlled releases into the Chernaya River channel in the event of a threat of severe floods. Since the river flows into Sevastopol Bay, these measures directly determine the hydrological characteristics of the near-mouth area of the bay, especially during dry periods and flood seasons. For example, study [5] showed that during an emergency release from the reservoir in January 2024, the surface water layer of a significant part of the estuary was freshened by 2 to 17‰.

High-resolution satellite data combined with the Normalized Difference Water Index (NDWI) make it possible to effectively monitor changes in the water surface area of water bodies [17–20]. Previously, studies [14, 15] analyzed the variability of the water surface areas of Crimean reservoirs, including the Chernorechenskoe Reservoir, up to 2021 based on satellite measurements with a spatial resolution

[1)] Reports on the Production Program in the Field of Cold Water Supply of the State Unitary Enterprise "Vodokanal". Available at: https://sevvodokanal.org.ru/pages/programma [Accessed: 13 May 2026] (in Russian).

of 30 m. This paper presents an approach for operational assessment of the water surface area and estimated volume of a water body using automated algorithms for processing high-resolution Sentinel-2 satellite data (10 m) and bathymetric data.

This work is aimed at quantifying the morphometric characteristics of the Chernorechenskoe Reservoir and analysing their long-term dynamics.

Materials and methods

We used optical satellite data from Sentinel-2 MSI with a spatial resolution of 10 m (from 2015 to the present). Three satellites are in operation: Sentinel-2A, Sentinel-2B and Sentinel-2C, launched in 2015, 2017 and 2024, respectively. The nominal repeat cycle for one satellite is 10 days. When two satellites operate together, this interval is reduced to five days, and a constellation of three satellites makes it possible to obtain consecutive daily images of the study area.

The data were obtained from the Copernicus Data Space Ecosystem Browser (URL: https://browser.dataspace.copernicus.eu/). A total of 164 cloud-free images were processed over the study period. Thus, the annual number of images varies from 5 in 2015–2016 to 23 in 2025. This data archive made it possible to analyse the seasonal and interannual dynamics of changes in the area and volume of the reservoir. The number of images for the study period was distributed as follows:

Jan.	7	May	10	Sept.	23
Febr.	8	June	13	Oct.	15
March	7	July	21	Nov.	12
April	20	Aug.	26	Dec.	2

The boundaries of the Chernorechenskoe Reservoir were delineated based on NDWI [18] using spectral channels in the green (B03, ~ 560 nm) and near-infrared (B08, ~ 842 nm) regions:

$$\mathrm{NDWI} = (\mathrm{B03} - \mathrm{B08}) / (\mathrm{B03} + \mathrm{B08}).$$

This combination of bands effectively enhances the contrast between water bodies, characterised by high reflectance in the green range and strong absorption in the near-infrared range, and other land surface types. A key feature of the developed algorithm is the use of adaptive NDWI threshold values, taking into account seasonal changes in the state of the water surface and coastal vegetation, for different months of the year. Using a single threshold value can lead to systematic errors in calculations: in winter months, to overestimation of the area due to the impact of snow cover and ice, and in summer, to its underestimation due to increased water turbidity. The threshold brightness values (R_{crit}) for the water mask were selected empirically based on the average value for each month. We constructed two spatial transects through the water–land transition zone in characteristic areas of the water area. Along the brightness profiles, the nature of the change in values was analysed: a sharp brightness jump was recorded at the water–land interface, which made it possible to unambiguously identify the threshold value for distinguishing between the water surface and land. The final threshold value was taken as the average of the results of several transects for a given month.

Thus, the R_{crit} values were:

$$R_{crit} = [0.15; 0.09; 0.08; 0.06; 0.05; 0.01; 0.05; 0.05; 0.05; 0.05; 0.05; 0.05].$$

Then the number of pixels identified as water was converted into units of area (hectares). At 10 m resolution, each pixel at the reservoir boundary can include both water and land. The relative error can be 3–7% of the maximum water surface area (≈ 600 ha).

The reservoir volume was calculated based on a combined analysis of bathymetric data obtained during field surveys [8] and the water surface mask derived from satellite images. For each image, the binary water surface mask was overlaid on the bathymetric grid, making it possible to extract depths only within the water-covered area. According to the survey data, the maximum depths in the reservoir reach 28 m. Depth values corresponding to land were filtered out to exclude them from the calculation. For each case, the minimum depth in the reservoir was determined, which was taken as the conditional zero level.

To analyse the effect of precipitation on the water volume of the Chernorechenskoe Reservoir, we used data from the global atmospheric reanalysis MERRA-2 (Modern-Era Retrospective Analysis for Research and Applications, Version 2), obtained from the GIOVANNI (Geospatial Interactive Online Visualization ANd aNalysis Infrastructure) portal (URL: https://giovanni.gsfc.nasa.gov/giovanni/). The spatial resolution of MERRA-2 data is 0.5° in latitude and 0.625° in longitude (approximately 50 km). In this work, we used hourly precipitation data, which were subsequently averaged to monthly mean values. Precipitation was considered within the catchment basin of the Chernorechenskoe Reservoir, which includes theslopes of Mount Ai-Petri and the Baydar Valley [2]. The spatial extent of the area is defined by a rectangle with corner coordinates: 44° 25′ N, 33° 42′ E and 44° 33′ N, 33° 58′ E.

Results and discussion

Based on the developed algorithm, a time series of the water surface area of the Chernorechenskoe Reservoir from 2015 to the present was obtained. Analysis of these data revealed significant interannual and seasonal variability in the reservoir area.

The obtained water surface contours of the reservoir were compared with higher-resolution data available in Google Earth (up to 0.3 m). For this purpose, the water surface contours of the reservoir obtained from Sentinel-2 data for the nearest date (11 April 2020) were overlaid on a Maxar (WorldView) satellite image of 08 April 2020 (Fig. 1). As a result, despite the significant difference in spatial resolution of the compared images (10 and 0.3 m), which caused a lack of detail in some zones, the water surface boundaries obtained from Sentinel-2 data almost completely corresponded to the reference image.

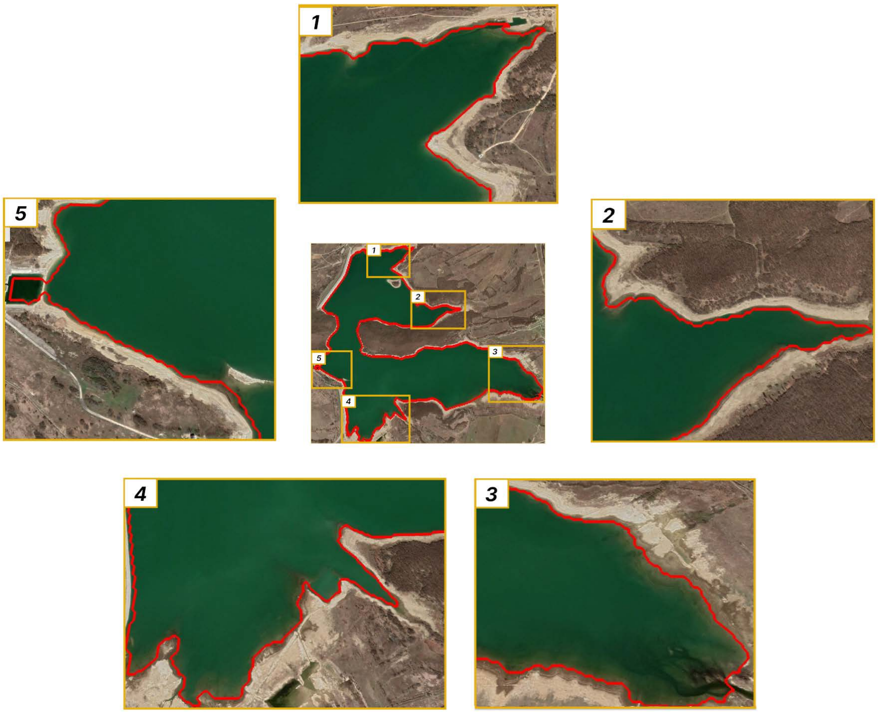

F i g . 1 . A Maxar satellite image of 08 April 2020 with an overlay of the reservoir water body contour (red line) derived from Sentinel-2 data of 11 April 2020

Satellite data analysis revealed that, on average, over the entire study period, the minimum water surface areas were observed from September to November after the dry summer season. Then, after the flood period (November–December), gradual filling of the reservoir and recovery of its area were observed in January–February. Fig. 2 shows, as an example, the reservoir waterline boundaries and the variability of its water surface area in January (Fig. 2, *a*) and September (Fig. 2, *b*) over the entire observation period of 2015–2026, as the waterline contours in these months correspond to two phases of the reservoir regime. The minimum area for the entire observation period was recorded on 6 January 2021 and was 178.1 hectares (Fig. 2, *a*), which is significantly higher than the historical minimum of 1994, but reflects the tense situation with water resources after the extremely low-water year of 2020.

The minimum water surface area in September (Fig. 2, *b*) was recorded on 27 September 2025 and was 254.7 hectares, which was the absolute minimum for this month over the entire observation period of 2015–2026 and was 45 hectares less than the corresponding value for 2020. Such a significant reduction in area is due to the water deficit accumulated since spring of 2024. As of February 2026, the reservoir area was 434.12 hectares, which corresponds to the values recorded in February 2020.

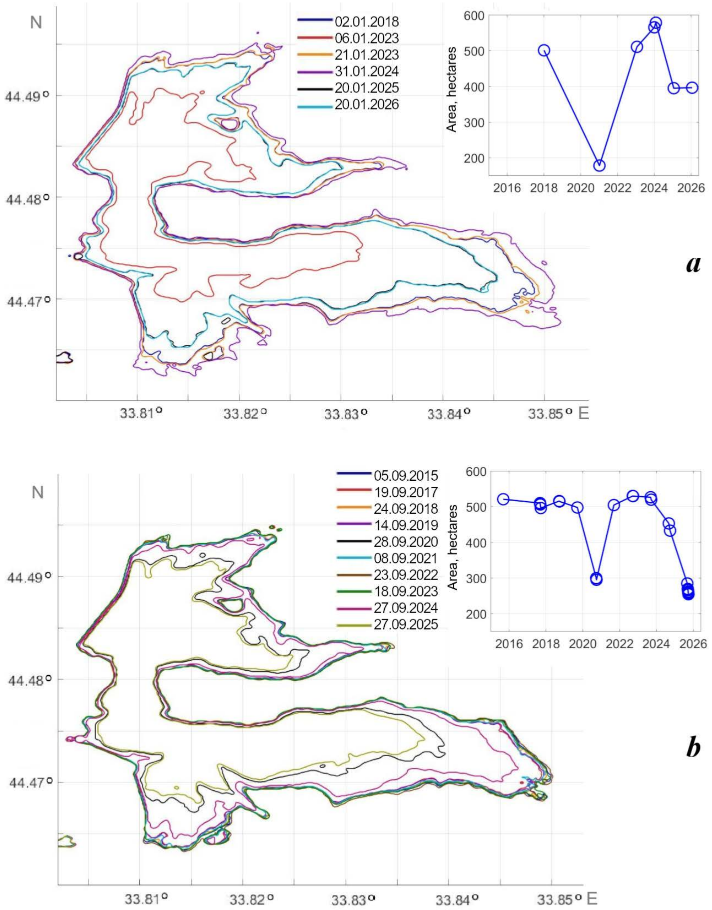

F i g . 2 . Waterline contours and water surface area dynamics of the Chernorechenskoe Reservoir based on Sentinel-2 data for January (*a*) and September (*b*) of 2015–2026

The maximum values for January were observed in 2024 (Fig. 2, *a*), and for September, in 2022 (Fig. 2, *b*).

Combining satellite data on water surface area with a bathymetric model allowed us to estimate the reservoir volume for each acquisition date. Fig. 3 shows the waterline data for February (period of water volume recovery) and October (characteristic period of minimum values) for the lowest-water years of the study period (2020 and 2025), as well as for February of the current year, 2026. In February 2020, the volume was 32.3 million m³ (Fig. 3, *a*), and in October it decreased to 16.4 million m³ (Fig. 3, *b*). Even lower values were recorded in 2025: 26.8 million m³ in February (see Fig. 2, *a*) and 12.2 million m³ in October. As of 20 January 2026, the volume and area of the reservoir approached the values for the same period of the previous year (395 ha and 26 million m³, respectively).

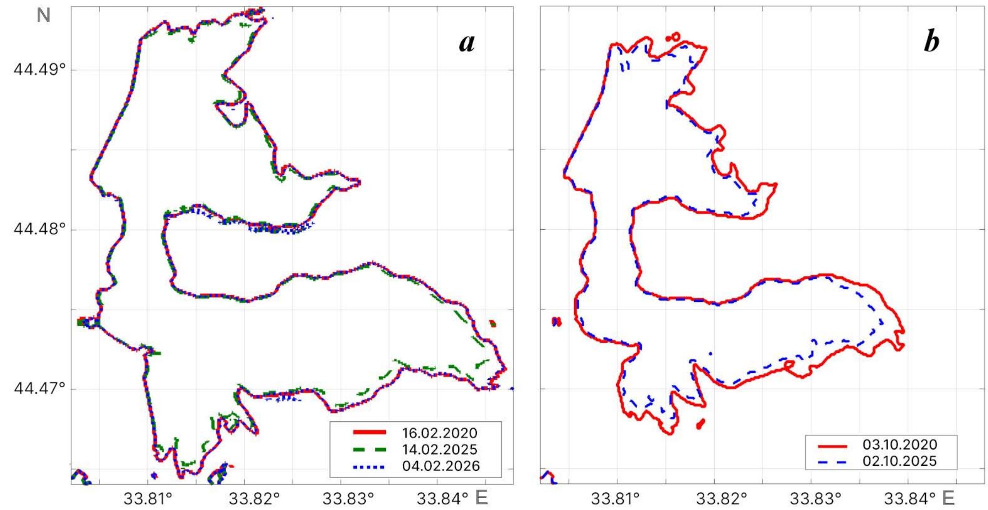

F i g . 3 . The Chernorechenskoe Reservoir waterline contours in February 2020, 2025 and 2026 (*a*) and in October 2020 and 2025 (*b*).

Fig. 4 shows the variability of the reservoir water surface area from satellite images and the amount of precipitation over the study area according to MERRA-2 reanalysis data (Fig. 4, *a*), as well as the dynamics of water volume (Fig. 4, *b*) and average water level (Fig. 4, *c*) for January from 2015 to 2026, relative to the maximum filling of the reservoir in February 2018. Analysis of these time series revealed a relationship: a decrease in precipitation leads to a reduction in the reservoir area (Fig. 4, *a*), and, accordingly, to a decrease in water volume (Fig. 4, *b*) and water level (Fig. 4, *c*).

The most pronounced low-water periods were observed in 2020 and 2025, which corresponds to the minimum values of accumulated precipitation in 2018–2020 and 2024–2025. The reservoir demonstrates significant inertia of the hydrological system: even after the amount of precipitation returns to long-term average values, the water surface area recovers gradually, over several months. In addition, in winter precipitation can fall as snow, which leads to water inflow into the reservoir only after snowmelt at above-zero temperatures. It is also important to consider that the reservoir regime is artificially regulated: during severe floods, water is released.

Except for 2021, the annual dynamics demonstrate an increase in reservoir volume from December to May, followed by a subsequent decrease. As noted earlier, the absolute minimum values for the entire study period were recorded in early January 2021, when the reservoir volume decreased to 7.4 million m³, and the level dropped by more than 11 m relative to the level of February 2018. Nevertheless, later

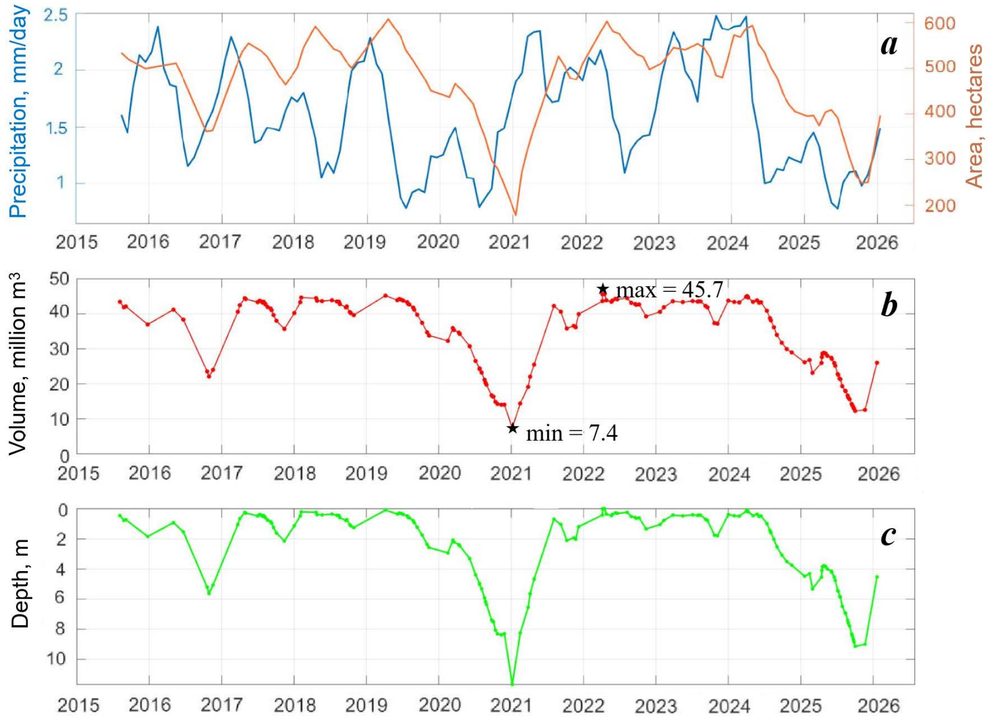

Fig. 4. Dynamics of the reservoir water-surface area and mean monthly precipitation (*a*), reservoir volume (*b*) and water level (*c*)

the volume increased rapidly, and a positive trend persisted throughout the year, which ultimately led to the maximum volume for the study period of 45.7 million m³ in April 2022. A local minimum was also noted in October–November 2016, when the reservoir volume dropped to 22 million m³. However, already in 2017–2018, high-water conditions were observed: the volume reached 43 million m³, which corresponded to the near-maximum filling of the reservoir basin.

The estimates of the Chernorechenskoe Reservoir volume obtained from satellite data were compared with information published in open sources [2)] by the State Unitary Enterprise "Vodokanal" [2]. According to these data, as of 5 February 2020, the water volume in the reservoir was 30.456 million m³, and as of 31 August 2020, 21.857 million m³. For correct comparison, satellite images with acquisition dates as close as possible to the measurements taken by Vodokanal were selected. In the image acquired on 16 February 2020 (Fig. 5, *a*), the estimated volume was 32.3 million m³, and on 29 August 2020, 19.7 million m³ (Fig. 5, *b*). Thus, the discrepancy between the Vodokanal data and the satellite measurements was 6.1 and 9.9%, respectively. It should be noted that the identified difference may be

2) Available at: https://sevvodokanal.org.ru/news/2020-02-05/163 [Accessed: 13 May 2026] (in Russian).

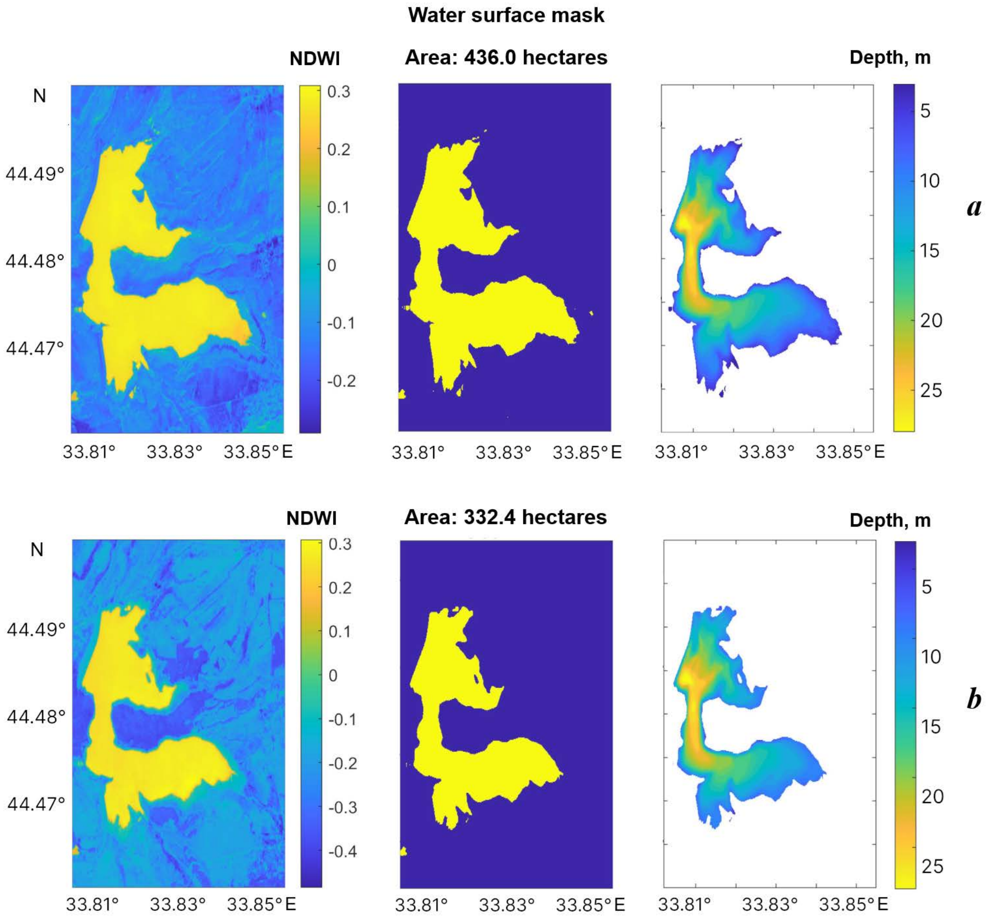

F i g . 5 . Identification of the Chernorechenskoe Reservoir water surface from satellite imagery on 16 February 2020 (*a*) and 29 August 2020 (*b*)

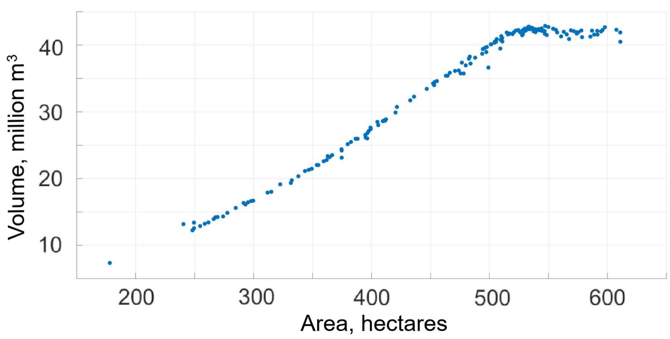

F i g . 6 . Dependence of the water volume on the reservoir water-surface area from satellite data and the bathymetric model due both to the time lag between the compared datasets (5–11 days) and to the uncertainty of the method for calculating the volume using satellite images and the bathymetric model used.

Analysis of the reservoir volume dependence on the water surface area revealed a non-linear nature of this relationship (Fig. 6). A positive correlation (R = 0.95) is observed between these parameters, but when the threshold area reaches about 450 ha, the reservoir volume reaches a plateau, showing a slight increase with a further increase in the water surface area. This is explained by the morphometric features of the reservoir bed. When the main basin is filled, a further increase in water level leads to flooding of relatively flat coastal areas with shallow depths.

Conclusion

We developed and tested an algorithm for determining the water surface area of the Chernorechenskoe Reservoir based on *Sentinel*-2 satellite data using the Normalised Difference Water Index (NDWI) and adaptive threshold values for different seasons of the year. A spatial resolution of 10 m provides high accuracy in determining the water body boundaries.

A time series of the water surface area of the Chernorechenskoe Reservoir for the period 2015–2026 with high temporal resolution was obtained. It was found that the minimum area for the study period was 178.1 ha and was observed on 6 January 2021, after the low-water year of 2020. A repeated critical reduction in area was recorded in September 2025.

Integration of satellite data on water surface area with a bathymetric model was performed, which allowed us to calculate the reservoir volume for each observation date. The minimum volume was 7.4 million m^3 (6 January 2021); the maximum volume over the observation period did not exceed 45.7 million m^3, which is 23% less than the design usable volume.

A clear correlation was found between the amount of precipitation (according to MERRA-2 reanalysis data) and the reservoir water surface area. It was shown that the reservoir demonstrates significant inertia of the hydrological system: even after the amount of precipitation returns to long-term average values, the water surface area recovers gradually, over several months. The most critical low-water periods of 2020 and 2025 are due to precipitation deficits in the previous two to three years.

A non-linear dependence of the reservoir volume on the water surface area with a plateau at an area of about 450 ha was determined, which is due to the morphometric features of the reservoir.

The developed algorithm can be subsequently applied to process satellite data with higher spatial resolution. The use of refined bathymetry obtained during the period of maximum reservoir filling will significantly improve the accuracy of volume calculations.

REFERENCES

1. Oliferov, A.N. and Timchenko, Z.V., 2005. [*Rivers and Lakes of Crimea*]. Simferopol: DOLYA, 214 p. (in Russian).

2. Degterev, A.Kh., 2022. [*The Filling Rates of Crimea's Reservoirs During the Closure of the North Crimean Canal*]. Sevastopol: SevGU, 70 p. (in Russian).

3. Volosukhin, Ya.V., 2019. Safety of Facilities of the Chernorechensk Reservoir Used for Sevastopol Water Supply. *Prirodoobustrojstvo*, (5), pp. 57–64 (in Russian).

4. Artemenko, V.M., Badyukov, D.D., Ivanov, V.A., Kondratev, S.I., Krasovsky, Z.I., Lyashenko, S.V. and Yastreb, V.P., 2003. Hydrological and Chemical Peculiarities of Chernorechenskoe Storage Pool Water in Summer. *Ecological Safety of Coastal and Shelf Zones and Comprehensive Use of Shelf Resources*, 9, pp. 67–75 (in Russian).

5. Minkovskaya, R.Ya., Demidov, A.N. and Narivonchik, S.V., 2024. The Effect of the Runoff of the Chernaya River (Sevastopol Region) on the Estuarine Coast During Floods. *Hydrosphere. Hazard Processes and Phenomena*, 6(2), pp. 138–156. https://doi.org/10.34753/HS.2024.6.2.138 (in Russian).

6. Vasilenko, V.A., 2019. Water Resources as an Impediment to Social and Economic Development in Crimea. Region: *Ekonomika i Sotsiologiya*, (4), pp. 245–267. https://doi.org/10.15372/REG20190411 (in Russian).

7. Kobechinskaya, V.G., Yarosh, O.B., Ivashov, A.V. and Apostolov, V.L., 2020. Issues of Drinking Water Quality in the Western Part of Crimea. *Water and Ecology*, (3), pp. 50–62. https://doi.org/10.23968/2305-3488.2020.25.3.50-62 (in Russian).

8. Grechushnikova, M.G., Kositsky, A.G., Ajbulatov, D.N., Shkolny, D.I., Alekseeva, A.A. and Karashova, M.I., 2020. Transformation of Water Runoff and Sedimentation in the Chernorechensk Reservoir. *Lomonosov Geography Journal*, (1), pp. 97–104 (in Russian).

9. Piskun, E.I. and Kamynina, A.A., 2021. Dynamic Analysis of the Factors of Influence on the Standard of Living of Sevastopol. *HronoEconomics*, (2), pp. 67–74 (in Russian).

10. Minkovskaya, R.Ya., 2009. Water Balance of the Sevastopol Region. *Reports of the National Academy of Sciences of Ukraine*, (3), pp. 137–140 (in Russian).

11. Prusov, A.V., Min'kovskaya, R.Ya. and Ovcharenko, I.A., 2009. Reserves of Fresh Water Resources of the Sevastopol Region. *Ecological Safety of Coastal and Shelf Zones and Comprehensive Use of Shelf Resources*, 19, pp. 143–153 (in Russian).

12. Kayukova, E.P. and Yurovsky, Y.G., 2016. Water Resources of the Crimea. *Geoekologiya. Inzheneraya Geologiya, Gidrogeologiya,Geokriologiya*, (1), pp. 25–32 (in Russian).

13. Nikolenko, I.V., Karimov, E.A., Bokov, S.A. and Avdeeva, D.V., 2022. Analysis of Water Resource Losses from Natural Runoff Reservoirs of the Republic of Crimea and Sevastopol. *Construction and Industrial Safety*, 27, pp. 111–123 (in Russian).

14. Shinkarenko, S.S., Solodovnikov, D.A., Bartalev, S.A., Vasilchenko, A.A. and Vypritskii, A.A., 2021. Dynamics of the Reservoirs Areas of the Crimean Peninsula. *Sovremennye Problemy Distantsionnogo Zondirovaniya Zemli iz Kosmosa*, 18(5), pp. 226–241. https://doi.org/10.21046/2070-7401-2021-18-5-226-241 (in Russian).

15. Ignatieva, M., 2023. Application of Remote Research Methods to Analyze Changes in the Area of the Chernorechenskoe Reservoir (Sevastopol, Crimean Peninsula). In: A. B. Kitaev, O. V. Larchenko and V. G. Kalinin, eds., 2023. *Modern Problems of Reservoirs and their Catchments: Proceedings of the IX All-Russian Scientific-Practical Conference with International Participation (Perm, May 25-28, 2023)*. Perm: Perm State University. Vol. 1, pp. 76–80 (in Russian).

16. Lubkov, A.S. and Voskresenskaya, E.N., 2021. Neural Network Method for Climate Forecasting Water Content of the Chernorechensk Reservoir. *Monitoring Systems of Environment*, (2), pp. 16–28. https://doi.org/10.33075/2220-5861-2021-2-16-28 (in Russian).

17. McFeeters, S.K., 1996. The Use of the Normalized Difference Water Index (NDWI) in the Delineation of open Water Features. *International Journal of Remote Sensing*, 17(7), pp. 1425–1432. https://doi.org/10.1080/01431169608948714

18. Militino, A.F., Montesino-SanMartin, M., Pérez-Goya, U. and Ugarte, M.D., 2020. Using RGISTools to Estimate Water Levels in Reservoirs and Lakes. *Remote Sensing*, 12(12), 1934. https://doi.org/10.3390/rs12121934

19. Du, Y., Zhang, Y., Ling, F., Wang, Q., Li, W. and Li, X., 2016. Water Bodies' Mapping from Sentinel-2 Imagery with Modified Normalized Difference Water Index at 10-m Spatial Resolution Produced by Sharpening the SWIR Band. *Remote Sensing*, 8(4), 354. https://doi.org/10.3390/rs8040354

20. Kataev, M.Yu. and Bekerov, A.A., 2017. Methodology of the Water Objects Detection from Multi-Spectrum Satellite Measurements. *Proceedings of The Tusur University*, 20(4), pp. 105–108. https://doi.org/10.21293/1818-0442-2017-20-4-105-108 (in Russian).

Submitted 19.02.2026; accepted after review 04.03.2026;
revised 19.03.2026; published 30.06.2026.

About the authors:

Anna A. Aleskerova, Senior Researcher, Marine Hydrophysical Institute of RAS (2 Kapitanskaya St., Sevastopol, 299011, Russia), PhD (Geogr.), **ORCID ID: 0000-0003-1451-3440, ResearcherID: F-2966-2017, Scopus Author ID: 57021552600**, *annete08@mail.ru*

Nadezhda V. Vasilenko, Junior Researcher, Marine Hydrophysical Institute of RAS (2 Kapitanskaya St., Sevastopol, 299011, Russia), **ResearcherID: JZT-8108-2024, Scopus Author ID: 57358387000**, *nadinkot.nk@gmail.com*

Pavel N. Lishaev, Researcher, Marine Hydrophysical Institute of RAS (2 Kapitanskaya St., Sevastopol, 299011, Russia), PhD (Phys.-Math.), **Scopus Author ID: 57193071072, ResearcherID: A-7770-2019, ORCID ID: 0000-0002-5259-3309**, *pavellish@mail.ru*

Arseny A. Kubryakov, Deputy Director for Research, Marine Hydrophysical Institute of RAS (2 Kapitanskaya St., Sevastopol, 299011, Russia), DSc (Phys.-Math.), **Scopus Author ID: 37072750100, WoS ResearcherID: F-8921-2014, ORCID ID: 0000-0003-3561-5913**, *arskubr@yandex.ru*

Sergey V. Stanichny, Senior Researcher, Marine Hydrophysical Institute of RAS (2 Kapitanskaya St., Sevastopol, 299011, Russia), PhD (Phys.-Math.), **ORCID ID: 0000-0002-1033-5678, ResearcherID: F-8915-2014, Scopus Author ID: 6602344280**, *sstanichny@mail.ru*

Maria G. Grechushnikova, Leading Researcher, Lomonosov Moscow State University, Faculty of Geography (Leninskie Gory, GSP-1, Moscow, 119991, Russia), PhD (Phys.-Math.), **ORCID ID: 0000-0001-6376-2473, ResearcherID: L-5317-2013, Scopus Author ID: 6507726807**, *allavis@mail.ru*

Contribution of the authors:

Anna A. Aleskerova – paper concept, formulation of the study goals and objectives, calculations, information collection, data analysis, interpretation of results, writing the paper manuscript, preparation of graphic materials

Pavel N. Lishaev – calculations, data analysis, interpretation of results

Nadezhda V. Vasilenko – analysis of literary sources, information collection, interpretation of results, writing the text of the article, preparation of graphic materials

Arseny A. Kubryakov – scientific supervision of research, interpretation of results

Sergey V. Stanichny – scientific supervision of research, interpretation of results

Maria G. Grechushnikova – field work, bathymetric data collection

All the authors have read and approved the final manuscript.

ISSN 2413-5577, Ecological Safety of Coastal and Shelf Zones of Sea, No. 2, pp. 57–75 (2026)

Original paper

Features of the Functioning of the Microbial "Loop" in the Black Sea

A. V. Parkhomenko

A. O. Kovalevsky Institute of Biology of the Southern Seas of RAS, Sevastopol, Russia
e-mail: parkhomenko.46@mail.ru

Abstract
The article analyses biotic interactions (competition, predation and commensalism) between the main components of the microbial "loop" during summer and winter in the upper mixed layer of the Black Sea pelagic zone. In summer, the interaction between bacteria and phytoplankton in a phosphate-deficient environment resulted in a high contribution of bacteria and phytoplankton to the total phosphate uptake by microplankton, which was 47 and 53%, respectively, indicating a strong competition between bacteria and phytoplankton for uptake of this nutrient. The high total rate of phosphate uptake by bacteria and phytoplankton ($119\cdot10^{-4}$ μM·h^{-1}) and its low concentrations in the upper mixed layer ensured a short turnover time of 1.9 hours, which contributed to accelerated phosphate recycling in this layer. In the interaction (predator–prey) between protozoa and picofraction (bacteria + picophytoplankton), high values of the specific rate of phosphate excretion by protozoa (zooflagellates, ciliates) were noted. This suggests their active participation in the consumption of bacteria, picophytoplankton and heterotrophic nanoplankton, thus indicating the high functional activity of the microbial "loop". In winter, in the upper mixed layer above the pycnocline, at a temperature of 5.5–10°C, the production and daily coefficient P/B of bacteria, picophytoplankton, zooflagellates, and ciliates decreased significantly compared to the summer period, with the exception of high levels of phytoplankton biomass and production. The contribution of the picofraction (bacteria + pico-phytoplankton) to the total phosphate uptake decreased to 8% compared to summer. The average total rate of phosphate uptake by microplankton decreased to $15\cdot10^{-4}$ μM·h^{-1} relative to the summer period, with an interval of $9\cdot10^{-4}$–$24\cdot10^{-4}$ μM·h^{-1}. At the same time, the phosphate turnover time in the upper mixed layer increased to 38 hours, indicating a slowdown in its recycling and a low level of functional activity in the microbial "loop". A data analysis suggests that the uptake of nutrients by bacteria and phytoplankton and their excretion by protozoa are subject to seasonal fluctuations, which should be taken into account when calculating the annual balance of matter and energy in the Black Sea pelagic zone.

Keywords: Black Sea, microbial loop, bacteria, protozoa, picophytoplankton, nanophytoplankton, phosphate uptake, phosphate excretion

Acknowledgments: The study was carried out under IBSS state research assignment "Transformation of the structure and functions of marine pelagic ecosystems under conditions of anthropogenic impact and climate change" (state registration number 124030400057-4).

For citation: Parkhomenko, A.V., 2026. Features of the Functioning of the Microbial "Loop" in the Black Sea. *Ecological Safety of Coastal and Shelf Zones of Sea*, (2), pp. 57–75.

© Parkhomenko A. V., 2026

This work is licensed under a Creative Commons Attribution-Non Commercial 4.0 International (CC BY-NC 4.0) License

Оценка функциональной активности микробиальной «петли» в Черном море

А. В. Пархоменко

ФГБУН ФИЦ «Институт биологии южных морей имени А. О. Ковалевского РАН», Севастополь, Россия

e-mail: parkhomenko.46@mail.ru

Аннотация

Анализируются биотические взаимодействия – соревнование (конкуренция), хищничество и комменсализм – между основными компонентами микробиальной «петли» в летнее и зимнее время в верхнем перемешанном слое пелагиали Черного моря. В летний период во взаимодействии между бактериями и фитопланктоном в условиях дефицита фосфата в среде отмечался высокий вклад бактерий и фитопланктона в суммарное усвоение фосфата микропланктоном (47 и 53 % соответственно), что указывает на жесткую конкуренцию бактерий и фитопланктона в усвоении этого вещества. Высокая суммарная скорость усвоения фосфата бактериями и фитопланктоном ($119 \cdot 10^{-4}$ мкМ·ч$^{-1}$) и низкие его концентрации в верхнем перемешанном слое обеспечивали малое время его оборота (1.9 ч), что способствовало ускоренному рециклингу фосфата в этом слое. Во взаимодействии хищник – жертва между простейшими и пикофракцией (бактерии + пикофитопланктон) отмечалась высокая удельная скорость экскреции фосфата простейшими (зоофлагелляты, инфузории), что свидетельствует об их активном участии в выедании бактерий, пикофитопланктона и гетеротрофного нанопланктона. Это указывает на высокую функциональную активность микробиальной «петли». В зимний период в верхнем перемешанном слое над пикноклином при температуре 5.5–10 ºС продукция и коэффициент P/B за сутки бактерий, пикофитопланктона, зоофлагеллят и инфузорий относительно летнего периода резко снижались. Исключение составляли высокие показатели биомассы и продукции фитопланктона. Вклад пикофракции (бактерии + пикофитопланктон) в суммарное усвоение фосфата относительно летнего периода снижался до 8 %. Средняя суммарная скорость усвоения фосфата микропланктоном относительно летнего периода уменьшалась до $15 \cdot 10^{-4}$ с интервалом $(9–24) \cdot 10^{-4}$ мкМ·ч$^{-1}$. При этом время оборота фосфата в верхнем перемешанном слое возрастало до 38 ч, что указывает на замедление его рециклинга и низкий уровень функциональной активности МП. Анализ данных позволяет заключить, что усвоение биогенных веществ бактериями и фитопланктоном и их экскреция простейшими подвержены сезонным колебаниям, которые необходимо учитывать при расчете годового баланса вещества и энергии в пелагиали Черного моря.

Ключевые слова: Черное море, микробиальная петля, бактерии, простейшие, пикофитопланктон, нанофитопланктон, усвоение фосфата, экскреция фосфата

Благодарности: исследование выполнено в рамках государственного задания ФИЦ ИнБЮМ по теме «Трансформация структуры и функций экосистем морской пелагиали в условиях антропогенного воздействия и изменения климата» (№ госрегистрации 124030400057-4).

Для цитирования: *Пархоменко А. В.* Оценка функциональной активности микробиальной «петли» в Черном море // Экологическая безопасность прибрежной и шельфовой зон моря. 2026. № 2. С. 57–75. EDN PIVBVA.

Introduction

In recent decades, the role and interactions of microbial communities (viruses, bacteria, picophytoplankton, nanophytoplankton and protozoa) have received considerable attention, since the results of these studies provide deeper insight into the functioning mechanisms of plankton communities in marine and freshwater bodies [1–8]. The widely accepted concept of the microbial "loop" (ML), developed in [9], significantly expanded the understanding of the classical linear food chain (LFC). The components of the ML include picophytoplankton, nanophytoplankton, heterotrophic bacteria, protozoa (heterotrophic flagellates and ciliates) and viruses [9–11]. It follows from general reviews [6, 10] that the microbial food chain is an integral part of the marine and freshwater pelagic LFC in the transfer of matter and energy. Heterotrophic bacteria and protozoa are recognized as separate trophic links of the microbial food chain: they serve as an intermediate element in the transformation of matter from autotrophic organisms to metazoan plankton. Before entering the LFC, the main part of organic matter is transformed through trophic interactions between the principal components of the ML (picophytoplankton, nanophytoplankton, heterotrophic bacteria and protozoa) [11–13].

Along with phytoplankton, heterotrophic bacteria actively participate in the uptake and cycling of nutrients (nitrogen and phosphorus). Protozoa, by grazing on bacteria and picophytoplankton together with the nutrients accumulated in them, transform organic matter into mineral forms of nitrogen and phosphorus, subsequently excreting them into the environment, thereby influencing nutrient recycling [6]. Consequently, one of the most important functions of the ML is to enhance the level of nutrient recycling under conditions of low ambient concentrations, including owing to the small size of bacteria, picophytoplankton, nanophytoplankton and protozoa, which ensures a high level of metabolic intensity for these organisms [14]. Depending on seasonal variability, the total rate of uptake of mineral forms of nitrogen and phosphorus by bacteria and phytoplankton, the concentrations of these elements in the environment, the excretion rate by protozoa, and the turnover time of nutrients in the euphotic zone can vary from several days to several hours. This can serve as an indicator of the acceleration or deceleration of nutrient recycling in the Black Sea pelagic zone [15].

Phosphate uptake by bacteria and different phytoplankton fractions and phosphate excretion by protozoa are interrelated and depend on the physiological activity of these organisms, which throughout the year ensure either the acceleration or deceleration of nutrient recycling and, as a consequence, a particular level of functional activity of the ML. It should be noted that to date, the seasonal variability of the interaction intensity between the principal components of the ML and its functional activity in the Black Sea pelagic zone has been scarcely studied.

The aim of the paper is to estimate the seasonal variability of the functional activity of the ML in the Black Sea pelagic zone based on our own data on the rate of phosphate uptake by bacteria, pico-, nano- and microphytoplankton, and phosphate excretion by protozoa, as well as on literature data characterising the structural and functional indicators of bacteria, phytoplankton and protozoa.

Materials and Methods

In studying phosphate uptake by different size fractions of microplankton (bacteria + phytoplankton) in the open Black Sea under near-*in situ* conditions, we used our own data obtained for the summer [16] and winter [17] periods. The study material consisted of microplankton in water samples collected from various horizons of the euphotic zone using a rosette of 10-litre Niskin bottles of the MARK-III CTD profiling system. The methods of water sampling, incubation conditions for experimental bottles, filtration of water samples through membrane filters with different pore sizes taking into account vacuum pressure, preparation of samples with radioactive phosphorus, the efficiency of measuring ^{32}P radioactivity with different radiometric setups and the estimation of the phosphate uptake rate by microplankton are described in detail in [18–23].

In this paper, it was assumed that the microplankton fraction retained on filters with a pore size of 0.2–1.5 μm conditionally corresponded to bacteria; that retained on filters with a pore size of 0.2–3 μm corresponded to the picofraction (bacteria + picophytoplankton); that retained on filters with a pore size of 3–20 μm corresponded to nanophytoplankton; and that retained on a nylon sieve with a mesh size larger than 20 μm corresponded to microphytoplankton.

The phosphate uptake rate by different microplankton fractions was estimated using the radioisotope method with radioactive ^{32}P in the form of carrier-free orthophosphoric acid, taking into account several methodological features [15, 18, 19–22]. In winter, radiometry of membrane filters and water samples placed in standard 20 mL counting vials was performed on an automated liquid scintillation analyser 1219-Rack Beta (LKB Wallac) using OptiPhase Hisafe II scintillation cocktail at 95% counting efficiency for beta particles emitted by ^{32}P decay. In summer, the radioactivity of water samples and membrane filters was measured using a PSO2-0.8 device with a gas-discharge end-window counter SBT-13 in a lead shield DS-000 with a ^{32}P counting efficiency of no more than 45% (https://works.doklad.ru/view/14BuMVjpSUo/5.html).

In studies of phosphorus metabolism in microplankton, the method of measuring ^{32}P with a gas-discharge and a scintillation counters has often been applied; therefore, it became necessary to compare the data obtained with these counters and to calculate the absolute rate of phosphorus uptake by bacteria and phytoplankton. For this purpose, in methodological study [21] we performed experiments to measure ^{32}P radioactivity in the same water samples and membrane filters. The influence of the following factors was studied: the volume of the water aliquot, the addition of the scintillation cocktail (as well as its absence), the volume of filtered water and the radiometry conditions for membrane filters (with and without a backing under different counting geometries). Measurements were performed using an SBT-13 gas-discharge end-window counter and on a scintillation analyser (1219-Rack Beta), both with and without the addition of the scintillation cocktail to the vials being radiometrically measured.

Analysis of these data showed that currently three technical methods of measuring ^{32}P in the studied samples can be used, provided that identical ^{32}P counting conditions are maintained for water and filters with microplankton. However, it should be taken into account that when measuring ^{32}P with an SBT-13 gas-discharge end-window counter, it is necessary to ensure not only the appropriate counting geometry for the water aliquot and the filters with microplankton, but also identical backscattering conditions for beta particles. This is achieved by using aluminium backings of equal thickness (0.5 mm) for membrane filters and water aliquots. In this case, the estimation of balance convergence (when the radioactivity of water before filtration equals the sum of the radioactivities of the filter and filtrate according to ^{32}P radiometry) obtained on the RPS gas-discharge setup gave satisfactory counting error estimates of 1.19 (±0.11) [19]. Similar estimates were obtained when measuring ^{32}P on a scintillation analyser (1219-Rack Beta) for membrane filters with microplankton and water aliquots (volume up to 1.0 mL) without adding the scintillation cocktail (Cherenkov effect) into the counting vials. The same result was obtained when measuring ^{32}P on a scintillation detector with the addition of 10 mL of scintillation coctail. However, in this case, the water aliquot (volume not exceeding 0.1 mL) must be applied onto the same type of membrane filter that is used for filtering microplankton. This allows identical ^{32}P counting conditions for water and the membrane filter with microplankton to be created [19].

If the identity of radiometry conditions for water aliquots and membrane filters with microplankton is violated, the results of ^{32}P measurements using a gas-discharge end-window counter, compared with data obtained using a scintillation detector without adding the scintillation cocktail to counting vials, can be underestimated by a factor of 1.19 (±0.11), and with the addition of 10 mL of the scintillation cocktail to the counting vials by a factor of 1.82 (±0.36) [19].

In connection with the above, the methodological nuances revealed when measuring ^{32}P with gas-discharge and scintillation counters were taken into account by the author when generalising the data from the gas-discharge device in order to correctly determine the rate of phosphate uptake by microplankton in the summer period.

The phosphate uptake rate for the exposure time of experimental bottles under near-*in situ* conditions was calculated from the change in phosphate radioactivity on filters using the formula [22, 24]:

$$V = (r - r_1) \cdot P / (R \cdot U \cdot t), \quad (1)$$

where V is the phosphate uptake rate by microplankton, μM·h^{-1}; r is the ^{32}P radioactivity recorded on the filters with microplankton after the exposure of the experimental bottles, counts·min^{-1}; r_1 is the ^{32}P radioactivity sorbed on filters and planktonic organisms (when mercuric chloride was added to the bottles), counts·min^{-1}; R is the ^{32}P radioactivity in water at the initial time, counts·min^{-1}·L^{-1}; P is the phosphate concentration in seawater, μM; U is the volume of filtered water, L; t is the exposure time of the experimental bottles, h.

The phosphate turnover time in the studied layer was calculated as the ratio of the phosphate concentration in seawater to its uptake rate by microplankton. The phosphate concentration in seawater was measured using a standard method [1]. In summer, when a phosphate deficiency was observed in the photosynthetic zone, the isotope dilution method [25] was used for its measurement.

The calculation of phosphate excretion by heterotrophic organisms was based on literature data on the size and species structure of zooplankton obtained in the open Black Sea [26]. To estimate the contribution of different zooplankton systematic groups to the total phosphate excretion, literature data on the mean weight of dominant zooplankton species, the mean weight of animals belonging to particular trophoecological groups, and their biomass were used. In these works, zooplankton was presented in the form of trophoecological groups united by feeding type and relatively homogeneous in size: protozoa (*a*), nanophages (*f*), euryphages (*v*), Oithona (*s*), Sagitta (*p*), Noctiluca (*n*), Pleurobrachia (q_1), Aurelia (q_2), Mnemiopsis (q_3) [26]. The rate of phosphate excretion by planktonic animals was calculated based on the experimentally established equality of the metabolic rate measured as the oxygen consumption rate and the phosphate excretion rate [27]. The total rate of phosphate excretion by planktonic animals E_Φ (mg P·m^{-2}·day^{-1}) was calculated using the formula [28]:

$$E_\Phi = \sum_{i=a}^{q} R_i \cdot N_i \cdot Z_i \cdot F_i\,, \tag{2}$$

where R_i is the daily metabolic expenditure for the mean weight of an individual, µcal·ind^{-1}·day^{-1}; *i* is the index of the trophoecological group of animals to which the individual belongs; N_i is the biomass of organisms in the trophoecological group, mg·m^{-2}; Z_i is the phosphorus content per unit body weight and its caloric value, mg P·mg^{-1}·µcal^{-1}; F_i is the temperature correction, which was introduced when calculating the metabolic rate of heterotrophic organisms from different trophoecological zooplankton groups, taking into account their occurrence in layers above and below the thermocline, and was calculated using the formula $F = Q_{10}^{(t-20)/10}$, $Q_{10} = 2.25$.

Results and discussion

As can be seen from the diagram (see figure), the ML is an integral part of the classical LFC and expands the possibilities of studying the transformation and transfer of matter and energy in the LFC to higher trophic levels [11]. According to the conceptual principles of the ML, the interaction intensity between its main components was assessed considering three types of biotic interactions: competition, predation and commensalism [9]. Competition was considered as the interaction within the ML branch between heterotrophic bacteria and picophytoplankton, nanophytoplankton and microphytoplankton during phosphate uptake, while predation was considered as the interaction within the branch between protozoa (zooflagellates + ciliates) and the picofraction (bacteria + picophytoplankton). Commensalism was defined as the interaction within the ML branch between heterotrophic bacteria, picophytoplankton and protozoa, associated with the uptake of phosphate excreted by protozoa and bacteria during the transformation of dissolved organic matter (DOM), as well as by phytoplankton, both through vital activity and upon cell death and decay.

---

[1] Bordovsky, O.K. and Ivanenkov, V.N., eds., 1978. [*Methods of Hydrochemical Studies of the Ocean*]. Moscow: Nauka, 271 p. (in Russian).

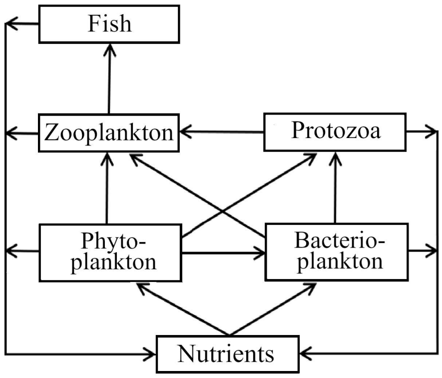

Diagram of the microbial "loop" and its connection with the classical linear food chain (according to [11])

Interaction in the ML branch between heterotrophic bacteria and picophytoplankton, nanophytoplankton and microphytoplankton during phosphate uptake in summer. In summer, a well-defined thermocline is observed in the Black Sea pelagic zone, limiting the supply of nutrients to the upper mixed layer (UML). As a consequence, low concentrations of nutrients, in particular phosphate, varying in the range of 0.02–0.07 μM, were recorded in the upper 0–40 m layer [4]. Against this background, analysis of multi-year data in the 0–100 m layer showed that the vertical profiles of the total phosphate uptake rate by microplankton (bacteria + phytoplankton), regardless of the season, exhibited a common pattern [15]. In summer, in the UML of the Black Sea pelagic zone, the average phosphate uptake rate by microplankton was $119 \cdot 10^{-4}$ $\mu M \cdot h^{-1}$, varying within the range of $(51–193) \cdot 10^{-4}$ $\mu M \cdot h^{-1}$, and its turnover time was 1.9 h. In the thermocline layer, the average value of this rate decreased to $(72 \pm 27) \cdot 10^{-4}$ $\mu M \cdot h^{-1}$, and in the cold intermediate layer at depths of 40 m and 50–100 m, the value dropped to a minimum of $(5 \pm 3) \cdot 10^{-4}$ $\mu M \cdot h^{-1}$ [15].

Analysis of the data obtained in summer in the UML on the contribution of heterotrophic bacteria, picophytoplankton, nanophytoplankton and microphytoplankton to the total phosphate uptake by microplankton (bacteria + phytoplankton) shows that the contribution of the bacterial fraction (size 0.2–1.5 μm) was 47%, while that of the picofraction (bacteria + picophytoplankton, size 0.2–3 μm) was 62% (Table) [15, 16]. The contribution of the picophytoplankton fraction (1.5–3 μm) was calculated as the difference between the contribution of the picofraction (bacteria + picophytoplankton) and that of the bacterial fraction (0.2–1.5 μm). The contributions of the picophytoplankton, nanophytoplankton and microphytoplankton fractions to the total phosphate uptake were 15, 33 and 5%, respectively, while the share of the bacterial fraction was 3.1, 1.4 and 9.4 times higher than the contribution of picophytoplankton, nanophytoplankton and microphytoplankton, respectively (see table). This indicates a strong competition for phosphate uptake between heterotrophic bacteria and picophytoplankton, nanophytoplankton and microphytoplankton.

Bacteria accounted for 47% and phytoplankton for 53% of the total phosphate uptake by microplankton. Similar ratios (with the bacterial share ranging from 50 to 96%) have been obtained in nutrient-poor freshwater and oceanic waters [24, 29, 30]. The ratio of the contributions of bacteria and phytoplankton to the total nutrient uptake during the annual cycle likely depends on a number of factors, such as

Average values of total phosphate uptake by bacterio- and phytoplankton (V, $\mu M \cdot h^{-1}$) and their contribution (%) in the upper mixed layer of the Black Sea pelagic zone in summer and winter

Fraction	Summer		Winter	
	$V \cdot 10^{-4}$	Contribution	$V \cdot 10^{-4}$	Contribution
Total bacteria and phytoplankton (over 0.2 μm)	119.0	100	15.00	100
Picofraction (bacteria + picophytoplankton) (0.2–3 μm)	73.7	62	1.20	8
Including:				
bacterial (0.2–1.5 μm)	55.9	47	0.75	5
picophytoplankton (1.5–3 μm)	17.8	15	0.45	3
Nanophytoplankton (3–20 μm)	39.3	33	4.35	29
Microphytoplankton fraction (over 20 μm)	6.0	5	9.45	63

Note: Information on the contribution of size fractions to the total uptake of phosphate by bacterial and phytoplankton according to [16, 17].

water temperature, light intensity, nutrient content, dissolved organic matter (DOM) concentration and the atomic C:N and C:P ratios in it. These factors influence the physiological activity of heterotrophic bacteria and the size and species structure of phytoplankton [15, 31].

Heterotrophic bacteria possess a number of structural and physiological features that ensure a high level of phosphate uptake relative to phytoplankton during the warm season when waters experience a nutrient deficiency. These features include: a high surface-to-volume ratio of bacterial cells; the presence of active transport systems; a twofold higher intracellular phosphorus content compared to phytoplankton cells (on average 3% of dry weight); and a high growth rate and short life cycle of bacteria [6, 24]. Heterotrophic bacteria not only participate in the transformation of DOM and particulate organic matter (POM) into inorganic forms of nitrogen and phosphorus with their subsequent release into the environment, but under certain conditions they are also capable of actively taking up these nutrients from the environment. At high C:N and C:P ratios in DOM, indicating a low nitrogen and phosphorus content in DOM and a nutrient deficiency in the environment, the rate of phosphate and ammonium uptake by heterotrophic bacteria increases, whereas the rate of mineralisation of these elements decreases [32].

The most efficient substrate utilisation at its minimum environmental concentration is achieved through an increase in the surface-to-volume ratio of organisms [33]. Studies conducted in spring–summer and autumn showed that at most horizons of the aerobic zone in the Black Sea pelagic zone, high values of this indicator were characteristic of bacteria, since the average volume of their single cells varied within 0.065–0.256 μm^3 (mean 0.097 μm^3) [34]. At the same time, phytoplankton biomass was formed mainly by coccolithophorids and dinoflagellates with an average cell volume of 456 μm^3 [35, 36]. A comparison shows that the average cell volume of bacteria is considerably smaller than that of phytoplankton cells, while the phosphorus content in bacterial cells is almost twice as high as in phytoplankton cells. This means that in summer, the advantage of bacteria in phosphate uptake is ensured both by their high surface-to-volume ratio and by their greater demand for phosphate uptake compared to phytoplankton. Most likely, in summer, in the euphotic zone of the Black Sea pelagic zone under phosphate deficiency, a significant portion of this element is taken up by heterotrophic bacteria. This is accompanied by competition between bacteria and picophytoplankton, nanophytoplankton and microphytoplankton in the process of phosphate uptake and a short turnover time of 1.9 h [15].

In the upper layer of the euphotic zone, the structural and physiological indicators of bacteria were characterised by high values: production varied on average from 20 to 50 $mg \cdot m^{-3} \cdot day^{-1}$, and the specific production (P/B) ranged from 0.5 to 0.7 day^{-1}, indicating a high level of physiological activity of bacteria [1]. With increasing depth in the 40–100 m layer, corresponding to the oxygen-deficient zone and the cold intermediate layer, bacterial production decreased 10–50-fold to 2–8 $mg \cdot m^{-3} \cdot day^{-1}$, and the P/B coefficient varied within 0.05–0.1 [1].

In summer and early autumn in the Black Sea, phytoplankton biomass was mainly formed by peridinians (20–75%) and small flagellates (10–60%). Coccolithophorids dominated in terms of abundance, but their contribution to total biomass was small, amounting to only 20% [35]. The mean monthly values of phytoplankton production in June–September were 270, 340, 340 and 390 $mg\ C \cdot m^{-2} \cdot day^{-1}$, respectively, with an average of 335 $mg\ C \cdot m^{-2} \cdot day^{-1}$ for the open Black Sea [37]. In the same region, the daily P/B coefficient of phytoplankton, calculated from the average primary production (400 $mg\ C \cdot m^{-2} \cdot day^{-1}$) and biomass (714 $mg\ C \cdot m^{-2}$) for July–September, was 0.56 day^{-1} [38].

As can be seen from the presented data, in summer, despite the nutrient deficiency in the euphotic layer, the structural and physiological indicators of biomass, primary production, and the daily P/B coefficient were high, indicating a relatively high physiological activity of phytoplankton. Therefore, in summer, in the upper heated layer within the ML branch in which bacteria and different phytoplankton fractions interact, heterotrophic bacteria play a key role in the transformation of organic carbon (from 40 to 80%) produced by primary producers [39].

The contribution of these bacteria to phosphate uptake is no less significant: they account for up to 47% of its total uptake by microplankton (Table). Under conditions of nutrient deficiency in the euphotic layer, the main role of bacteria is not the regeneration of inorganic nitrogen and phosphorus compounds, but their uptake from the environment and transfer along the microbial trophic chain to protozoa in the form of particles enriched with these elements.

Predator–prey relationships in the ML branch between protozoa and the picofraction (bacteria + picophytoplankton) in summer. According to literature data, protozoa in the Black Sea pelagic zone include colourless flagellates, ciliates and amoebae. The highest abundance among colourless flagellates in open seas is represented by heterotrophic (achlorophyllous) or mixotrophic representatives of the classes Phytomastigophorea and Zoomastigophorea [40].

In spring–summer and autumn, in the aerobic zone of the open Black Sea, the biomass of heterotrophic nanoflagellates (zooflagellates and dinoflagellates) (less than 10 μm), as well as small (less than 25 μm) and large (over 25 μm) ciliates in the 0–100 m layer, were concentrated predominantly in the 0–50 m layer [41–44]. In summer, the main biomass of heterotrophic nanoflagellates smaller than 10 μm in the 0–50 m layer was 70 $mg \cdot m^{-3}$. Below the thermocline, in the 50–100 m layer, as the temperature decreased from 10 to 7°C, the biomass of zooflagellates decreased from 10 to 2 $mg \cdot m^{-3}$ (in the core of the cold intermediate layer) [41]. In later studies, a similar pattern of vertical distribution of heterotrophic nanoflagellate production was noted in spring–summer and autumn as well [43].

On the whole, a similar pattern of vertical distribution of abundance and biomass was also observed for ciliates, as the ciliate community was concentrated mainly in the 0–50 m layer, accounting for 88.4–96.0% of the total abundance and 79.4–96.3% of the total biomass in the water column of the sea's aerobic zone. Large ciliates (over 25 μm) with a holozoic feeding mode predominated over the other size groups of ciliates. In autumn, their biomass in the 0–50 m layer accounted for 51.3%, and from May to June, 28.1–66.6% of the total ciliate biomass in the water column [44].

According to literature data, in the aerobic zone of the open Black Sea, the pattern of vertical distribution of ciliates may be determined by: 1) the availability of food (its shortage limits the vertical distribution of ciliates in the 0–100 m layer); 2) the ability of ciliates to perform vertical migrations [44]; 3) the effect of low temperatures (7–10°C) in the 50–100 m layer on the physiological activity of protozoa [26]. The influence of temperature on the vertical distribution of protozoa can be confirmed by the limited structural and physiological indicators of protozoa obtained for heterotrophic nanoflagellates in summer (June) in the upper layer

(0–44 m) and the 50–70 m layer of the Black Sea (its open part), which differ in temperature regime [42]. The average values of biomass, production and the P/B coefficient of heterotrophic nanoplankton in the 0–44 m layer were 16.2 $mg \cdot m^{-3}$, 11.1 $mg \cdot m^{-3} \cdot day^{-1}$ and 0.68, respectively. However, with increasing depth and decreasing temperature in the 50–70 m layer, a sharp decline in their biomass from 2.93 to 0.52 $mg \cdot m^{-3}$, a decline in production from 0.68 to 0.11 $mg \cdot m^{-3} \cdot day^{-1}$, and a decrease in the specific production P/B value by a factor of 3.2, averaging 0.21, were observed [42].

Studies of the nutrition of nanoflagellates smaller than 10 μm show that, being well adapted to grazing on bacteria and picophytoplankton at natural concentrations, they are the main consumers of these organisms. Zooflagellates exhibit higher activity in consuming bacteria and picophytoplankton than dinoflagellates [6]. At the same time, for heterotrophic nanoplankton larger than 10 μm, bacteria were not the main component of the diet, but their biomass in autumn reached 49–76% of the total heterotrophic nanoplankton biomass, and in May–June it varied from 29 to 64%. These data indicate the key role of heterotrophic dinoflagellates, cryptomonads and chrysomonads in the functioning of the plankton community of the Black Sea aerobic zone, as they serve as an important component of the fraction of food particles ranging from 2 to 20 μm in size [43]. Ciliates consume not only bacteria and picophytoplankton, but also, to a considerable extent, zooflagellates and dinoflagellates [44, 45].

Thus, the consumers of bacteria and picophytoplankton are zooflagellates, dinoflagellates and ciliates. Ciliates consume not only bacteria, but also zooflagellates and dinoflagellates. However, the main component of the diet of protozoa (60–80% of the total food volume consumed per hour) is composed of bacteria and picophytoplankton. On the whole, in various regions of the Black Sea, the ciliate community grazed on from 0.04 to 20.9% of daily primary production and from 1.0 to 44.2% of daily bacterial production [46]. It should be noted that during the period of spring and summer phytoplankton development in the Black Sea, intensive bacterial growth was observed despite high rates of bacterial grazing by protozoa and lysis by viruses and bacterial biomass reached values typical of temperate latitudes [6]. The consumers of bacteria, picophytoplankton, heterotrophic nanoflagellates and ciliates include representatives of microzooplankton, such as fish larvae, nauplii, tintinnids, radiolarians and appendicularians (*Oikopleura dioica*). They act as intermediaries in the transfer of matter and energy from the ML to the LFC [6, 11].

During feeding, protozoa, microzooplankton and mesozooplankton release DOM and POM into the environment [47], as well as inorganic forms of nitrogen and phosphorus [26, 32, 48, 49], which are actively taken up by bacteria, picophytoplankton, nanophytoplankton and microphytoplankton in the euphotic zone. In summer and early autumn, the main internal sources of nutrients (nitrogen and phosphorus) in the euphotic layer of the Black Sea include their excretion by protozoa and mesozooplankton, as well as the release of dissolved organic substances resulting from the lysis of bacterial and phytoplankton cells by viruses. Viruses close the nutrient cycle in chemical-biological processes by returning mineral compounds to the environment, thereby partially replenishing their pool for re-uptake by bacteria and phytoplankton [6]. The rate of these processes affects both the content of nutrients and DOM in the euphotic layer and the level of primary production.

Against this background, the results of studies on phosphate excretion by protozoa, mesozooplankton and gelatinous macroplankton in the Black Sea pelagic zone are of interest [26]. These results, obtained during the annual cycle, allow for an indirect assessment of the intensity of the predator–prey interaction between protozoa and the picofraction (bacteria + picophytoplankton). According to estimates by the author of [26], the average annual contributions of protozoa, mesozooplankton and gelatinous macroplankton in the Black Sea pelagic zone to the total phosphate excretion by zooplankton was 51, 32 and 17%, respectively; that is, protozoa make the greatest contribution to the total phosphate excretion by zooplankton. Comparable values of the protozoan contribution (47%) were also obtained in a mesotrophic area of the tropical Pacific Ocean [28]. In marine oligotrophic waters, the contribution of heterotrophic nanoplankton 1–15 μm in size to total ammonium excretion varied from 50 to 64% [48].

According to our data [26], during the warm season, the average specific rates of phosphate excretion normalised to the dry weight of zooflagellates and zooflagellates + ciliates in the Black Sea pelagic zone were 29.01 and 19.43 $\mu g\ P \cdot mg^{-1} \cdot day^{-1}$, respectively. This indicates a high level of metabolic intensity, in contrast to the values of this indicator for mesozooplankton – 3.70 $\mu g\ P \cdot mg^{-1} \cdot day^{-1}$ and gelatinous macroplankton – 0.05 $\mu g\ P \cdot mg^{-1} \cdot day^{-1}$. During the cold season, the average value of this indicator for zooflagellates decreased to 15.41 $\mu g\ P \cdot mg^{-1} \cdot day^{-1}$, for protozoa (zooflagellates + ciliates) – to 9.75 $\mu g\ P \cdot mg^{-1} \cdot day^{-1}$, for mesozooplankton – to 1.55 $\mu g\ P \cdot mg^{-1} \cdot day^{-1}$, and for gelatinous macroplankton – to 0.03 $\mu g\ P \cdot mg^{-1} \cdot day^{-1}$ [26].

The specific excretion rate of nutrients is inversely proportional to the size of zooflagellates, dinoflagellates and ciliates. Therefore, zooflagellates smaller than 10 μm and dinoflagellates larger than 10 μm play a key role in the excretion of ammonium and phosphate [26, 32]. In the warm period, as a result of the predator–prey interaction between protozoa and the picofraction (bacteria + picophytoplankton), the excretion of nutrients (nitrogen and phosphorus) by protozoa ensures the replenishment of the nutrients taken up by bacteria and picophytoplankton from the euphotic environment, as well as a feedback loop of nutrient fluxes within the ML [6].

In summer, in the predator–prey interaction branch between the picofraction (bacteria + picophytoplankton) and protozoa, not only was a high level of nutrient (ammonium and phosphate) excretion by protozoa observed, but also clearly pronounced commensalism between protozoa and the picoplankton. This interaction is manifested in the uptake by bacteria, picophytoplankton and nanophytoplankton of phosphate excreted by protozoa and zooplankton, as well as in the uptake and transformation by bacteria of DOM produced during phytoplankton vital activity and the breakdown of its cells upon grazing by zooplankton. Commensalism was most active in the warm season during the uptake by bacteria, picophytoplankton, nanophytoplankton and microphytoplankton of phosphate released by protozoa, mesozooplankton and gelatinous macroplankton. The average annual contribution of protozoa to the total phosphate excretion by zooplankton during this period was 51% [2]. Therefore, it can be assumed that in summer, under phosphate deficiency in the euphotic layer of the Black Sea pelagic zone, commensalism plays an important role in maintaining biological balance in the functioning of the main ML components and the plankton community as a whole.

Thus, one of the most important functions of the ML is manifested in the active predator–prey interaction between protozoa and the picofraction (bacteria + picophytoplankton), which ensures a high rate of phosphate excretion by protozoa into the euphotic zone. By actively taking up nutrients and having small cell sizes with a low sinking rate from the euphotic zone, bacteria, picophytoplankton and nanophytoplankton are able to retain nutrients within the plankton community for a long time, ensuring their multiple recirculation. This, in turn, contributes to the acceleration of nutrient recycling, prevents its rapid removal from the euphotic layer and thereby supports a high functional level of the ML.

Relationships between bacteria, protozoa, picophytoplankton, nanophytoplankton and microphytoplankton in the functioning of the ML in winter. In winter, in the upper mixed layer (0–30 m) of the open Black Sea at a temperature of 5.5–10°C, a rise in the upper boundary of the main pycnocline, intensive convective mixing of waters and turbulent diffusion were observed. As a result, the concentration of nutrients (nitrogen and phosphorus, in particular phosphate) increased significantly compared to the summer period, reaching 0.11–0.6 μM. The phosphate concentration was 2–4 times higher than the level limiting phytoplankton development [3].

At the same time, the average total rate of phosphate uptake by microplankton decreased significantly compared to the summer period – to an average of $15 \cdot 10^{-4}$ μM·h^{-1}, varying within the range of $(9–24) \cdot 10^{-4}$ μM·h^{-1} (Table). High phosphate concentrations in the upper 0–40 m layer and the low rate of phosphate uptake by microplankton contributed to an increase in the phosphate turnover time – on average up to 38 h, indicating a slowdown in the recycling of this nutrient relative to the summer period [15]. The contribution of the picofraction (bacteria + picophytoplankton) to the total phosphate uptake sharply decreased and did not exceed 8%. The shares of bacteria and picophytoplankton were 5 and 3%, respectively, which was 9.4 and 5 times less than in summer (Table).

The observed decrease in the rate of phosphate uptake by bacteria and picophytoplankton and phosphate excretion by protozoa is largely associated with the effect of low water temperature (5.5–10°C) on their physiological activity. This is fully consistent with the results of studies on the influence of abiotic and biotic factors on the physiological activity of bacteria, picophytoplankton and protozoa during the cold season in water bodies of temperate latitudes, according to which the activity of these organisms, mainly regulated by temperature, decreases upon water cooling [2, 15, 26, 31].

In the winter–early spring period, when high values of biomass and primary production were observed and DOM was actively released by phytoplankton, the values of production and the daily P/B coefficient of bacteria were minimal compared to the summer period. According to data from [2], bacterial biomass in winter varied within 80–120 mg·m^{-3}. On average, it was 100 mg·m^{-3} and remained approximately at the same level as in summer (99 mg·m^{-3}). The low level of bacterial biomass was primarily due to reduced bacterial production – on average 12.5 mg·m^{-3}·day^{-1} (from 10 to 15 mg·m^{-3}·day^{-1}) and daily specific production values P/B of 0.1 (from 0.08 to 0.15) [2]. The average values of bacterial production and P/B were 3.7–5.5 times lower than in summer.

A similar downward trend in functional indicators was also noted for protozoa. Thus, in summer, with increasing depth and a sharp temperature drop in the 50–70 m layer of the open Black Sea, a decrease in the biomass of nanoheterotrophs was observed relative to the upper layer (0–44 m): from 2.93 to 0.52 mg·m^{-3} (by a factor of 5.6), a decrease in production from 0.63 to 0.11 mg·m^{-3}·day^{-1} (by a factor of 5.7) and a decrease in daily specific production P/B by a factor of 3.2, averaging 0.21 [42].

To assess the physiological activity of picophytoplankton in summer and winter, the results of seasonal variability in the trophodynamics of picophytoplankton obtained in the surface layer of coastal waters at the entrance to Sevastopol Bay were used [7]. In summer, the average values of the daily specific production of picophytoplankton and its grazing were 0.47 and 0.80, respectively, and were 1.9 and 2.7 times higher than the average values obtained in winter [7]. Consequently, in winter, in the Black Sea pelagic zone, a significant decrease in the physiological activity of heterotrophic bacteria, picophytoplankton and protozoa was observed, which contributed to the weakening of their biotic interactions (competition, predation, commensalism) and, as a result, a decline in the functional activity of the ML.

However, a different situation was observed with regard to nanophytoplankton and microphytoplankton. The contribution of nanophytoplankton to the total phosphate uptake by microplankton in winter was 29%, which almost corresponded to the contribution value (33%) for the summer period (Table). The contribution of the microphytoplankton fraction with a cell size over 20 μm averaged 63%, which was 12.6 times higher than in summer. Thus, the total contribution of the nanophytoplankton and microphytoplankton fractions was 92%, indicating the dominance of phytoplankton in phosphate uptake relative to heterotrophic bacteria. This is due to the predominance of cold-adapted diatom species in the phytoplankton composition and the absence of competition between these algae and bacteria in the total phosphate uptake (Table). The mean monthly values of phytoplankton production in January–March in the central regions of the open Black Sea were high, amounting to 420, 685 and 700 mg C·m^{-2}·day^{-1}, respectively [37]. The daily P/B coefficient calculated for the entire phytoplankton community in the water column was 0.25, with an average primary production value for February and March of 600 mg C·m^{-2}·day^{-1} and a phytoplankton biomass of 2381 mg C·m^{-2} [38].

Thus, the average indicators of primary production and phytoplankton biomass in winter were 1.5 and 3.3 times higher than in summer [38]. The high values of primary production and phytoplankton biomass in the upper layer above the pycnocline in the open Black Sea during the winter–early spring period were mainly caused by the high position of the pycnocline, an increase in the concentration of nutrients (nitrogen and phosphorus), and the progressive increase in the level of solar radiation. To a lesser extent, these processes were regulated by temperature, which together created favourable conditions for the growth and development of cold-adapted diatoms [3, 37]. Moreover, the observed increase in phytoplankton biomass and production in the upper 0–40 m layer is largely associated with a weakening of zooplankton grazing pressure on phytoplankton at low water temperatures (5.5–10°C), which affects the metabolic rate reduction of zooplankton organisms [3, 26].

Conclusion

Analysis of the literature and our own data showed that in the competition interaction branch between heterotrophic bacteria and various size fractions of phytoplankton in summer in the UML, a high contribution of bacteria (47%) and phytoplankton (53%) to the total phosphate uptake by microplankton was observed. The picofraction (bacteria + picophytoplankton) accounted for 62%, indicating its predominant role in phosphate uptake. In the predator–prey interaction branch between the picofraction (bacteria + picophytoplankton) and protozoa, the grazing of the picofraction was accompanied by a high specific rate of phosphate excretion (29.01 and 19.43 μg P·mg^{-1}·day^{-1}, normalised to the dry weight of zooflagellates and zooflagellates + ciliates, respectively). The contribution of protozoa to the total excretion by zooplankton was 51%. Since the specific phosphate excretion rate is inversely proportional to the size of zooflagellates, dinoflagellates and ciliates, zooflagellates and dinoflagellates smaller than 10 μm play a key role in phosphate excretion. Against this background, commensalism was actively noted in the branch between protozoa and the picofraction, manifested in the uptake by mesozooplankton and gelatinous macroplankton of phosphate excreted by protozoa. Heterotrophic bacteria actively participate not only in the utilisation of DOM and POM but also in the uptake of nutrients (nitrogen and phosphorus). In summer, the main components of the ML are bacteria, picophytoplankton and nanophytoplankton and protozoa, which play a key role in regulating phosphate uptake and excretion, ensuring the acceleration of its recycling and indicating a high level of functional activity of the ML. In winter, with a decrease in temperature in the UML, a substantial decrease (relative to the summer period) was observed in the average values of the specific production of heterotrophic bacteria by a factor of 3.7, the P/B coefficient for picophytoplankton and its grazing by a factor of 1.9 and 2.7, respectively, and the production and P/B coefficient for heterotrophic nanoplankton by a factor of 5.7 and 3.2, respectively. The decline in the physiological activity of heterotrophic bacteria, picophytoplankton and protozoa contributed to the weakening of their biotic interactions among the main components of the ML, leading to a slowdown in phosphate recycling in the environment and a decrease in the level of functional activity of the ML. The materials considered above allow us to conclude that the intensity of microbiological processes in the nitrogen and phosphorus cycle is subject to significant seasonal fluctuations, which should be taken into account when calculating the annual balance of matter and energy in the Black Sea pelagic zone.

REFERENCES

1. Sorokin, Yu.I. and Avdeev, V.A., 1991. Bacterial Production and Chemosynthesis. In: M. E. Vinogradov, ed., 1991. [*Variability of the Black Sea ecosystem: Natural and Anthropogenic Factors*]. Moscow: Nauka, pp. 157–166 (in Russian).
2. Sorokin, Jy.I., Sorokin, P.Ju., Sorokin, O.V., Sorokin, D.Ju. and Sukhomlin, A.V., 1992. Distribution and Microflora Functional Activity in the Water Column of the Black Sea in Winter-Early Spring 1991. In: IO RAS, 1992. *Ecosystem of the Open Black Sea in Winter*. Moscow: Institute of Oceanology RAS, 1992, pp. 89–102 (in Russian).
3. Sorokin, Jy.I., Sukhomlin, A.V. and Sorokina, O.V., 1992. Phytoplankton Primary Production in the Black Sea in Winter-Early Spring 1991. In: IO RAS, 1992. *Ecosystem of the Open Black Sea in Winter*. Moscow: Institute of Oceanology RAS, pp. 72–76 (in Russian).
4. Vedernikov, V.I. and Demidov, A.B., 1997. Vertical Distribution of Primary Production and Chlorophyll During Different Seasons in the Deep Regions of the Black Sea. *Oceanology*, 37(3), pp. 376–384.
5. Azam, F., 1998. Microbial Control of Oceanic Carbon Flux: the Plot Thickens. *Science*, 280(5364), pp. 694–696. https://doi.org/10.1126/science.280.5364.694
6. Kopylov, A.I. and Kosolapov, D.B., 2011. [*Microbial "Loop" on Planktonic Communities in Marine and Fresh-Water Ecosystems*]. Izhevsk: KnigoGrad, 332 p. (in Russian).
7. Mukhanov, V.S., Rylkova, O.A., Churilova, T.Y., Sakhon, E.G. and Pimenov, N.V., 2016. Structure and Seasonal Trophodynamics of Picophytoplankton in Sevastopol Bay and Adjacent Waters (the Black Sea). *Microbiology*, 85(5), pp. 553–561. https://doi.org/10.1134/S002626171605012X
8. Mukhanov, V., Sakhon, E., Rodionova, N. and Tsai A.-Y., 2022. *Journal of Marine Systems*, 234, 103779. https://doi.org/10.1016/j.jmarsys.2022.103779
9. Azam, F., Fenchel, T., Field, J.G., Gray, J.S., Meyer-Reil, L.A. and Thingstad F., 1982. The Ecological Role of Water – Column Microbes in the Sea. *Marine Ecology Progress Series*, 10, pp. 257–263. https://doi.org/10.3354/meps010257
10. Pace, M.L., 1993. Heterotrophic Microbial Processes. In: S. R. Carpenter and J. F. Kitchell, eds., 1993. *The Trophic Cascade in Lakes*. Cambridge: Cambridge University Press. pp. 252–277.
11. Boulion, V.V., 2002. [The Structure and Function of the "Microbial Loop" in the Plank-ton of Lake Ecosystems]. *Biologiya Vnutrennih Vod*, (2), pp. 5–14 (in Russian).
12. Baines, S.B. and Pace, M.L., 1991. The Production of Dissolved Organic Matter by Phytoplankton and Its Importance to Bacteria: Patterns Across Marine and Freshwater Systems. *Limnology and Oceanography*, 36(6), pp. 1078–1090. https://doi.org/10.4319/lo.1991.36.6.1078
13. Sommaruga, R., 1995. Microbial and Classical Food Webs: a Visit to a Hypertrophic Lake. *FEMS Microbiology Ecology*, 17(4), pp. 257–270. https://doi.org/10.1016/0168-6496(95)00030-E
14. Boulion, V.V., Nikulina, V.N., Pavelyeva, E.B., Stepanova, L.A. and Khlebovich, T.V., 1998. Biotic Interactions in the Ecosystem of a Potential Eutrophic Lake. *Doklady Akademii Nauk*, 359(2), pp. 277–279 (in Russian).
15. Parkhomenko, A.V., 2009. Seasonal Variability of Mineral Phosphorus Uptake by Microplankton in Deep-Water Area of the Black Sea. *Marine Ekological Journal*, 8(2), pp. 5–23 (in Russian).
16. Parkhomenko, A.V., 2009. Phosphates Uptake by Different Size Fractons of Microplankton in Open Part of the Black Sea. *Ecology of the Sea*, 77, pp. 5–10 (in Russian).

17. Parkhomenko, A.V., 2000. Quantitative Estimation of Phosphate Uptake by Microplankton in the Black Sea During Winter Period. *Ecology of the Sea*, 51, pp. 14–19 (in Russian).
18. Parkhomenko, A.V., 1984. The Use of Phosphorus-32 in Estimation of the Membrane Filter Retentivity in Experiments with Microplankton. *Gidrobiologicheskiy Zhurnal*, 20(2), pp. 76–79 (in Russian).
19. Popovichev, V.N. and Parkhomenko, A.V., 2001. Methodological Aspects of the Phosphorus-32 Beta-Emission Registration by the Gas-Discharge and Scintillation Counters in the Investigations of the Phosphoric Metabolism of the Sea Particulate Matter. *Ecology of the Sea*, 56, pp. 107–112 (in Russian).
20. Parkhomenko, A.V. and Kirikova, M.V., 2004. Uptake and Turnover Time of Inorganic Phosphorus in Black Sea Waters over the Autumn Season. *Marine Ekological Journal*, 3(2), pp. 5–23 (in Russian).
21. Popovichev, V.N. and Egorov, V.N., 1992. Uptake of Inorganic Phosphorus by Suspended Matter in the Photic Zone. In: Polikarpov, G.G., 1992. *Molismology of the Black Sea*. Kiev: Naukova Dumka, pp. 62–70 (in Russian).
22. Popovichev, V.N. and Egorov, V.N., 2003. Phosphorus Exchange of Natural Suspended Matter in the Estuaries of Danube and Corukh Rivers. *Marine Ekological Journal*, 2(1), pp. 83–97 (in Russian).
23. Gutelmakher, B.L. and Pashkevich, A.I., 1987. [Methods for Measuring the Rates at which Inorganic Phosphorus is Converted into Seston and the Availability of this Element to Algae]. In: N. A. Petrova and B. L. Gutelmakher, eds., 1987. [*Elements of Phosphorus Turnover in Water Bodies*]. Leningrad: Nauka, pp. 32–39 (in Russian).
24. Sorokin, Yu.I., 1985. [Quantitative Assessment of Mineral Phosphorus Fluxes in Pelagic Plankton Communities]. *Zhurnal Obshchey Biologii*, 46(5), pp. 606–624 (in Russian).
25. Parkhomenko, A.V., 1984. Determination of Low Concentrations of Mineral Phosphorus in the Sea Water with Application of ^{32}P. *Gidrobiologicheskiy Zhurnal*, 20(3), pp. 92–96 (in Russian).
26. Parkhomenko, A.V., 2005. Phosphorus Excretion by Zooplankton in the Black Sea. *Marine Ekological Journal*, 4(4), pp. 17–32 (in Russian).
27. Gutelmakher, B.L., 1986. [*Plankton Metabolism as a Unified Whole: Trophometabolic Interactions Between Zooplankton and Phytoplankton*]. Leningrad: Nauka, 154 p. (in Russian).
28. Lebedeva, L.I., 1987. [Planktonic Animals and Phosphorus Regeneration in the Ocean]. *Okeanologiya*, 27(6), pp. 980–984 (in Russian).
29. Vadstein, O., Olsen, Y. and Reinertsen, H., 1993 The Role of Planktonic Bacteria in Phosphorus Cycling in Lakes – Sink and Link. *Limnology and Oceanography*, 38(7), pp. 1539–1544. https://doi.org/10.4319/lo.1993.38.7.1539
30. Donald, K.M., Joint, I., Rees, A.P., Woodward, E.M.S. and Savidge, G., 2001. Uptake of Carbon, Nitrogen and Phosphorus by Phytoplankton Along the 20°W Meridian in the NE Atlantic between 57.5°N and 37°N. *Deep Sea Research Part II: Topical Studies in Oceanography*, 48(4–5), pp. 873–897. https://doi.org/10.1016/S0967-0645(00)00102-8
31. Shish, F.-K. and Ducklow, H.W., 1994. Temperature Regulation of Heterotrophic. Bacterioplankton Abundance, Production, and Specific Growth Rate in Chesapeake Bay. *Limnology and Oceanography*, 39(6), pp. 1243–1258. https://doi.org/10.4319/lo.1994.39.6.1243
32. Goldman, J.C. and Dennett, M.R., 1991. Ammonium Regeneration and Carbon Utilization by Marine Bacteria Grown on Mixed Substrates. *Marine Biology*, 109(3), pp. 369–378. https://doi.org/10.1007/BF01313502

33. Dolan, J.R., 1997. Phosphorus and Ammonia Excretion by Planktonic Protists. *Marine Geology*, 139(1–4), pp. 109–122. https://doi.org/10.1016/S0025-3227(96)00106-5

34. Sazhin, A.F. and Kopylov, A.I., 1989. Bacterioplankton in the Oxygen Zone of the Black Sea Open Area. In: M. E. Vinogradov, M. V. Flint, eds., 1989. [*The Structure and Productivity Characteristics of Planktonic Communities in the Black Sea*]. Moscow: Nauka, pp. 122–139 (in Russian).

35. Senichkina, L.G., Georgieva, L.V., Nesterova, D.A., Fashchuk, D.Ya and Lifshiz, A.V., 1991. Phytoplankton of the Black Sea in Summer Period, 1989: Biomass and Connection with Hydrological Conditions. In: M. E. Vinogradov, ed., 1991. [*Variability of the Black Sea ecosystem: Natural and Anthropogenic Factors*]. Moscow: Nauka, pp. 157–166 (in Russian).

36. Churilova, T.Y., Berseneva, G.P. and Georgieva, L.V., 2004. Variability of the Biooptical Characteristics of Phytoplankton in the Black Sea. *Oceanology*, 44(2), pp. 192–204.

37. Vedernikov, V.I. and Demidov, A.B., 1992. Seasonal Variability of the Primary Production and Chlorophyll in the Open Regions of the Black sea. In: M. E. Vinogradov, ed., 1992. *Ecosystem of the Open Black Sea in Winter*. Moscow: Institute of Oceanology RAS, pp. 77–89 (in Russian).

38. Shushkina, E.A. and Vinogradov, M.E., 1991. [Long-Term Changes in Plankton Biomass in the Open Waters of the Black Sea]. *Okeanologiya*, 31(6), pp. 973–980 (in Russian).

39. Ducklow, H.W., 1999. The Bacterial Component of the Oceanic Euphotic Zone. *FEMS Microbiology Ecology*, 30(1), pp. 1–10. https://doi.org/10.1016/S0168-6496(99)00031-8

40. Vinogradov, M.E., Sapozhnikov, V.V. and Shushkina, E.A., 1992. [*Ecosystem of the Black Sea*]. Moscow: Nauka, 112 p. (in Russian).

41. Moiseev, E.V., 1980. [Zooflagellates from the Open Waters of the Black Sea]. In: M. E. Vinogradov, ed., 1980. [*Pelagic Ecosystems of the Black Sea*]. Moscow: Nauka, pp. 174–179 (in Russian).

42. Kopylov, A.I. and Sazhin, A.F., 1989. Reproduction Rate and Production of Heterotrophic Nanoplankton in the Open Areas of the Black Sea. In: M. E. Vinogradov and M. V. Flint, eds., 1989. [*The Structure and Productivity Characteristics of Planktonic Communities in the Black Sea*]. Moscow: Nauka, pp. 180–187 (in Russian).

43. Kopylov, A.I. and Sazhin, A.F., 1989. Heterotrophic Nanoplankton in the Oxygen Zone of the Black Sea. In: M. E. Vinogradov and M. V. Flint, eds., 1989. [*The Structure and Productivity Characteristics of Planktonic Communities in the Black Sea*]. Moscow: Nauka, pp. 139–155 (in Russian).

44. Kopylov, A.I., 1989. Ciliates of the Oxygen Zone of the Black Sea. In: M. E. Vinogradov and M. V. Flint, eds., 1989. [*The Structure and Productivity Characteristics of Planktonic Communities in the Black Sea*]. Moscow: Nauka, pp. 156–172 (in Russian).

45. Fenchel, T.S., 1986. The Ecology of Heterotrophic Microflagellates. In: K. C. Marshall, ed., 1986. *Advances in Microbial Ecology*. Boston: Springer. Vol. 9, pp. 35–42. https://doi.org/10.1007/978-1-4757-0611-6_2

46. Kopylov, A.I. and Tumantseva, N.I., 1991. Nano- and Microplankton Protozoans in the Oxygen Zone of the Black Sea in Spring, 1988. In: M. E. Vinogradov, ed., 1991. [*Variability of the Black Sea ecosystem: Natural and Anthropogenic Factors*]. Moscow: Nauka, pp. 118–196 (in Russian).

47. Nagata, T., Takai, K., Kawabata, K., Nakanishi, M. and Urabe, J., 1996. The Trophic Transfer via Picoplankton – Flagellate – Copepod Food Chain During a Picocyanobacterial Bloom in Lake Biwa. *Archiv für Hydrobiologie*, 137(2), pp. 145–160. https://doi.org/10.1127/archiv-hydrobiol/137/1996/145

48. Le Corre, P., Wafar, M., L'Helguen, S. and Maguer, J.F., 1996. Ammonium Assimilation and Regeneration by Size-Fractionated Plankton in Permanently Well-Mixed Temperature Waters. *Journal of Plankton Research*, 18(3), pp. 355–374. https://doi.org/10.1093/plankt/18.3.355

49. Harrison, W.G., 1992. Regeneration of Nutrients. In: P. G. Falkowski, A. D. Woodshed, K. Vivirito, eds., 1992. *Primary Productivity and Biogeochemical Cycles in the Sea*. New York: Plenum press, pp. 385–407. https://doi.org/10.1007/978-1-4899-0762-2_21

Submitted 17.11.2025; accepted after review 14.02.2026;
revised 19.03.2026; published 30.06.2026

About the author:

Aleksandr V. Parkhomenko, Senior Researcher, A. O. Kovalevsky Institute of Biology of the Southern Seas of the Russian Academy of Sciences (2 Nakhimov Ave., Sevastopol, 299011, Russia), PhD (Biol.), **ORCID ID: 0000-0002-4070-434X**, **Scopus Author ID: 7006612604**, **ResearcherID: W-3623-2019**, *parкhomenko.46@mail.ru*

The author has read and approved the final version of the manuscript.

ISSN 2413-5577, Ecological Safety of Coastal and Shelf Zones of Sea, No. 2, pp. 76–92 (2026)

Original paper

Results of Hydrological, Hydrochemical and Biological Studies in the Waters of the Mussel and Oyster Farm in 2023–2024 (Black Sea, the Resort Town of Koreiz)

S. V. Shchurov *, N. V. Pospelova, O. A. Troshchenko, N. P. Kovrigina, E. V. Lisitskaya, A. S. Priymak

A. O. Kovalevsky Institute of Biology of the Southern Seas, RAS, Sevastopol, Russia
* *email: shchur@ibss-ras.ru*

Abstract
The paper presents results of comprehensive hydrological, hydrochemical and hydrobiological investigations of the coastal waters off Koreiz (Southern Coast of Crimea, Black Sea). In 2023–2024, a total of six seasonal sampling sessions were conducted within the area near a mussel and oyster farm, thus ensuring comprehensive coverage of all seasons. In the surface layer (0–0.5 m), 61 samples were collected, and 720 hydrochemical analyses were performed. Phytoplankton was sampled at stations *1–5* in the surface layer. Meroplankton samples were collected with a Juday net (entry ring diameter 36 cm, gas size no. 49) in the 0–10 m layer at coastal stations *1*, *5* and *7*. It was shown that the temperature and salinity levels of the surface layer during the study period exhibited a consistent increase compared to the long-term means for the Yalta area. However, these parameters remained within the range 7–25°C and 17–20‰, which is conducive for cultivation of bivalve molluscs. The dissolved oxygen concentrations in all seasons remained substantially above the threshold values specified by fisheries water quality standards. The values of five-day biochemical oxygen demand (BOD_5) and the pollution coefficient Kz corresponded to the category of “unpolluted” waters. Concentrations of inorganic forms of nitrogen and phosphorus were in most cases low and spatially homogeneous. The local hotspots of elevated ammonium, nitrate and organic nitrogen and phosphorus were identified in the mussel and oyster farm area and a coastal station influenced by domestic wastewater. In the phytoplankton, 77 microalgal species were identified; diatoms dominated numerically throughout the year, while in the cold and spring seasons a substantial part of the biomass was formed by taxa considered food for mussels and oysters. The meroplankton community was found to comprise larvae of 43 benthic invertebrate species; larvae of the cultivated bivalves *Mytilus galloprovincialis* and *Magallana gigas* occurred within the temperature ranges characteristic of these species. The obtained data indicate that the coastal waters off Koreiz can be regarded as an environmentally favourable area for the operation of a mussel and oyster farm.

Keywords: hydrochemical indicators, phytoplankton, meroplankton, mariculture, Black Sea

Acknowledgments: This work was carried out within the framework of the state assignment of IBSS “Comprehensive study of the functioning mechanisms of marine biotechnological complexes with the aim of obtaining bioactive substances from hydrobionts” (124022400152-1).

© Shchurov S. V., Pospelova N. V., Troshchenko O. A., Kovrigina N. P., Lisitskaya E. V., Priymak A. S., 2026

This work is licensed under a Creative Commons Attribution-Non Commercial 4.0 International (CC BY-NC 4.0) License

For citation: Shchurov, S.V., Pospelova, N.V., Troshchenko, O.A., Kovrigina, N.P., Lisitskaya, E.V. and Priymak, A.S., 2026. Results of Hydrological, Hydrochemical and Biological Studies in the Waters of the Mussel and Oyster Farm in 2023–2024 (Black Sea, the Resort Town of Koreiz). *Ecological Safety of Coastal and Shelf Zones of Sea*, (2), pp. 76–92.

Результаты гидролого-гидрохимических и биологических исследований в акватории мидийно-устричной фермы в 2023–2024 годах (Черное море, поселок Кореиз)

С. В. Щуров *, Н. В. Поспелова, О. А. Трощенко, Н. П. Ковригина, Е. В. Лисицкая, А. С. Приймак

ФГБУН ФИЦ «Институт биологии южных морей имени А.О. Ковалевского РАН», Севастополь, Россия

* *email: shchur@ibss-ras.ru*

Аннотация

Представлены результаты комплексных гидролого-гидрохимических и гидробиологических исследований прибрежной акватории поселка Кореиз (Южный берег Крыма, Черное море). В 2023–2024 гг. в районе мидийно-устричной фермы выполнены шесть съемок, охватывающих все сезоны. В поверхностном слое (0–0.5 м) отобрана 61 проба, выполнено 720 гидрохимических анализов. Пробы фитопланктона отбирали на станциях *1–5* в поверхностном слое. Пробы меропланктона отбирали сетью Джеди (диаметр входного кольца 36 см, размер газа № 49) в слое 0–10 м на прибрежных станциях *1*, *5* и *7*. Показано, что температура и соленость поверхностного слоя в годы наблюдений устойчиво превышали среднемноголетние значения для района Ялты, однако оставались в пределах 7–25 °С и 17–20 ‰, благоприятных для культивирования двустворчатых моллюсков. Содержание растворенного кислорода во все сезоны было значительно выше рыбохозяйственных нормативов. Значения $БПК_5$ и коэффициента загрязнения *Kz* соответствовали категории незагрязненных вод. Концентрации минеральных форм азота и фосфора в большинстве случаев были однородными и не превышали предельно допустимых концентраций. Выявленные локальные очаги повышенного содержания аммонийного азота, нитратов и органических форм азота и фосфора ограничивались районом фермы и прибрежной станцией, подверженной влиянию хозбытовых стоков. В фитопланктоне идентифицировано 77 видов микроводорослей, при этом круглый год по численности доминировали диатомовые водоросли, а в холодный и весенний сезоны значительную часть биомассы составляли кормовые для мидий и устриц таксоны. В состав меропланктона входили личинки 43 видов донных беспозвоночных, личинки культивируемых моллюсков *Mytilus galloprovincialis* и *Magallana gigas* встречались в характерных для этих видов температурных диапазонах. Совокупность полученных данных позволяет рассматривать район пос. Кореиз как экологически благоприятную акваторию для функционирования мидийно-устричной фермы.

Ключевые слова: гидрохимические показатели, фитопланктон, меропланктон, марикультура, Черное море

Благодарности: работа выполнена в рамках государственного задания ФИЦ ИнБЮМ по теме: «Комплексное исследование механизмов функционирования морских биотехнологических комплексов с целью получения биологически активных веществ из гидробионтов» (регистрационный номер: 124022400152-1).

Для цитирования: *Щуров С. В., Поспелова Н. В., Трощенко О. А., Ковригина Н. П. и др.* Результаты гидролого-гидрохимических и биологических исследований в акватории мидийно-устричной фермы в 2023–2024 годах (Черное море, поселок Кореиз) // Экологическая безопасность прибрежной и шельфовой зон моря. 2026. № 2. С. 76–92. EDN FBVCKA.

Introduction

Mussel and oyster mariculture represents one of the most promising areas for the rational utilisation of biological resources in the coastal zone of the Black Sea. Bivalve molluscs, on the one hand, serve as a commercially and aquaculturally valuable resource, and on the other, participate in biofiltration and redistribution of matter within coastal ecosystems, thereby influencing the quality of the marine environment. In the context of climate change and increasing anthropogenic pressure on the coastal zone, assessing the suitability of shelf areas for aquaculture development requires comprehensive consideration of hydrological, hydrochemical and biological characteristics. For water areas with existing mariculture facilities, ecological safety is determined by the variability of hydrophysical parameters, dissolved oxygen and nutrient concentrations, as well as the structure of phyto- and meroplankton, which form the trophic base and ensure natural recruitment of populations of cultivated species.

Phytoplankton constitutes the primary link in the trophic pyramid of the coastal zone and largely determines the food availability for cultivated molluscs. Small-celled diatoms and dinoflagellates are considered the most nutritionally valuable food organisms for mussels and oysters [1, 2], whereas the growth of toxic dinoflagellates, principally *Dinophysis* and *Alexandrium*, can result in toxin accumulation in mollusc tissues [3, 4]. Water temperature and salinity substantially influence the timing of mollusc reproduction and the abundance of their pelagic larvae in the plankton [5]. Accordingly, a comprehensive investigation in the area of a mussel and oyster farm makes it possible not only to evaluate the current ecological impact of the farm on the coastal ecosystem, but also to support the sustainable operation of the farm from the perspective of ecological safety.

The object of the study was a functioning mussel-oyster farm of approximately 7 ha situated in the coastal zone of the settlement of Koreiz. The area under investigation extends approximately 2.4 km along the coast, with a maximum distance from the shore of 700 m and depths ranging from 8 to 32 m. Koreiz is a settlement on the Southern Coast of Crimea (SCC), characterized by a subtropical Mediterranean-type climate. The absence of well-defined bays promotes frequent wave action, particularly during the cold season, which is significant for water exchange and the formation of concentration fields of dissolved and suspended substances. Three small rivers discharge into the sea within the study area (the Khosma-Bash, Uzen-Chesme and Zagmata) which may influence the hydrological regime.

Several large sanatoriums and coastal residential structures are located in the vicinity and may serve as sources of anthropogenic pollution.

Studies analogous to those presented in this paper were previously carried out by the authors in the waters of mussel-oyster farms in Goluboy Bay near the settlement of Katsiveli [6], in Lake Donuzlav, and in the coastal waters off Sevastopol [7, 8]. Data on water quality assessment in the Yalta Harbour area are also available [9]. However, the coastal area of Koreiz has been scarcely studied.

The aim of the present work is to examine the spatial distribution of the principal hydrological and the characteristics of phyto- and meroplankton in the area of the Koreiz mussel-oyster farm, and to assess the suitability of these waters for bivalve mollusc cultivation.

Materials and Methods

Hydrological, hydrochemical and hydrobiological studies in the Koreiz area were conducted from March 2023 to September 2024, encompassing all seasons: winter (February 2024), spring (March and May 2023, May 2024), summer (August 2023) and autumn (September 2024). A total of six comprehensive surveys were carried out in accordance with the station scheme (Fig. 1).

Surveys were conducted from a small motor vessel. Samples were collected primarily in the surface layer (0–0.5 m); a total of 61 samples were taken, and approximately 720 analyses were performed. The suite of hydrological and hydrochemical analyses included measurement of temperature and salinity, determination of dissolved oxygen content, five-day biochemical oxygen demand (BOD_5), permanganate index in an alkaline medium, silicate concentration, as well as inorganic

Fig. 1. Schematic map of the study area (the figures are station numbers, farm – the mussel and oyster farm). Adopted from: Google Maps (Available at: https://www.google.ru/maps)

and organic forms of nitrogen and phosphorus. Analyses were performed according to standard methods [1), 2)]. The pollution coefficient (*Kz*) defined as the ratio of BOD_5 to permanganate index, was calculated following the approach described in the study [3)].

Phytoplankton samples were collected at stations *1–5* in the surface layer (0–1 m) and processed in accordance with standard guidelines [4)]. Microalgae were identified using identification keys [5), 6), 7)]. Mean cell volumes and phytoplankton biomass were determined using dedicated software [10]. A total of 29 samples were collected and processed. Phytoplankton abundance and biomass were distributed according to taxonomic group (diatoms – *Dia*; dinoflagellates – *Dino*; others – *Other*) and by suitability as food for cultivated molluscs (forage vs. non-forage) [1]. Meroplankton samples were collected with a Juday net (entry ring diameter 36 cm, mesh size no. 49) in the 0–10 m layer at coastal stations *1*, *5* and *7* (Fig. 1). The material was processed alive; larvae of benthic invertebrates were counted in a Bogorov chamber under MBS-9 and Mikmed-5 light microscopes. A total of 15 samples were collected; processing methods corresponded to those applied in previous studies [7, 11].

Results

In the analysis of thermohaline characteristics, the newly obtained data were compared with long-term baseline values for the Yalta area for the period 1900–2011 [12].

Temperature. The February 2024 survey revealed anomalously high surface-layer water temperature (12.1°C) relative to the long-term mean (7.7°C). The recorded values exceeded both the long-term maximum (9.7°C) and the absolute maximum for February (10.4°C). In March 2023, surface-layer temperature ranged from 8.8 to 9.2°C, corresponding to long-term maximum values. Spring surveys (May 2023 and May 2024) showed temperatures ranging from 14.4 to 15.0°C, which likewise exceeded the long-term mean (13.9°C). In August 2023, temperatures reached 26.8°C, exceeding the long-term mean by 3.5°C. In September,

---

[1)] Guideline documents РД 52.24.420-2019, РД 52.24.383-2018, РД 52.24.380-2017, РД52.24.381-2017, РД 52.24.382-2019, РД 52.24.432-2018, РД 52.10.805-2013, РД 52.24.387-201 (in Russian).

[2)] *On the Approval of Water Quality Standards for Water Bodies of Commercial Fishing Importance, Including Standards for Maximum Permissible Concentrations of Harmful Substances in the Waters of Water Bodies of Commercial Fishing Importance*: Order of the Federal Agency for Fishery dated May 26, 2025, No. 296 (in Russian).

[3)] Skopintsev, B.A., 1975. [*Formation of the Modern Chemical Composition of the Black Sea Waters*]. Leningrad: Gidrometeoizdat, 335 p. (in Russian).

[4)] Moncheva, S. and Parr, B., 2010. *Manual for Phytoplankton Sampling and Analysis in the Black Sea*. 67 p.

[5)] Kiselev, I.A., 1950. [*A Faunal Guide to the USSR. Armoured Dinoflagellates (Dinoflagellata) of the Seas and Freshwaters of the USSR*]. Moscow; Leningrad: Izd-vo AN SSSR, 280 p. (in Russian).

[6)] Proshkina-Lavrenko, A.I., 1955. [*Diatom Algae of the Black Sea Plankton*]. Moscow, Leningrad: Izd. AN SSSR, 224 p. (in Russian).

[7)] Tomas, C.R., ed., 1993. *Marine Phytoplankton: A Guide to Naked Flagellates and Coccolithophorids.* Academic Press, 263 p.

temperatures at all stations were 24.7°C, surpassing the long-term mean by 3.9°C. The spatial distribution of surface-layer temperature was homogeneous across all surveys.

Salinity. Mean area-averaged salinity values in the surface layer in all surveys exceeded long-term means by 0.28÷0.56‰, with the exception of August 2023. The August survey recorded the minimum salinity value for the entire study period at all stations (17.63‰) and a spatially uniform distribution throughout the study area. It should be noted that despite the small spatial extent of the study area, the salinity distribution in February, March and September was characterized by heterogeneity, with inter-station differences of 0.30÷0.36‰.

Hydrochemical conditions. Minimum, maximum and mean values of hydrochemical indicators in the surface layer of the coastal waters off Koreiz in 2023–2024 are presented in Table 1.

Dissolved oxygen, BOD_5 and permanganate index. The distribution of dissolved *oxygen concentration* was relatively homogeneous throughout the study period, with values ranging from 7.44 to 10.07 mg/dm³. The minimum was recorded in September 2024 at stations *2* and *3*. Survey-mean values ranged from 7.49 to 9.92 mg/dm³. Relative dissolved oxygen saturation varied between 91.3 and 124.5%. The minimum saturation was recorded on 6 March 2023 at coastal station *1*, and the maximum was recorded on 25 August 2023 at station *5* in the farm area. Survey-mean saturation values ranged from 94.5% (6 March 2023) to 116% (25 August 2023). The minimum dissolved oxygen saturation exceeded the regulatory threshold (40%) by a factor of 2.3.

BOD_5 values ranged from 0.17 to 2.58 mg/dm³ (Fig. 2); the maximum was recorded on 15 May 2023 at offshore station *3*, situated abeam of the farm. At the remaining stations, BOD_5 values were considerably lower and did not exceed the regulatory limit (2.1 mg/dm³ according to fisheries water quality standards [2)]); exceedances were not observed on any other sampling date.

Permanganate index during the observation period varied from 2.75 to 6.02 mgO/dm³ (Fig. 3), with the minimum value recorded in February 2024 at offshore station 6 (Fig. 1).

Exceedances of the regulatory threshold (4.0 mgO/dm³) were observed in May and August 2023 at all stations, and in September 2024 at stations *2* and *5* (an offshore station abeam of Cape Kommunarov and a coastal station in the farm area, respectively). The maximum permanganate index in August 2023 was recorded in the farm area and was attributed to pollution with organic matter. During the warm season of 2023, survey-mean permanganate index values exceeded the regulatory limit by 0.75 mgO/dm³ (May) and 1.52 mgO/dm³ (August). The pollution coefficient *Kz*, calculated as the ratio of BOD_5 to permanganate index following Skopintsev [10], varied from 0.09 to 0.55.

Nutrients. Nitrite nitrogen concentrations in the surface layer were low, ranging from 0.4 to 2.5 µg/dm³. The minimum was recorded in May 2024 at station *4*, T a b l e 1 . Average and extreme values of hydrochemical parameters in the surface layer of the water area under study (2023–2024)

Date	Value	BOD_5, mg/dm^3	PI, mgO/dm^3	Content, µg/dm^3						
				NO_2	NO_3	NH_4	N_{org}	PO_4	P_{org}	Si
26.03. 2023	Mean	0.50	2.78	1.2	2.9	7.8	535	4.0	23.9	109.5
	Min	0.17	2.40	0.8	2.1	3.5	377	2.4	20.8	87.4
	Max	0.75	3.53	2.1	4.8	12.5	645	7.6	31.7	188.8
15.05. 2023	Mean	1.41	4.75	1.1	4.8	7.4	308	1.7	18.6	95.4
	Min	0.77	4.11	0.6	2.8	6.6	261	0.6	15.8	83.4
	Max	2.58	5.59	2.5	6.8	9.4	372	2.7	21.4	105.8
25.08. 2023	Mean	N/D	5.52	1.1	8.7	16.7	2407	4.6	26.6	24.7
	Min	N/D	4.11	0.7	3.6	7.4	2080	1.9	21.2	17.9
	Max	N/D	6.02	1.8	22.4	36.8	3154	7.9	28.7	30.5
14.02. 2024	Mean	0.64	2.75	1.9	12.1	17.3	496	8.6	31.6	148.3
	Min	0.31	2.19	1.7	5.1	5.3	399	3.8	25.7	122.6
	Max	1.04	3.43	2.3	23.1	62.0	747	20.4	41.0	172.9
07.05. 2024	Mean	0.77	3.70	0.6	6.6	3.5	429	4.1	5.3	111.9
	Min	0.51	3.45	0.4	3.1	2.6	179	3.1	2.7	108.0
	Max	0.98	4.02	1.1	14.0	4.7	1142	6.3	8.0	117.9
12.09. 2024	Mean	0.61	3.70	0.7	10.5	29.5	592	6.3	12.0	69.7
	Min	0.38	3.04	0.5	6.4	12.8	159	5.8	8.3	64.9
	Max	0.82	4.42	0.9	14.9	57.3	1014	6.9	25.1	78.8

Note: N/D – no data.

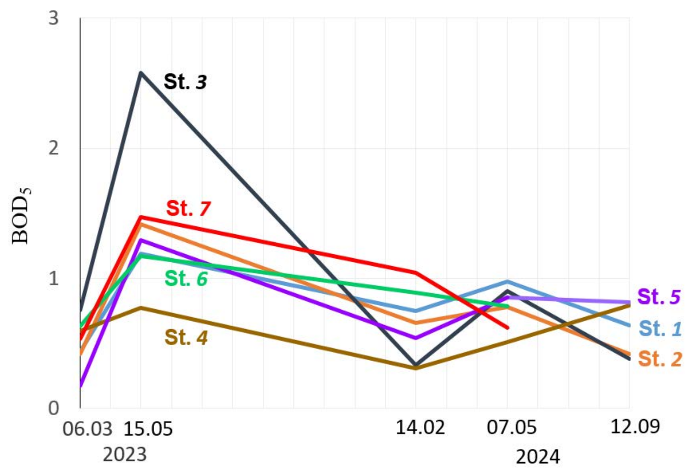

F i g . 2 . Distribution of five-day biochemical oxygen demand (BOD_5) in the coastal waters off Koreiz (2023–2024)

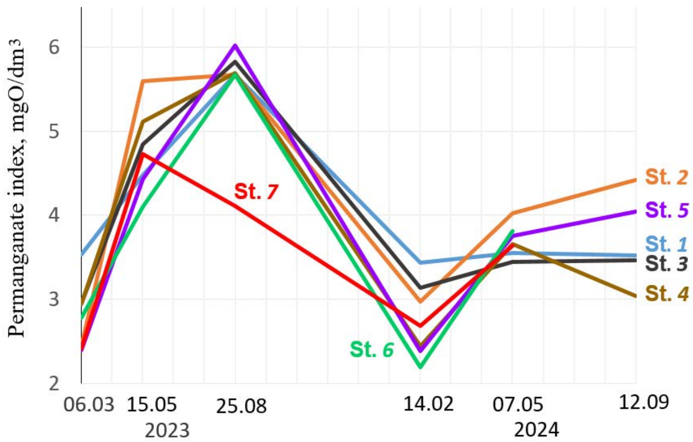

F i g . 3 . Distribution of permanganate index in the coastal waters off Koreiz (2023–2024)

and the maximum in May 2023 at station *3* (Table 1). Nitrate nitrogen concentrations in the surface layer ranged from 2.1 to 23.1 μg/dm³, with the minimum recorded in March 2023 at offshore station *3* and the maximum in February 2024 at coastal station *7*. *Ammonium nitrogen* concentrations were low, varying from 2.6 to 62.0 μg/dm³. Minimum values were recorded at stations *1* and *2* in May 2024; maximum values were recorded at station *7* in February 2024. Elevated ammonium nitrogen concentrations were observed at all stations in September 2024, with the highest values at stations *4* and *5* in the immediate vicinity of the farm.

Elevated organic nitrogen and phosphorus concentrations were also recorded at these stations. The maximum ammonium nitrogen concentration at coastal station *7* coincided with elevated concentrations of phosphate (20.4 μg/dm³), total phosphorus (56.8 μg/dm³) and nitrate (23.1 μg/dm³).

Organic nitrogen concentrations ranged widely, from 159 to 3154 μg/dm³, with extreme values in the Cape Kommunarov area: the minimum at coastal station *1* in September 2024 and the maximum at offshore station *2* in August 2023. Elevated organic nitrogen concentrations were observed at all stations in August 2023. No pronounced seasonal dynamics in the concentrations of inorganic and organic forms of nitrogen and phosphorus in the surface layer were detected during the study period.

Silicate concentrations ranged from 17.9 to 188 μg/dm³, with the minimum recorded at station *5* in August 2023 and the maximum at coastal station *1* in March 2023.

Phytoplankton community structure. During the study period, 77 microalgal species were identified in the coastal waters off Koreiz, including 45 diatom species, 24 dinoflagellate species and 8 species from other taxonomic groups (chrysophytes, silicoflagellates, cyanobacteria). Phytotoxin-producing microalgae of the genera *Prorocentrum* and *Dinophysis* were recorded throughout the year but at very low abundance. Diatoms dominated numerically in all seasons (Table 2). In March and August 2023, they accounted for 90–95% of total abundance at most stations, while the proportion of dinoflagellates generally did not exceed 5–10%.

In summer 2023, diatoms retained their numerical dominance, but the biomass of non-forage taxa increased to 90–98% due to large-celled microalgae. In spring (May 2023 and May 2024), forage taxa comprised up to 80% of biomass at several stations, while in winter–spring 2024, forage taxa predominated numerically at most stations (Fig. 4).

Meroplankton composition and dynamics. During the study period, pelagic larvae of 43 benthic invertebrate species belonging to various taxa were recorded in the coastal waters off Koreiz (Table 3).

Larvae bivalvia were present in the plankton throughout the study period. Velikoncha of *M. galloprovincialis* were recorded in March and May at water temperatures of 9.0–14.9°C, although their density did not exceed 12 ind.·m^{-3}. Another species of the family Mytilidae, *M. lineatus*, dominated in density in August (93–195 ind.·m^{-3}) and September (52–118 ind.·m^{-3}) at water temperatures above 24.7°C. Species of the families Cardiidae and Veneridae were recorded during the warm season, with densities not exceeding 32 ind.·m^{-3}. Larvae of the giant oyster *M. gigas* were found in August at water temperatures of 26.7°C and in September at 24.7°C. The larvae were at the velikoncha stage, with sizes of 275–300 μm and densities of 1–2 ind.·m^{-3}. Larvae of the invasive species *A. inaequivalvis* were discovered during the same period, with densities ranging from 17 to 68 ind.·m^{-3}. Pelagic stages of the gastropods *B. reticulatum* and species of the family Rissoidae dominated in August (118–234 ind.·m^{-3}).

T a b l e 2 . Abundance and biomass of the main groups of phytoplankton in the coastal waters off Koreiz (2023–2024)

Date	Station	Abundance, thous. cells·L^{-1}				Biomass, µg·L^{-1}			
		Dia	*Dino*	*Other*	Total	*Dia*	*Dino*	*Other*	Total
06.03. 2023	*1*	58.50	0.04	2.00	60.5	345.40	0.01	0.50	345.7
	2	7.50	0.02	0.30	14.4	7.75	0	0.30	8.9
	3	195.00	0	11.70	206.7	448.90	0	2.00	451.0
	4	18.50	0.07	1.60	20.2	7.44	0.2	0.20	7.8
	5	53.30	0	5.90	59.2	149.10	0	1.10	150.2
15.05. 2023	*1*	13.20	4.40	0	17.6	13.20	27.0	0	38.1
	2	23.10	1.40	0	24.6	27.10	34.5	0	61.6
	3	8.20	7.10	3.40	18.7	5.90	59.8	0.05	72.5
	4	6.42	3.30	0	9.7	85.70	12.1	0	97.8
	5	6.50	17.10	3.10	11.4	2.70	37.5	0.60	8.2
25.08. 2023	*1*	31.80	0.90	0.50	33.3	217.00	10.8	1.70	229.5
	2	21.20	2.50	0.40	24.1	334.40	22.2	0.90	357.5
	3	4.20	0.20	0	4.3	88.70	2.9	0	91.6
	4	20.90	1.10	0.30	22.3	281.5	4.7	0.40	286.6
	5	47.50	0.70	0	48.2	523.50	8.7	0	532.2
14.02. 2024	*1*	11.90	1.20	118.90	131.9	158.70	4.6	34.20	197.5
	2	7.90	1.10	53.20	62.2	66.80	10.9	11.50	89.3
	3	6.70	1.30	67.60	75.5	153.70	23.9	18.30	195.9
	4	1.80	0.90	49.60	52.3	17.20	4.2	2.00	30.5
	5	47.50	0.70	0	48.2	523.50	8.7	0	532.2
07.05. 2024	*1*	52.30	0.20	0	52.3	34.20	9.5	0	43.8
	2	65.50	1.20	0.05	66.8	25.80	12.0	0.30	38.1
	3	756.00	1.10	0.07	757.2	284.10	5.2	0.20	289.5
	4	52.90	1.70	0.04	54.6	43.80	11.4	0.20	55.4
	5	6.90	0.90	0	7.9	49.70	10.9	0	60.7
12.09. 2024	*1*	9.50	0.70	0.10	10.4	29.50	11.8	0.70	41.9
	2	5.20	1.10	0	6.3	31.40	16.2	0	47.6
	3	4.40	0.70	0.06	5.1	25.80	15.4	0.40	41.6
	4	5.30	0.40	0	5.6	21.80	4.5	0	26.2

N o t e : *Dia* – diatoms, *Dino* – dinophytes, *Other* – other taxonomic groups.

T a b l e 3 . Taxonomic composition of meroplankton in the Koreiz coastal waters

Taxon, species	Taxon, species
Type Annelida, class Polychaeta	**Type Mollusca, class Bivalvia**
Nephthys hombergii Savigny, 1818	*Anadara inaequivalvis* (Bruguière, 1789)
Harmothoe reticulata (Claparède, 1870)	*Magallana gigas (Thunberg, 1793)*
Pholoe inornata Johnston, 1839	*Mytilus galloprovincialis* Lamarck, 1819
Lysidice ninetta Aud. et M. Edw., 1833	*Mytilaster lineatus* (Gmelin, 1791)
Spio decorata Bobretzky, 1870	*Modiolus* sp.
Malacoceros fuliginosus (Claparède, 1868)	*Spisula subtruncata* (Da Costa, 1778)
Scolelepis squamata (Müller, 1806)	*Teredo navalis* Linnaeus, 1758
Prionospio sp.	*Chamelea gallina* (Linnaeus, 1758)
Spionidae gen. sp	Veneridae gen. sp.
Magelona rosea Moore, 1907	Cardiidae gen. sp.
Phyllodoce sp.	Larvae Bivalvia
Capitellidae gen. sp.	
	Class Gastropoda
Nereididae gen.sp.	*Bittium reticulatum* (Da Costa, 1778)
	Rissoa splendida Eichwald, 1830
Type Arthropoda, class Crustacea	*Rissoa parva* (Da Costa, 1778)
Decapoda	*Rissoa* sp.
Clibanarius erythropus (Latreille, 1818)	*Retusa truncatula* (Bruguiere, 1792)
Hippolyte leptocerus (Heller, 1863)	*Tricolia pullus* (Linnaeus, 1758)
Palaemon sp.	*Caecum trachea* (Montagu, 1803)
Pachygrapsus marmoratus (Fabricius, 1787)	Larvae Gastropoda
Pilumnus hirtellus (Linnaeus, 1761)	**Type Cnidaria**
Larvae Brachyura	Planula Hydrozoa
Cirripedia	**Type Bryozoa**
Amphibalanus improvisus Darwin, 1854	Larvae Bryozoa
Verruca spengleri Darwin, 1854	**Type Bryozoa**
	Larvae Kamptozoa

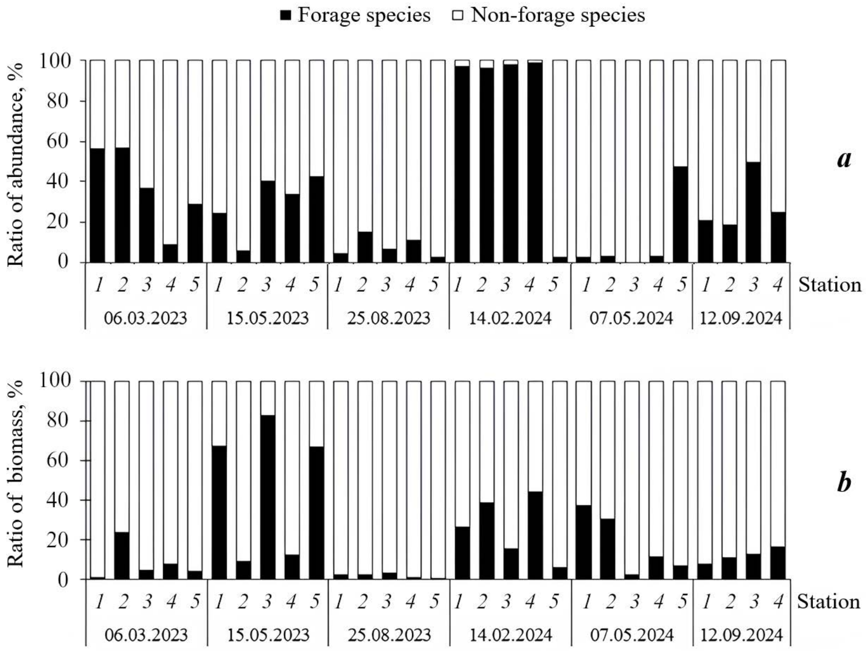

F i g . 4 . Ratio (%) of abundance (*a*) and biomass (*b*) of forage and non-forage microalgal species in the plankton of the Koreiz coastal waters (2023–2024)

Polychaete larvae were recorded throughout the study period, with Spionidae (*S. decorata*, *M. fuliginosus*, *Prionospio* sp.) predominating. In May, at water temperatures of 14.5–15.0°C, nectochaetae of *Ph. inornata* (12–14 ind.$\cdot$m^{-3}) dominated. Notably, larvae of *M. rosea* were found in all May samples (3–5 ind.$\cdot$m^{-3}); polychaetes of this species predominate in areas with good water exchange and aeration. Nauplii of the barnacle *A. improvisus* were present in all samples at densities not exceeding 15 ind.$\cdot$m^{-3}; this species is abundant on hard substrates in coastal fouling communities. Nauplii of another barnacle species, *V. spengleri*, were recorded in August 2023 at a density of only 2 ind.$\cdot$m^{-3}. Larvae Decapoda were recorded only as single specimens during the warm season at water temperatures above 24°C. Planulae of hydroid polyps (Hydrozoa) were recorded in May and September at densities of up to 6 ind.$\cdot$m^{-3}. In September, larvae of *B.* cf. *benedeni* (Entoprocta) were recorded at a density of 8 ind.$\cdot$m^{-3}, along with rare bryozoan cyphonautes larvae (Bryozoa). Total meroplankton density in the coastal waters off Koreiz was generally low, with maximum values of 325 ind.$\cdot$m^{-3} (August) and 326 ind.$\cdot$m^{-3} (September) at all stations, and minimum values of 6–7 ind.$\cdot$m^{-3} in March 2023.

Discussion

The thermohaline data obtained for the coastal waters off Koreiz in 2023–2024 indicate a consistent prevalence of elevated temperature and salinity values relative to the long-term means for the Yalta area for the period 1900–2011 [12]. This is consistent with the previously identified trend towards warming and increasing salinity for both the Black Sea as a whole [13] and the coastal waters of Crimea [14]. Temperatures in the range of 7–25°C and salinity values of 17–20‰ are considered favourable for mollusc cultivation [5, 15], as confirmed by the present observations. No influence of the temporary temperature and salinity anomalies on hydrochemical and plankton fields was detected, which may be attributable to the insufficient duration and frequency of the surveys, as well as the absence of long-term hydrochemical and hydrobiological baseline data for the Koreiz area.

The dissolved oxygen regime indicates good aeration of the surface layer and favourable conditions for molluscs: minimum relative oxygen saturation values (91.3%) are substantially above the fisheries regulatory threshold (40%).

BOD_5 values corresponded in most cases to unpolluted waters, and the pollution coefficient *Kz* remained considerably below unity. The single exceedance of the BOD_5 limit and the elevated permanganate index values observed during the warm season of 2023 in the farm area and at certain coastal stations are most likely attributable to the influence of localised organic matter sources (river runoff and domestic wastewater). Within the study area, localised nutrient enrichment hotspots were identified (station *7*), where maximum nitrate and phosphate concentrations also appear likewise to be associated with domestic wastewater discharge.

Silicate concentrations in the study area were characterised by considerable variability. The absence of pronounced seasonal silicate depletion, against the background of constant diatom numerical dominance, indicates that phytoplankton biomass limitation in the Koreiz area is more closely linked to nitrogen supply than to silicon deficiency.

The taxonomic composition and structure of phytoplankton in the farm area were broadly consistent with data reported for the SCC [16, 17]. During the winter–spring period (March 2023, February 2024), enhanced vertical mixing and nitrogen and silicon availability, the proportion of forage taxa, represented primarily by diatoms, increased. In summer (August 2023 and 2024), stable stratification and depletion of nitrogen and silicate reserves led to the dominance of non-forage taxa by biomass (large diatoms and dinoflagellates). Consequently, the high proportions of forage microalgae in spring indicate favourable feeding conditions and growth of molluscs, whereas the summer shift towards non-forage taxa reduces food availability while overall biomass is maintained.

Potentially toxic dinoflagellates of the genera *Dinophysis* and *Prorocentrum* were recorded throughout the year at low abundance without evidence of mass bloom events. This is consistent with current understanding of the patchy occurrence of harmful microalgae along the Crimean coast and underscores the necessity of regular phytoplankton monitoring in the mariculture area [3, 4].

The meroplankton of the Koreiz area is diverse. The timing and temperature ranges of benthic invertebrate larval occurrence in the plankton were consistent with those characteristic of the coastal waters of Crimea [6, 7], indicating the preservation of natural reproductive cycles and the potential for replenishment of benthic populations. The water temperature range (24.7–26.7°C) in August and September, when *M. gigas* oyster larvae were recorded in the study area, fell within the optimum range for early developmental stages of the Pacific oyster (23–30°C) [18, 19]. The combination of the present findings and previously published records of *M. gigas* larvae in the Black Sea [11] corroborates projections of range expansion for this species under climate warming conditions [20].

The relatively low overall meroplankton density, with warm-season maxima of up to 325–326 ind.$\cdot$m^{-3}, is characteristic of open coastal waters with good water exchange. The presence of larvae of abundant fouling species (*A. improvisus*, *V. spengleri*) and hydropolyps in the meroplankton reflects the general tendency for complex fouling communities to develop on farm structures.

Taken together, the hydrological, hydrochemical, phytoplankton and meroplankton characteristics indicate that the Koreiz area represents an environmentally favourable area for the development of bivalve mollusc mariculture. Further development of the farming operation should be accompanied by comprehensive monitoring of hydrochemical indicators and mero- and phytoplankton. Particular attention should be directed to localised organic pollution hotspots and the dynamics of potentially toxic microalgae.

Conclusion

During 2023–2024, the hydrological and hydrochemical regime of the coastal waters off Koreiz was characterised by elevated surface-layer temperature and salinity relative to the long-term means established for the SCC. Dissolved oxygen concentration remained at high levels (7.44–10.07 mg/dm^3) throughout the study period and did not fall below fisheries regulatory thresholds. The pollution coefficient (*Kz*) did not exceed unity, allowing the study area to be classified as “unpolluted”. Concentrations of inorganic forms of nitrogen and phosphorus were low and spatially homogeneous, which is typical of unpolluted coastal waters. The identified localised hotspots of elevated ammonium nitrogen (62.0 µg/dm^3), nitrate (23.1 µg/dm^3) and organic nitrogen and phosphorus (3154 and 41.0 µg/dm^3, respectively) were confined to the mussel-oyster farm area and to the coastal station subject to the influence of river and domestic wastewater. Silicate concentrations remained sufficient for diatom development throughout the year.

In the phytoplankton, diatoms consistently dominated numerically (up to 95%), and during the cold and spring seasons, taxa that serve as food for mussels and oysters constituted a substantial proportion of both biomass and abundance. The summer increase in the proportion of non-forage taxa was transient and was not accompanied by blooms of potentially toxic species, indicating a stable food supply for the cultivated bivalve molluscs. The meroplankton of the Koreiz area comprised larvae of 43 benthic invertebrate species, including pelagic stages of cultivated bivalves and invasive species. Larvae of *Mytilus galloprovincialis* were recorded at water temperatures of 9.0–14.9°C, while larvae of *Magallana gigas* and *Anadara inaequivalvis* were found at 24.7–26.7°C.

Thus, the thermohaline conditions, persistent diatom dominance with a high contribution of forage taxa, high dissolved oxygen concentrations, a low level of nutrient pollution with localised and manageable enrichment in organic forms of nitrogen and phosphorus in the farm vicinity, and the availability of bivalve larvae collectively support the conclusion that the coastal waters off Koreiz are environmentally favourable for the operation of the existing mussel-oyster farm.

REFERENCES

1. Pospelova, N.V. and Priimak, A.S., 2021. The Feeding of *Mytilus galloprovincialis* Lam. Cultivating in Coastal Waters of Sevastopol. *Proceedings of the T. I. Vyazemsky Karadag Scientific Station – Nature Reserve of the Russian Academy of Sciences*, 6(1), pp. 24–34. https://doi.org/10.21072/eco.2021.17.03 (in Russian).
2. Ryabushko, L.I., Pospelova, N.V., Balycheva, D.S., Kovrigina, N.P., Troshchenko, O.A. and Kapranov, S.V., 2017. Epizoon Microalgae of the Cultivated Mollusk Mytilus galloprovincialis Lam. 1819, Phytoplankton, Hydrological and Hydrochemical Characteristics in the Mussel-and-Oyster Farm Area (Sevastopol, Black Sea). *Marine Biological Journal*, 2(4), pp. 67–83. https://doi.org/10.21072/mbj.2017.02.4.07 (in Russian).
3. Blanco, J., 2018. Accumulation of *Dinophysis* Toxins in Bivalve Molluscs. *Toxins*, 10(11), 453. https://doi.org/10.3390/toxins10110453
4. Reguera, B., Riobó, P., Rodríguez, F., Díaz, P.A., Pizarro, G., Paz, B., Franco, J.M. and Blanco, J., 2014. Dinophysis Toxins: Causative Organisms, Distribution and Fate in Shellfish. *Marine Drugs*, 12(1), pp. 394–461. https://doi.org/10.3390/md12010394
5. Holodov, V.I., Pirkova, A.V. and Ladygina, L.V., 2017. *Cultivation of Mussels and Oysters in the Black Sea*. Voronezh: OOO “IZDAT-PRINT”, 508 p. (in Russian).
6. Troshchenko, O.A., Kuftarkova, E.A., Lisitskaya, T.V., Pospelova, N.V., Rodionova, N.Yu., Subbotin, A.A. and Eremin, I.Yu., 2012. Results of Complex Ecological Research on the Mussel-Oyster Far, Waters of (the Blue Bay, Crimea, the Black Sea). *Ecological Safety of Coastal and Shelf Zones and Comprehensive Use of Shelf Resources*, 26(1), pp. 291–309 (in Russian).
7. Ryabushko, V.I., Shchurov, S.V., Kovrigina, N.P., Lisitskaya, E.V. and Pospelova, N.V., 2020. Comprehensive Research of the Environmental Status of Coastal Waters of Sevastopol (Western Crimea, Black Sea). *Ecological Safety of Coastal and Shelf Zones of Sea*, (1), pp. 104–119. https://doi.org/10.22449/2413-5577-2020-1-104-119 (in Russian).
8. Ryabushko, V.I., Shchurov, S.V., Kovrigina, N.P., and Popov, M.A., 2021. Hydrological, Hydrochemical and Hydrobiological Studies of Lake Donuzlav (Western Crimea, Black Sea) based on the Results of Expeditions in 2018. *Ecological Safety of Coastal and Shelf Zones of Sea*, (2), pp. 80–93. https://doi.org/10.22449/2413-5577-2021-2-80-93 (in Russian).
9. Mezentseva, I.V., Sovga, E.E. and Khmara, T.V., 2025. Self-Purification Capacity of the Yalta Port Ecosystem in Relation to Inorganic Forms of Nitrogen for 2012–2022. *Ecological Safety of Coastal and Shelf Zones of Sea*, (3), pp. 41–53.

10. Lyakh, A.M. and Bryantseva, Yu.V., 2001. Computer's Program for the Calculation of Basic Phytoplankton Parameters. *Ecology of the Sea*, 58, pp. 87–90 (in Russian).

11. Lisitskaya, E.V. and Shchurov, S.V., 2024. The First Record of Larval *Crassostrea gigas* (Thunberg 1793) (Bivalvia, Ostreidae) from the Black Sea. *Zoologicheskiy Zhurnal*, 103(5), pp. 11–15. https://doi.org/10.31857/S0044513424050028 (in Russian).

12. Ilyin, Yu.P., Repetin, L.N., Belokopytov, V.N., Goryachkin, Yu.N., Dyakov, N.N., Kubryakov, A.A. and Stanichny, S.V., 2012. *Hydrometeorological Conditions of the Ukrainian Seas. Vol. 2. The Black Sea*. Sevastopol: ECOSI-Gidrofizika, 421 p. (in Russian).

13. Belokopytov, V.N. and Zhuk, E.V., 2024. Climatic Variability of the Black Sea Thermohaline Characteristics (1950–2023). *Physical Oceanography*, 31(6), pp. 788–801.

14. Kapranov, S.V., Kovrigina, N.P., Troshchenko, O.A. and Rodionova, N.Yu., 2020. Long-Term Variations of Thermohaline and Hydrochemical Characteristics in the Mussel Farm Area in the Coastal Waters off Sevastopol (Black Sea) in 2001–2018. *Continental Shelf Research*, 206, 104185. https://doi.org/10.1016/j.csr.2020.104185

15. Keskin, İ., Ekici, A. and Serdar, S., 2020. Determination of the Growth Performance of Mytilus Galloprovincialis in Nets at Gökçeada Island. *The European Zoological Journal*, 87(1), pp. 559–570. https://doi.org/10.1080/24750263.2020.1818856

16. Stelmakh, L., Kovrigina, N. and Gorbunova, T., 2023. Phytoplankton Seasonal Dynamics under Conditions of Climate Change and Anthropogenic Pollution in the Western Coastal Waters of the Black Sea (Sevastopol Region). *Journal of Marine Science and Engineering*, 11(3), 569. https://doi.org/10.3390/jmse11030569

17. Silkin, V., Mikaelyan, A.S., Pautova, L. and Fedorov, A., 2021. Annual Dynamics of Phytoplankton in the Black Sea in Relation to Wind Exposure. *Journal of Marine Science and Engineering*, 9(12), 1435. https://doi.org/10.3390/jmse9121435

18. Gagnaire, B., Frouin, H., Moreau, K., Thomas-Guyon, H. and Renault, T., 2006. Effects of Temperature and Salinity on Haemocyte Activities of the Pacific Oyster, *Crassostrea gigas* (Thunberg). *Fish and Shellfish Immunology*, 20(4), pp. 536–547. https://doi.org/10.1016/j.fsi.2005.07.003

19. Heo, J.-M., Kim, S.-S., Kim, D.-Y., Lee, S.W., Lee, J.S., Kang, M.H. and Kim, S.E., 2023. Impact of Exposure Temperature Rise on Mass Mortality of Tidal Flat Pacific Oysters. *Frontiers in Marine Science*, 10, 1275521. https://doi.org/10.3389/fmars.2023.1275521

20. King, N.G., Wilmes, S.B., Smyth, D., Tinker, J., Robins, P.E., Thorpe, J., Jones, L., Malham, S.K., 2021. Climate Change Accelerates Range Expansion of the Invasive Non-Native Species, the Pacific Oyster, *Crassostrea gigas*. *ICES Journal of Marine Science*, 78(1), pp. 70–81. https://doi.org/10.1093/icesjms/fsaa189

Submitted 15.11.2025; accepted after review 14.01.2026;
revised 19.03.2026; published 30.06.2026

About the authors:

Sergey V. Shchurov, Researcher, A.O. Kovalevsky Institute of Biology of the Southern Seas of RAS (2 Nakhimov Ave., Sevastopol, 299011, Russia), **ORCID ID: 0000-0002-8913-2637**, **Scopus Author ID: 57214992790**, **ResearcherID: AAC-9044-2022**, *shchur@ibss-ras.ru*

Natalia V. Pospelova, Leading Researcher, A.O. Kovalevsky Institute of Biology of the Southern Seas of RAS (2 Nakhimov Ave., Sevastopol, 299011, Russia), PhD (Biol.), **ORCID ID: 0000-0002-3165-2090**, **Scopus Author ID: 56884605100**, **ResearcherID: C-7572-2016**, *nv.pospelova@ibss-ras.ru*

Oleg A. Troshchenko, Senior Researcher, A.O. Kovalevsky Institute of Biology of the Southern Seas of RAS (2 Nakhimov Ave., Sevastopol, 299011, Russia), PhD (Geogr.), **ORCID ID: 0000-0001-5200-9996**, **Scopus Author ID: 57218589904**, **ResearcherID: AAC-9364-2022**, *oleg_tr59@mail.ru*

Nelya P. Kovrigina, Senior Researcher, A.O. Kovalevsky Institute of Biology of the Southern Seas of RAS (2 Nakhimov Ave., Sevastopol, 299011, Russia), PhD (Geogr.), **ORCID ID: 0000-0002-6734-8285**, **Scopus Author ID: 6507114864**, **ResearcherID: AAC-9395-2022**, *npkovrigina@yandex.ru*

Elena V. Lisitskaya, Senior Researcher, A.O. Kovalevsky Institute of Biology of the Southern Seas of RAS (2 Nakhimov Ave., Sevastopol, 299011, Russia), PhD (Biol.), **ORCID ID: 0000-0002-8219-4616**, **Scopus Author ID: 6504112143**, **ResearcherID: T-1970-2017**, *lisitskaya@ibss.su*

Anastasia S. Priymak, Junior Researcher, A.O. Kovalevsky Institute of Biology of the Southern Seas of RAS (2 Nakhimov Ave., Sevastopol, 299011, Russia), **ORCID ID: 0000-0003-4366-474X**, **Scopus Author ID: 57215722245**, **ResearcherID: A-5754-2019**, *priymaklimova@ibss-ras.ru*

Contribution of the authors:

Sergey V. Shchurov – development of the concept, formulation and statement of the research problem, literature review on the research topic, analysis and interpretation of hydrological and hydrochemical results, formulation of conclusions

Natalia V. Pospelova – literature review on the research topic, analysis and interpretation of phytoplankton results, statistical analysis, formulation of conclusions

Oleg A. Troshchenko – analysis and interpretation of hydrological and hydrochemical results, formulation of conclusions

Nelya P. Kovrigina – analysis and interpretation of hydrological and hydrochemical results, formulation of conclusions

Elena V. Lisitskaya – literature review on the research topic, analysis and interpretation of meroplankton results, formulation of conclusions

Anastasia S. Priymak – analysis of phytoplankton results

All the authors have read and approved the final manuscript.

ISSN 2413-5577, Ecological Safety of Coastal and Shelf Zones of Sea, No. 2, pp. 93–109 (2026)

Original paper

Microplastics in the Lower Volga–Northern Caspian System: Spatial Distribution in the Water Mixing Zone and Sources of Input

M. A. Antsiferova *, A. V. Kleshchenkov, A. M. Korshun

Federal State Budgetary Institution of Science "Federal Research Center Southern Scientific Center of the Russian Academy of Sciences", Rostov-on-Don, Russia

* *e-mail: m12antsiferova@mail.ru*

Abstract

The influence of hydrological and hydrochemical conditions on the spatial distribution of microplastics in estuarine zones has been poorly studied. The study aims to assess microplastics spatial distribution and their quantitative and qualitative characteristics in the Lower Volga–Northern Caspian system. The data were collected during an expedition on R/V *Deneb* in September 2023. The samples were taken using a neuston trawl net (0.3 mm mesh) in the surface layer (0–0.2 m), followed by processing according to a modified NOAA method and direct visual sorting under a microscope. The polymers were identified using the Raman and Fourier-transform infrared spectroscopy, with the PHI hazard index calculated. In parallel, hydrochemical, hydrological and meteorological parameters of the environment were measured, including ion composition. In the Lower Volga, the average particle concentration was 81 particles/m^3, with peak values of 100 particles/m^3 (following a downpour in Kalmykia), as well as 92 particles/m^3 near Volgograd and 98 particles/m^3 near Astrakhan, indicating anthropogenic runoff as the primary source. In the Northern Caspian Sea, particle concentrations were significantly lower (ranging from 3 to 44 particles/m^3, with an average of 13 particles/m^3), showing a pronounced downward gradient from the estuary. Fine microplastics (0.3–2 mm) in the form of fibres and fragments predominated, mainly consisting of polyethylene, polyethylene terephthalate and polyamide, which are classified as hazard class 2 according to the PHI index. The spatial distribution of particles correlates with variations in salinity and ionic composition (a 20- and 80-fold decrease in the Ca^{2+}/Cl^- and HCO_3^-/Cl^- ratios), turbulent mixing following a storm and shower precipitation. In the estuary zone, the dilution of river water with sea-water leads to a significant reduction in particle count: from 98 to 44 particles/m^3, and subsequently to 13 particles/m^3. The primary source of microplastics is anthropogenic runoff from the Volga, including diffuse runoff from urbanised areas. The specific nature of the Caspian Sea as a closed basin with a significant river runoff results in relatively higher microplastics concentrations than those found in open seas. The obtained data justify the need to control surface runoff and monitor estuarine geochemical barriers.

Keywords: microplastics, Northern Caspian Sea, Lower Volga, mixing zone, ionic composition, anthropogenic pollution

© Antsiferova M. A., Kleshchenkov A. V., Korshun A. M., 2026

This work is licensed under a Creative Commons Attribution-Non Commercial 4.0 International (CC BY-NC 4.0) License

Acknowledgements: The article was prepared under state assignment of SSC RAS no. 125012100503-4. The work was performed using equipment of the Shared Research Facility of SSC RAS, no. 501994.

For citation: Antsiferova, M.A., Kleshchenkov, A.V. and Korshun, A.M., 2026. Microplastics in the Lower Volga–Northern Caspian System: Spatial Distribution in the Water Mixing Zone and Sources of Input. *Ecological Safety of Coastal and Shelf Zones of Sea*, (2), pp. 93–109.

Микропластик в системе Нижняя Волга – Северный Каспий: пространственное распределение в зоне смешения вод и источники поступления

М. А. Анциферова *, А. В. Клещенков, А. М. Коршун

Федеральный исследовательский центр Южный научный центр Российской академии наук, Ростов-на-Дону, Россия

* *e-mail: m12antsiferova@mail.ru*

Аннотация

Влияние гидрологических и гидрохимических условий на пространственное распределение микропластика в эстуарных зонах изучено слабо. Цель работы – оценка его пространственного распределения, количественных и качественных характеристик в системе Нижняя Волга – Северный Каспий. Материал получен в ходе экспедиционного рейса на НИС «Денеб» в сентябре 2023 г., пробы отбирали тралением нейстонной сети (ячея 0.3 мм) в поверхностном горизонте (0–0.2 м) с последующей обработкой по модифицированной методике *NOAA* и прямой визуальной сортировкой под микроскопом. Идентификация полимеров выполнена методами рамановской и ИК-Фурье-спектроскопии с расчетом индекса опасности *PHI*. Параллельно измеряли гидрохимические, гидрологические и метеорологические параметры среды, в частности ионный состав. В Нижней Волге среднее содержание частиц составило 81 шт/м^3, пиковые значения – 100 шт/м^3 (после ливня в Калмыкии), а также 92 шт/м^3 у Волгограда и 98 шт/м^3 у Астрахани, что указывает на антропогенный сток как основной источник. В Северном Каспии концентрации частиц существенно ниже (от 3 до 44 шт/м^3, среднее 13 шт/м^3) с выраженным нисходящим градиентом от устья. Преобладает мелкий микропластик (0.3–2 мм) в виде волокон и фрагментов, преимущественно из полиэтилена, полиэтилентерефталата и полиамида, которые отнесены ко 2-му классу опасности согласно индексу *PHI*. Пространственное распределение частиц коррелирует с динамикой солености, ионного состава (снижение коэффициентов Ca^{2+}/Cl^- и HCO_3^-/Cl^- в 20 и 80 раз), турбулентным перемешиванием после шторма и ливневыми осадками. В эстуарной зоне разбавление речных вод морскими приводит к значительному снижению количества частиц: с 98 до 44 шт/м^3, а затем до 13 шт/м^3. Основной источник микропластика – антропогенный сток Волги, включая диффузный смыв с урбанизированных территорий. Уникальность Каспия как замкнутого водоема с мощным речным стоком обусловливает относительно повышенные концентрации микропластика по сравнению с открытыми морями. Полученные данные обосновывают необходимость контроля поверхностного стока и мониторинга эстуарных геохимических барьеров.

Ключевые слова: микропластик, Северный Каспий, Нижняя Волга, зона смешения, ионный состав, антропогенное загрязнение

Благодарности: публикация подготовлена в рамках реализации госзадания ЮНЦ РАН, № госрегистрации 125012100503-4. Работа выполнена на оборудовании ЦКП «Объединенный центр научно-технологического оборудования ЮНЦ РАН (исследование, разработка, апробация)», № 501994.

Для цитирования: *Анциферова М. А., Клещенков А. В., Коршун А. М.* Микропластик в системе Нижняя Волга – Северный Каспий: пространственное распределение в зоне смешения вод и источники поступления // Экологическая безопасность прибрежной и шельфовой зон моря. 2026. № 2. С. 93–109. EDN EUXOMX.

Introduction

Microplastics (MPs) are solid, water-insoluble particles of synthetic polymers characterised by heterogeneity of properties, composition, and characteristics [1]. The key criterion for classifying plastics into this group is particle size – from 0.1–0.3 mm (depending on sampling methods [2]) to 5 mm. The considerable variability of MP characteristics gives rise to a number of unresolved issues, e.g., concerning particle sources, transport patterns, quantitative assessment, and, most importantly, the degree of MP impact on living organisms and ecosystems as a whole. One of the main challenges in assessing MP concentrations in the environment remains the lack of unified standardised protocols for sampling, sample preparation, and particle identification.

MP pollution of freshwater environments has long been studied less intensively than that of marine environments; however, the number of relevant studies has been growing recently [3–5]. The study area is the shelf zone of the Caspian Sea – the largest inland water body on the planet. Its drainage basin generates a runoff of about 300 km³, over 80% of which (255 km³) is contributed by the Volga River [6]. This makes the northern part of the sea particularly important as an extensive mixing zone where river runoff is transformed. Despite the importance of the region, the problem of its MP pollution remains poorly studied. Existing publications mainly address the southern (Iranian) [7, 8] and western (Kazakhstan) [9] coasts. For the southern Caspian Sea, mean and median MP concentrations are 15 and 12 items/kg in bottom sediments, and 710 and 650 items/m³ in the water column [10]. However, comprehensive studies of the Volga–Caspian mixing zone have not been carried out so far.

Our study, in addition to the Northern Caspian Sea, covers the Lower Volga, since rivers are recognised as the main source of anthropogenic litter entering the seas. The Lower Volga has been studied previously: earlier studies [11] confirmed the presence of MPs in surface waters and aquatic organisms. A comprehensive survey of both water bodies makes it possible to assess the spatial distribution patterns of pollution and its sources.

The present paper is aimed at estimating the MP content in the waters of the Lower Volga and the Northern Caspian Sea, analysing the specifics of their input and spatial distribution in the mixing zone of river and sea waters, and determining the qualitative characteristics and polymer composition of particles against the background of changing hydrochemical water parameters.

Materials and methods

The material for the study was collected during an expedition of the Southern Scientific Centre of the Russian Academy of Sciences on board the R/V *Deneb* in September 2023. Sampling stations covered the Lower Volga (from the exit of the Volga–Don Shipping Canal to the mouth area) and the northwestern part of the Caspian Sea (from the Volga–Caspian Shipping Canal (VCSC) to the Izberbash area).

Concentrated samples were taken by trawling with a neuston trawl net (0.3 mm mesh) in the surface layer (0–0.2 m). During sampling, the colour of the ship's side and deck was taken into account to minimise secondary contamination.

Samples were processed according to a modified NOAA method [12]. The main sample preparation steps included filtration through a fine-mesh (100 μm) nylon filter, wet oxidation in hydrogen peroxide with the addition of iron (Fenton's reaction), and density separation in a zinc chloride solution ($ZnCl_2$, $\rho = 1.6$ g/cm^3). Thus, the sample was cleaned of the bulk of accompanying organic and mineral material.

Quantitative, morphometric, and morphological analyses were performed by direct visual sorting under an optical microscope (stereo Micromed MS-1 var. 2C Digital, 20× magnification), during which the number of particles was counted, normalised to 1 m^3 of filtered water, and their characteristics were described: shape (fibre, fragment, granule, film), colour, and size.

The composition of particles preliminarily identified as MPs by the hot needle method was analysed using Raman spectroscopy (RAMOS S120) and Fourier-transform infrared spectroscopy (FSM 2202). Initially, both methods were used in parallel for the most representative samples from the dataset; subsequently, they complemented each other to cover a larger number of samples and establish a broad list of polymers.

Based on the polymer composition data, the overall Polymer Hazard Index (PHI) was calculated in accordance with the methodology, adapted for MP mixtures in [13], as proposed in [14] using the formula

$$PHI = \sum Pn \times Sn,$$

where Pn is the percentage share of particles of a specific polymer type; Sn is the hazard score of that polymer according to Table 2 in [14, pp. 3312–3315]. The obtained value was compared with threshold ranges (Table 1 in [14, p. 3311]): less than 10 – class I (low risk), 10–100 – II (moderate risk), 100–1000 – III (significant risk), over 1000 – IV (high risk). It should be noted that, although the PHI index is widely used for preliminary risk assessment, it is a simplified tool because it does not account for the full set of particle characteristics such as size, morphology, presence of additives, and degree of degradation, which significantly affect the ecotoxicological potential of particles. Therefore, the obtained PHI values should be interpreted as a primary hazard indication.

Quality control was carried out at all stages of the work; only glass laboratoryware was used, the filters used were thoroughly rinsed with distilled water, and all reagents were filtered through fine-mesh filters (100 μm). Under laboratory conditions, blank samples were analysed, and open Petri dishes with distilled water were exposed to monitor background MP content in the air. The lower limit of particle detection was 0.3 mm, which is determined by the mesh size of the sampling net. Therefore, the obtained concentrations should be regarded as underestimated relative to actual values [15].

In parallel with MP sampling, monitoring of aquatic environment parameters was carried out. Profiles of temperature, salinity, turbidity, and density were measured with a CTD-48 hydrological probe. Meteorological parameters were recorded by an automatic shipboard station.

Water samples for hydrochemical analysis were taken using standard oceanological methods with a bathometer from the surface layer (down to 0.5 m). In the laboratory of the SSC RAS, water hardness (PND F 14.1:2.98-97) and the concentrations of major ions of the salt composition were determined by direct analysis of chlorides (PND F 14.1:2.96-97), sulphates (PND F 14.1:2.108-97), bicarbonates (PND F 14.2.99-97), and calcium ions (PND F 14.1:2.95-97). Magnesium ion concentration was calculated from the difference between hardness and calcium concentration in equivalent form. The total concentration of sodium and potassium ions was determined as the difference between the sum of anion concentrations (chlorides, bicarbonates, and sulphates) and the sum of cation concentrations (calcium and magnesium ions) in equivalent form (RD 52.24.514-2009).

To compare water areas with different mineralisation, ion contents were calculated in percent equivalents (%-equiv), whereby the sum of anions, like the sum of cations, in water was taken as 100% [1)]. Changes in the percent-equivalent concentrations of salt-forming ions were used as an indicator of salt composition transformation.

To identify the factors governing the spatial distribution of MPs in the river–sea mixing zone, hydrological and hydrochemical parameters were analysed in parallel with MP sampling. The variability of the ionic composition of the Northern Caspian Sea waters is shaped primarily by the Volga River runoff. Statistical data processing was performed in Microsoft Excel.

Results and Discussion

Quantity and spatial distribution of microplastics

MPs were detected in the aquatic environment at all stations.

In the Lower Volga, the average particle concentration was 81 particles/m³ [16]. The highest content (100 particles/m³) was observed in the Kalmykia area after a heavy downpour, indicating a likely contribution of diffuse runoff and atmospheric precipitation. High values were also recorded near major urbanised centres: 92 particles/m³ at St. *1v* near Volgograd and 98 particles/m³ at St. *5v* near Astrakhan (Fig. 1). The minimum (58 particles/m³) was recorded downstream of the Buzan distributary branch.

[1)] Alekin, O.A., 1970. [*Hydrochemistry Basics. A Study Guide*]. Leningrad: Gidrometeoizdat, 442 p. (in Russian).

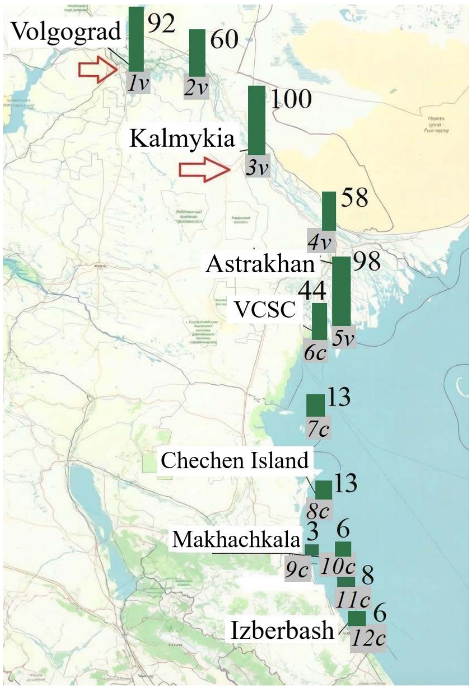

F i g . 1 . Schematic map of microplastics distribution in the Lower Volga and North Caspian (September 2023). The arrows show areas of elevated pollution, the black numbers are station numbers, the green ones are MP concentrations (particles/m^3)

In the Northern Caspian Sea, MP particle concentrations markedly decrease with distance from the Volga mouth. The highest value (44 particles/m^3) was recorded in the Volga–Caspian Canal. Elevated MP content relative to the rest of the sea also persists at the next two stations (St. *7c* and *8c* in Fig. 1) near Chechen Island (13 particles/m^3). The minimum particle concentration (3 particles/m^3) was recorded near the coast in the area of Kaspiysk (St. *9c*). The average value for the northwestern part of the Caspian Sea, given such a wide scatter of values, is 13 particles/m^3 [17]. The obtained values are consistent with the global range of MP concentrations in water bodies and are at the level of average values (from 0.3 to 150 particles/m^3) [3–5].

The revealed pattern confirms that the Lower Volga, like many river systems of the world, is an important source of microplastic input into the marine environment [18]. The established MP content in the river (average 81 particles/m^3) exceeds concentrations in the Northern Caspian Sea (13 particles/m^3). Peak microplastics concentration values near large cities (Volgograd, Astrakhan) point to an anthropogenic source of their input – surface runoff from urbanised areas. The maximum concentration (100 particles/m^3) after a downpour in the Kalmykia area indicates a probable contribution of atmospheric precipitation and diffuse runoff. A direct link has not been proven, but a similar situation has been described in other studies [19], and atmospheric precipitation is generally considered one of the important pathways for microplastics entering water bodies.

With distance from the Volga mouth in the marine area, a clear trend towards a decrease in particle concentration is observed, followed by a slight increase (see Fig. 1). The specific nature of the Caspian Sea as a closed basin with a significant river runoff means that the average concentration of MP particles in its north-western part (13 particles/m³) exceeds levels typical of many open marine waters [2].

Morphological and morphometric characteristics; polymer composition of particles

Analysis of the qualitative characteristics of microplastics revealed differences between particles in the river and sea areas. In the waters of the Lower Volga, mainly transparent filamentous fibres up to 1 mm in length (modal value 0.7 mm) were found. Coloured particles (most common colours: black, white, blue) and those of other shapes (mainly fragments) occurred less frequently (Fig. 2, Table 1).

A more diverse assemblage is observed in the Northern Caspian Sea: along with fibres (54%), fragments (32%) are widely represented, as well as occasional granules and films. The colour palette of particles is diverse, but, as in the river, transparent samples predominate; among coloured particles, white and pink are the most common. In the sea, particles from 0.5 to 2 mm in length dominate the size range (Fig. 2, Table 1); other size fractions (0.3–0.5 and 2–5 mm) occurred significantly less frequently.

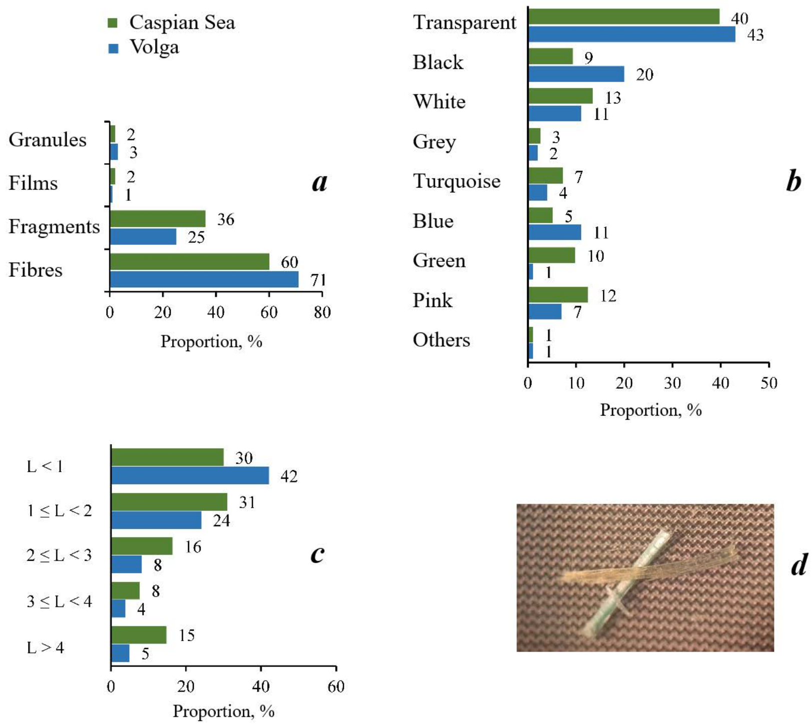

F i g . 2 . Microplastics distribution by characteristics in the Lower Volga and Northern Caspian Sea: by shape (*a*), colour (*b*) and size, mm (*c*). Particle samples (*d*)

T a b l e 1 . Statistical indicators of the microplastics length, mm

Water body	Average ($\bar{x}$)	Mode (M_o)	Median (M_e)
Lower Volga	1.5	0.7	1.0
Northern Caspian Sea	1.9	0.7	1.3

In general, for both water bodies, the width of MP fibres ranges from 0.01 to 0.05 mm, and that of fragments from 1 to 3 mm.

In the Volga waters, low- and high-density polyethylene (PE), polyethylene terephthalate (PET), and polyamide (PA) predominate. In marine samples, the bulk is also composed of PET and PE, while the proportion of ethylene vinyl acetate (EVA) increases (Fig. 3). In both water bodies, polystyrene (PS) (see Fig. 3), polypropylene (PP) and occasional polyurethane (PU), polyvinyl chloride (PVC), polyvinyl acetate (PVA), polyoxymethylene (POM) and polymethyl methacrylate (PMMA) were detected in smaller quantities.

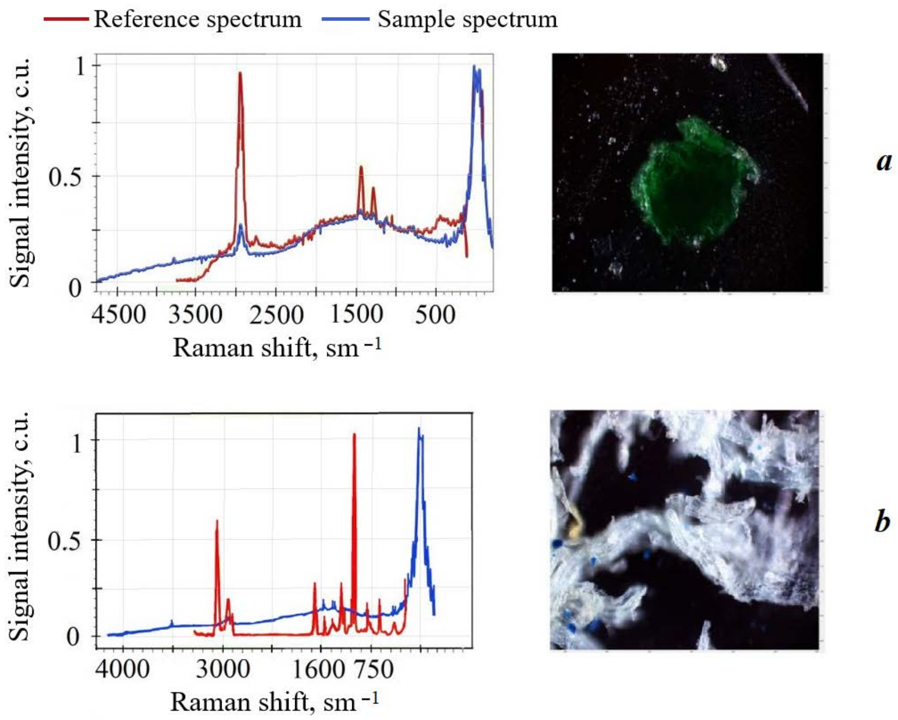

F i g . 3 . Spectra of Raman scattering (*right*) and photos (*left*) of polymers collected in the Caspian Sea: *a* – polyethylene-vinyl-acetate; *b* – polystyrene

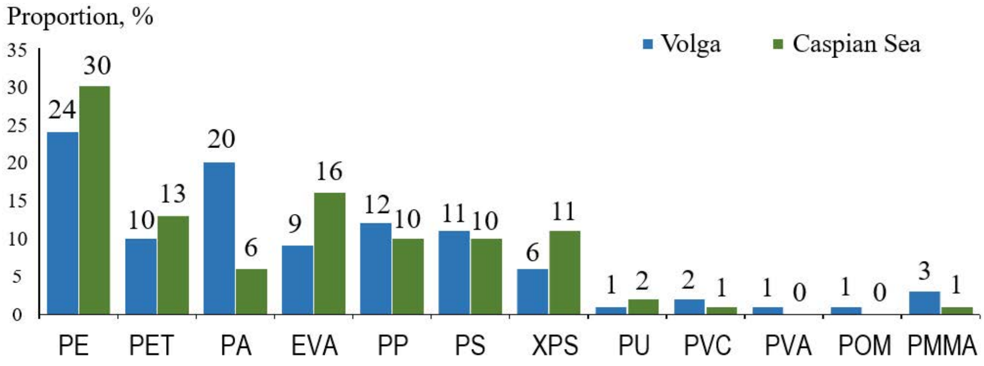

F i g . 4 . Percentage of particles by polymer type. Notations: PE – polyethylene, PET – polyethylene terephthalate, PA – polyamide, EVA – (poly)ethylene vinyl acetate, PP – polypropylene, PS – polystyrene, XPS – extruded polystyrene, PU – polyurethane, PVC – polyvinyl chloride, PVA – polyvinyl acetate, POM – polyoxymethylene, PMMA – polymethyl methacrylate.

According to PHI calculations, most of the polymers – PE, PET, PA, EVA, PP, and PS – belong to hazard class 2 (Fig. 4). Polymers of higher hazard classes were found in single particles: PU, PVC, PVA, POM, and PMMA.

Qualitative analysis revealed differences in particle characteristics. The predominance of fine fibres with high bioaccumulation potential is typical of the river. In the sea, the proportion of larger fragments increases, and the polymer composition changes (with an increase in the share of ethylene vinyl acetate), which is likely associated with sedimentation, fragmentation, and selective transport. Although most of the identified polymers belong to hazard class 2 according to the PHI index, the actual ecotoxicological threat may be higher. As Raman spectroscopy showed, particles contain chemical additives (e.g., flame retardants, dyes) that have greater mobility and biological activity than the base polymer. This confirms the need for a comprehensive assessment of microplastic hazard, considering not only the polymer composition but the entire spectrum of associated contaminants.

Meteorological conditions and hydrological factors of the aquatic environment

During the expedition, meteorological conditions varied from moderate when entering the Volga (air temperature 13.8°C) to consistently warm in the Caspian Sea (21–21.8°C) with easterly and north-easterly winds. Shower precipitation was recorded in the Kalmykia area. A storm occurred on 23 September.

Shower precipitation had a noticeable effect on the local distribution of the pollutant: the maximum MP particle concentration in the Kalmykia area (100 particles/m^3) is likely associated with the effect of diffuse runoff after heavy rain, demonstrating the importance of diffuse sources of pollutant input.

A pattern can be traced in the distribution of MPs: higher particle concentration values are recorded in the river and relatively low values in the sea, with a gradual decrease in the water mixing zone (the seaward edge of the delta). This is evident during the transition from the river station (*6c*) to the first sea stations (*7c* and *8c*) and is due to the dilution of river runoff with seawater. Storm-induced mixing also probably affected the distribution dynamics; according to expedition observations, it led to the displacement of water masses, which is reflected in salinity values and explains the similar MP concentrations (13 particles/m^3) at the stations before and after Chechen Island.

Water salinity increased from 0.19–0.20 PSU at the river stations to 2.89–11.4 PSU in the open sea. Turbidity was maximal (75.1 FTU) at the transitional station *7c*, then decreased (Table 2).

Thus, a combined influence of various factors and events on the spatial dynamics of MPs was noted: direct meteorological events (downpours, storms) provoking diffuse input and mixing of waters, and hydrological factors, among which river runoff plays a key role as the main source of particle input into the sea.

Table 2. Hydrological parameters of the aquatic environment

Station	*S*, PSU	Density, kg/m^3	pH	Turbidity, FTU	*T*, °C	Transparency, m
1v	0.19	998.38	7.83	4.70	19.80	2.10
2v	0.19	998.40	7.75	7.50	19.70	2.60
3v	0.20	998.44	7.68	8.20	19.60	1.60
4v	0.20	998.39	7.84	9.83	19.00	1.40
5v	0.19	998.40	7.79	7.28	19.80	1.10
6c	0.20	998.43	7.36	15.40	19.60	–*
7c	2.89	1000.18	7.31	75.10	21.00	0.30
8c	10.31	1005.73	6.50	55.70	21.20	0.50
9c	11.17	1006.29	6.33	16.70	21.60	0.80
10c	11.34	1006.28	6.23	8.94	22.20	1.40
11c	11.36	1006.46	6.31	2.88	21.50	5.00
12c	11.29	1006.37	5.97	6.14	21.70	8.00

* Transparency was not measured because the samples were taken in the evening.
Note: *S* – salinity; *T* – temperature.

Ionic composition of waters in the mixing zone

Within the framework of this research, the ionic composition is considered exclusively as a background environmental parameter characterising the physicochemical conditions of the water area. A detailed comparison of data on the composition and distribution of MP particles is not carried out; however, understanding the basic hydrochemical setting is necessary for the correct interpretation of the mixing zone as an area of potential pollutant accumulation. Since MPs are part of suspended matter, similar distribution patterns are expected for MP particles and suspended matter [20]. Therefore, the ionic composition of the study water area was simultaneously analysed (see Figs. 5 and 6).

The ionic composition of the Northern Caspian Sea is shaped by several factors, the main one being the Volga River runoff, whose influence extends over the entire water column of this shallow part of the sea. In the eastern part, Ural waters, which differ from the Volga waters in the content of certain components, have an impact. From the south, water from the Middle Caspian arrives with an already established ionic composition. As a result of the displacement of these water masses in the Northern Caspian Sea, waters of different ionic composition are formed – from freshened waters with chlorinity less than 1‰ to those close to true Caspian waters [2)].

The spatial variability of the ionic composition of the northwestern Caspian waters, which are under the dominant influence of the Volga River runoff, reflects complex processes of mixing, dilution, physicochemical interaction, and biological transformation. The ionic composition of the Volga and Caspian waters is presented in Table 3. Sharp fluctuations in water mineralisation are observed in the estuarine zone.

The analysis of the transformation of ionic composition at the river–sea boundary is most representative when considering the relative ion concentrations (%-equiv.). In the mixing zone of the Volga freshwater with the saline waters of the Caspian Sea, with increasing mineralisation, a so-called salt barrier is observed, characterised by changes in the relative concentrations of anions and cations (Fig. 5).

In the estuarine zone, where a sharp increase in mineralisation is observed, the following patterns have been revealed. In the anion group, chlorides become dominant already at a mineralisation above 4.46 g/kg, reaching values of more than 60%-equiv. In contrast, sulphates show a slight decreasing trend. Bicarbonate ion concentrations, which never take a leading position in marine waters, decrease most sharply at the river–sea boundary: in the mixing zone, their relative values decrease more than 10-fold.

Among the cations in the mixing zone, the sodium ion dominates, and its share increases monotonically with increasing mineralisation (from 30 to 65%-equiv.). A positive trend is also characteristic of magnesium ions: with distance from the mouth, their relative concentration gradually increases. In contrast, the calcium ion,

---

[2)] Pakhomova, A.S. and Zatuchnaya, B.M., 1966. [*Hydrochemistry of the Caspian Sea*]. Leningrad: Gidrometeoizdat, 342 p. (in Russian).

T a b l e 3. Spatial variability of the ion-salt composition in the Lower Volga and Northern Caspian waters in September 2023 (the period of expeditionary studies of the Southern Scientific Center of the Russian Academy of Sciences)

1. Lower Volga

Station	Mineralisation, mg/L	Concentration, mg/L					
		Cl^-	HCO_3^-	SO_4^{2-}	Ca^{2+}	Mg^{2+}	Na^++K^+
1v	286.70	31.91	117.16	48.10	56.87	12.16	20.50
2v	299.68	39.00	122.04	46.49	53.95	10.70	27.50
5v	309.58	35.45	129.36	46.49	47.15	13.13	38.00

2. Northern Caspian

Station	Mineralisation, g/kg	Concentration, g/kg					
		Cl^-	HCO_3^-	SO_4^{2-}	Ca^{2+}	Mg^{2+}	Na^++K^+
7c	4.46	1.77	0.17	0.96	0.13	0.21	1.22
9c	13.38	5.32	0.24	3.17	0.33	0.72	3.60
11c	13.32	5.14	0.24	3.36	0.34	0.76	3.48
12c	13.97	5.67	0.26	3.17	0.34	0.77	3.76

which is predominant in fresh mouth waters (over 40%-equiv. in the Lower Volga) at a mineralisation of up to 1 g/L, sharply loses its significance upon contact with the marine environment: already at the first sea station (*7c*), its relative concentration decreases approximately 5-fold.

The work "On the Formation of the Salt Barrier in the Azov, Caspian, and Aral Seas" shows that during the mixing of waters in estuarine zones, all transition stages between hydrocarbonate-calcium and chloride-sodium waters are observed [21]. The evolution of the ionic composition in the mixing zone of river and sea waters has a pronounced stage-by-stage character. The first and most dynamic stage (mineralisation from 0.3 to 4.46 g/kg) is accompanied by a fundamental restructuring of the salt complex: a sharp increase in the share of chlorides against the background of decreasing sulphate and bicarbonate concentrations leads to the transition from the hydrocarbonate water class to the chloride class, and from calcium to sodium dominance in the cation composition. At the second stage (mineralisation from 4.46 to 13.38 g/kg), the ionic composition of the mixing zone waters approaches the composition of the Northern Caspian waters. Finally, at the third stage (mineralisation above 13.38 g/kg), the dominant influence of the marine component is preserved, but the intensity of water enrichment with marine ions (chlorides and sodium) significantly decreases.

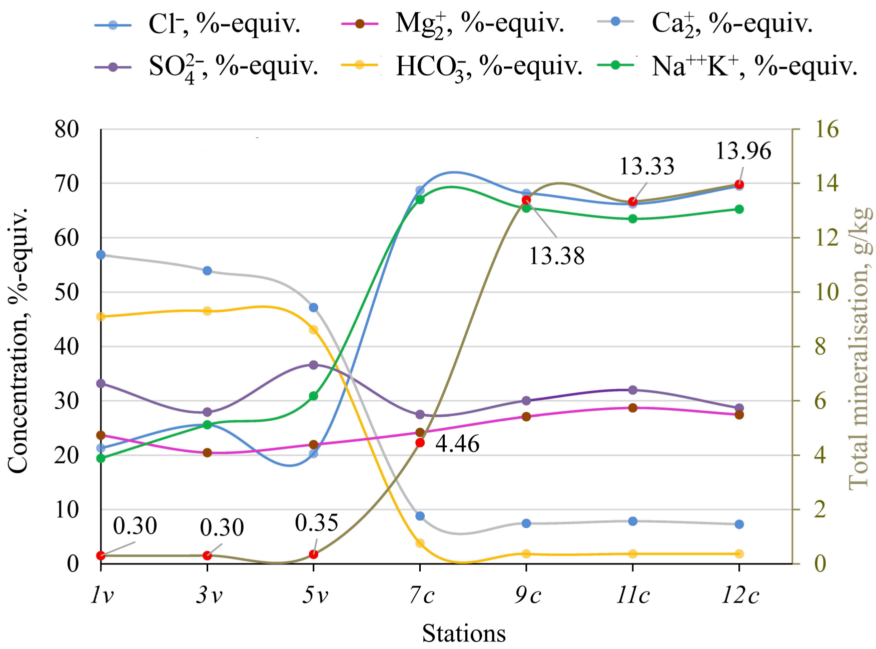

F i g . 5 . Spatial variability in the relative concentrations of the ionic and salinity composition of waters in the Lower Volga and the Northern Caspian Sea in September 2023 (the period of expeditionary studies of SSC RAS)

The transition from fresh waters to the mixing zone waters is illustrated in Fig. 6. The change in key interionic coefficients demonstrates pronounced non-linearity in the mixing zone. At the first stage, in the salinity interval 0–0.2 PSU, the maximum values of the key interionic ratios are recorded. However, already in the next range of 0.2–2.89 PSU, a sharp decrease occurs. At the second, more prolonged mixing stage (salinity 2.89–11.36 PSU), the metamorphosis of the water mass intensifies. The coefficients Ca^{2+}/Cl^{-} and HCO_3^{-}/Cl^{-}, the most sensitive to the input of seawater, decrease significantly – approximately 20-fold and 80-fold, respectively, compared to their values in the Volga water at the seaward delta edge, while the coefficients $Na^{+}+K^{+}/Cl^{-}$ and SO_4^{2-}/Mg^{2+}, with an overall increase in salinity, decrease only 1.62- and 1.60-fold, which indicates their relative stability [12].

It is important to note that the sharp decrease in MP concentration (from 44 to 13 particles/m^3) occurs synchronously with the first, most contrasting stage of ionic composition transformation (mineralisation from 0.3 to 4.46 g/kg, salinity up to ~ 3 PSU) during the change of the water chemical composition from carbonate-calcium to chloride-sodium.

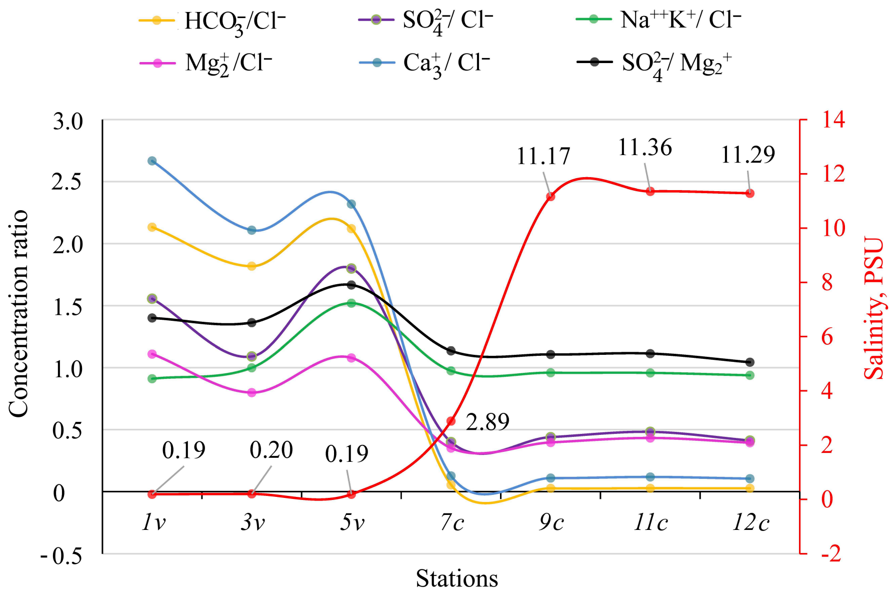

Fig. 6. Relative values of salt-forming components and salinity of water in the Lower Volga and the Northern Caspian in September 2023 (the period of expedition studies at the SSC RAS)

With distance from the Volga mouth, a subsequent increase in mineralisation from 4.46 to 13.38 g/kg is observed, which corresponds to the phase of active adjustment of the mixed water composition to the characteristics of the Northern Caspian marine environment. At the transition between these zones (distance from the river–sea boundary), the most significant decrease in the amount of MPs for the Caspian Sea is recorded: from 44 particles/m³ at St. *6c* to 13 particles/m³ at the next two stations, *7c* and *8c*. With an increase in mineralisation to 13.38 g/kg (salinity over 11 PSU), the process of increasing marine ion concentrations slows down substantially, which indicates that the system has reached a stage of relative chemical stabilisation, or complete dilution of river waters by marine waters. The minimum amount of MPs (3 particles/m³) and a noticeable change in the fractional composition of particles are observed upon transition to the region of marine ion stabilisation (salinity over 11 PSU).

The revealed correlation suggests that the processes forming the geochemical barrier in the estuary (coagulation, flocculation, sedimentation of suspended matter) probably also affect MP transport. This assumption agrees with the concept of the marginal filter, the active gravitational step of which in the Caspian Sea is located between the isohalines of 0.2 and 2 PSU [22] – it is precisely in this salinity interval that the most significant drop in MP concentrations is observed.

Thus, the distribution of MPs in the coastal-shelf zone of the Northern Caspian is influenced by a set of factors, including: 1) the intensity and localisation of anthropogenic load in the river basin; 2) the river runoff regime; 3) meteorological and hydrodynamic conditions (e.g., storm-induced mixing recorded during the survey period). Accounting for these factors is necessary for the development of a scientifically grounded monitoring system and measures to ensure the environmental safety of the vulnerable ecosystem of the Caspian Sea.

Conclusions

MPs were detected at all stations in the waters of the Lower Volga and the Northern Caspian Sea. In the river, their quantity varies from 58 to 100 particles/m³, averaging 81 particles/m³; peak values were recorded near large cities and after heavy atmospheric precipitation. This confirms the role of the river as the main source of anthropogenic plastic input into the Northern Caspian. In the sea itself, the extreme values of MP particle concentrations range from 3 to 44 particles/m³, with an average of 13 particles/m³. The relatively elevated numerical values compared to other open seas are due to the closed nature of the water body and the powerful river inflow.

The maximum decrease in the amount of MPs (from 44 to 13 particles/m³) occurs in parallel with the phase of sharp ionic composition transformation (0.3–4.46 g/kg), while the lowest value (3 particles/m³) and a change in the fractional composition are observed simultaneously with the attainment of chemical stabilisation in highly mineralised waters (over 13.38 g/kg). Since plastic is chemically inert, the transformation of waters itself does not affect its distribution; however, the mechanism of dilution and subsequent distribution of particles in a larger water mass volume affects the observed spatial dynamics.

The qualitative characteristics of MPs have been determined. Predominantly transparent samples, fine fibres (up to 2 mm), and coloured fragments of polyethylene, PET, and polyamide prevail, belonging to potential hazard class 2. The detection of toxic additives (dyes, flame retardants) in the particles points to the need for assessing the integrated chemical risk, not just that of the polymer matrix.

The aquatic environment where MP pollution is considered is a mixing zone with a pronounced stage-by-stage transformation of water masses. The restructuring of the water chemical composition occurs at the initial stage, up to a mineralisation of 4.46 g/kg, at which the change from the hydrocarbonate-calcium to the chloride-sodium class is recorded. The high contrast of the environment is confirmed by the non-linear change in interionic coefficients (Ca^{2+}/Cl^-, HCO_3^-/Cl^-), which decrease by tens of times. This indicates a heterogeneous hydrochemical background, which determines the specific conditions of settling and transit of suspended matter in the area of anthropogenic pollution.

The obtained results can serve as a scientific basis for developing a monitoring system and measures to reduce anthropogenic load. They highlight the critical importance of controlling surface runoff from urbanised areas and preserving the functional integrity of estuarine mixing zones to ensure the long-term environmental safety of the unique and vulnerable coastal-shelf ecosystem of the Caspian Sea.

REFERENCES

1. Rochman, C.M., Brookson, C., Bikker, J., Djuric, N., Earn, A., Bucci, K., Athey, S., Huntington, A., McIlwraith, H. et al., 2019. Rethinking Microplastics as a Diverse Contaminant Suite. *Environmental Toxicology and Chemistry*, 38(4), pp. 703–711. https://doi.org/10.1002/etc.4371
2. Chubarenko, I.P., Esyukova, E.E., Khatmullina, L.I., Lobchuk, O.I., Isachenko, I.A. and Bukanova, T.V., 2021. [*Microplastics in the Marine Environment*]. Moscow: Nauchny Mir, 520 p. (in Russian).
3. Frank, Yu.A., Vorobiev, E.D., Rakhmatullina, S.N., Trifonov, A.A. and Vorobiev D.S., 2022. Screening of Microplastic Content in Surface Waters of Russian Rivers. *Ecology and Industry of Russia*, 26(9), pp. 67–71. https://doi.org/10.18412/1816-0395-2022-9-67-71 (in Russian).
4. Frank, Y.A., Vorobiev, E.D., Vorobiev, D.S., Trifonov, A.A., Antsiferov, D.V., Soliman Hunter, T., Wilson, S.P. and Strezov, V., 2021. Preliminary Screening for Microplastic Concentrations in the Surface Water of the Ob and Tom Rivers in Siberia, Russia. *Sustainability*, 13(1), 80. https://doi.org/10.3390/su13010080
5. Gao, S., Orlowsky, N., Bopf, F.K. and Breuer, L., 2024. Review on Microplastics in Large European Rivers. *WIREs Water*, 11(3), e1713. https://doi.org/10.1002/wat2.1713
6. Mikhailov, V.N., 1997. [*River Mouths in Russia and Neighbouring Countries: Past, Present and Future*]. Moscow: GEOS, 413 p. (in Russian).
7. Nematollahi, M.J., Moore, F., Keshavarzi, B., Vogt, R.D., Saravi, H.N. and Busquets, R., 2020. Microplastic Particles in Sediments and Waters, South of Caspian Sea: Frequency, Distribution, Characteristics, and Chemical Composition. *Ecotoxicology and Environmental Safety*, 206, 111137, https://doi.org/10.1016/j.ecoenv.2020.111137
8. Manbohi, A., Mehdinia, A., Rahnama, R., Hamzehpour, A. and Dehbandi, R., 2023. Distribution of Microplastics in Upstream and Downstream Surface Waters of the Iranian Rivers Discharging to the Southern Caspian Sea. *Environmental Science and Pollution Research*, 30(40), pp. 92359–92370. https://doi.org/10.1007/s11356-023-28898-8
9. Taghizadeh Rahmat Abadi, Z., Abtahi, B., Grossart, H.-P. and Khodabandeh, S., 2021. Microplastic Content of Kutum Fish, *Rutilus frisii kutum* in the Southern Caspian Sea. *Science of The Total Environment*, 752. 141542. https://doi.org/10.1016/j.scitotenv.2020.141542
10. van Emmerik, T.H.M., González-Fernández, D., Laufkötter, C., Blettler, M., Lusher, A., Hurley, R. and Ryan, P.G., 2023. Focus on Plastics from Land to Aquatic Ecosystems. *Environmental Research Letters*, 18(4), 040401. https://doi.org/10.1088/1748-9326/acc086
11. Litvinov, K.V., Kalmykov, A.P. and Biryukova, M.G., 2020. Microplastics as a New Component in the Ecosystem of the Lower Zone of the Volga Delta. *Astrakhan Bulletin of Ecological Education*, (6), pp. 147–152. https://doi.org/10.36698/2304-5957-2020-19-6-147-152 (in Russian).
12. Zobkov, M.B. and Esiukova, E.E., 2018. Microplastics in a Marine Environment: Review of Methods for Sampling, Processing, and Analyzing Microplastics in Water, Bottom Sediments, and Coastal Deposits. *Oceanology*, 58(1), pp. 137–143. https://doi.org/10.1134/S0001437017060169
13. Xu, P., Peng, G., Su, L., Gao, Y., Gao, L. and Li, D., 2018. Microplastic Risk Assessment in Surface Waters: A Case Study in the Changjiang Estuary, China. *Marine Pollution Bulletin*, 133, pp. 647–654. https://doi.org/10.1016/j.marpolbul.2018.06.020
14. Lithner, D., Larsson, Å. and Dave, G., 2011. Environmental and Health Hazard Ranking and Assessment of Plastic Polymers Based on Chemical Composition. *Science of the Total Environment*, 409(18), pp. 3309–3324. https://doi.org/10.1016/j.scitotenv.2011.04.038
15. Antsiferova, M.A., Glushko, A.E., Bespalova, L.A., Kleshchenkov, A.V. and Nazarenko, A.V., 2025. Microplastics in Water and Problems of Its Identification (the Water Bodies in the South of the European Part of Russia are Example). *Proceedings of Voronezh State University. Series: Geography. Geoecology*, (1), pp. 115–124. https://doi.org/10.17308/geo/1609-0683/2025/1/115-124 (in Russian).

16. Antsiferova, M.A., 2024. Polymer Microparticles: Content, Distribution in the Lower Volga. *Ekologia. Ekonomika. Informatika. Seriya: Sistemny Analiz i Modelirovanie Ekonomicheskikh i Ekologicheskikh Sistem*, 1(9), pp. 19–21 (in Russian).
17. Antsiferova, M.A., 2024. Concentrations of Microplastics in the Waters of the Northern Caspian Sea. In: SSC RAS, 2024. *Strategic Problems, Threats, and Risks of the Sea of Azov Basin and the Sea of Azov Region ("Hazardous Phenomena–V"). Proceedings of the 5th International Scientific Conference in Memory of Corresponding Member RAS D.G. Matishov (Rostov-on-Don, 10–14 July 2024)*. Rostov-on-Don: SSC RAS Publishers, pp. 277–279 (in Russian).
18. Yakushev, E., Gebruk, A., Osadchiev, A., Pakhomova, S., Lusher, A., Berezina, A., van Bavel, B., Vorozheikina, E., Chernykh, D. et al., 2021. Microplastics Distribution in the Eurasian Arctic is Affected by Atlantic Waters and Siberian Rivers. *Communications Earth and Environment*, 2, 23. https://doi.org/10.1038/s43247-021-00091-0
19. Werbowski, L.M., Gilbreath, A.N., Munno, K., Zhu, X., Grbic, J., Wu, T., Sutton, R., Sedlak, M.D., Deshpande, A.D. et al., 2021. Urban Stormwater Runoff: a Major Pathway for Anthropogenic Particles, Black Rubbery Fragments, and Other Types of Microplastics to Urban Receiving Waters. *ACS ES&T Water*, 1(6), pp. 1420–1428. https://doi.org/10.1021/acsestwater.1c00017
20. Kravchishina, M.D., Klyuvitkin, A.A., Lukashin, V.N., Politova, N.V., Novigatsky, A.N. and Lisitsyn, A.P., 2018. Distribution of Suspended Particulate Matter in the Caspian Sea. *Russian Meteorology and Hydrology*, 43(10), pp. 697–705. https://doi.org/10.3103/S1068373918100096
21. Tsytsarin, A.G. and Lobov, A.L., 1995. Formation of Salt Barriers in the Sea of Azov, the Caspian and Aral Seas. *Meteorologiya i Gidrologiya*, (6), pp. 84–94 (in Russian).
22. Lisitsyn, A.P., 1994. A Marginal Filter of the Oceans. *Oceanology*, 34(5), pp. 735–747 (in Russian).

Submitted 04.02.2026; accepted after review 09.03.2026;
revised 19.03.2026; published 30.06.2026

About the authors:

Marina A. Antsiferova, Junior Researcher, Federal Research Centre the Southern Scientific Centre of RAS (41 Chekhov Ave., Rostov-on-Don, 344006, Russia), PhD (Geogr.), **ORCID ID: 0009-0006-6549-8606**, *m12antsiferova@mail.ru*

Aleksei V. Kleshchenkov, Leading Researcher, Federal Research Centre the Southern Scientific Centre of RAS (41 Chekhov Ave., Rostov-on-Don, 344006, Russia), PhD (Geogr.), **ORCID ID: 0000-0002-7976-6951, Scopus Author ID: 57016697100, ResearcherID: E-6619-2014**, *kle-aleksej@yandex.ru*

Anna M. Korshun, Researcher, Federal Research Centre the Southern Scientific Centre of RAS (41 Chekhov Ave., Rostov-on-Don, 344006, Russia), PhD (Geogr.), *a_korshyn@mail.ru*

Contribution of the authors:

Marina A. Antsiferova – obtaining material during expedition cruises, sampling and sample processing, interpretation of microplastics content data, drafting the manuscript text and graphic material

Aleksei V. Kleshchenkov – general supervision of the work, obtaining and interpretation of expedition hydrological and meteorological data, drafting the manuscript text and graphic material

Anna M. Korshun – interpretation of data on the ionic composition of waters, drafting the manuscript text and graphic material

All the authors have read and approved the final manuscript.

ISSN 2413-5577, Ecological Safety of Coastal and Shelf Zones of Sea, No. 2, pp. 110–123 (2026)

Original paper

Microbiological Characteristics of the North Crimean Canal Water: A Current Status

N. V. Burdiyan *, Yu. V. Doroshenko, N. Yu. Mirzoeva, E. V. Guseva, O. V. Soloveva

A. O. Kovalevsky Institute of Biology of the Southern Seas of RAS, Sevastopol, Russia

* *e-mail: burdiyan_nv@ibss-ras.ru*

Abstract

The North Crimean Canal, which supplies water to the territory of the Crimea, was closed in April 2014. After an eight-year break, in 2022, the Dnieper River water was again channelled along the riverbed of the Canal. After destruction of the Kakhovka hydroelectric power station (June 2023), the water supply stopped. To assess the current state of the canal ecosystem, microbiological studies of its aquatic environment are required. The aim of this study is to assess the current state of the waters in the North Crimean Canal and the adjacent Black Sea waters based on microbiological indicators. Between April 2022 and June 2024, water and sediment samples were collected at 13 stations. The abundance of heterotrophic, hydrocarbon-oxidising, lipolytic and phenol-oxidising bacteria in the water samples was determined using the limiting dilution method on selective media. Temperature, redox potential and dissolved oxygen content were measured. The abundance of heterotrophic bacteria in the canal bed ranged from $4.5 \cdot 10^2$ to $2.5 \cdot 10^7$ cells·mL^{-1}. In 85% of the samples, this corresponded to the mesosaprobic zone (10^3–10^5 cells·mL^{-1}). Hydrocarbon-oxidising, lipolytic and phenol-oxidising bacteria were found throughout the study area. The proportion of hydrocarbon-oxidising bacteria within the heterotrophic bacterial community did not exceed 2%, indicating the absence of chronic oil pollution. A positive correlation was found between hydrocarbon-oxidising and lipolytic bacteria ($R = 0.73$; $n = 19$; $\alpha < 0.05$) and between heterotrophic and phenol-oxidising bacteria ($R = 0.66$; $n = 16$; $\alpha < 0.05$). No significant correlation was found between the abundance of the observed microorganisms and parameters such as water temperature, redox potential and pH. The presence of lipolytic, hydrocarbon-oxidising and phenol-oxidising bacteria indicates that the water body under study is undergoing self-purification to remove contamination by the relevant pollutants. Further observations are required for long-term monitoring.

Keywords: North Crimean Canal, bottom sediments, ecological and trophic groups of microorganisms, microbiological monitoring, Crimean Peninsula, water quality, water pollution

Acknowledgments: The work was carried out under IBSS state research assignment “Study of biogeochemical patterns of radioecological and chemoecological processes in the ecosystems of water bodies of the Sea of Azov–Black Sea Basin in comparison with other areas of the World Ocean and individual aquatic ecosystems of their drainage basins to ensure sustainable development in the southern seas of Russia” (no. 124030100127-7) as part of

© Burdiyan N. V., Doroshenko Yu. V., Mirzoeva N. Yu., Guseva E. V., Soloveva O.V., 2026

This work is licensed under a Creative Commons Attribution-Non Commercial 4.0 International (CC BY-NC 4.0) License

the implementation of the Russian Science Foundation grant "The role of the irrigation system of the North Crimean Canal in the transfer of long-lived radionuclides of Chernobyl origin, heavy metals, and hydrocarbons from Dnieper water to irrigated farmland in Crimea" (No. 23-26-00128). The authors are thankful to the staff of the Department of Radiation and Chemical Biology at the IBSS: leading engineers I. N. Moseichenko and M. O. Vakhrushev; and to the staff of the Department of Aquaculture and Marine Pharmacology at the IBSS: senior researcher, PhD (Geogr.) N. P. Kovrigina, leading engineer D. S. Borisova and junior researcher N. Yu. Rodionova.

For citation: Burdiyan, N.V., Doroshenko, Yu.V., Mirzoeva, N.Yu., Guseva, E.V. and Soloveva, O.V., 2026. Microbiological Characteristics of the North Crimean Canal Water: A Current Status. *Ecological Safety of Coastal and Shelf Zones of Sea*, (2), pp. 110–123.

Микробиологическая характеристика водной среды Северо-Крымского канала в современный период

Н. В. Бурдиян *, Ю. В. Дорошенко, Н. Ю. Мирзоева, Е. В. Гусева, О. В. Соловьёва

ФГБУН ФИЦ «Институт биологии южных морей имени А. О. Ковалевского РАН», Севастополь, Россия

* *e-mail: burdiyan_nv@ibss-ras.ru*

Аннотация

Северо-Крымский канал, обеспечивающий водой территорию Крыма, был перекрыт в апреле 2014 г. В 2022 г., после восьмилетнего перерыва, днепровская вода вновь была пущена по руслу канала. После разрушения Каховской ГЭС (июнь 2023 г.) подача воды прекратилась. Для оценки современного состояния экосистемы канала необходимо проводить микробиологические исследования водной экосистемы канала. Цель работы – оценка современного состояния вод в русле Северо-Крымского канала и прилегающих к нему акваториях Черного моря по микробиологическим показателям. С апреля 2022 г. по июнь 2024 г. отбирали пробы воды и донных отложений на 13 станциях. В пробах воды определяли численность гетеротрофных, углеводородокисляющих, липолитических и фенолокисляющих бактерий методом предельных разведений на элективных средах. Измеряли температуру, окислительно-восстановительный потенциал и содержание растворенного кислорода. Численность гетеротрофных бактерий в русле канала варьировала от $4.5 \cdot 10^2$ до $2.5 \cdot 10^7$ кл.·мл$^{-1}$. В 85 % проб она соответствовала мезосапробной зоне (10^3–10^5 кл.·мл$^{-1}$). Углеводородокисляющие, липолитические и фенолокисляющие бактерии обнаружены повсеместно. Доля углеводородокисляющих бактерий в составе гетеротрофных бактерий не превышала 2 %, что указывает на отсутствие хронического нефтяного загрязнения. Выявлена положительная корреляция между углеводородокисляющими и липолитическими бактериями ($R = 0.73$; $n = 19$; $\alpha < 0.05$), а также между гетеротрофными и фенолокисляющими бактериями ($R = 0.66$; $n = 16$; $\alpha < 0.05$). Достоверная зависимость между численностью наблюдаемых микроорганизмов и значениями таких показателей, как температура, окислительно-восстановительный потенциал и pH воды, не выявлена. Наличие липолитических, углеводородокисляющих и фенолокисляющих бактерий свидетельствует о самоочищении исследуемой акватории от загрязнений соответствующими поллютантами. Для долгосрочного мониторинга необходимо продолжить наблюдения.

Ключевые слова: Северо-Крымский канал, донные отложения, эколого-трофические группы микроорганизмов, микробиологический мониторинг, Крымский полуостров, качество вод, загрязнение вод

Благодарности: работа выполнена в рамках государственного задания ФИЦ ИнБЮМ по теме «Изучение биогеохимических закономерностей радиоэкологических и хемоэкологических процессов в экосистемах водоемов Азово-Черноморского бассейна в сравнении с другими акваториями Мирового океана и отдельными водными экосистемами их водосборных бассейнов для обеспечения устойчивого развития на южных морях России» (номер госрегистрации № 124030100127-7), в рамках реализации гранта РНФ «Роль оросительной системы Северо-Крымского канала в процессах переноса долгоживущих радионуклидов чернобыльского происхождения, тяжелых металлов, а также углеводородов с днепровской водой на поливные сельхозугодья Крыма» (№ 23-26-00128). Авторы выражают благодарность сотрудникам Отдела радиационной и химической биологии ФИЦ ИнБЮМ ведущим инженерам И. Н. Мосейченко и М. О. Вахрушеву, сотрудникам отдела Аквакультуры и морской фармакологии ФИЦ ИнБЮМ с. н. с. канд. геогр. наук Н. П. Ковригиной, ведущему инженеру Д. С. Борисовой, м. н. с. Н. Ю. Родионовой.

Для цитирования: *Бурдиян Н. В., Дорошенко Ю. В., Мирзоева Н. Ю., Гусева Е. В. и др.* Микробиологическая характеристика водной среды Северо-Крымского канала в современный период // Экологическая безопасность прибрежной и шельфовой зон моря. 2026. № 2. С. 110–123. EDN KRHDAH.

Introduction

The North Crimean Canal (NCC) is an irrigation and water supply canal drawing water from the Kakhovka Reservoir, which was specially constructed on the lower reaches of the Dnieper River. The Canal was built between 1961 and 1971 to supply water to the arid and drought-prone areas of the Kherson and Crimean Regions. The NCC is the longest of its kind in Europe: the length of the main bed exceeds 402 km, and the total length of all spillways is 11,000 km; the maximum depth of the canal is 7 m, and its width is 150 m. A significant portion of the main bed is lined with concrete to reduce water losses [1]. Until 2013, the NCC supplied 80–87% of the water consumed by the population of Crimea [2].

For many years, the quality of water withdrawn from the lower reaches of the Dnieper was rather poor [1), 2)], as this part of the river received contaminated industrial and domestic effluent from major cities and industrial centres. Intensive irrigation of the agricultural areas adjacent to the NCC has led to an increase in the volume of return water discharged from irrigation systems. This water is generally contaminated with allochthonous organic matter, and subsequently it enters natural water bodies, including the Black Sea bays.

Between 2014 and 2022, no water was supplied to Crimea from the Dnieper. In February 2022, water supply to the Crimean Peninsula via the NCC resumed.

[1)] Denisova, A.I., Timchenko, V.M., Nakhshina, E.P., Novikov, B.I., Ryabov, A.K. and Bass, Ya.I., 1989. [*Hydrology and Hydrochemistry of the Dniper River and its Reservoirs*]. Kiev: Naukova Dumka, 216 p. (in Russian).

[2)] [*State of the Crimean Environment*]. 2025. [online] Available at: https://ru.ruwiki.ru/wiki/Состояние_природной_ среды_Крыма [Accessed: 14 October 2025].

Before the initiation of the primary water flow through the NCC, water quality was assessed using microbiological indicators. The results indicated that the surface waters of the NCC were classified as the oligosaprobic (slightly polluted) zone [3]. In June 2023, following the destruction of the Kakhovka Hydroelectric Power Station, the flow of Dnieper water to Crimea via the NCC ceased once again, and the water level in the canal bed dropped to the point of drying up in some sections. To ensure the long-term operation of the NCC, the local authorities intend to maintain the water level in it using pumps to be installed on the Dnieper [3)]. Given the importance of the NCC for supplying water to the Crimean Peninsula, further research is required to assess the quality of water entering the canal.

Heterotrophic microbiota are a significant component of biocoenoses in any aquatic ecosystem. Their primary function is the assimilation and transformation of organic compounds, including anthropogenic pollutants. An increase in the abundance of certain bacterial groups may indicate the entry of various chemical pollutants into the water body [4, 5]. Hydrocarbon-oxidising microbiota participate in the oil oxidation and exert a mineralising effect depending on the chemical nature of the petroleum hydrocarbons [4)] [6]. A widely used parameter for diagnosing water quality, in addition to the abundance of heterotrophic (HB) and hydrocarbon-oxidising (HOB) bacteria, is the abundance of phenol-oxidising (POB) and lipolytic (LLB) bacteria.

Phenol and its compounds are among the most common pollutants entering water bodies with industrial effluents. Phenol is a highly toxic substance; its maximum permissible concentration (MPC) in water is 0.001 mg/L. When entering water bodies, wastewater contaminated with phenol and its compounds increases the water toxicity, which results in deterioration of the water body sanitary condition [5)]. The abundance of phenol-oxidising microorganisms is used as an indicator of environmental contamination by phenolic compounds. Lipids are also common pollutants of water bodies.

The main sources of lipids are industrial and domestic wastewater. In addition, lipids may be formed during the microbial oxidation of n-alkanes in crude oil or may be metabolic products of phytoplankton and zooplankton [7]. The negative impact of lipids on aquatic ecosystems is associated with a significant chemical stability of this pollutant [8].

The study is aimed to assess the current state of the NCC waters and the adjacent Black Sea waters based on microbiological indicators.

[3)] Sinyavskaya, E. and Zhdanov, V., 2023. [*Krymchane Nazvali Posledstviya Podryva Kakhovskoy Ges Dlya Vodosnabzheniya Poluostrova*]. MK, 29048, 14 June. [online]. Available at: https://www.mk.ru/economics/2023/06/13/krymchane-nazvali-posledstviya-podryva-kakhovskoy-ges-dlya-vodosnabzheniya-poluostrova.html [Accessed: 24 May 2026] (in Russian).

[4)] Morales, M., Ayala, M., Vazquez-Duhan, R. and Le Borgne, S., 2010. Application of Microorganisms to the Processing and Upgrading of Crude Oil and Fractions. In: S. Lee, ed., 2010. *Consequences of Microbial Interactions with Hydrocarbons, Oils, and Lipids: Production of Fuels and Chemicals. Handbook of Hydrocarbon and Lipid Microbiology*. Cham: Springer, pp. 2767–2785. https://doi.org/10.1007/978-3-319-50436-0_205

[5)] Drozdovskaya, O.A., 2000. [*Search for Microorganisms–Phenol Indicators and Degraders in Coastal Waters of Far East Seas*]. PhD Thesis. Vladivostok: DVGU, 156 p. (in Russian).

Materials and methods

The samples used for microbiological analysis consisted of water and bottom sediment samples collected from various sections of the NCC main bed, including pumping stations and the reservoir (Fig. 1). In addition, control samples of seawater and bottom sediments were taken in Karkinita Bay near the canal branch (which receives irrigation water from the NCC), as well as on a beach in Kerch. (Fig. 1). At some canal sections, bottom sediments were absent, therefore, their samples were not taken. The coordinates of the sampling sites for microbiological analyses are presented in Table 1.

The first samples for microbiological analysis were taken a few days after the initial water release in March 2022. Sampling continued in the spring, summer and autumn of 2023, and in the spring and summer of 2024. Water samples were collected into sterile 50 cm^3 test tubes, and bottom sediment samples were put in sterile jars. In all samples, the abundance of heterotrophic, hydrocarbon-oxidising, lipolytic and phenol-oxidising groups of bacteria was determined by the method of tenfold dilutions using liquid selective media. For HB, a peptone medium was used [6]. For HOB and LLB, the Voroshilova–Dianova medium [9] was used, to which sterile petroleum or lipid (1% by volume) was added as the only source of carbon and energy. For POB, a modified Kalabina–Rogovskaya medium [10] was used. The most probable number of microorganisms per unit volume was calculated using McCready's table (in triplicate), based on the method of variational statistics [7].

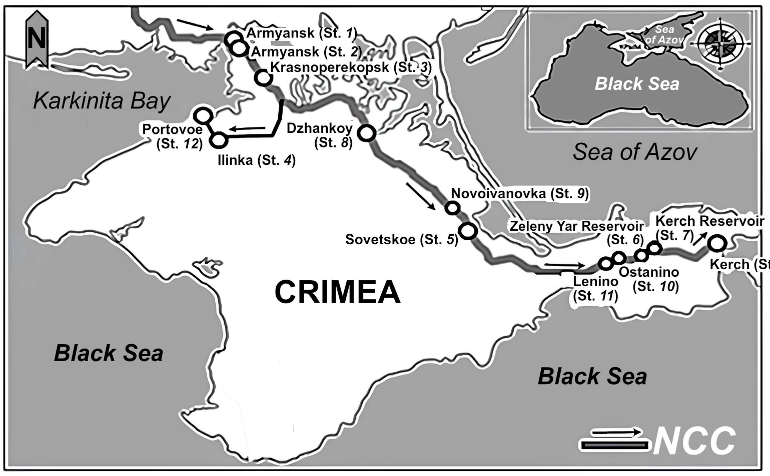

Fig. 1. The schematic map of sampling stations

[6] Mironov, O.G., ed., 1988. [*Biological Aspects of Oil Pollution of the Marine Environment*]. Kiev: Naukova Dumka, 247 p. (in Russian).

[7] Netrusov, A.I., ed., 2005. [*Practical Course on Microbiology*]. Moscow: Akademiya, 608 p. (in Russian).

T a b l e 1 . Sampling coordinates at the sites of the North Crimean Canal (NCC) and adjacent territories

Station number	Geographical coordinates, N, E	Sampling area
1	46.119673, 33.690343	Main bed, Armyansk area, first NCC hydroelectric complex (on the peninsula)
2	46.119887, 33.690445	Main bed, Armyansk area, near a highway bridge
3	45.957321, 33.821749	Main bed, Krasnoperekopsk area
4	45.834547, 33.762471	Main bed, the village of Ilinka area
5	45.834591, 33.762660	Main bed, second pumping station, The village of Sovetskoe
6	45.344203, 36.010135	Main bed, third pumping station
7	45.339563, 36.044696	Second Kerch Water Reservoir
8	45.701458, 34.439761	Main bed, Dzhankoy area
9	45.465167, 34.804000	Main bed, the village of Novoivanovka area
10	45.313176, 35.875492	Main bed, the village of Ostanino area
11	45.287740, 35.786521	Main bed, the settlement of Lenino area
12	45.853261, 33.482983	Karkinita Bay, the village of Portovoe, beach
13	45.363455, 36.502351	Cherepashka Beach, Kerch

In all *in situ* water samples, hydrochemical parameters were measured to compare microbiological data: temperature, pH and oxidation-reduction potential (Eh), using a portable multi-parameter pH/Eh/conductivity/oxygen meter HI98194 (Hanna Instrument, Romania). The instrument underwent primary calibration upon delivery (Federal State Information System *Arshin*) and is listed in the National Register of Measuring Instruments of the Russian Federation (reg. no. 77745-20).

The instrument was calibrated using the manufacturer's calibration solutions supplied with the unit (pH – three-point calibration with automatic recognition: 4.01; 6.86; 9.18). The accuracy of pH determination is ±0.02, that of Eh is ±1.0 mV. The instrument was calibrated for the determination of dissolved oxygen in water using a manufacturer's solution with zero oxygen content. From April 2022 to November 2023, in addition to the mentioned parameters, the dissolved oxygen content was determined in the water samples. The obtained results were compared using standard values for fishery water bodies [8)].

Results and discussion

The results of microbiological monitoring showed that, over the study period, the HB abundance in the surface water layer at stations located in the main bed varied from $4.5 \cdot 10^2$ to $2.5 \cdot 10^7$ cells·mL^{-1} (Fig. 2). Although HB consume oxygen for cellular respiration and oxidation of organic matter, dissolved oxygen (O_2) was high in the waters of the main bed and adjacent areas, ranging from 5.76 mg/L (station *2*, Armyansk) to 9.61 mg/L (station *3*, Krasnoperekopsk). The lowest value, at station *2*, was only 0.24 mg/L below the recommended fishery threshold (6.0 mg/L).

The highest HB abundance was detected in the October 2023 samples at stations *6* and *7*. This increase appeared to be localised. The lowest HB abundance was recorded in only two samples: at stations *2* and *3*. The abundance of HB may depend on both climatic conditions and the time of year, as well as on the pollution level of the water body. The water quality can be judged by the quantity of heterotrophic microbiota: an abundance of HB up to 10^3 cells·mL^{-1} corresponds to clean, or oligosaprobic, water; 10^4–10^5 cells·mL^{-1} corresponds to mesosaprobic waters, in which the mineralisation of organic matter occurs; 10^6 cells·mL^{-1} and above corresponds to polysaprobic waters (an indicator of high pollution) [9)]. In 85% of the samples taken from the NCC bed in 2023–2024, the bacterial abundance was

---

8) *On the Approval of Water Quality Standards for Water Bodies of Commercial Fishing Importance, Including Standards for Maximum Permissible Concentrations of Harmful Substances in the Waters of Water Bodies of Commercial Fishing Importance*: Order of the Federal Agency for Fishery dated May 26, 2025, No. 296 (in Russian).

9) Labinskaya, A.S., Blinkova, L.P. and Eshchina, A.S., eds., 2004. [*General and Sanitary Microbiology, Including Microbiological Testing Techniques: A Study Guide*]. Moscow: Meditsina, 576 p. (in Russian).

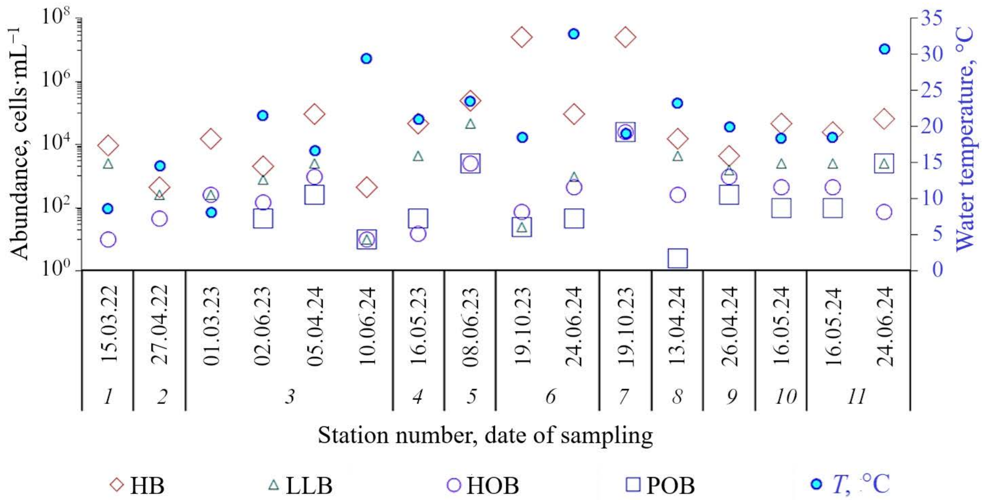

F i g . 2 . Bacterial abundance of the studied bacterial groups and the water temperature in the main part of the North Crimean Canal and reservoirs

within the range of 10^3–10^5 cells·mL^{-1}, which classifies the NCC waters as meso-saprobic. Of note, according to the results of microbiological studies conducted at station *1* in March 2022 (a few days before the main water flow was initiated), the NCC waters were classified as oligosaprobic (slightly polluted) [3]. In April 2022, following the release of water into the canal, the HB abundance in the water varied between 10^2 and 10^3 cells·mL^{-1} (see Fig. 2). The increase in HB abundance observed in the NCC water samples in 2023–2024 is most likely attributable to reduced flow after the dam collapse. This led to a higher influx of organic matter into the canal, partly from riparian runoff.

The concentrations of HOB (the primary degraders of oil pollution in water bodies) in the NCC ranged from 10 to $2.5 \cdot 10^3$ cells·mL^{-1} (see Fig. 2). HOB were detected in all water samples. The maximum HOB value in samples from the canal bed was recorded near the second pumping station (station *5*). A mosaic distribution of HOB was observed, caused by the uneven distribution of the substrate itself, i. e. hydrocarbons. It is known that in clean water bodies, the proportion of HOB usually does not exceed 0.1–1.0% of the total heterotrophic bacterial community, whereas in oil-contaminated areas, this proportion can rise [10] up to 80%. The HOB percentage in the bacterial community during the study period varied within 0.1–2% in the vast majority of samples, which does not exceed the values established for water bodies contaminated with petroleum products. Moreover, the MPC of

[10] Mishustina, I.E., Shcheglova, I.K. and Mitskevich, I.N., 1985. [*Marine Microbiology*]. Vladivostok: DVGU, 184 p. (in Russian).

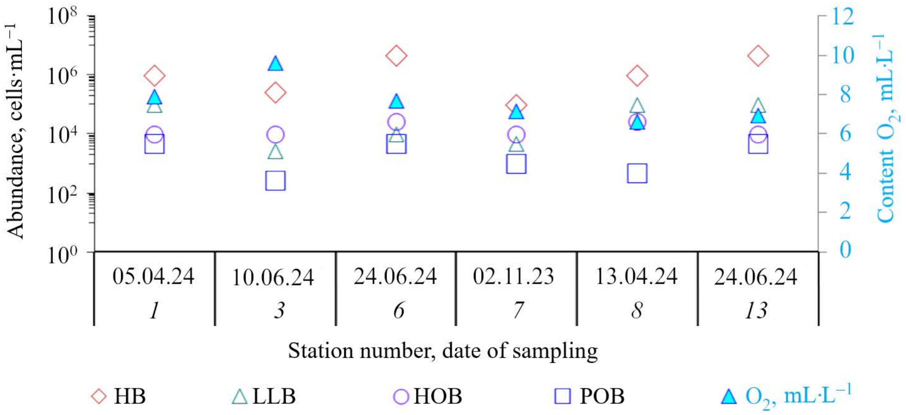

F i g . 3 . Bacterial abundance of the studied bacterial groups and the dissolved oxygen content in the main bed of the North Crimean Canal

petroleum products in fishery waters [11] (0.05 mg/L) corresponds [12] to less than 1,000 HOB per 1 mL. All this indicates that the surface waters of the NCC were not affected by chronic pollution with petroleum products.

The lipolytic group of bacteria was observed at all stations located in the main bed of the canal; the concentration of LLBs ranged from 10 to $4.5 \cdot 10^4$ cells·mL^{-1} (see Fig. 2). The maximum LLB concentration, like that of HOB, was recorded at station *5*, near the second pumping station. It was noted [13] that the distribution of LLB was similar to that of HOB, because the quantitative indicators of LLB reflect the transformation rate of oil degradation intermediates. This is confirmed by the identified positive correlation between the abundances of HOB and LLB ($R = 0.73$; $n = 19$, $\alpha < 0.05$). The minimum LLB concentration was recorded in the NCC waters near the third pumping station (station *6*) in October 2023. In 67% of the samples, the LLB count was within the range of 10^3–10^4 cells·ml^{-1}, indicating active microbial self-purification of the NCC waters of lipid components. The quantitative indicators for LLB obtained in 2024 are comparable with the results from 2022 [3].

POB were detected in all water samples taken at stations along the NCC main bed. POB concentrations ranged from 10 to $2.5 \cdot 10^3$ cells·mL^{-1} (see Fig. 2). The highest concentration of POB was recorded near the village of Sovetskoe (second pumping station, station *5*) in the June sample. This may be associated

---

[11] State Standard, 1977. [*17.1.2.04-77. Nature Protection. Hydrospere, Indicators of the Condition and Rules for Assessment of Fisheries Water Bodies*]. Moscow: Izdatelstvo Standartov, 17 p. (in Russian).

[12] Verbina, N.M., 1980. [*Hydromicrobiology with the Fundamentals of General Microbiology: A Study Guide for Students*]. Moscow: Pishchevaya Promyshlennost, 288 p. (in Russian).

[13] Abakumov, V.A., ed., 1983. [*A Guide to Methods for the Hydrobiological Analysis of Surface Waters and Sediments*]. Leningrad: Gidrometeoizdat, 240 p. (in Russian).

with an active phytoplankton bloom, since phenolic derivatives are present in plants and their degradation products [11]. In relatively clean river areas, high POB abundance had previously been recorded, according to [12], due to the natural content of humic substances. High POB levels may also be associated with pollution from faecal effluent or organochlorine pesticides, as well as with the activities of various industrial complexes [1)]. The correlation coefficient between the abundances of HB and POB was $R = 0.66$ ($n = 16$, $\alpha < 0.05$), suggesting possible water self-purification from phenolic compounds, mediated by the studied microbiota.

High concentrations of the studied groups of microorganisms were recorded in the waters of the Kerch Reservoir (station *7*), where, during sampling, so-called stagnation phenomena were visually marked: a persistent odour of hydrogen sulphide, massive algal blooms and siltation of the bed. In terms of bacterial abundance, the studied section of the reservoir falls within the high-pollution zone, i. e. it is classified as polysaprobic water. A high abundance (over $2.5 \cdot 10^4$ cells·mL^{-1}) of indicator bacterial groups was also noted there. The obtained data are consistent with the results of a water chemical analysis at this station [13]. The authors [13] note an increase in the content of aliphatic hydrocarbons in the water, as well as the presence of high-molecular-weight homologues, with an even number of carbon atoms predominating over an odd number in the chromatograms. This type of n-alkane composition is characteristic of bacterial biofilms. Thus, the overall increase in the concentration of hydrocarbons and other organic substances may be due not to their additional input, but to their accumulation in the water body.

The bacterial abundances in the water at the control sampling points in Karkinita Bay and on the beach in Kerch are presented in Table 2. The studied bacterial groups were detected at all locations. Relatively high levels of indicator bacterial groups (LLB – over $2.5 \cdot 10^4$ cells·mL^{-1}, HOB – $9.5 \cdot 10^2$ cells·mL^{-1}, POB – $4.5 \cdot 10^2$ cells·mL^{-1}) were recorded in the waters of Karkinita Bay (station *12*) in samples taken in May 2023. Such microorganism counts indicate an anthropogenic load on the study area and are often characteristic of wastewater discharge sites [14]. However, the results of repeat water sampling from the bay in June 2024 show that the abundances of HOB and POB did not exceed 5 cells·mL^{-1}, indicating that the inflow of pollutants into the bay's coastal waters is of a local nature. In a seawater sample taken near Kerch (Cherepashka Beach, station *13*), the abundance of HB was $2.5 \cdot 10^4$ cells·mL^{-1}, whereas that of the other ecological and trophic groups of bacteria ranged from 4.0 to 250 cells·mL^{-1} (Table 2).

Throughout the observation period, the microbial community was developing within a wide range of water temperatures: from 8.6 to 32.9°C (see Fig. 2). However, no correlation was found between the abundance of the studied bacterial groups and temperature. The pH of fresh Dnieper water entering the NCC waterway varied between 6.0 and 8.5 (Table 3), peaking in March 2022 when the flow resumed following the dam collapse. The obtained pH values were generally consistent with the pH range recorded previously in the Kakhovka Reservoir [1)].

Table 2. Water temperature, values of the hydrogen index (pH), redox potential (Eh) and quantitative indicators of the microbiota in the surface water layer of the coastal water area of the Karkinita Bay (station *12*) and the beach waters in Kerch (station *13*)

Sampling date	Station number	*T*, °C	pH	Eh, mV	Abundance, cells·mL^{-1}			
					HB	LLB	HOB	POB
16.05.2023	*12*	21.1	8.1	+174	$9.5 \cdot 10^4$	$> 2.5 \cdot 10^4$	$9.5 \cdot 10^2$	$4.5 \cdot 10^2$
19.10.2023	*13*	17.0	8.0	+180	$2.5 \cdot 10^4$	$2.5 \cdot 10^2$	45.0	4.0
10.06.2024	*12*	31.6	8.5	+145	$1.5 \cdot 10^6$	$1.5 \cdot 10^2$	5.0	1.0

The measured pH values of the aquatic environment at the study sites fell within the range of standard values for this parameter (6.5–8.5) adopted in the Russian Federation for fishery water bodies [8)]. No statistically significant correlation was found between the water pH and the abundance of the observed microorganisms.

Eh values ranged from +120 to +426 mV (Table 3), indicating an oxidation environment characterised by the presence of free oxygen, which, in turn, is typical of surface waters and favourable for the growth of the studied groups of microorganisms. However, no statistically significant correlations were found between the bacterial abundance and Eh values. Note that factors such as influx of various substances into the canal bed following the dam collapse, surface runoff from agricultural land and changes in flow velocity and water temperature within the canal bed may have influenced the formation of pH and Eh in the canal's aquatic environment.

Table 3. Values of the hydrogen index pH and redox potential Eh of water at the studied stations

Sampling date	Station number	pH	Eh, mV
15.03.2022	*1*	8.5	+171
27.04.2022	*2*	6.3	+210
01.03.2023	*3*	6.2	+168
02.06.2023	*3*	6.9	+150
05.04.2024	*3*	6.5	+220
10.06.2024	*3*	6.5	+158
16.05.2023	*4*	6.5	+215
08.06.2023	*5*	6.5	+177
19.10.2023	*6*	7.0	+170
24.06.2024	*6*	6.5	+426
19.10.2023	*7*	6.0	+153
13.04.2024	*8*	6.5	+143
26.04.2024	*9*	6.5	+172
16.05.2024	*10*	6.5	+120
16.05.2024	*11*	6.0	+134
24.06.2024	*11*	6.0	+356

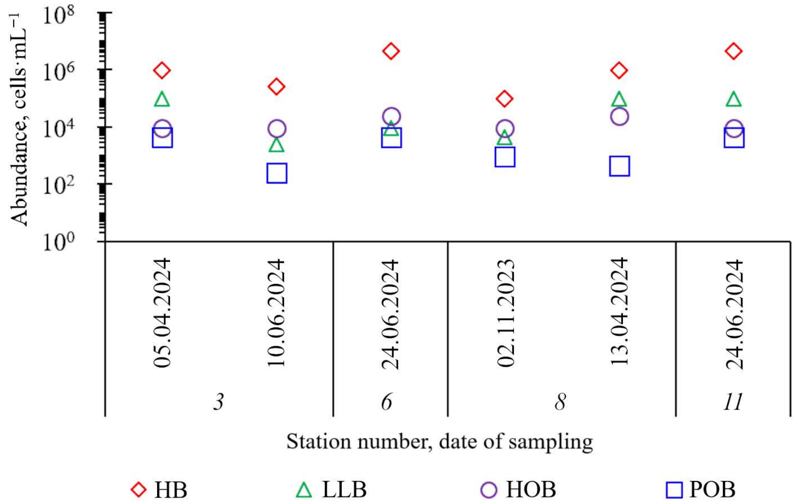

F i g. 4. Bacterial abundance in the bottom sediments of the North Crimean Canal during the study period

The bacterial counts in the bottom sediment of the NCC varied within the following ranges: HB – from $9.5 \cdot 10^4$ to $4.5 \cdot 10^6$ cells·g^{-1}, HOB – from 9.5×10^3 to $2.5 \cdot 10^4$ cells·g^{-1}, LLB – from $2.5 \cdot 10^3$ to $9.5 \cdot 10^4$ cells·g^{-1}, POB – from $2.5 \cdot 10^2$ to $4.5 \cdot 10^3$ cells·g^{-1} (Fig. 4). The bacterial abundance in all sediment samples exceeded that recorded in the water samples.

Conclusions

From the initiation of the main water flow in 2022 until June 2024, microbiological surveys of individual NCC sections showed that the waters were classified as mesosaprobic according to HB abundance. In 85% of the samples, this parameter varied within the range of 10^3–10^5 cells·mL^{-1}. The bacterial abundance and high oxygen content suggest recent contamination of the canal's waters with readily degradable organic matter.

Indicator groups of bacteria were detected throughout the water and bottom sediment, indicating self-purification of the water body from the respective pollutants. A quantitative analysis of HOB revealed no chronic petroleum contamination in the NCC surface waters. The proportion of HOB in the HB population did not exceed 2%. The quantitative indicators for HOB and POB in the NCC waters ranged from 10 to $2.5 \cdot 10^3$ cells·mL^{-1}, while the abundance of LLB was between 10 and $4.5 \cdot 10^4$ cells·mL^{-1}. A positive correlation was identified between HOB and LLB ($R = 0.73$; $n = 19$; $\alpha < 0.05$) and between HB and POB ($R = 0.66$; $n = 16$; $\alpha < 0.05$). No significant relationship was found between the abundance of the observed microorganisms and parameters such as water temperature, Eh and pH.

References

1. Sharovarina, E.S., 2018. The North Crimean Channel and the Crimean Environment. In: Russian NPLSaT, 2018. *Proceedings of the Fourth International Professional Forum "Book. Culture Education. Innovations" – "Crimea-2018". Sudak, June 18–22, 2018*. Moscow: Russian NPLSaT, pp. 353−359 (in Russian).
2. Baydakova, E.V., Krovopuskova, V.N. and Dunaev, A.I., 2022. Problems of Resuming Work and Operation the North Crimean Canal. *Vestnik of the Bryansk State Agricultural Academy*, (5), pp. 68−72 (in Russian).
3. Mirzoeva, N.Yu., Soloveva, O.V., Doroshenko, Yu.V., Tikhonova, E.A. and Burdiyan, N.V., 2023. Assessment of Water Quality and Bottom Sediments of the North Crimean Canal Before the Launch of the Main Flow of Water by the Content of Hydrocarbons and Some Microbiological Indicators (Spring 2022, Crimean Peninsula). *Bulletin of Higher Educational Institutions. North Caucasus Region. Natural Sciences*, (4), pp. 118−125. https://doi.org/10.18522/1026-2237-2023-4-118-125 (in Russian).
4. Kondrat'eva, L.M., Fisher, N.K. and Berdnikov, N.V., 2009. Microbiological Estimate of Water Quality in the Amur and Sungari Rivers After a Technogenic Accident in China in 2005. *Water Resources*, 36(5), pp. 548−559. https://doi.org/10.1134/S0097807809050078
5. Mironov, O.G., 2000. Biological Problems of Oil Contamination of Seas. *Hydrobiological Journal*, 37(4), pp. 52−67. https://doi.org/10.1615/hydrobj.v37.i4.50
6. Pandolfo, E., Caracciolo, A.B. and Rolando, L., 2023. Recent Advances in Bacterial Degradation of Hydrocarbons. *Water*, 15(2), 375. https://doi.org/10.3390/w15020375
7. Ermakova, E.P. and Gavrilova, E.I., 2004. [Long-Term Trends in Certain Microbiological Parameters of the Seawater at Sheshkharis in Novorossiysk Bay]. *Izvestiya Vuzov. Severo-Kavkazskii Region. Natural Science*, (2), pp. 85−88 (in Russian).
8. Kolotova, O.V., Sokolova, I.V., Vladimtseva, I.V., Belen'kova, T.V. and Shevtsova, V.S., 2017. [Isolation and Study of Lipid-Oxidising Microorganisms Inhabiting the Northern Caspian Sea]. *Herald of Technological University*, 20(6), pp. 135−138 (in Russian).
9. Voroshilova, A.A. and Dianova, E.V., 1952. [Oil-Oxidizing Bacteria – Performance Indices of Oil Biological Oxidation under Natural Conditions]. *Mikrobiologiya*, 21(4), pp. 408–415 (in Russian).
10. Ermolaev, K.K. and Mironov, O.G., 1975. The Role of Phenol Microorganisms in Degradation of Phenol in the Black Sea. *Mikrobiologiya*, 44(5), pp. 928–932 (in Russian).
11. Sokolova, I.V., Kolotova, O.V., Vladimtseva, I.V., Vodovsky, N.B. and Kochetkova, E.A., 2017. [A Study of Phenol-Oxidising Bacterial Strains Isolated from the Waters of the Northern Caspian Sea]. *Herald of Technological University*, 20(10), pp. 119−123 (in Russian).
12. Tekanova, E., Makarova, E. and Kalinkina, N., 2015. An Assessment of the Condition of the Water of Lake Onego Inflowing Streams under Human Impact Influence Using Microbiological and Toxicological Parameters. *Transactions of KarRC RAS*, (9), pp. 44–52. https://doi.org/10.17076/lim35 (in Russian).
13. Soloveva, O.V., Tikhonova, E.A. and Mirzoeva, N.Y., 2025. Features of the spatial and seasonal distribution of hydrocarbons in water of the North Crimean Canal, Crimea. *Acta Geochimica*, 44(2), pp. 247–259. https://doi.org/10.1007/s11631-024-00719-w

14. Rubtsova, S.I., Tikhonova, E.A., Burdiyan, N.V. and Doroshenko, Yu.V., 2013. The Estimation of the Ecological State of Sevastopol Bays on Basic Chemical and Microbiological Criteria. *Marine Ekological Journal*, 12(2), pp. 38–50 (in Russian).

Submitted 06.08.2025; accepted after review 25.11.2025;
revised 19.03.2026; published 30.06.2026

About the authors:

Nataliya V. Burdiyan, Senior Researcher, A. O. Kovalevsky Institute of Biology of the Southern Seas of RAS (2 Nakhimova Ave., Sevastopol, 299011, Russia), PhD (Biol.), **ORCID ID: 0000-0001-8030-1556, Scopus Author ID: 57208497483, ResearcherID: AAD-1704-2022,** *burdiyan_nv@ibss-ras.ru*

Yuliya V. Doroshenko, Researcher, A.O. Kovalevsky Institute of Biology of the Southern Seas of RAS (2 Nakhimova Ave., Sevastopol, 299011, Russia), PhD (Biol.), **ORCID ID: 0000-0003-0498-3369; Scopus Author ID: 57211643141, ResearcherID: AAD-1706-2022**, *doroshenko_yuv@ibss-ras.ru*

Natalya Yu. Mirzoeva, Leading Researcher, A. O. Kovalevsky Institute of Biology of the Southern Seas of RAS (2, Nakhimov Ave., Sevastopol, 299011, Russia), PhD (Biology), **ORCID ID: 0000-0002-8538-2436, Scopus Author ID: 55623414000, ResearcherID: Q-9393-2016**, *mirzoyevanyu@ibss-ras.ru*

Elena V. Guseva, Junior Researcher, A.O. Kovalevsky Institute of Biology of the Southern Seas of RAS (2 Nakhimova Ave., Sevastopol, 299011, Russia), **Scopus Author ID: 57208488324,** *guseva_ev@ibss-ras.ru*

Olga V. Soloveva, Leading Researcher, A. O. Kovalevsky Institute of Biology of the Southern Seas of RAS (2 Nakhimova Ave, Sevastopol, 299011, Russian Federation), PhD (Biol.), **ORCID ID: 0000-0002-1283-4593, Scopus Author ID: 57208499211, ResearcherID: X-4793-2019**, *soloviova@ibss-ras.ru*

Contribution of the authors:

Nataliya V. Burdiyan – statement of the objectives of the microbiological study, analysis of the results obtained in the microbiological study, results discussion, manuscript writing, microbiological works to determine the abundance of indicator groups of bacteria

Yuliya V. Doroshenko – analysis of the obtained results in the microbiological study, results discussion, manuscript writing, microbiological works to determine the abundance of indicator groups of bacteria

Natalya Yu. Mirzoeva – statement of the aim and objectives of the microbiological and hydrochemical studies

Elena V. Guseva – preparation of the literature review, creation of graphic materials

Olga V. Soloveva – statement of the field work objectives, water and sediment sampling, measurement of hydrological parameters

All the authors have read and approved the final manuscript

ISSN 2413-5577, Ecological Safety of Coastal and Shelf Zones of Sea, No. 2, pp. 124–144 (2026)

Original paper

Photosynthetic Parameters of Phytoplankton and Primary Production in Coastal Waters of the Black Sea: Seasonal Features

D. V. Kalmykova, T. Ya. Churilova, T. V. Efimova *, N. A. Moiseeva, E. Yu. Skorokhod

A.O. Kovalevsky Institute of Biology of the Southern Seas of RAS, Sevastopol, Russia
* *e-mail: tefimova@ibss-ras.ru*

Abstract
This paper studies seasonal variability of phytoplankton photosynthetic parameters in the Black Sea coastal waters near the Crimean Peninsula. Primary production was estimated using a full spectral approach that took into account phytoplankton spectral light absorption coefficient, spectral downwelling irradiance and quantum yield of photosynthesis. In the coastal waters near the village of Katsiveli, the annual dynamics of chlorophyll a concentration was characterized by maximal values in winter and minimal (half as many) in summer, while in the waters near Sevastopol, the maximum was recorded in early October and March, which is likely due to the "bloom" of phytoplankton. High annual variability of both the phytoplankton spectrally weighted chlorophyll a specific absorption coefficient (~ 3 times) and maximum quantum yield of photosynthesis (~ 7 times) was noted, with maximal values in summer and winter, respectively. In the vertical profile, the minimal values of the quantum yield were observed in the sea surface layer associated with the high photosynthetically active radiation incident on the sea surface. The variability in photosynthetic parameters, caused by phytoplankton adaptation to changing environmental factors, resulted in a strong annual variability of primary production, which varied ~8-fold over the study period. The obtained patterns of variability of the basic photosynthetic parameters of phytoplankton (the ability to absorb light quanta and use them in photochemical reactions) are necessary for understanding the mechanism of formation of primary production in the studied water region.

Keywords: chlorophyll a, quantum yield of photosynthesis, light absorption, photosynthetically available radiation, spectral downwelling irradiance

Acknowledgements: We thank E. A. Zemlyanskaya for her efficient contribution to the sample treatments and E. A. Khvalkov for assistance with translation. The present study was carried out within the framework of state assignment no. 124030100106-2 "Study of regional bio-optical properties for development of satellite algorithm for assessment of multi-scale variability of primary production characteristics of pelagic ecosystems".

© Kalmykova D. V., Churilova T. Ya., Efimova T. V., Moiseeva N. A., Skorokhod E. Yu., 2026

This work is licensed under a Creative Commons Attribution-Non Commercial 4.0 International (CC BY-NC 4.0) License

For citation: Kalmykova, D.V., Churilova, T.Ya., Efimova, T.V., Moiseeva, N.A. and Skorokhod, E.Yu., 2026. Photosynthetic Parameters of Phytoplankton and Primary Production in Coastal Waters of the Black Sea: Seasonal Features. *Ecological Safety of Coastal and Shelf Zones of Sea*, (2), pp. 124–144.

Фотосинтетические характеристики фитопланктона и первичная продукция в прибрежных водах Черного моря: сезонные особенности

Д. В. Калмыкова, Т. Я. Чурилова, Т. В. Ефимова *, Н. А. Моисеева, Е. Ю. Скороход

ФГБУН ФИЦ «Институт биологии южных морей имени А. О. Ковалевского РАН», Севастополь, Россия

* *e-mail: tefimova@ibss-ras.ru*

Аннотация

Исследована сезонная изменчивость фотосинтетических характеристик фитопланктона в прибрежных водах Черного моря у побережья Крымского полуострова. Первичную продукцию оценивали с использованием полного спектрального подхода, учитывающего спектральные показатели поглощения света пигментами фитопланктоном, спектральную освещенность и квантовый выход фотосинтеза. В прибрежных водах у поселка Кацивели годовая динамика концентрации хлорофилла *a* характеризовалась максимальными значениями зимой и минимальными (в два раза меньше) летом, тогда как в водах вблизи Севастополя максимум концентрации хлорофилла *a* был отмечен в начале октября и в марте, что, вероятно, обусловлено «цветением» фитопланктона. Отмечена высокая годовая вариабельность как удельной эффективности поглощения света пигментами фитопланктона (примерно в три раза), так и максимального квантового выхода фотосинтеза (примерно в семь раз) с наблюдаемыми максимальными значениями летом и зимой соответственно. В вертикальном распределении квантового выхода минимальные значения были отмечены в поверхностном слое, что связано с высокой фотосинтетически активной радиацией, падающей на поверхность моря. Вариабельность фотосинтетических характеристик, обусловленная адаптацией фитопланктона к изменяющимся факторам среды, привела к значительной годовой изменчивости первичной продукции, которая за исследуемый период варьировала примерно в восемь раз. Полученные закономерности изменчивости основных фотосинтетических характеристик фитопланктона (способности поглощать кванты света и использовать их в фотохимических реакциях) необходимы для понимания механизма формирования первичной продукции в исследуемой акватории.

Ключевые слова: хлорофилл *a*, квантовый выход фотосинтеза, поглощение света, фотосинтетически активная радиация, спектральная освещенность

Благодарности: благодарим Е. А. Землянскую за весомый вклад в обработку проб и Е. А. Хвалькова за помощь в переводе. Работа выполнена в рамках государственного задания ФИЦ ИнБЮМ № 124030100106-2 по теме «Исследование региональных особенностей биооптических показателей водоемов как основы дешифрования данных дистанционного зондирования для оценки мультимасштабной изменчивости первично продукционных характеристик пелагических экосистем».

Для цитирования: *Kalmykova D. V., Churilova T. Ya., Efimova T. V., Moiseeva N. A. et al.* Photosynthetic parameters of phytoplankton and primary production in coastal waters of the Black Sea: seasonal features // Экологическая безопасность прибрежной и шельфовой зон моря. 2026. № 2. С. 124–144. EDN KIQVDM.

Introduction

Phytoplankton uses the sunlight energy during the primary synthesis of organic matter from inorganic compounds, the daily rate of which is called primary production (PP) [1]. PP ensures functioning of all trophic levels in food web of water ecosystems [1, 2]. The rate of photosynthesis depends on photosynthetically available radiance (PAR), the nutrient supply and temperature [2]. The coastal waters of the Black Sea (BS) are subject to strong anthropogenic impacts [3], which results in an increase in the concentration of nutrients, organic and suspended matter in the sea [4]. Elevated nutrient (mineral compounds of nitrogen, phosphorus and silicon) concentrations in the upper mixed level (UML) contribute to higher photosynthesis rates and enhance the growth of planktonic microalgae [5]. The photosynthetic and productive characteristics of phytoplankton determine the functioning of all other levels of the aquatic ecosystem's food web. Therefore, assessment of the current state of phytoplankton productivity in the BS coastal waters is highly relevant. Light intensity and its spectral properties change with depth in the sea associated with light absorption and scattering by optically active components (OAC), namely phytoplankton, colored dissolved organic matter (CDOM), non-algal particles (NAP) and pure water [6]. Consequently, a spectral approach to primary productivity (PP) estimation provides more accurate estimates than other approaches, which are based on PAR (i. e. light intensity integrated for wavelengths of 400–700 nm) [7, 8]. For the BS region, a full spectral algorithm was developed [9]. This approach considers the spectral properties of downwelling irradiance, light absorption by phytoplankton and the quantum yield (efficiency of absorbed photon use in photosynthesis), which determines the accuracy of the PP estimate [9–11].

This study focuses on the seasonal dynamics of PP, chlorophyll a concentration, photosynthetic parameters of phytoplankton, namely spectrally weighted chlorophyll a-specific phytoplankton absorption coefficient and the quantum yield of photosynthesis in the BS coastal waters. Additionally, the aim of this study is to investigate the influence of the spectral composition of light on the spectrally weighted chlorophyll a-specific phytoplankton absorption coefficients.

Methods

Study area

The study was carried out in the BS coastal waters. The BS is an inland sea, the easternmost of the seas of the Atlantic Ocean basin. In the southwest it connects to the Sea of Marmara through the Bosphorus Strait, in the northeast it connects to the Sea of Azov through the Kerch Strait. The BS is one of the largest and deepest inland seas. Its greatest depths are in the range of 2210–2258 m. About 1000 large and small rivers flow into the BS. Due to the large river runoff, the BS surface waters salinity is 18‰ [12].

Bio-optical properties and phytoplankton photosynthetic parameters were measured at two fixed stations in the coastal waters of the Crimean Peninsula:

1. A station located about a mile offshore outside of Sevastopol Bay (44°38′ N, 33°29′ E) with a depth of ~50 m (to the bottom) (22.02.2022; 16.06.2022; 13.07.2022; 06.10.2022; 09.11.2022; 29.11.2022; 07.03.2023; 21.03.2023);

2. The oceanographic platform of the Marine Hydrophysical Institute (MHI) of the Russian Academy of Sciences located in the coastal waters ~ 0.37 mile offshore from the village of Katsiveli with a depth of ~ 30 m (to the bottom) (44°23′ N, 33°59′ E) (08.06.2023; 24.01.2024).

Water sampling

The downwelling irradiance spectra $E_d(\lambda)$ were measured in increments of 1 m within the euphotic zone using a RAMSES submersible spectroradiometer (TrioOS, Germany). The euphotic zone depth (Z_{eu}) is limited to the depth at which 1% photosynthetically available radiation (PAR) penetrates. Water samples (5 L) were collected using Niskin bottles at the depths selected based on water transparency and temperature profiles. Water transparency was assessed based on Secchi disk depth (Z_s).

Pigment Analysis

The sum of chlorophyll a and pheopigment concentrations (TChl-*a*) was determined by the spectrophotometric method [13, 14] with 90% acetone using Whatman GF/F glass fiber filters (25 mm diameter, 0.7 μm size pore). The optical density (OD) of the acetone-extracted phytoplankton pigments was measured with a Lambda 35 dual-beam spectrophotometer (PerkinElmer).

Absorption Measurements

The spectral light absorption coefficients of phytoplankton ($a_{ph}(\lambda)$), NAP ($a_{NAP}(\lambda)$) and CDOM ($a_{CDOM}(\lambda)$) were measured in accordance with modern protocols [15, 16] using a Lambda 35 dual-beam spectrophotometer (PerkinElmer) equipped with an integrating sphere. The chlorophyll a-specific phytoplankton light absorption coefficient of ($a^*_{ph}(\lambda)$) ($m^2 \cdot mg^{-1}$) was calculated by dividing $a_{ph}(\lambda)$ by TChl-*a*.

Spectrally weighted chlorophyll a-specific absorption coefficients of phytoplankton $\bar{a}^*_{ph}(z)$, $m^2 \cdot mg^{-1}$, were calculated as

$$\bar{a}^*_{ph}(z) = \frac{\int_{400}^{700} a^*_{ph}(\lambda, z) \cdot E_d(\lambda, z) d\lambda}{\int_{400}^{700} E_d(\lambda, z) d\lambda \cdot \text{TChl-}a}.$$

Primary production

PP, $mgC \cdot m^{-3} \cdot d^{-1}$, was determined according to the full spectral approach [9]:

$$PP = 12000 \cdot \phi(z) \cdot PUR_{psp}(z),$$

where 12000 – moles to mg carbon conversion ratio; ϕ – the quantum yield of photosynthesis, and PUR_{psp} – the amount of quanta absorbed by photosynthetically active pigments, per TChl-*a* unit.

The ϕ values (mol C·mol quanta^{-1}), were calculated as [17]:

$$\phi(z) = \phi_{max}(z) \cdot \tanh\left(\frac{I_k(z)}{PAR(z)}\right),$$

where ϕ_{max} is the maximum quantum yield of photosynthesis; I_k is the light intensity saturating relative electron transfer rate (rETR), which corresponds to I_k for the photosynthesis rate [17].

The ϕ_{max}, mol C·mol quanta^{-1}, was assessed based on the parameters of variable chlorophyll a fluorescence:

$$\phi_{max} = \left(\frac{F_v}{F_m}\right) / (K_c \cdot 2),$$

where F_m is the maximal fluorescence of chlorophyll a with closed reaction centers (RC) of photosystem II (PSII); F_v is the difference between F_m and the minimal fluorescence of chlorophyll a with open RC PSII (F0); K_c is the number of electrons required to fix a single CO_2 molecule [18]; 2 is the number of photons required for the transfer of one electron along the photosynthetic electron transport chain [2].

F_m, F0 and rETR were measured in the laboratory with a chlorophyll fluorescence kinetic measurement system (fluorimeter Smart) developed at the Department of Biophysics, Faculty of Biology, Lomonosov Moscow State University [19].

K_c, mol electrons·mol C^{-1}, was calculated in accordance with [20]:

$$K_c = 0.85\mathrm{PAR} + 6.55.$$

I_k, μmol quanta·m^{-2}·s^{-1}, was calculated as [21]:

$$I_k = \frac{\mathrm{rETR}_{max}}{\alpha},$$

where rETR_{max} is the maximal value of rETR; α is the tangent of the initial slope of the light curve of rETR. The light curve of rETR was fitted using the equation [22]:

$$\mathrm{rETR} = \mathrm{rETR}_{max}\left(1 - \exp\left(\frac{\alpha \cdot \mathrm{PAR}}{\mathrm{rETR}_{max}}\right)\right) \cdot \exp\left(\frac{\beta \cdot \mathrm{PAR}}{\mathrm{rETR}_{max}}\right),$$

where β is the tangent of the slope of the curve on the declining section.

PUR_{psp}, μmol quanta·m^{-3}·s^{-1}, was calculated as [23]:

$$\mathrm{PUR}_{psp}(z) = k_{psp} \cdot \mathrm{PUR}(z),$$

where k_{psp} is a coefficient reflecting the contribution of photosynthetic pigments to light absorption by all pigments, PUR is the number of quanta absorbed by all phytoplankton pigments. The k_{psp} was calculated as [23]:

$$k_{psp} = (1 - \mathrm{NPSP}) / (1 + \mathrm{NPSP}),$$

where NPSP is the weight fraction of photoprotective pigments in the total amount of phytoplankton pigments. The NPSP, g·g^{-1}, was calculated using its dependence on the daily average light intensity in the UML (PAR_{uml}) [24]:

$$\mathrm{NPSP} = 0.0202\,(\mathrm{PAR}_{uml} - 2.92).$$

PAR_{uml}, μmol·quanta·m^{-2}·s^{-1}, was calculated as [23]:

$$\mathrm{PAR}_{uml} = \mathrm{PAR}_0 \cdot \frac{1 - \exp\left(-4.6\,\frac{Z_{uml}}{Z_{eu}}\right)}{4.6\,\frac{Z_{uml}}{Z_{eu}}},$$

where PAR_0 is the daily PAR incident on the sea surface [25]; Z_{uml} is the depth of the upper mixed layer. Z_{uml} was determined using a temperature gradient [26].

PUR, μmol quanta·m^{-3}·s^{-1}, was calculated as:

$$\mathrm{PUR}(z) = \int_{400}^{700} \mathrm{Ed}(z,\lambda) \cdot a_{ph}(z,\lambda)\,d\lambda.$$

Results and discussion

Hydrological parameters

In summer (June, July 2022), the sea surface temperature (SST) varied in the range from 19 to 25°C and the average PAR_0 equaled 59 ± 1 mol quanta·m^{-2}·day^{-1}. At the station located near Sevastopol, the seasonal thermocline was well-developed (vertical temperature gradient > 2°C·m^{-1}). It divides the euphotic layer into two layers: the UML and thermocline with a part of the euphotic zone located below. During stratification, the UML waters are characterized by higher light intensity, temperature and dissolved oxygen concentration in comparison to the waters under the thermocline [27]. The coastal waters in the Katsiveli area were characterized by the absence of a thermocline in early June. The water temperature was 19°C over the entire water column. This is probably due to the high dynamic activity of the coastal waters near the Southern Coast of Crimea [28, 29]. In autumn, SST varied from 15 to 20°C, the average PAR_0 equaled 27 ± 8 mol quanta·m^{-2}·day^{-1}. Water stratification was only observed in early October. In winter, SST varied from 10 to 14°C and the PAR_0 on average was 22 ± 5 mol quanta·m^{-2}·day^{-1}. In spring, SST was 9°C, and the averaged PAR_0 was 32 ± 5 mol quanta·m^{-2}·day^{-1}. During the winter and early spring, the water was well-mixed due to convection and winds at both stations. The water transparency and Z_{eu} at the stations significantly differed by season (Fig. 1).

Spectral downwelling irradiance and euphotic zone

Light is the main factor for photosynthesis. An electron needs the energy of a photon of the visible spectrum to move from the ground state to the excited state [2]. The attenuation of light with depth, as well as the change in the spectral characteristics of light, occurs due to scattering and absorption of light by suspended matter, CDOM and pure water [6] (Fig. 2, *a*). A comparison of the $E_d(\lambda)$ spectrum shape showed (Fig. 2) that the wavelength of the $E_d(\lambda)$ spectrum maximum at a depth of 1% PAR shifted from ~ 495 nm to ~ 561 nm, since the surface total non-water light absorption at 438 nm ($a_{tot\text{-}w}(438) = a_{ph}(438) + a_{NAP}(438) + a_{CDOM}(438)$) increased from 0.204 m^{-1} in February to 0.328 m^{-1} in October (Fig. 3, *a*).

The light attenuation depends on the OAC content in water [6]. A decrease in the OAC content is accompanied by an increase in the water transparency, and light penetrates to greater depths than in waters with lower transparency [6]. The transparency determines the Z_{eu} (Fig. 3, *b*). In summer, at the beginning of June, with $a_{tot\text{-}w}(438)$ equal to 0.138 m^{-1} in the surface layer, Z_{eu} was 24 m. With a double increase in $a_{tot\text{-}w}(438)$ (0.253 m^{-1}) in mid-July, the Z_{eu} decreased by ~ 1.6 times (15 m). In winter, a different pattern was noticed: with relatively identical $a_{tot\text{-}w}(438)$ values in the surface layer, Z_{eu} was in the range from 28 to 38 m (Fig. 3, *b*). As a result, link Z_{eu} vs. $a_{tot\text{-}w}$ was weak in the surface layer, likely due to the inhomogeneous vertical distribution of OAC and to the influence of light scattering (Fig. 3, *b*). Suspended matter both absorbs and scatters light. Therefore, an increase in microalgae biomass and NAP in water (Fig. 3, *c*) can lead to a decrease in Z_{eu} due to an increase in the contribution of backscattering to light attenuation. It is worth noting that the effect of backscattering on transparency is manifested to a greater extent in the presence of mineral particles [30].

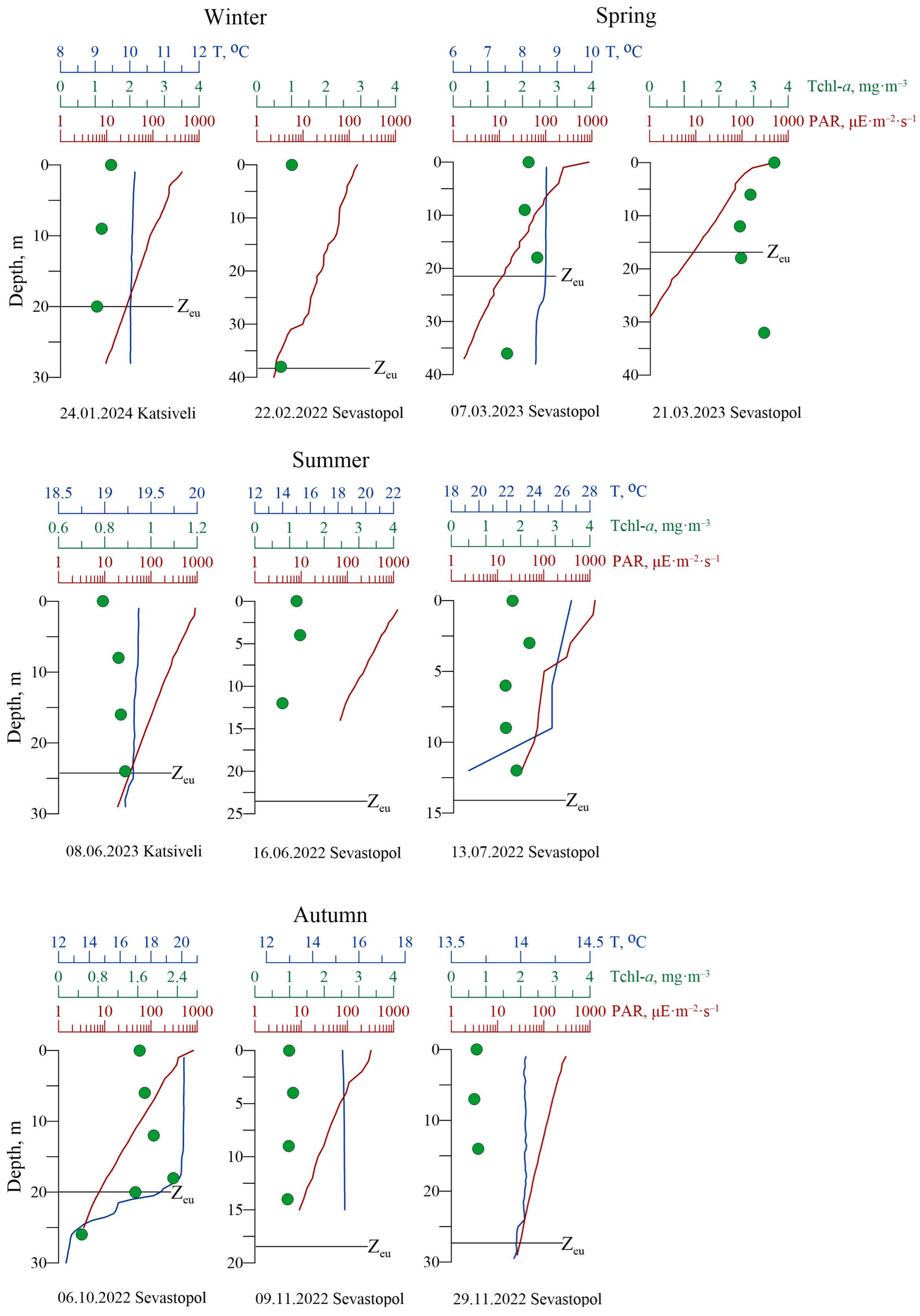

F i g. 1. Vertical profiles of temperature T (blue line), photosynthetically available radiance PAR (red line) and chlorophyll a plus pheopigment concentrations TChl-*a* (green circles) near Sevastopol and Katsiveli

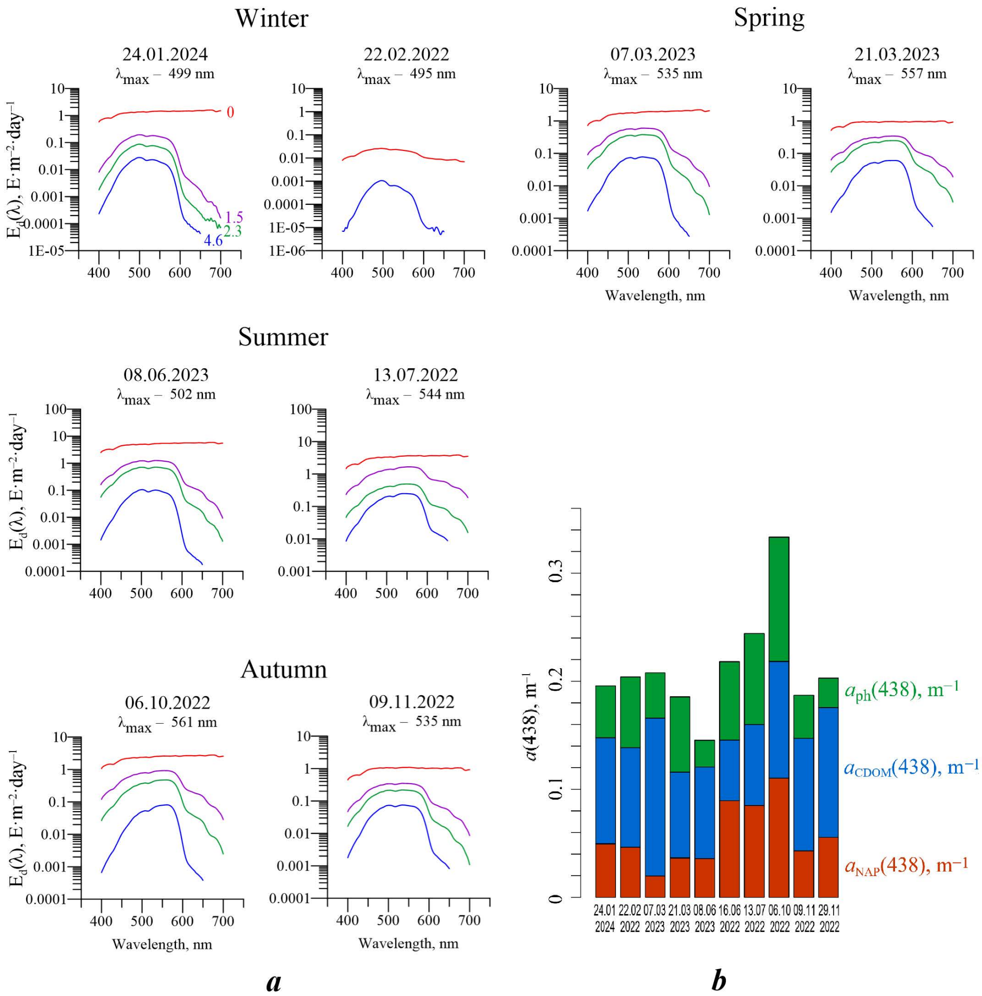

F i g . 2 . Spectral downwelling irradiance $E_d(\lambda)$ at optical depths of 0 (red curve), 1.5 (purple curve), 2.3 (green curve), 4.6 (blue curve) (*a*); light absorption at 438 nm by non-algal particles $a_{NAP}(438)$ (red), colored dissolved organic matter $a_{CDOM}(438)$ (blue) and phytoplankton $a_{ph}(438)$ (green) (*b*) at the surface of the Black Sea

Pigment concentration

In summer, in coastal waters near Sevastopol, the vertical TChl-*a* distribution was relatively uniform throughout the studied layer (including the UML and the thermocline layer) (Fig. 4, *a*). On average, TChl-*a* in the UML was 1.5 ± 0.4 mg·m^{-3}, which exceeded the winter values at this station by almost 2 times (0.8 ± 0.2 mg·m^{-3} in the UML). At the station near Katsiveli, the opposite situation was observed: winter TChl-*a* values (1.2 ± 0.2 mg·m^{-3} in the UML) were 2 times higher than summer

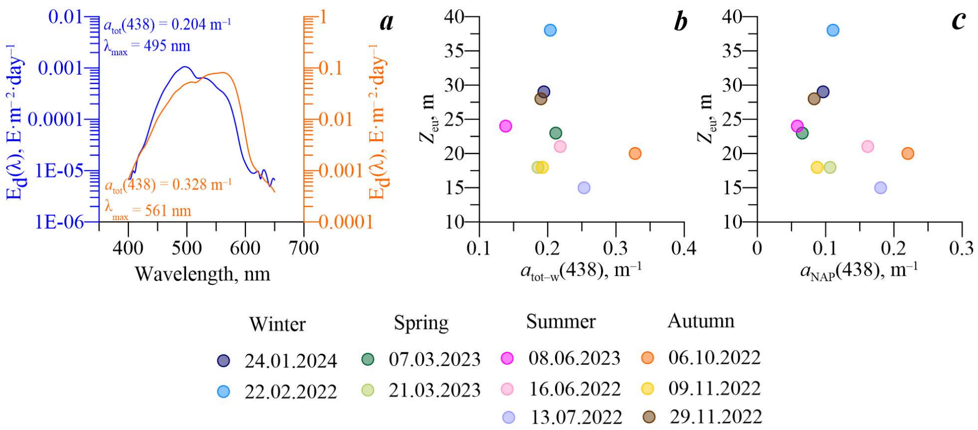

Fig. 3. Spectral downwelling irradiance $E_d(\lambda)$ at the euphotic zone depth Z_{eu} on 22.02.2022 (blue line) and 06.10.2022 (orange line) (*a*); relationship between the total non-water light absorption at 438 nm $a_{tot\text{-}w}(438)$ and Z_{eu} (*b*); relationship between the non-algal particles absorption coefficients at 438 nm $a_{NAP}(438)$ and Z_{eu} (*c*)

ones (0.6 ± 0.1 mg·m^{-3} in the UML). Such an increase of TChl-*a* in winter compared to summer is typical for the deep-water areas of the Black Sea [31, 32]. The maximum TChl-*a* values for the study period were recorded in March (2.3 ± 0.5 mg·m^{-3} in the UML) and at the beginning of October (3.1 ± 0.2 mg·m^{-3} in the UML) (Fig. 4, *a*). The obtained data are consistent with the known patterns of phytoplankton bloom. Spring bloom is often observed in March in the coastal waters of the Black Sea due to the nutrients supply and increase of solar radiance [33, 34]. Autumn phytoplankton bloom is caused by an increase in the nutrients supply [33].

Spectrally weighted chlorophyll a specific absorption coefficient of phytoplankton

Change of $\overline{a}^*_{ph}(z)$ with depth in different seasons is shown (Fig. 4, *b*). The $\overline{a}^*_{ph}(z)$ values in the surface layer (0–1 m) almost tripled from the minimal values (0.009 m^2·mg^{-1}) in early March to the maximal values (0.024 m^2·mg^{-1}) in summer (Fig. 4, *b*). In March, the $\overline{a}^*_{ph}(z)$ increased from 0.009 to 0.015 m^2·mg^{-1}. The maximal values (0.023–0.024 m^2·mg^{-1}) were recorded in summer at both stations near Katsiveli and Sevastopol. In autumn $\overline{a}^*_{ph}(z)$ was lower (0.018 m^2·mg^{-1}) than in summer. In winter the $\overline{a}^*_{ph}(z)$ values differed between stations by a factor of two: 0.021 m^2·mg^{-1} near Sevastopol and 0.012 m^2·mg^{-1} near Katsiveli.

In the surface layer, where $E_d(\lambda)$ spectra have the same shape (Fig. 2), the seasonal dynamics of $\overline{a}^*_{ph}(z)$ depends only on $a^*_{ph}(\lambda)$ (equation 1). The minimal values of the $a^*_{ph}(438)$ were noted in winter near Katsiveli (0.032 m^2·mg^{-1}) and in spring near Sevastopol (0.023 m^2·mg^{-1} and 0.035 m^2·mg^{-1}) (Fig. 5, *b*). The maximal values of $a^*_{ph}(438)$ (0.058 m^2·mg^{-1}) were recorded in summer (June, July) at both stations.

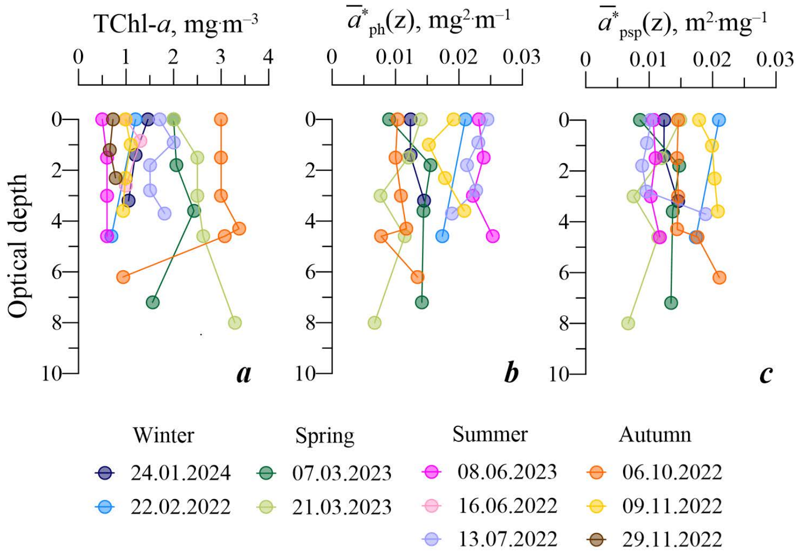

F i g . 4 . Vertical distribution of the chlorophyll a plus pheopigment concentrations TChl-*a* (*a*); the spectrally weighted chlorophyll a-specific phytoplankton absorption coefficient $\overline{a}^*_{ph}(z)$ (*b*); and $\overline{a}^*_{ph}(z)$ calculated for photosynthetically active pigments $\overline{a}^*_{psp}(z)$ (*c*) in the Black Sea coastal waters

High winter values of $a^*_{ph}(438)$ in the coastal waters of Sevastopol (0.055 $m^2 \cdot mg^{-1}$ in February) are most likely associated with the predominance of small-celled algae species. In autumn, intermediate values of $a^*_{ph}(438)$ were observed: 0.037 $m^2 \cdot mg^{-1}$ in October and 0.045 $m^2 \cdot mg^{-1}$ in November.

The changes in $a^*_{ph}(\lambda)$ are caused by the "pigment package effect", which is associated with intracellular pigment concentration and phytoplankton cell size composition [35]. The intracellular pigment concentration changes as a result of microalgal adaptation to environmental factors (PAR, the nutrient availability, temperature) [36], which vary throughout the year. The PAR_0 varies from 22.1 ± 4.6 $E \cdot m^{-2} \cdot day^{-1}$ in winter to 59.4 ± 0.9 $E \cdot m^{-2} \cdot day^{-1}$ in summer [25]. As a result of adaptive changes in the intracellular composition and concentration of pigments, $a^*_{ph}(\lambda)$ differed seasonally [37].

Seasonal changes in $a^*_{ph}(438)$ (2.5 times) led to almost the same (2.7 times) changes in $\overline{a}^*_{ph}(z)$. A positive correlation was obtained between $\overline{a}^*_{ph}(z)$ and $a^*_{ph}(438)$ (Fig. 5, *a*).

In addition to photosynthetically active pigments, phytoplankton cells also contain photoprotective pigments that absorb excess solar radiation to protect the RC cells from photodestruction [38]. This applies to a greater extent to microalgae living in the sea surface layer. In spring, the daily PAR incident at the sea surface averaged 32.4 ± 5.5 mol quanta$\cdot m^{-2} \cdot day^{-1}$, while NPSP averaged 0.014 ± 0.010 $g \cdot g^{-1}$. In summer,

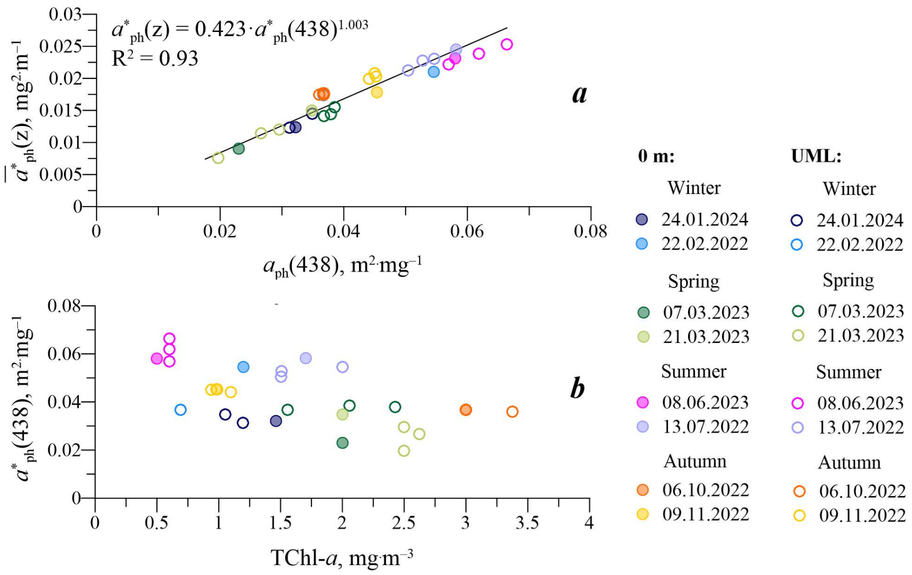

F i g . 5 . Dependence of the spectrally weighted chlorophyll a specific absorption coefficient by phytoplankton $\bar{a}^*_{ph}(z)$ on the chlorophyll a specific light absorption coefficient of phytoplankton at 438 nm $a^*_{ph}(438)$ (*a*); dependence of $a^*_{ph}(438)$ on chlorophyll a plus phaeopigment concentrations TChl-*a*(z) (*b*)

when the PAR values were maximal – on average 59.4 ± 0.9 mol quanta·m^{-2}·day^{-1}, NPSP increased to 0.39 ± 0.28 g·g^{-1} as a result of adaptation. In autumn, PAR decreased to 27.0 ± 7.9 mol quanta·m^{-2}·day^{-1}, which led to a decrease in NPSP to 0.096 g·g^{-1}. The lowest level of PAR_0 was observed in winter – 22.1 ± 4.6 mol quanta·m^{-2}·day^{-1}, for these conditions no photoprotective pigments were obtained.

Only light quanta absorbed by photosynthetically active pigments are used during photosynthesis [2]. The annual dynamics of NPSP (0–0.39) led to varying degrees of change in $\bar{a}^*_{psp}(z)$ relative to $\bar{a}^*_{ph}(z)$. In summer, near Katsiveli and Sevastopol, the values of $\bar{a}^*_{psp}(z)$ in the sea surface layer were 2.2 and 2.4 times less than the value of $\bar{a}^*_{ph}(z)$, correspondingly (Fig. 4, *c*). The value of $\bar{a}^*_{psp}(z)$ in early October in the sea surface layer was 1.2 times less than $\bar{a}^*_{ph}(z)$. Winter and spring $\bar{a}^*_{psp}(z)$ values were almost equal to $a^*_{ph}(0)$ due to low (almost zero) content of photoprotective pigments. As a result, the values of $\bar{a}^*_{psp}(z)$ changed 2.3 times from 0.009 m^2·mg^{-1} in early March to 0.021 m^2·mg^{-1} in late February (Fig. 4, *c*). Thus, the variability range of the $\bar{a}^*_{psp}(z)$ values was narrowed compared to that of $\bar{a}^*_{ph}(z)$.

Quantum yield of photosynthesis

Values of ϕ depend on the environmental conditions. Theoretically, ϕ_{max} is ~ 0.125 mol C·mol quanta^{-1} [39], whereas in practice, ϕ_{max} is lower [40], which is associated with the inhibitory effect of high PAR and nutrients availability [41].

In the sea surface layer, where the PAR values are maximal, the lowest values of ϕ_{max} were noted: from 0.003 mol C·mol quanta^{-1} in early June to 0.025 mol C·mol quanta^{-1} in late February. The ϕ_{max} increased with depth due to decreasing PAR. As a result, the ϕ_{max} near the bottom of the euphotic zone increased from 0.044 mol C·mol quanta^{-1} in early June to 0.053 mol C·mol quanta^{-1} in early October (Fig. 6, *a*).

Seasonal variability of I_k values is associated with the acclimation of phytoplankton to changes in the light level in the sea [2]. In summer, in coastal waters near Sevastopol, I_k values varied from 280 μmol quanta·m^{-2}·s^{-1} in June to 320 μmol quanta·m^{-2}·s^{-1} in July in the surface layer. The I_k decreased with depth by 1.5 and 2.5 times in June and July, respectively (Fig. 6, *b*). The average I_k value in the UML was 270 ± 30 μmol quanta·m^{-2}·s^{-1}. The I_k values were higher in autumn (on average 290 ± 30 μmol quanta m^{-2}·s^{-1} in the UML) and varied in the sea surface layer from 310 μmol quanta·m^{-2}·s^{-1} in October to 330 μmol quanta·m^{-2}·s^{-1} in November. At the beginning of October, a more pronounced decrease in I_k with depth was noted than in November (Fig. 6, *b*). High winter values were noted in the UML of the Sevastopol coastal waters (on average 310 ± 25 μmol quanta m^{-2} s^{-1}). In the sea surface layer by the end of November, I_k was equal to 315 μmol quanta·m^{-2}·s^{-1}, and at the end of February it was 350 μmol quanta·m^{-2}·s^{-1}. A more uniform vertical distribution of this parameter was observed in winter. The I_k values at the beginning of spring were similar to those in winter (315 ± 30 μmol quanta·m^{-2}·s^{-1} in the UML). In the surface layer, the I_k was 300 μmol quanta·m^{-2}·s^{-1} in early March and increased up to 350 μmol quanta·m^{-2}·s^{-1} in late March.

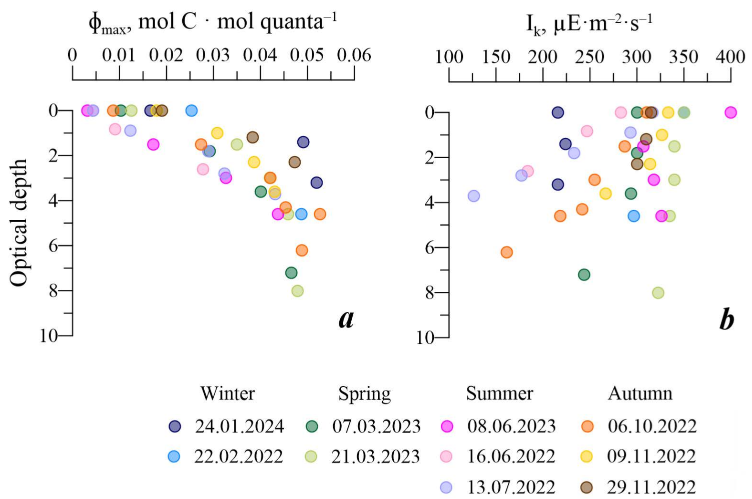

Fig. 6. Vertical distribution of the maximum quantum yield of photosynthesis ϕ_{max} (*a*) and the light intensity saturating the photosynthesis I_k (*b*) in the Black Sea coastal waters

In summer, the I_k values in the coastal waters of Katsiveli averaged 320 ± ± 15 μmol quanta·m^{-2}·s^{-1} in the UML (340 μmol quanta·m^{-2}·s^{-1} at 0 m), which exceeded I_k values near Sevastopol. The vertical distribution of the I_k was uniform near Katsiveli, which is due to the absence of thermal vertical stratification. In winter, the lowest I_k values were recorded in the coastal waters of Katsiveli over the entire study period: 220 ± 5 μmol quanta·m^{-2}·s^{-1} in the UML. In summer and early October, a decrease in the I_k with depth by ~ 2 times was noted in the coastal waters of Sevastopol due to temperature stratification of the waters. During the rest of the study period, when temperature vertical stratification was not observed, the depth-dependent variability of the I_k values was insignificant. The variability of the I_k values among seasons and with depth noted in the study is a result of phytoplankton adaptation to light conditions and depends on the so-called light history of phytoplankton [42]. Within the UML, phytoplankton is in constant vertical movement, and therefore, the photosynthetic parameters of phytoplankton are determined by the average light intensity for this layer [23, 43]. Temperature (density) gradient is a barrier to the vertical mixing of water. As a result, phytoplankton in the layers (above and below the thermocline) exist under different environmental factors, such as light intensity, nutrients and temperature. This determines the pronounced variation in the phytoplankton photosynthetic parameters with depth [44].

One of the key parameters for estimating PP is ϕ [2]. It expresses the efficiency of phytoplankton carbon fixation per quantum of light absorbed by the photosynthetic apparatus of the cell [45]. The ϕ varied with depth and by season. Light conditions determine the content of photoprotective pigments, which reduce the ϕ values [2, 17]. Due to the high PAR values in the sea surface layer, the ϕ values were minimal: at the station near Katsiveli in summer, the ϕ was equal to 0.005 mol C·mol quanta^{-1}, whereas at the station near Sevastopol, the average summer values were lower and equaled 0.003 ± 0.003 mol C·mol quanta^{-1}. Within the UML, ϕ increased by ~ 6 times at both stations. Autumn ϕ values reached 0.005 mol C·mol quanta^{-1}, increasing with depth in the UML by ~ 8 times. In winter, when the PAR values were minimal, the ϕ was maximal: at the station near Katsiveli, the ϕ in the sea surface layer was equal to 0.007 mol C·mol quanta^{-1} (increasing in the UML by ~ 7 times), while at the station near Sevastopol it was 0.010 mol C·mol quanta^{-1} (increasing in the UML by ~ 5 times) and 0.012 mol C·mol quanta^{-1} (increasing in the UML by ~ 5 times) on 22.02.2022 and 29.11.2022, respectively. With the increase of PAR in spring, the ϕ values began to decrease and amounted to 0.007 ± 0.001 mol C·mol quanta^{-1} in the sea surface layer, increasing within the UML by ~ 6 times (Fig. 7, *a*). It was found that in winter in the sea surface layer near Sevastopol, the ϕ values were ~3 times higher than in summer. Such significant seasonal dynamics of the ϕ is a consequence of the phytoplankton acclimation to changing light conditions.

A comparison of the ϕ values with PUR^*_{psp} showed a relationship between these parameters, which was described by a power function (Fig. 7, *b*).

Primary production

For the entire study period, the same types of vertical PP profiles were observed with a maximum in the sea surface layer. The profiles varied significantly throughout

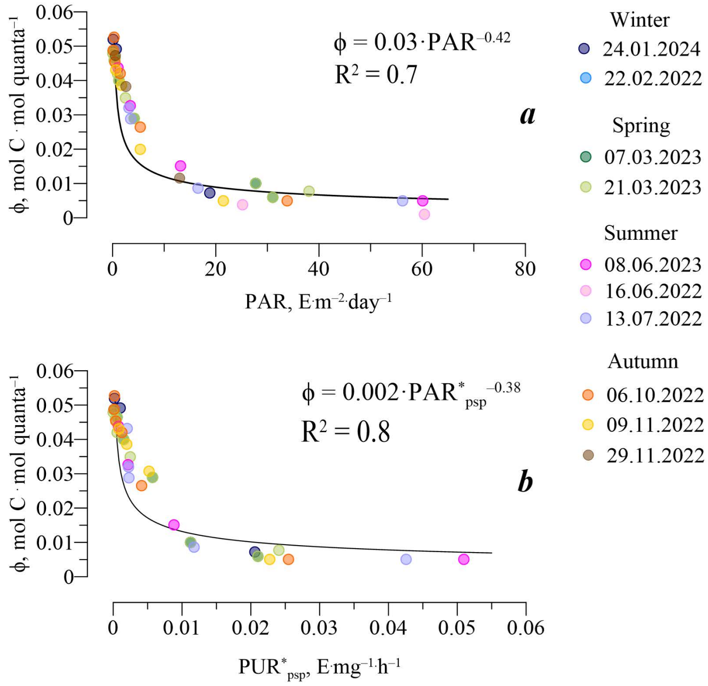

F i g . 7 . Dependence of the quantum yield of photosynthesis ϕ on PAR in the UML (*a*) and on the amount of quanta absorbed by photosynthetically active pigments, per chlorophyll a unit PUR^*_{psp} in the UML (*b*)

the year: from 11 mgC·m^{-3}·day^{-1} in early November to 84 mgC·m^{-3}·day^{-1} in early October (Fig. 8, *a*). The winter PP values at the stations near Katsiveli and Sevastopol equaled 21 mgC·m^{-3}·day^{-1} and 16 mgC·m^{-3}·day^{-1}, respectively. During March, the PP increased from 43 mgC·m^{-3}·day^{-1} to 58 mgC·m^{-3}·day^{-1}.The summer PP values were higher in the coastal waters of Sevastopol (72 mgC·m^{-3}·day^{-1}) than in those of Katsiveli (34 mgC·m^{-3}·day^{-1}).

The maximal photosynthesis rate in the sea surface layer was observed in October (7.8 mgC·m^{-3}·h^{-1}), and relatively high values were also observed in March (4.0 mgC·m^{-3}·h^{-1} and 4.5 mgC·m^{-3}·h^{-1}) and July (4.4 mgC·m^{-3}·h^{-1}) (Fig. 8, *c*). The high photosynthesis rate corresponded to the maximum TChl-*a* values and minimum ϕ values. In summer, the TChl-*a* values varied between stations by 3.4 times, while the PP values differed by 2 times. In November, a decrease in the TChl-*a* values also led to a 6-fold decrease in the PP values.

The values of assimilation number (AN) in the sea surface layer increased from early November (1.3 mgC·mgTChl-*a*$^{-1}$·h^{-1}) to July (2.6 mgC·mgTChl-*a*$^{-1}$·h^{-1}) at the station near Sevastopol and from winter (1.8 mgC·mgTChl-*a*$^{-1}$·h^{-1}) to summer

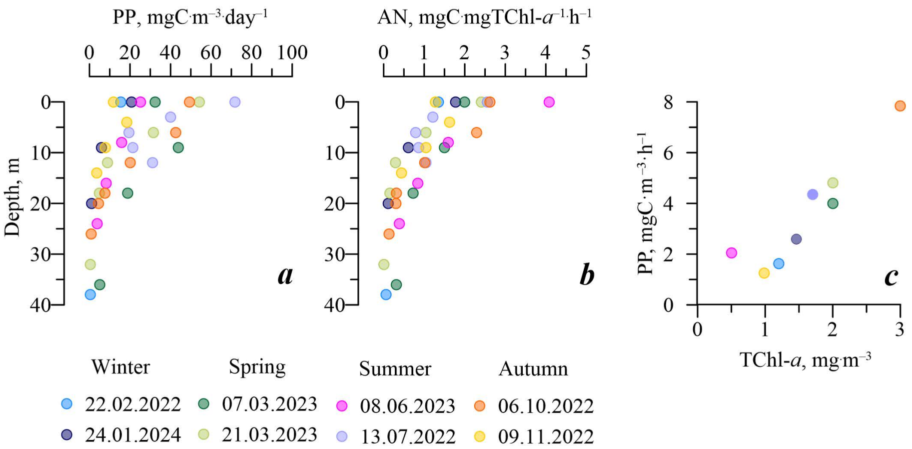

F i g . 8 . Vertical distribution of the PP (*a*) and the assimilation number AN (*b*); dependence of the PP on chlorophyll a plus phaeopigment concentrations TChl-*a* at 0 m (*c*)

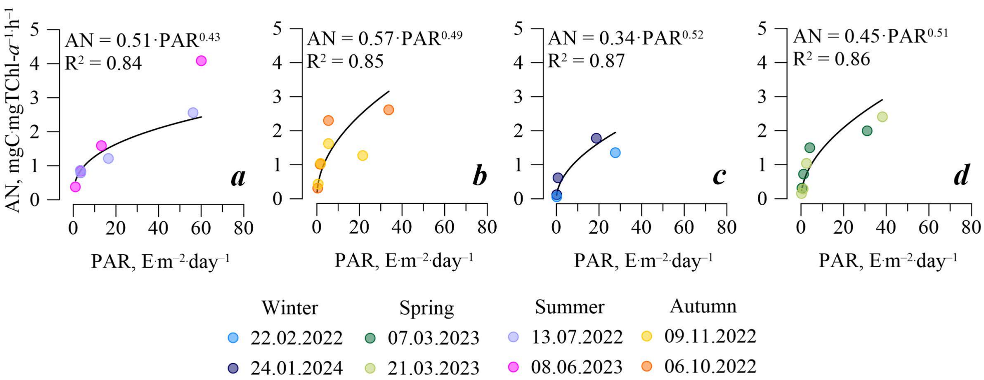

F i g . 9 . Dependence of the AN on the PAR in the UML of the Black Sea coastal waters in summer (*a*), autumn (*b*), winter (*c*) and in spring (*d*)

(4.0 mgC·mgTChl-a^{-1}·h^{-1}) at the station near Katsiveli (Fig. 8, *b*). The analysis showed that the AN varied among seasons, which was more pronounced in the sea surface layer (Fig. 8, *b*). The AN depends mainly on light intensity and to a lesser extent on other abiotic factors such as temperature and nutrients availability [42]. A comparison of the AN with the light intensity allowed us to reveal dependencies for individual seasons (Fig. 9):

for summer, $AN = 0.51\ PAR^{0.43}$, $n = 9$, $r^{r2} = 0.83$; (3)

for autumn, $AN = 0.57\ PAR^{0.49}$, $n = 10$, $r^{r2} = 0.85$; (4)

for winter, $AN = 0.34\ PAR^{0.52}$, $n = 5$, $r^{r2} = 0.87$; (5)

for spring, $AN = 0.45\ PAR^{0.51}$, $n = 8$, $r^{r2} = 0.86$. (6)

The revealed dependencies of the AN on the PAR (equations 3–6) reflect seasonal differences in the AN under the same light conditions (Fig. 9).

Annual cycle

In the most productive surface layer of the sea (Fig. 8, *a*), ϕ_{max} varied ~ 7-fold during the year, which exceeded the degree of variability of other photosynthetic parameters. An analysis of the seasonal dynamics showed that ϕ_{max} (Fig. 10, *d*) was related inversely to PAR_0, whereas I_k was directly related to PAR_0 and showed a twofold seasonal variation (Fig. 10, *e*). Since the ϕ depends on the ϕ_{max} and

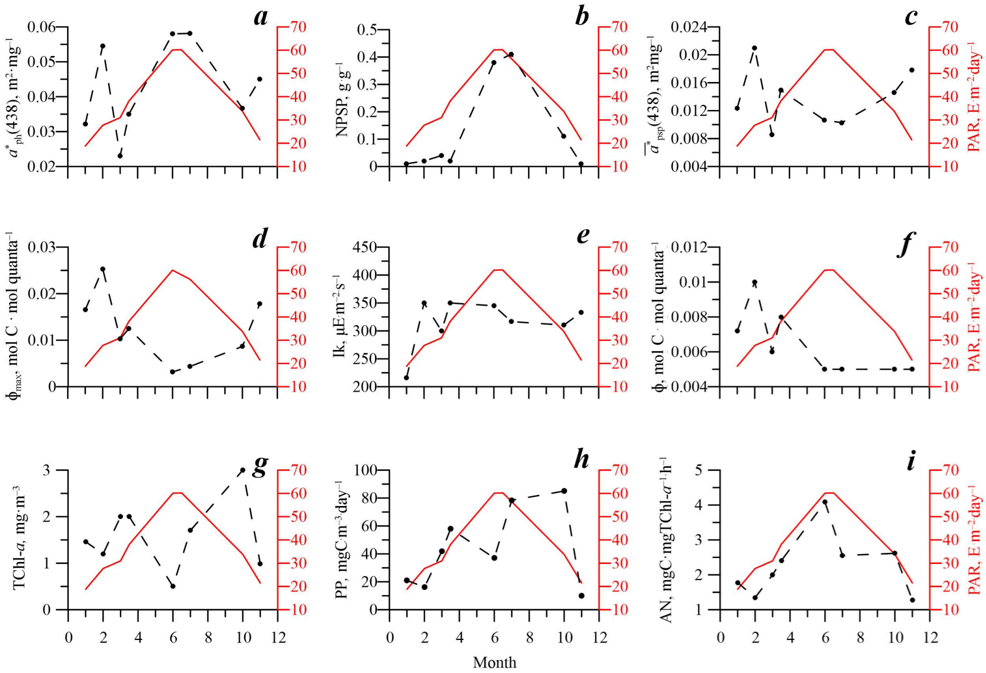

F i g . 1 0 . Annual cycle of the studied parameters. The red line is photosynthetically available radiance PAR at surface water. The dashed lines denote chlorophyll a-specific light absorption coefficient of phytoplankton $a^*_{ph}(438)$ (*a*); intracellular content of photoprotective pigments and their share NPSP in the total amount of phytoplankton pigments (*b*); the spectrally weighted chlorophyll a specific absorption coefficient calculated for photosynthetically active pigments $\overline{a}^*_{psp}(z)$ (*c*); maximum quantum yield of photosynthesis ϕ_{max} (*d*); the light intensity saturating the photosynthesis I_k (*e*); quantum yield of photosynthesis ϕ (*f*); chlorophyll a plus phaeopigment concentrations TChl-*a* (*g*); primary production PP (*h*); assimilation number AN (*i*)

I_k (equation 2), and since ϕ_{max} was the most variable seasonally, the ϕ was directly related to PAR, yet to a lesser extent than ϕ_{max} (Fig. 10, *f*). The intra-annual variability of $a^*_{ph}(438)$ in the surface layer spanned a factor of three and was directly related to PAR_0, except the high a^*_{ph} values in February (Fig. 10, *a*), which may be associated with small-celled species of phytoplankton [35], in particular coccolithophores. The abundance of coccolithophores in the phytoplankton increased in the last decade in the Black Sea [46]. However, the seasonal dynamics of $\overline{a}^*_{psp}$ (Fig. 10, *c*), which determines the rate of photosynthesis, differed from a^*_{ph}. This was due to the proportion of photoprotective pigments (Fig. 10, *b*), which depended directly on the light intensity in the UML [23]. In the annual cycle of $\overline{a}^*_{psp}$, a peak was observed in February. The peak is associated with the dominance of small-cell phytoplankton species, and the decline in March is due to the bloom of large diatoms. However, in general, a U-shaped type of cycle was observed with relatively lower values in summer, with their increase in other seasons. The annual AN cycle (Fig. 10, *i*) differs in type from ϕ and $\overline{a}^*_{psp}$. This is due to the fact that AN also depends on the light intensity. Consequently, the light factor has a predominant influence on the intra-annual dynamics of the AN. The TChl-*a* in the sea surface layer varied 6 times during the year. The annual cycle of TChl-*a* has two peaks (Fig. 10, *g*): spring and autumn, which is associated with the bloom of phytoplankton in these seasons. The intra-annual variability of PP was 8-fold and was similar to the annual cycle of TChl-*a* (Fig. 10, *i*).

Conclusions

We analysed seasonal dynamics of photosynthetic characteristics of phytoplankton in the BS coastal waters near the Crimean Peninsula. The seasonal variability of PP was caused by acclimation of phytoplankton to environmental conditions. The PAR incident on the sea surface increased approximately threefold from winter (22 ± 5 mol quanta·m^{-2}·day^{-1}) to summer (59 ± 1 mol quanta·m^{-2}·day^{-1}). This caused photoadaptive transformations in the pigment complex of microalgae, namely changes in the concentration of chlorophyll a and accessory pigments, including photoprotective pigments, which affect the capacity of phytoplankton to absorb light in the sea and use it during photosynthesis. The seasonal variability of the TChl-*a* occurred. High values of TChl-*a* in the sea were observed in early October and in March, which may be associated with phytoplankton bloom, while low values were observed in summer (twice as little). The $\overline{a}^*_{ph}(z)$ varied significantly among seasons: from minimal values in spring (on average 0.012 m^2·mg^{-1}) to maximal values in summer (on average 0.024 m^2·mg^{-1}) with intermediate values in autumn and winter (on average 0.017 m^2·mg^{-1}). The variability of the $\overline{a}^*_{ph}(z)$ is mainly due to the intra-annual variability of the a^*_{ph}. The $\overline{a}^*_{psp}$ was minimal in summer (on average 0.010 m^2·mg^{-1}) due to the highest relative content of photoprotective pigments (on average 0.35 g·g^{-1}). The ϕ in the surface layer varied among seasons by ~ 3 times from the lowest values in summer (0.003 mol C·mol quanta^{-1}) to the highest values (0.010 mol C·mol quanta^{-1}) in winter, which is associated with the annual dynamics of sea surface insolation. The variability of ϕ within the euphotic zone was greatest (up to 8.7 times) compared to other parameters. PP values varied widely in the sea surface layer, decreasing with depth. The AN changed during the year by ~ 2 times from 1.3 to 4 mgC·mgTChl-a^{-1}·h^{-1}, which is associated with its dependence on PAR.

REFERENCES

1. Falkowski, P.G. and Knoll, A.H., 2011. *Evolution of Primary Producers in the Sea*. Academic Press, 456 p.
2. Falkowski, P.G. and Raven, J.A., 2007. *Aquatic Photosynthesis*. Third edition. New Jersey: Princeton University Press, 501 p.
3. Shalovenkov, N., 2000. Scales of Ecological Processes and Anthropogenous Loads on the Coastal Ecosystems of the Black Sea. *Estuarine, Coastal and Shelf Science*, 50(1), pp. 11–16.
4. Cociasu, A., Dorogan, L., Humborg, C. and Popa, L., 1996. Longterm Ecological Changes in Romanian Coastal Waters of the Black Sea. *Marine Pollution Bulletin*, 32(1), pp. 32–38. https://doi.org/10.1016/0025-326X(95)00106-W
5. Lillebø, A.I., Stålnacke, P. and Gooch, G.D., 2015. *Coastal Lagoons in Europe: Integrated Water Resource Strategies*. London: IWA Publishing, 228 p. https://doi.org/10.2166/9781780406299
6. Kirk, J., 2011. *Light and Photosynthesis in Aquatic Ecosystems*. Cambridge University Press, 524 p.
7. Morel, A., 1991. Light and Marine Photosynthesis: A Spectral Model with Geochemical and Climatological Implications. *Progress in Oceanography*, 26, pp. 263–306. https://doi.org/10.1016/0079-6611(91)90004-6
8. Smyth, T.J., Tilstone, G.H. and Groom, S.B., 2005. Integration of Radiative Transfer into Satellite Models of Ocean Primary Production. *Journal of Geophysical Research: Oceans*, 110(C10), C10014. https://doi.org/10.1029/2004JC002784
9. Churilova, T.Ya., Suslin, V.V., Krivenko, O.V., Efimova, T.V. and Moiseeva, N.A., 2016. Spectral Approach to Assessment of Phytoplankton Photosynthesis Rate in the Black Sea Based on Satellite Information: Methodological Aspects of the Regional Model Development. *Journal of Siberian Federal University. Biology*, 9(4), pp. 367–384. https://doi.org/10.17516/1997-1389-2016-9-4-367-384 (in Russian).
10. Churilova, T. and Suslin, V., 2010. Parameterization of Light Absorption by all In-Water Optically Active Components in the Black Sea: Impact for Underwater Irradiance and Primary Production Modelling. In: H. Dahlin, M. J. Bell, N. C. Flemming and S. E. Petersson, eds., 2010. *Proceedings of the Fifth International Conference on EuroGOOS: Coastal to Global Operational Oceanography: Achievements and Challenges, 20–22 May 2008, Exeter, UK*. EuroGOOS Office, Vol. 28, pp. 199–205.
11. Churilova, T., Kryvenko, O., Suslin, V., Efimova, T. and Moiseeva, N., 2016. Primary Production of the Black Sea: Spectral Approach. *Marine Biological Journal*, 1(3), pp. 50–53. https://doi.org/10.21072/mbj.2016.01.3.08 (in Russian).
12. Ivanov, V.A. and Belokopytov, V.N., 2013. *Oceanography of the Black Sea*. Sevastopol: ECOSI-Gidrofizika, 210 p.
13. Jeffrey, S.W. and Humphrey, G.F., 1975. New Spectrophotometric Equations for Determining Chlorophylls a, b, c1 and c2 in Higher Plants, Algae and Natural Phytoplankton. *Biochemie und Physiologie der Pflanzen*, 167(2), pp. 191–194. https://doi.org/10.1016/s0015-3796(17)30778-3
14. Lorenzen, C.J., 1967. Determination of Chlorophyll and Pheopigments: Spectrophotometric Equations. *Limnology and Oceanography*, 12, pp. 343–346. https://doi.org/10.4319/lo.1967.12.2.0343

15. Neeley, A.R. and Mannino, A., 2018. *Inherent Optical Property Measurements and Protocols: Absorption Coefficient.* IOCCG Protocol Series Ocean Optics & Biogeochemistry Protocols for Satellite Ocean Colour Sensor Validation, vol. 1. Dartmouth, NS, Canada, 83 p. https://doi.org/10.25607/OBP-119
16. Mannino, A., Novak, M.G., Nelson, N.B., Belz, M., Berthon, J.-F., Blough, N.V., Boss, E., Bricaud, A., Chaves, J. et al., 2019 Measurement Protocol of Absorption by Chromophoric Dissolved Organic Matter (CDOM) and Other Dissolved Materials. In: A. Mannino, and M. G. Novak, eds., 2019. *Inherent Optical Property Measurements and Protocols: Absorption Coefficient.* IOCCG Ocean Optics and Biogeochemistry Protocols for Satellite Ocean Colour Sensor Validation, vol. 5.0. Dartmouth, NS, Canada: IOCCG, 77 p.
17. Marra, J., Trees, C.C., Bidigare, R.R. and Barber, R.T., 2000. Pigment Absorption and Quantum Yields in the Arabian Sea. *Deep Sea Research. Part II: Topical Studies in Oceanography*, 47(7–8), pp. 1279–1299. https://doi.org/10.1016/S0967-0645(99)00144-7
18. Lawrenz, E., Silsbe, G., Capuzzo, E., Ylöstalo, P., Forster, R.M., Simis, S.G., Prášil, O., Kromkamp, J.C., Hickman, A.E. et al., 2013. Predicting the Electron Requirement for Carbon Fixation in Seas and Oceans. *PLoS ONE*, 8(3), e58137. https://doi.org/10.1371/journal.pone.0058137
19. Antal, T., Konyukhov, I., Volgusheva, A., Plyusnina, T., Khruschev, S., Kukarskikh, G. and Rubin, A., 2019. Chlorophyll Fluorescence Induction and Relaxation System for the Continuous Monitoring of Photosynthetic Capacity in Photobioreactors. *Physiologia Plantarum*, 165(3), pp. 476–486. https://doi.org/10.1111/ppl.12693
20. Zhu, Y., Ishizaka, J., Tripathy, S.C., Wang, S., Sukigara, C., Goes, J., Matsuno, T. and Suggett, D.J., 2017. Relationship Between Light, Community Composition and the Electron Requirement for Carbon Fixation in Natural Phytoplankton. *Marine Ecology Progress Series*, 580, pp. 83–100. https://doi.org/10.3354/meps12310
21. Cruz, S. and Serôdio, J., 2008. Relationship of Rapid Light Curves of Variable Fluorescence to Photoacclimation and Non-Photochemical Quenching in a Benthic Diatom. *Aquatic Botany*, 88(3), pp. 256–264. https://doi.org/10.1016/j.aquabot.2007.11.001
22. Platt, T., Gallegos, C.L. and Harrison, W.G., 1980. Photoinhibition of Photosynthesis in Natural Assemblages of Marine Phytoplankton. *Journal of Marine Research*, 38, pp. 687–701.
23. Babin, M., Morel, A., Claustre, H., Bricaud, A., Kolber, Z. and Falkowski, P.G., 1996. Nitrogen-and Irradiance-Dependent Variations of the Maximum Quantum Yield of Carbon Fixation in Eutrophic, Mesotrophic and Oligotrophic Marine Systems. *Deep-Sea Research. Part I: Oceanographic Research Papers*, 43(8), pp. 1241–1272.
24. Churilova, T.Ya., Suslin, V.V. and Sosik, H.M., 2021. Dependence of the Photosynthetic Quantum Yield on Phytoplankton Light Absorption: Equations for Assessing Primary Production in the Black Sea. *Physical Oceanography*, 28(1), pp. 67–77. https://doi.org/10.22449/1573-160X-2021-1-67-77
25. Suslin, V.V., Korolev, S.N., Kucheryaviy, A.A., Churilova, T.Ya. and Krivenko, O.V., 2015. Photosynthetically Available Radiation on Surface of the Black Sea Based on Ocean Color Data. In: O. A. Romanovskii, ed., 2015. *Vol. 9680: Proceedings of SPIE. 21st International Symposium Atmospheric and Ocean Optics: Atmospheric Physics*. Tomsk, 96800T. https://doi.org/10.1117/12.2203660
26. de Boyer Montégut, C., Madec, G., Fischer, A.S., Lazar, A. and Iudicone, D., 2004. Mixed Layer Depth over the Global Ocean: An Examination of Profile Data and a Profile-Based Climatology. *Journal of Geophysical Research: Oceans*, 109(C12), C12003. https://doi.org/10.1029/2004JC002378

27. Becker, V., Huszar, V.L.M. and Crossetti, L.O., 2009. Responses of Phytoplankton Functional Groups to the Mixing Regime in a Deep Subtropical Reservoir. *Hydrobiologia*, 628, pp. 137–151. https://doi.org/10.1007/s10750-009-9751-7
28. Ivanov, V.A. and Mikhaylova, E.N., 2008. [*Upwelling in the Black Sea*]. Sevastopol: ECOSI-Gidrofizika, 92 p. (in Russian).
29. Shokurova, I.G., Plastun, T.V., Kasianenko, T.E., Stanichnaya, R.R., Krasheninnikova, S.B. and Simonova, Yu.V., 2023. Winds Favorable for Upwellings near the Southern Coast of Crimea. *Physical Oceanography*, 30(4), pp. 398–409.
30. Stramski, D. and Kiefer, D.A., 1991. Light Scattering by Microorganisms in the Open Ocean. *Progress in Oceanography*, 28(4), pp. 343–383. https://doi.org/10.1016/0079-6611(91)90032-h
31. Berseneva, G.P., Churilova, T.Ya. and Georgieva, L.V., 2004. Seasonal Variability in Pigment Concentration, Taxonomic Structure of Phytoplankton Community in Western Part of the Black Sea. *Oceanology*, 44(3), pp. 362–371.
32. Finenko, Z.Z., Suslin, V.V. and Kovaleva, I.V., 2014. Seasonal and Long-Term Dynamics of the Chlorophyll Concentration in the Black Sea According to Satellite Observations. *Oceanology*, 54(5), pp. 596–605. https://doi.org/10.1134/S0001437014050063
33. Finenko, Z.Z., Stelmakh, L.V., Mansurova, I.M., Georgieva, E.Ju. and Tsilinsky, V.S., 2017. Seasonal Dynamic of Structural and Functional Characteristics of the Phytoplankton Community in the Sevastopol Bay. *Monitoring Systems of Environment*, 9, pp. 73–82 (in Russian).
34. Finenko, Z.Z. and Krupatkina, D.K., 1993. Primary Production in the Black Sea During Winter–Spring Period. *Okeanologiya*, 33(1), pp. 97–104 (in Russian).
35. Morel, A. and Bricaud, A., 1981. Theoretical Results Concerning Light Absorption in a Discrete Medium, and Application to Specific Absorption of Phytoplankton. *Deep Sea Research. Part A: Oceanographic Research Papers*, 28(11), pp. 1375–1393. https://doi.org/10.1016/0198-0149(81)90039-x
36. Churilova, T.Ya., Finenko, Z.Z. and Akimov, A.I., 2008. [Pigments of Microalgae]. In: Yu. N. Tokarev, Z. Z. Finenko and N. V. Shadrin, eds., 2008. *The Black Sea Microalgae: Problems of Biodiversity Preservation and Biotechnological Use*. Sevastopol: ECOSI-Gidrofizika, pp. 301–319 (in Russian).
37. Churilova, T., Suslin, V., Krivenko, O., Efimova, T., Moiseeva, N., Mukhanov, V. and Smirnova, L., 2017. Light Absorption by Phytoplankton in the Upper Mixed Layer of the Black Sea: Seasonality and Parametrization. *Frontiers in Marine Science*, 4, 90. https://doi.org/10.3389/fmars.2017.00090
38. Raven, J.A., 2011. The Cost of Photoinhibition. *Physiologia Plantarum*, 142(1), pp. 87–104. https://doi.org/10.1111/j.1399-3054.2011.01465.x
39. Emerson, R. and Lewis, C.M., 1943. The Dependence of the Quantum Yield of Chlorella Photosynthesis on the Wavelength of Light. *American Journal of Botany*, 30(3), pp. 165–178. https://doi.org/10.2307/2437236 30:165–178
40. Woźniak, B., Ficek, D., Ostrowska, M., Majchrowski, R. and Dera, J., 2007. Quantum Yield of Photosynthesis in the Baltic: A New Mathematical Expression for Remote Sensing Applications. *Oceanologia*, 49(4), pp. 527–542. Available at: https://www.iopan.gda.pl/oceanologia/494wozni.pdf (Accessed: 25 May 2026).
41. Babin, M., 2008. Phytoplankton Fluorescence: Theory, Current Literature and In Situ Measurement. In: M. Babin, C. S. Roesler and J. J. Cullen, eds., 2008. *Real-Time Coastal Observing Systems for Marine Ecosystem Dynamics and Harmful Algal Blooms: Theory, Instrumentation and Modelling*. Paris: UNESCO Publishing, pp. 237–280. Available at: https://unesdoc.unesco.org/ark:/48223/pf0000160000 (Accessed: 25 May 2026).

42. Falkowski, P.G., 1981. Light-Shade Adaptation and Assimilation Numbers. *Journal of Plankton Research*, 3(2), pp. 203–216. https://doi.org/10.1093/plankt/3.2.203
43. Cullen, J.J. and Lewis, M.R., 1988. The Kinetics of Algal Photoadaptation in the Context of Vertical Mixing. *Journal Plankton Research*, 10(5), pp. 1039–1063. https://doi.org/10.1093/plankt/10.5.1039
44. Prézelin, B.B., Putt, M. and Glover, H.E., 1986. Diurnal Patterns in Photosynthetic Capacity and Depth-Dependent Photosynthesis-Irradiance Relationships in Synechococcus spp. and Larger Phytoplankton in Three Water Masses in the Northwest Atlantic Ocean. *Marine Biology*, 91, pp. 205–217. https://doi.org/10.1007/BF00569436
45. Marra, J., Chamberlain, W.S. and Knudson, C., 1993. Proportionality Between In Situ Carbon Assimilation Bio-Optical Measures of Primary Production in the Gulf of Maine in Summer. *Limnology and Oceanography*, 38(1), pp. 232–238. https://doi.org/10.4319/lo.1993.38.1.0232
46. Mikaelyan, A.S., Sergeeva, A.V., Pautova, L.A., Chasovnikov, V.K. and Gagarin, V.I., 2024. 75-Year Dynamics of the Black Sea Phytoplankton in Association with Eutrophication and Climate Change. *Science of the Total Environment*, 954, 176448. https://doi.org/10.1016/j.scitotenv.2024.176448

Submitted 26.12.2025; accepted after review 22.01.2026;
revised 19.03.2026; published 30.06.2026

About the authors:

Daria V. Kalmykova, Junior Researcher, A.O. Kovalevsky Institute of Biology of the Southern Seas of RAS (2, Nakhimov Ave., Sevastopol, 299011, Russia), Laboratory of Photosynthesis and Marine Bio-optics, **ORCID ID: 0000-0002-3097-9913**, **Scopus Author ID: 58688288100**, *daria-k.kalmykova@ibss-ras.ru*

Tanya Ya. Churilova, Senior Researcher, A.O. Kovalevsky Institute of Biology of the Southern Seas of RAS (2, Nakhimov Ave., Sevastopol, 299011, Russia), Laboratory of Photosynthesis and Marine Bio-optics, PhD (Biol.), **ORCID ID: 0000-0002-0045-7284**, **Scopus Author ID: 6603622802**, **ResearcherID: O-8437-2016**, *tanya.churilova@ibss-ras.ru*

Tatiana V. Efimova, Senior Researcher, A.O. Kovalevsky Institute of Biology of the Southern Seas of RAS (2, Nakhimov Ave., Sevastopol, 299011, Russia), Head of Laboratory of Photosynthesis and Marine Bio-optics, PhD (Biol.), **ORCID ID: 0000-0003-3908-4160**, **Scopus Author ID: 57194423783**, **ResearcherID: X-1355-2019**, *tefimova@ibss-ras.ru*

Nataliia A. Moiseeva, Researcher, A.O. Kovalevsky Institute of Biology of the Southern Seas of RAS (2, Nakhimov Ave., Sevastopol, 299011, Russia), Laboratory of Photosynthesis and Marine Bio-optics, **ORCID ID: 0000-0003-1356-7981**, *moiseeva@ibss-ras.ru*

Elena Yu. Skorokhod, Researcher, A.O. Kovalevsky Institute of Biology of the Southern Seas of RAS (2, Nakhimov Ave., Sevastopol, 299011, Russia), Laboratory of Photosynthesis and Marine Bio-optics, **ORCID ID: 0000-0002-3057-3964**, *elenaskorokhod@ibss-ras.ru*

Contribution of the authors:

Daria V. Kalmykova – text drafting, reviewing and editing, data analysis, formal analysis, visualisation

Tanya Ya. Churilova – concept statement, text drafting, reviewing and editing, data analysis

Tatiana V. Efimova – data analysis, text reviewing and editing

Nataliia A. Moiseeva – data collection, text reviewing and editing

Elena Yu. Skorokhod – data collection, text reviewing and editing

All the authors have read and approved the final manuscript.

ISSN 2413-5577, Ecological Safety of Coastal and Shelf Zones of Sea, No. 2, pp. 145–161 (2026)

Original paper

Zooplankton Image Classification Using a FlowCam Flow Imaging Microscope

I. A. Minsky [1, 2], **D. A. Litvinyuk** [1, 2] *, **V. P. Evstigneev** [1, 2], **A. A. Pinaev** [1], **V. S. Mukhanov** [1, 2]

[1] *Sevastopol State University, Sevastopol, Russia*

[2] *A. O. Kovalevsky Institute of Biology of the Southern Seas of RAS, Sevastopol, Russia*

* *d.litvinyuk@ibss-ras.ru*

Abstract

For many years, a FlowCam flow imaging microscope (Yokogawa Fluid Imaging Inc., USA) has been used to study communities of marine organisms – their species composition, structure, and dynamics, as well as morphological characteristics of individual organisms. However, the problem of standardizing protocols for using these types of instruments in the field of visualization cytometry for processing plankton samples remains unsolved. The aim of the study was to develop a methodology for zooplankton image classification using *VisualSpreadsheet tools* – the software that controls the system operation. For the first time, an algorithm for automatic search of value filters was developed, and the ordering of class tabs in the *VisualSpreadsheet* classification window was formalized. The proposed method was applied to native samples of Black Sea zooplankton and, under certain conditions, enabled the correct classification of 100% of bivalve larvae (class *mollusca*) and the dinoflagellate *Noctiluca scintillans* (class *noctiluca*), 82% of the appendicularian *Oikopleura dioica* (class *oikopleura*), 71.2% of naupliar (larval) stages (class *nauplius*), and up to 70.2% of calanoid and cyclopod (class *copepoda*). Overall, the described approach can be used for any type of object studied with FlowCam, especially those with a complex morphology.

Keywords: FlowCam, VisualSpreadsheet, zooplankton, images classification, classification algorithm

Acknowledgment: The study was carried out under the state assignment of Sevastopol State University on the topic "Comprehensive Marine Interdisciplinary Research on the Research Vessel 'Pioneer-M' in the Shelf Zone and Continental Slope of the Black Sea under Conditions of Anthropogenic Impact and Climate Change" (FEFM-2024-0013); and under IBSS state research assignment "Transformation of the structure and functions of marine pelagic ecosystems under the anthropogenic load and climate change" (No. 124030400057-4).

For citation: Minsky, I.A., Litvinyuk, D.A., Evstigneev, V.P., Pinaev, A.A. and Mukhanov, V.S., 2026. Zooplankton Image Classification Using a FlowCam Flow Imaging Microscope. *Ecological Safety of Coastal and Shelf Zones of Sea*, (2), pp. 145–161.

© Minsky I. A., Litvinyuk D. A., Evstigneev V. P., Pinaev A. A., Mukhanov V. S., 2026

This work is licensed under a Creative Commons Attribution-Non Commercial 4.0 International (CC BY-NC 4.0) License

Классификация изображений зоопланктона на программно-аппаратном комплексе *FlowCam*

И. А. Минский [1, 2], Д. А. Литвинюк [1, 2] *, В. П. Евстигнеев [1], А. А. Пинаев [1], В. С. Муханов [1, 2]

[1] *ФГБОУ ВО Севастопольский государственный университет, Севастополь, Россия*

[2] *ФГБУН ФИЦ «Институт биологии южных морей имени А.О. Ковалевского РАН», Севастополь, Россия*

* *d.litvinyuk@ibss-ras.ru*

Аннотация

Многие годы программно-аппаратный комплекс *FlowCam* (*Yokogawa Fluid Imaging Inc.,* США) используется для исследования сообществ морских организмов – их видового состава, структуры и динамики, а также морфологических характеристик. Однако до сих пор не решена задача унификации протоколов применения такого типа приборов, относящихся к области визуализирующей цитометрии, для обработки планктонных проб. Цель работы заключается в разработке методики классификации изображений зоопланктона инструментами *VisualSpreadsheet* – программного продукта, управляющего работой комплекса. Впервые разработан алгоритм автоматического поиска фильтров значений (*value filters*) и проведена формализация порядка вкладок классов в окне классификации *VisualSpreadsheet*. Предложенная методика была применена на нативных пробах черноморского зоопланктона и позволила, при определенных условиях, корректно классифицировать 100 % личинок двустворчатых моллюсков (класс *mollusca*) и динофлагеллят *Noctiluca scintillans* (класс *noctiluca*), 82 % оболочников *Oikopleura dioica* (класс *oikopleura*), 71.2 % науплиальных стадий развития (класс *nauplius*) и до 70.2 % каланоидных и циклоподных копепод (класс *copepoda*). В целом описанный подход может быть использован для любых типов объектов, исследуемых на *FlowCam*, особенно со сложной морфологией.

Ключевые слова: *FlowCam*, *VisualSpreadsheet*, зоопланктон, классификация изображений, алгоритм классификации

Благодарности: исследование выполнено в рамках государственного задания Севастопольского государственного университета по теме «Комплексные морские междисциплинарные исследования на НИС «Пионер-М» в шельфовой зоне и континентальном склоне Черного моря в условиях антропогенного воздействия и климатических изменений» (FEFM-2024-0013); в рамках государственного задания ФИЦ ИнБЮМ по теме «Трансформация структуры и функций экосистем морской пелагиали в условиях антропогенного воздействия и изменения климата» (№ гос. регистрации 124030400057-4).

Для цитирования: *Минский И. А., Литвинюк Д. А., Евстигнеев В. П., Пинаев А. А. и др.* Классификация изображений зоопланктона на программно-аппаратном комплексе *FlowCam* // Экологическая безопасность прибрежной и шельфовой зон моря. 2026. № 2. С. 145–161. EDN WCIXSD.

Introduction

Zooplankton is the most important link in the trophic chain of aquatic ecosystems, determining the efficiency of matter and energy transfer from primary producers (phytoplankton) to higher-order consumers (planktivorous fish and invertebrates) [1, 2]. Ecological monitoring of marine areas includes zooplankton sampling, the processing and analysis of which make it possible to assess the structure of marine communities and their state [3, 4]. However, sample processing requires significant time expenditure, and the laboriousness and monotony of this type of work are accompanied by occasional errors of varying impact on the analysis result [5, 6]. Currently, the task of automating such a classical hydrobiological operation is becoming increasingly relevant, and efforts of many researchers all over the world are focused on its solution [7, 8]. One of the existing solutions for plankton sample processing is a FlowCam (FC) flow imaging microscope (Yokogawa Fluid Imaging Inc., USA).

FC is a combination of a microscope, flow cytometer, and a fluorimeter. The examined liquid is pumped through the FC system, where particles are captured by a high-speed camera. Together with the VisualSpreadsheet (VS) software, FC allows framing objects detected in the liquid flow and analysing their quantitative and qualitative characteristics. From the acquired images, VS automatically calculates over 40 parameters describing the morphometric and colour characteristics of the framed objects. In addition, the instrument can record their fluorescence intensity (trigger mode).

Studies have shown that, compared to traditional manual processing of plankton samples by light microscopy, imaging cytometry systems such as FC underestimate the concentration of objects in a liquid volume. Nevertheless, these systems provide correct estimates of the relative abundance of a particular taxon, which, combined with speed, opens prospects for partial automation of the sample processing procedure [9].

An important feature of the system is the semi-automated particle image classification function in VS [10]. Its essence lies in creating filters that sort images based on morphometric, colour, or fluorometric characteristics. A filter is a set of threshold constraints on parameter values that allows an object to be distinguished among many others in a single run. VS has a function to create a sequence of filters (classifier) designed to sort run images into user-defined classes. The information basis for filter creation is digital libraries – user-expanded collections of object images within classes. Ultimately, the libraries cover the entire range of values of discriminating features.

Despite the use of FC for plankton analysis, to date there is no clearly formulated and reproducible methodology for classifying zooplankton images using VS. In a review article [11], devoted to the experience of using FC in phytoplankton studies (a more common object for FC work), it is shown that slightly more than 10% of publications discuss image classification. At the same time, articles that mention filter creation and the autoclassification procedure, with rare exceptions [10, 12], do not contain a detailed description of a ready-to-use methodology for creating filters and a classifier. Descriptions of filter selection for identifying zooplankton organisms and creating a filter system in the VS classifier are completely absent from these publications.

This work is purposed at developing a methodology for identifying zooplankton organisms in native samples using the tools provided by VisualSpreadsheet. Information is presented on the materials used in the work and the libraries created on their basis; the key classification tools of VS and the chosen approach to library creation are described; general principles for creating filters and a classifier are formulated; an algorithm for creating filters and arranging tabs in the VS classification window is described; the process of creating a classifier for selected zooplankton object classes is given; finally, a brief review of publications where FC was applied for zooplankton research is presented, and based on it, we carried out the comparison of results with works where the image classification procedure is described in most detail.

Materials and methods

Sampling and material preparation. Zooplankton samples were collected with a Juday net (Ø = 37 cm, mesh size 150 μm) by total hauls from bottom to surface at the exit from Balaklava Bay (Crimea, Black Sea) during daytime in March and April 2025. The samples were fixed with 40% formaldehyde to a final concentration of 2%. Small particles were removed using a 100 μm filter.

FlowCam settings. A flow cell with an inlet diameter of 1000 μm (FOV1000) and a 2× magnification lens were installed on the FlowCam (model 8400). According to the FlowCam operating manual [1), 2)], automatic focusing was performed beforehand to obtain the best-quality images (Best Focus Image mode). The samples were passed through the FC system in Autoimage Mode, i.e. without using the laser. Software: VisualSpreadsheet, version 4.

Class identification and library creation. Zooplankton objects to be classified were divided by an expert (with over 18 years of experience in zooplankton sample processing) into the following classes: *nauplius* (naupliar stages of copepods), *cyclopoida* and *calanoida* (copepodid stages and adult *Copepoda* of the orders *Cyclopoida* and *Calanoida*), *noctiluca* (living cells of *Noctiluca scintillans* (Macartney) Kofoid & Swezy, 1921), *oikopleura* (appendicularians *Oikopleura* (Vexillaria) *dioica* Fol, 1872), *mollusca* (bivalve larvae).

[1)] Fluid Imaging Technologies Inc., 2020. *VisualSpreadsheet 5 User Guide. Version A*. Available at: https://www.fluidimaging.com/FlowCam-university/visp-5 [Accessed: 10 May 2026].

[2)] Fluid Imaging Technologies Inc., 2020. *FlowCam 8000 Series. Dynamic Imaging Particle Analyzer. User Guide*. *Version C*. Scarborough, Maine, 39 p.

All images of objects not belonging to zooplankton (debris particles of unknown nature and detritus, macrophyte fragments, clearly dead zooplankton organisms, empty copepod carapaces, large diatom and dinoflagellate cells, etc.) were assigned to the *garbage* class.

For each class, a corresponding image library was created: *calanoida* – 1479 images, *cyclopoida* – 374, *garbage* – 4081, *mollusca* – 26, *nauplius* – 383, *noctiluca* – 539, *oikopleura* – 45.

Computational experiments simulating VS operation were performed in the *R* statistical programming environment [3)].

Operation principle of filters and the VS classifier

The principle of image classification in the VS classification window is their sequential checking for compliance with a particular class. A tab is created in the classification window, into which one or more filters are placed. If the parameter values of an image satisfy the filter requirements, the object is assigned to the corresponding class. Objects are fed into the classifier in the order they were obtained during sample processing. An object is checked against the filter requirements in the order in which the class tabs are arranged. The object is assigned to the first class whose filters it satisfies.

In VS, there are two types of filters: *value* and *statistical*. A value filter (VF) sets intervals of permissible values for one or several parameters of objects. The intervals for a specific class can be set based on its library (a set of characteristic images of the class) or manually. One way to use a VF is to apply the *Like selected particles* (*Value*) *From* (LVF) function. The LVF function operates as a VF that includes intervals of all parameters determined by the library. Fig. 1, *a* schematically illustrates the VF principle.

The VS manual does not provide a detailed description of the statistical filter (SF) operation, except that an object is checked for class membership using basic statistical metrics (mean, standard deviation, as well as minimum and maximum parameter values) calculated from library data. The closer an object is to the ideal target particle [4)], for a given parameter, the lower the *Filter Score* (FS) value assigned to it. Practice shows that FS values can range from near unity (very strong match) to several hundred (very strong mismatch). A schematic interpretation of SF principle is given in Fig. 1, *b*.

[3)] R Core Team, 2021. *R: A Language and Environment for Statistical Computing. R foundation for statistical computing.* Vienna, Austria, 2021.

[4)] Fluid Imaging Technologies Inc., 2011. *FlowCam Manual Version 3.0.* 145 p. Available at: https://www.manualslib.com/manual/1628819/Fluid-Imaging-Technologies-*FlowCam*.html#manual [Accessed: 08 October 2025].

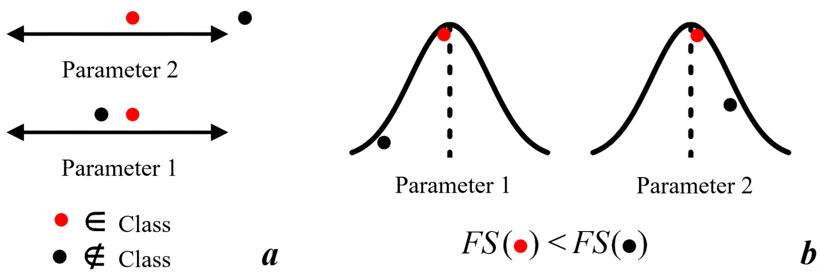

F i g . 1 . Principle of operation of value and statistical filters based on two parameters: *a* – the red object is assigned to the class because its parameter values fall within the specified intervals, whereas the black object is not assigned to the class because it exceeds the permissible range for the second parameter; *b* – the total deviation of the red object from the ideal particle (dashed line), calculated using two parameters, is smaller than that of the black object; therefore, the red object receives a lower *FS* value

For the SF, one or several parameters can also be selected, but manual adjustment of the metrics is unavailable and, unlike the VF, they are entirely determined by library data. VF and SF can be combined within a single filter and employ the same parameters.

Approach to determining the membership of zooplankton images to classes

When creating zooplankton libraries, an approach based on expert assessment of object class membership was applied. For each of the selected zooplankton classes, a single library was created. Only those images that met the following criteria were included in the library: a) the frame contained no garbage particles or only negligible amounts; b) according to expert assessment, a single specific zooplankton object is present in the image; c) the organism was alive at the time of sampling and fixation with formaldehyde; d) the object image is not cropped or only slightly cropped (this can happen if the object was at the periphery of the camera field of view at the moment of photofixation). A visual representation of the above-mentioned image selection criteria for a class is represented using *N. scintillans* as an example (Fig. 2).

Separating objects into a separate library (class) is advisable when their shape and colour variability are low. The parameter samples of such libraries are characterised by the absence or rare occurrence of extreme values and small variance. The boundaries of distributions of different samples on parameter axes, as a rule, turn out to be sufficiently narrow, which, when combining several parameters in filters, ensures high classification accuracy of images by classes.

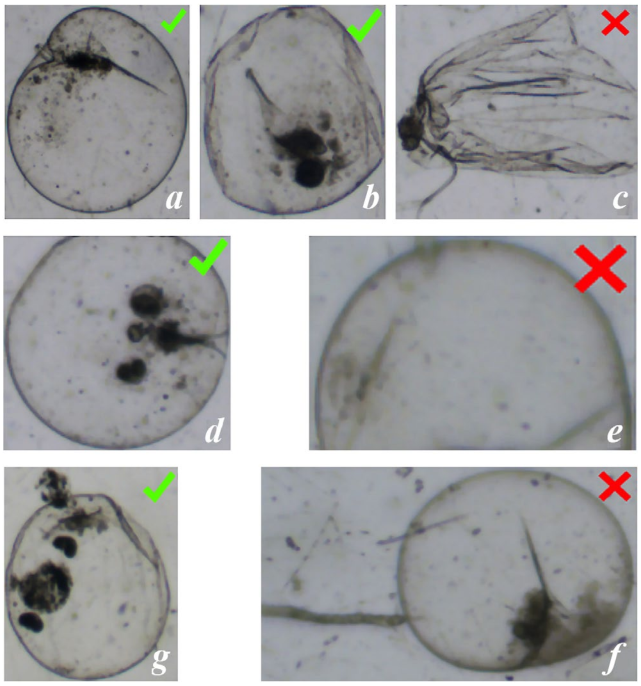

F i g . 2 . Images of *N. scintillans* obtained using FC: *a* – "ideal" state of the object; *b* – moderately deformed object; *c* – severely deformed object (the organism was most likely dead at the time of sample fixation); *d* – the image is moderately cropped at the top; *e* – the image is excessively cropped from below; *f* – a negligible amount of garbage; *g* – the garbage particle size is comparable in size to the object

Zooplankton, with rare exceptions, are objects of very complex shape, in contrast, for example, to non-colonial cells of many phytoplankton species, whose morphology can be reduced to simple geometric figures [12]. The presence in libraries of images of objects with extreme parameter values, as well as multimodality and pronounced asymmetry of parameter distributions, lead to overlapping of classes on numerical axes, which complicates the use of simple value filters (Fig. 3). A particular difficulty is posed by objects of the *garbage* class (e.g., detritus in the field of view), whose quantity and diversity call into question the possibility of completely excluding debris from the zooplankton class tabs (Fig. 3). Applying the LVF function under such conditions leads to numerous classification errors.

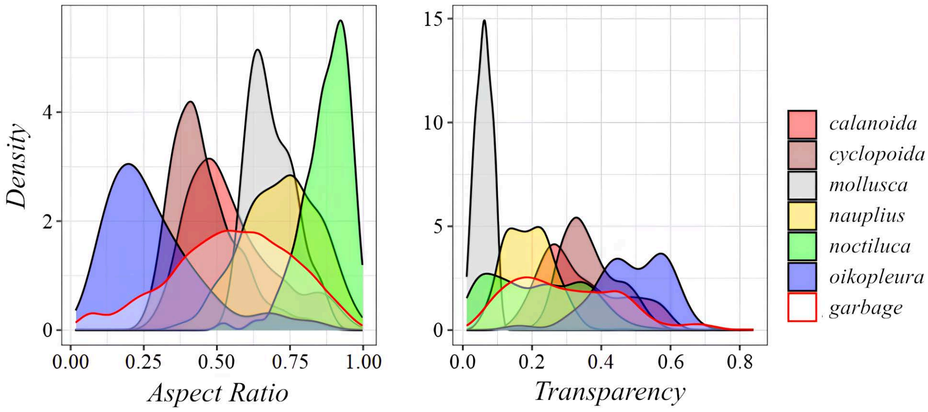

Fig. 3. Examples of probability density functions of parameters for selected zooplankton classes. The Aspect Ratio parameter is calculated as the ratio of the object's side lengths; The Transparency parameter indicates the degree of transparency of the object

A proposed solution for the classification task could be the additional introduction of subclasses in the classifier that reflect the most characteristic variants of the spatial arrangement of zooplankton objects in the FC camera field of view. As an example, class differentiation of copepods depending on their orientation in the frame can be given: a) ventral or dorsal orientation; b) lateral orientation of the object (Fig. 4). However, such subclass detailing apparently would not lead to a significant increase in classification accuracy. This is due to the enormous diversity of antennae and limb positions (or their absence due to mechanical damage),

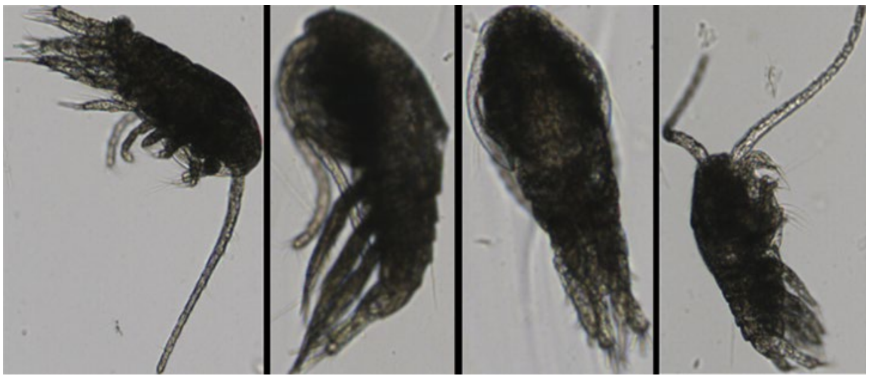

Fig. 4. Variability of spatial orientations of copepods in images obtained using a *FlowCam*

as well as the probability of anthropogenic or natural debris particles entering the field of view. Nevertheless, identifying all possible spatial orientations (i.e., "poses") of zooplankton organisms of various taxonomic classes and forming specialised image libraries based on them is a labour-intensive task that may negate the advantage of using the VS classifier (Fig. 4).

Principles of creating filters and the classifier

Taking into account the statistical properties of object parameter samples and peculiarities of the VS classification toolkit, the following principles for creating filters and constructing the classifier were formulated:

1. When creating filters, classical descriptive statistics methods are not used to identify the best parameters, since the classification logic in VS is based on the sequential application of threshold filters, not on statistical optimization of parameters. Moreover, the distributions of parameters of individual classes are often overlapping and multimodal (see Fig. 3).
2. Due to huge diversity of garbage particles and the impossibility of classifying them without using statistical methods, erroneous assignment of garbage objects to zooplankton classes is permissible, but not in large numbers.
3. In view of high variability of features within classes, pronounced asymmetry of their distributions, and the absence of a formalised description of FS calculation algorithm, only VFs are used when constructing the classifier.
4. The number of class tabs in the classification window should be minimal – one tab per class.

Methodology for creating filters and establishing the order of class tabs in the classifier

A total of 32 parameters are available for use in VFs. Methodology development was based on the hypothesis that in pairs of classifying features, a sufficient number of unique combinations of value intervals for each class can be identified. It is assumed that their combined use in the form of a set of value filters, each containing two parameters, can reveal most objects of the corresponding classes. In total, $C^2_{32} = 496$ parameter pairs are subject to consideration.

The essence of approach to creating class filters is to detect and approximate by rectangles those regions of the two-classifying-feature space that are occupied exclusively by objects (points) of one class. The rectangles must have sides parallel to the parameter axes. In this case, the coordinates of the rectangle length projections and width onto the corresponding axes determine the value intervals of two parameters of one filter. For the remaining filter parameters, intervals determined by the class library are set to reduce the probability of classification error when working with test samples. The number of filters obtained for a class based on two parameters equals the number of rectangles into which the region occupied by that class is divided. In the tabs of future classes, the OR mode is set; therefore, for an object to be assigned to a class, it must satisfy the requirements of any filter in the corresponding tab.

An algorithm for searching and creating such VFs was implemented in the *R* environment using the *sf* library [13]. The algorithm provides three main steps:

Step 1. Within one pair of parameters, *n* situations are formed (*n* – number of classes), in each of which two polygons are created (Fig. 5): polygon *A* – based on the convex hull of the point cloud of the given class; polygon *B* – based on the convex hull formed by the points of the remaining classes. If there is a section of polygon *A* lying outside polygon *B*, then a polygon *C* is formed from such a section (green area in Fig. 5).

Step 2. For polygon *C*, a bounding box is constructed and filled with a regular grid (Fig. 5). The regular grid created using the *sf* library tools is an array of rectangular polygons with sides parallel to the coordinate axes. Regardless of the class and the area of polygon *C*, the grid has a size of 20 × 20 polygons. Polygons that have common sections with polygon *A* or with polygon *C* (or with both) are removed from the grid. The remaining grid polygons are merged into a single polygon *D* (Fig. 5).

Step 3. Polygon *D* is divided into rectangular polygons according to the following algorithm:

(*i*) The lower-left vertex of polygon *D* is selected, then the vertex to its right, and the vertex above it. A rectangular polygon D_i is constructed from the three vertices;

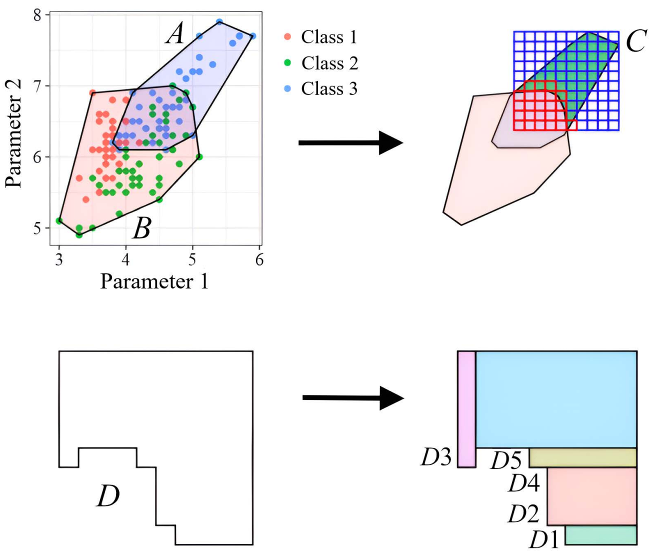

F i g . 5 . The value filter creation algorithm in a two-parameter space (*ii*) If polygon D_i does not extend beyond polygon D, then D_i is cut off from D. Action (*i*) is repeated for the truncated D, and so on until it is completely split into rectangles (Fig. 5);

(*iii*) If polygon D_i extends beyond polygon D, then polygon D is rotated by 90°. Actions (*iii*) and then (*i*) are repeated until condition (*ii*) is satisfied. If after three iterations condition (*ii*) is not met, further attempts to split polygon D (both as a whole and its resulting parts D_n, $i = 1, 2, ..., n$) are stopped.

In the example of Fig. 5, section C of class 3 was divided into D_n rectangles ($n = 5$). The coordinates of each length along parameter 1 and each width along parameter 2 are the intervals of two parameters that are set in separate filters. Thus, based on two parameters, five filters were created to identify objects of class 3.

The described algorithm can be applied iteratively depending on the chosen order of class tabs in the classifier window and the allowable error specified by the user. For example, if the obtained set of filters allowed unambiguous identification of objects of a class(-es), it makes sense to repeat the filter search for the remaining classes, excluding the recognised classes from the dataset. Obviously, tabs with such high filter efficiency should be placed first. Furthermore, if the percentage of erroneous assignment of other classes' objects or the percentage of unidentified objects of this class is small, it can be neglected in favour of increasing the efficiency of the subsequent classifier tabs.

Results

Classifier creation and its performance. The first run of the VF search algorithm was performed on the dataset including all seven classes (Table). As expected, the largest number of regions outside the boundaries of other classes (Fig. 5) was found for *garbage* – 700. Due to the high density of garbage objects in the pair-parameter space, the number for the remaining classes was significantly smaller (*mollusca* – 112, *noctiluca* – 185, *oikopleura* – 7, *nauplius* – 8, *calanoida* – 223, *cyclopoida* – 0), which in some cases led to low or zero detectability (Table). Since further identification efficiency increase (68.9%) of *garbage* objects proved impossible, the *garbage* tab with the VFs obtained in the first run was placed first in the classifier.

The second run of the algorithm was performed after removing all *garbage* objects from the dataset. The use of the obtained VF sets allowed increasing the proportion of detected objects for all classes. The detectability of the *mollusca* and *noctiluca* classes was 100%, so tabs for these classes with new VF sets were created next.

The next algorithm run took place after removing the aforementioned classes from the dataset. The new VF sets noticeably increased the proportion of detected *nauplius* objects (71.2%), which is particularly important in the context of the difficulty of distinguishing naupliar and adult copepod stages. No improvement in detectability was noted for the *oikopleura* class. A small increase in detected objects was achieved for calanoida – by 5.1% (to 51.9%). Despite a noticeable increase in the number of identified *cyclopoida*, their proportion remained low (Table).

For the final decision on creating the last three tabs of the classifier, the fourth algorithm run was performed on the dataset without *oikopleura*. The new VFs did not lead to a noticeable increase in classification efficiency, so the *nauplius*, *calanoida*, and *cyclopoida* tabs were filled with the VF sets obtained after the previous run.

Since it was not possible to indicate *cyclopoida* objects at the level of other classes, we made a separate attempt to search for VFs after combining *calanoida* and *cyclopoida* into a single class *copepoda* (Table, run number III.I).

Results of sequential application of filter sets in the *VisualSpreadsheet* classification window

Algorithm run number	Variations in classes composition	Number of identified objects / total number of class images (*identification rate, %*)						
		garbage	*mollusca*	*noctiluca*	*oikopleura*	*nauplius*	*calanoida*	*cyclopoida*
I	All classes	2815/4081 (*68.9*)	19/26 (*73.1*)	376/539 (*69.8*)	5/45 (*11.1*)	4/383 (*1.04*)	111/1479 (*7.5*)	0/374 (*0*)
II	– *garbage*	–	(*100*)	(*100*)	(*82*)	(*56.9*)	(*46.8*)	(*3.5*)
III	– *noctiluca, mollusca*	–	–	–	(*82*)	(*71.2*)	(*51.9*)	(*7.75*)
IV	– *oikopleura*	–	–	–	–	(*71.2*)	(*55.4*)	(*9.6*)
III.I	+ *oikopleura, calanoida* + +*cyclopoida* = = *copepoda*	–	–	–	(*82*)	(*69.5*)	1301/1853 (*70.2*)	

Note: "–" indicates that the class parameter data was not used during the subsequent run of the filter search algorithm, and the result (% of identifications) for the class remains the same as in the previous filter configuration; the order of classes corresponds to the order of tabs in the VS classification window.

A total of 1301 objects were identified; 1079 of them belonged to *calanoida* and 222 to *cyclopoida*. Thus, the number of identified objects was increased to 72.8% and 59.3%, respectively, but already within a single class.

Discussion

Most studies that mention zooplankton sample processing on FC are devoted to comparing organism size characteristics obtained by light microscopy and VS, and calculating biomass, biovolume, and other indicators based on them [2, 14–16], determining community structure, identifying and counting rare species [5, 17]. In some works, FC is appled to count particles whose number provides indirect information on zooplankton vital activity and its habitat [18, 19]. Literature analysis revealed the absence of publications with a detailed description of parameter selection for sorting zooplankton images or entirely devoted to the development of a classifier in VS.

We see the causes for the absence of such works in the difficulties that accompany work with this material. The most common FC models have insufficient capillary width of flow cells, which limits the ability to work with the lower boundary of the mesozooplankton size spectrum [15, 20]. In the case of the Black Sea, the FlowCam 8400 cannot process samples containing large specimens (over 1–1.5 mm) of calanoid copepods and sagittae. The length of sagittae reaches 3 mm or more. An additional obstacle in operation can be created by detritus particles and copepod aggregates, which tend to clog the flow capillary of the cell. If the goal is to process a sample with all zooplankton in it (from naupliar stages to adult copepods), an additional FlowCam model Macro or ZOOSCAN is required [21–23]. Given these difficulties and the fact that zooplankton images are poorly handled by the VS toolkit, it is more appropriate to use predominantly manual classification or ML libraries [5)] [24, 25]. It is worth noting that the increase in classification efficiency of calanoid and cyclopoid copepods (classes *calanoida* and *cyclopoida*) after merging into a single class *copepoda* is probably due to the morphological similarity of organisms of these groups.

In the previously mentioned work [12] the authors describe an approach to creating SFs for identifying microalgae cell images. They managed to achieve good results (filter accuracy criterion approached the maximum value of unity) for nine phytoplankton classes. At the same time, the classes were identified with much greater taxonomic depth (to genus and in some cases to species) compared to our study. However, the authors do not mention foreign particles, which undoubtedly must have been present in the samples, given the net sampling method. It should be noted that the filter accuracy decreased as the cell shape became morphologically

---

[5)] Grosjean, P., Denis, K. and Wacquet, G., 2018. *ZooImage: Analysis of Numerical Plankton Images. R package version*. Available at: https://cran.r-project.org/web/packages/zooimage/zooimage.pdf [Accessed: 31 May 2026].

more complex. These results allow us to conclude that the use of SFs for the tasks of our study is limited. The heterogeneity of samples (see Fig. 3) leads to incorrect calculation of the sample mean and standard deviation, which apparently entails a large number of errors.

In study [10], when solving the problem of identifying genera and species of colonial cyanobacteria and other microalgae, the authors, on the contrary, focused on selecting VFs. The minimum number of the most useful parameters for two filters was selected by manual adjustment based on 25 and 50 characteristic images of object classes. To improve classification accuracy, a third filter with the same parameters was created, but with value ranges formed by the intersections of the parameter ranges of the original filters. In [10] the authors report that the proposed approach allowed achieving almost 100% (99.8%) accuracy of object identification by genus; the accuracy when separating morphospecies varied from 42.6 to 93.7%. As in [12], the authors do not address the issue of foreign particles and do not describe the preprocessing of the image dataset.

Unlike [10, 12], where filters were created intuitively manually, in our study we attempted to automate filter selection and formalise the arrangement of class tabs in the VS classification window.

In version 6 of VS, an AI tool for working with protein aggregates appeared for the first time. However, until VS incorporates functionality allowing users to customise and train neural networks independently, the proposed algorithm may become an alternative to manual parameter selection. Presumably, the algorithm may be more effective when working with phytoplankton samples, and its efficiency can be improved by moving from pairs of parameters to triples, etc. In other words, increasing the dimensionality of the considered parameter spaces should lead to the identification of a larger number of filters with class-unique value intervals and an increase in the detectability of the corresponding objects.

Conclusions

In this work, a methodology for classifying zooplankton images obtained using a FlowCam system with the VisualSpreadsheet software tools has been developed for the first time. Within the framework of the proposed approach, an algorithm for the automatic generation of value filters was implemented; under certain conditions, it ensured 100% identification for the *mollusca* and *noctiluca* classes, 82% for *oikopleura*, 71.2% for *nauplius*, and 70.2% for *copepoda* (after merging *cyclopoida* and *calanoida*).

Since the algorithm does not require preliminary analysis of parameter distributions, the methodology can be applied to the study of a wide range of objects recorded by FlowCam. It is most advisable to use the developed methodology when working with objects that have complex morphology, in particular zooplankton. In the future, it is planned to implement a value filter search algorithm in parameter spaces of higher dimensionality and test it both on zooplankton objects and on other components of marine plankton, including phytoplankton.

REFERENCES

1. Piontkovski, S.A., Minsky, I.A. and Meger, Ya.V., 2023. Long-Term Variability Of Oceanic Zooplankton Biomass. *Aquatic Bioresources & Environment*, 6(3), pp. 52–65. https://doi.org/10.47921/2619-1024_2023_6_3_52 (in Russian).
2. Karnan, C., Jyothibabu, R., Manoj Kumar, T. M., Jagadeesan, L. and Arunpandi, N., 2017. On the Accuracy of Assessing Copepod Size and Biovolume Using *FlowCam* and Traditional Microscopy. *Indian Journal of Geo Marine Systems*, 46, pp. 1261–1264.
3. Chiba, S., Batten, S., Martin, C.S., Ivory, S., Miloslavich, P. and Weatherdon, L.V., 2018. Zooplankton Monitoring to Contribute Towards Addressing Global Biodiversity Conservation Challenges. *Journal of Plankton Research*, 40(5), pp. 509–518. https://doi.org/10.1093/plankt/fby030
4. Ratnarajah, L., Abu-Alhaija, R., Atkinson, A., Batten, S., Bax, N.J., Bernard, K.S., Canonico, G., Cornils, A., Everett, J.D. et al. Monitoring and Modelling Marine Zooplankton in a Changing Climate. *Nature Communications*, 14, 564. https://doi.org/10.1038/s41467-023-36241-5
5. Detmer, T.M., Broadway, K.J., Potter, C.G., Collins, S.F., Parkos III, J.J. and Wahl, D.H., 2019. Comparison of Microscopy to a Semi-Automated Method (FlowCam®) for Characterization of Individual-, Population-, and Community-Level Measurements of Zooplankton. *Hydrobiologia*, 838, pp. 99–110. https://doi.org/10.1007/s10750-019-03980-w
6. Culverhouse, P.F., Williams, R., Reguera, B., Herry, V. and González-Gil, S., 2003. Do Experts Make Mistakes? A Comparison of Human and Machine Identification of Dinoflagellates. *Marine Ecology Progress Series*, 247, pp. 17–25. https://doi.org/10.3354/meps247017
7. Zhang, W., Bi, H., Wang, D., Cheng, X., Cai, Z. and Ying, K., 2024. Automated Zooplankton Size Measurement Using Deep Learning: Overcoming the Limitations of Traditional Methods. *Frontiers in Marine Science*, 11, 1341191. https://doi.org/10.3389/fmars.2024.1341191
8. Drago, L., Panaïotis, T., Irisson, J.-O., Babin, M., Biard, T., Carlotti, F., Coppola, L., Guidi, L., Hauss, H. et al., 2022. Global Distribution of Zooplankton Biomass Estimated by In Situ Imaging and Machine Learning. *Frontiers in Marine Science*, 9, 894372. https://doi.org/10.3389/fmars.2022.894372
9. Kydd, J., Rajakaruna, H., Briski, E. and Bailey, S., 2017. Examination of a High-Resolution Laser Optical Plankton Counter and *FlowCam* for Measuring Plankton Concentration and Size. *Journal of Sea Research*, 133, pp. 2–10. http://doi.org/10.1016/j.seares.2017.01.003
10. Mirasbekov, Y., Zhumakhanova, A., Zhantuyakova, A., Sarkytbayev, K., Malashenkov, D.V., Baishulakova, A., Dashkova, V., Davidson, T.A., Vorobjev, I.A. et al., 2021. Semi-Automated Classification of Colonial Microcystis by *FlowCam* Imaging Flow Cytometry in Mesocosm Experiment Reveals High Heterogeneity During Seasonal Bloom. *Scientific Reports*, 11, 9377. https://doi.org/10.1038/s41598-021-88661-2
11. Owen, B.M., Hallett, C.S., Cosgrove, J.J., Tweedley, J.R. and Moheimani, N.R., 2022. Reporting of Methods for Automated Devices: A Systematic Review and Recommendation for Studies Using *FlowCam* for Phytoplankton. *Limnology and Oceanography: Methods*, 20(7), pp. 400–427. https://doi.org/10.1002/lom3.10496
12. Camoying, M.G. and Yñiguez, A.T., 2016. *FlowCam* Optimization: Attaining Good Quality Images for Higher Taxonomic Classification Resolution of Natural Phytoplankton Samples. *Limnology and Oceanography: Methods*, 14(5), pp. 305–314. https://doi.org/10.1002/lom3.10090

13. Pebesma, E. and Bivand, R., 2023. *Spatial Data Science: With Applications in R*. New York : Chapman and Hall/CRC, 314 p. https://doi.org/10.1201/9780429459016

14. Wong, E., Sastri, A.R., Lin, F.-S. and Hsieh, C.-h., 2017. Modified FlowCam Procedure for Quantifying Size Distribution of Zooplankton with Sample Recycling Capacity. *PLoS ONE*, 12(4), e0175235. https://doi.org/10.1371/journal.pone.0175235

15. Albini, D., Ransome, E., Dumbrell, A.J., Pawar, S., O'Gorman, E.J., Smith, T.P., Bell, T., Jackson, M.C. and Woodward, G., 2025. Warming Alters Plankton Body-Size Distributions in a Large Field Experiment. *Communications Biology*, 8, 162. https://doi.org/10.1038/s42003-024-07380-2

16. Lovecchio, E., Henson, S., Carvalho, F., Briggs, N., Hilder, H., Wolff, G.A., Giering, S.L.C., Cook, K., Baker, C.A. et al., 2025. Mesopelagic Particle Layers in the Dynamic Hypoxic Northern Benguela are Shaped by Zooplankton Activity. *Journal of Geophysical Research: Oceans*, 130(3), e2024JC021039. https://doi.org/10.1029/2024JC021039

17. Wang, Y., Castillo-Keller, M., Eustance, E., Sommerfeld, M., 2017. Early Detection and Quantification of Zooplankton Grazers in Algal Cultures by *FlowCam. Algal Research*, 21, pp. 98–102. https://doi.org/10.1016/j.algal.2016.11.012

18. Ide, K., Takahashi, K., Kuwata, A., Nakamachi, M. and Saito, H., 2008. A Rapid Analysis of Copepod Feeding Using *FlowCam. Journal of Plankton Research*, 30(3), pp. 275–281. https://doi.org/10.1093/plankt/fbm108

19. Minguez, L., Sperfeld, E., Berger, S.A., Nejstgaard, J.C. and Gessner, M.O., 2020. Changes in Food Characteristics Reveal Indirect Effects of Lake Browning on Zooplankton Performance. *Limnology and Oceanography*, 65(5), pp. 1028–1040. https://doi.org/10.1002/lno.11367

20. Lombard, F., Boss, E., Waite, A.M., Vogt, M., Uitz, J., Stemmann, L., Sosik, H.M., Schulz, J., Romagnan, J.-B. et al., 2019. Globally Consistent Quantitative Observations of Planktonic Ecosystems. *Frontiers in Marine Science*, 6, 196. https://doi.org/10.3389/fmars.2019.00196

21. Gorsky, G., Ohman, M.D., Picheral, M., Gasparini, S., Stemmann, L., Romagnan, J.-B., Cawood, A., Pesant, S., García-Comas, C. et al., 2010. Digital Zooplankton Image Analysis Using the Zooscan Integrated System. *Journal of Plankton Research*, 32(3), pp. 285–303. https://doi.org/10.1093/plankt/fbp124

22. Feliú, G., Pagano, M., Hidalgo, P. and Carlotti, F., 2020. Structure and Function of Epipelagic Mesozooplankton and Their Response to Dust Deposition Events During the Spring PEACETIME Cruise in the Mediterranean Sea. *Biogeosciences*, 17(21), pp. 5417–5441. https://doi.org/10.5194/bg-17-5417-202

23. Fierro-González, P., Pagano, M., Guilloux, L., Makhlouf, N., Tedetti, M. and Carlotti, F., 2023. Zooplankton Biomass, Size Structure, and Associated Metabolic Fluxes with Focus on its Roles at the Chlorophyll Maximum Layer During the Plankton-Contaminant MERITE-HIPPOCAMPE Cruise. *Marine Pollution Bulletin*, 193, 115056. https://doi.org/10.1016/j.marpolbul.2023.115056

24. Ershova, E.A., Berge, T., Aguirre, G.E., Reeve, M.J., Martinussen, M.B., Falkenhaug, T., 2025. Latitudinal Gradients in Zooplankton Communities in Norwegian Fjords Resolved by an Integrated Morphological and Molecular Approach. *ICES Journal of Marine Science*, 82(6), fsae147. https://doi.org/10.1093/icesjms/fsae147

25. Conradt, J., Börner, G., López-Urrutia, Á., Möllmann, C. and Moyano, M., 2022. Automated Plankton Classification with a Dynamic Optimization and Adaptation Cycle. *Frontiers in Marine Science*, 9, 868420. https://doi.org/10.3389/fmars.2022.868420

Submitted 26.11.2025; accepted after review 04.02.2026;
revised 19.03.2026; published 30.06.2026.

About the authors:

Ivan A. Minsky, Junior Researcher, Research Laboratory "Marine Ecosystems", Institute of Advanced Studies, Sevastopol State University (33, Universitetskaya St., 299053, Sevastopol, Russia); Leading Engineer, A. O. Kovalevsky Institute of Biology of the Southern Seas of RAS (2, Nakhimov Ave., 299011, Sevastopol, Russia), **ORCID ID: 0009-0009-6539-303X**, **Scopus Author ID: 58168623600**, *ivansimfer@yandex.ru*

Daria A. Litvinyuk, Senior Researcher, A. O. Kovalevsky Institute of Biology of the Southern Seas of RAS (2, Nakhimov Ave., 299011, Sevastopol, Russia), PhD (Biol.), **ORCID ID: 0000-0002-9732-1219**, **Scopus Author ID: 57195425970**, **ResearcherID: ABB-1684-2021**, *d.litvinyuk@ibss-ras.ru*

Vladislav P. Evstigneev, Leading Researcher, Sevastopol State University (33, Universitetskaya St., 299053, Sevastopol, Russia), PhD (Phys.-Math.), Associate Professor, **ORCID ID: 0000-0003-3064-2613**, **ResearcherID: G-1894-2014**, **Scopus Author ID: 12544785600**, *vald_e@rambler.ru*

Andrey A. Pinaev, Master's Degree Holder, Sevastopol State University (33, Universitetskaya St., 299053, Sevastopol, Russia), **ResearchID**: **rid125302**, *mrsend@mail.ru*

Vladimir S. Mukhanov, Leading Researcher, Head of the Plankton Department, A. O. Kovalevsky Institute of Biology of the Southern Seas of RAS (2, Nakhimov Ave., 299011, Sevastopol, Russia), PhD (Biol.), **Scopus Author ID: 7004040853**, **ORCID ID: 0000-0002-5324-045X**, **ResearcherID: H-4760-2014**, *v.s.mukhanov@ibss-ras.ru*

Contribution of the authors:

Ivan A. Minsky – problem formulation and statement, methodology development, computational experiments, literature review, field data acquisition, discussion of results, equipment preparation and maintenance, operation of equipment, manuscript preparation, conclusions formulation

Daria A. Litvinyuk – methodology development, literature review, field data acquisition, qualitative analysis of field data, discussion of results, manuscript preparation, manuscript revision

Vladislav P. Evstigneev – methodology development, literature review, discussion of results, manuscript revision

Andrey A. Pinaev – computational experiments, field data acquisition, equipment preparation and maintenance, operation of equipment, discussion of results, figure preparation

Vladimir S. Mukhanov – discussion of results, conclusions formulation, manuscript revision

All the authors have read and approved the final manuscript.